University of Southampton

Faculty of Natural and Environmental Science

Biological Sciences

The Role of Serine/Threonine Kinases in Translation Machinery Regulation and Antibiotic Susceptibility in Response to Nutrient Starvation in *Pseudomonas aeruginosa*

DOI…

by

Conor Patrick William Graham

Thesis for the degree of Doctor of Philosophy

2023

University of Southampton

Abstract

Faculty of Natural and Environmental Science

Biological Sciences

Thesis for the degree of Doctor of Philosophy

The Role of Serine/Threonine Kinases in Translation Machinery Regulation and Antibiotic Susceptibility in Response to Nutrient Starvation in *Pseudomonas aeruginosa*

by

Conor Patrick William Graham

Pseudomonas aeruginosa is a gram-negative opportunistic pathogen that produces highly antibiotic-tolerant biofilms that create an enormous therapeutic burden as they cause many types of chronic infections. The reason *P. aeruginosa* biofilms are problematic is in part due to reduced growth activity and downregulation of metabolic processes within biofilms that are typically the target of antibiotics. There is an unmet need for novel strategies that aim to either disrupt the biofilm itself or modulate metabolic activity and cell survical mechanisms within biofilms. A relatively unexplored mechanism for disrupting the metabolic adaptability of *P. aeruginosa* is via inhibition of serine/threonine phosphorylation pathways of eukaryote-like serine/threonine kinases in biofilms. These kinases are characterised by a catalytic Hanks-type domain that reversibly phosphorylates serine or threonine residues of various proteins in many cellular processes, including several regulatory proteins of other signalling cascades. The focus of this study was to investigate the role of eSTK's in *P. aeruginosa* biofilm development and their impact on metabolism and adaptive responses.

There are four eSTK's in the *P. aeruginosa* genome. All four of these genes were deleted from PAO1 individually and sequentially to produce a quadruple knockout mutant termed QKO. In addition, three were deleted individually from *P. aeruginosa* PA2192, a cyctic fibrosis clinical isolate. Using multiple strategies such as confocal microscopy and TMT-labelled proteomics analysis we showed that deletion of a single eSTK, YeaG, of PA2192 can inhibit aggregate formation, and that the metabolic adaptability of the QKO mutant of PAO1 is significantly disrupted and which leads to major alterations within intracellular signalling pathways. This leads to a compromised membrane phenotype that allows greater influx of positively charged compounds such as propidium iodide. Although we did not see any increase in the susceptibility of the QKO mutant to tobramycin in the model used, the apparent cellular stress exhibited by the

QKO mutant and the inhibited aggregation of the PA2192 suggest that eSTK's are potentially interesting drug targets with therapeutic potential in the control of *P. aeruginosa* biofilms.

Table of Contents

Table of Contents i

Table of Tables vii

Table of Figures ix

Research Thesis: Declaration of Authorship xv

Acknowledgements xvii

Definitions and Abbreviations xix

Chapter 1 Introduction 1

1.1 Hallmarks of a biofilm 1

1.1.1 Adhesion 1

1.1.2 Binary population growth and matrix formation 2

1.1.3 Dispersal 2

1.1.4 Characteristics of the EPS 3

1.2 Chemical gradients and physiological heterogeneity in biofilms contribute to multi-drug tolerance and persistence 5

1.2.1 Biofilm induced hypoxia 6

1.2.2 Amino acid and carbon starvation in antibiotic tolerance 7

1.3 Persister cells 8

1.3.1 Defining a persister cell: A historical perspective 8

1.4 The role of the stringent response and toxin anti-toxin systems in translation inhibition 10

1.4.1 Ribosome-independent mRNA interferases 11

1.4.2 Ribosome-dependent mRNA interferases 11

1.4.3 Other TA systems 12

1.4.4 Controversy surrounding Toxin Antitoxin Systems 12

1.5 The mechanisms and advantages of eukaryotic translation inhibition in response to cellular stress in the tumour microenvironment 13

1.5.1 Direct inhibition of translation machinery 13

1.5.2 Selective mRNA translation 15

1.6 Bacterial and eukaryotic translation: a comparison 16

1.6.1 Initiation 16
1.6.2 Elongation 17
1.7 Ubiquitous nature of translation machinery and the evolution of protein synthesis regulation 19
1.7.1 Translation initiation factors 19
1.7.2 Translation elongation factors 19
1.8 The bacterial vs human kinome 22
1.9 Translation machinery phosphorylation in response to nutrient deprivation in bacteria 23
1.10 The structure and activation of Hanks type serine/threonine kinases 24
1.10.1 Stk1 25
1.10.2 PpkA 26
1.10.3 YeaG 27
1.10.4 The role of adjacent phosphatases 27
1.11 Which translation factors are the most effective targets for cellular protein synthesis inhibition? 27
1.11.1 Initiation Factors 27
1.11.2 Elongation Factors 28
1.12 Aims and Hypothesis 29

Chapter 2 Creation of the eSTK deletion mutants identified in *Pseudomonas aeruginosa* 31

2.1 Introduction 31
2.1.1 Rationale for selecting the plasmid vector and marker to facilitate gene deletions in *P. aeruginosa* 32
2.1.2 Methodologies used to create recombinant constructs in plasmids 34
2.1.3 Method used to create a markerless deletion 35
2.2 Materials and Methods 36
2.2.1 Blast search, conserved domain search and multiple sequence alignment 36
2.2.2 Strains and plasmids relevant to this chapter 36
2.2.3 Primers used in this study 38

2.2.4 DNA extraction 38
2.2.5 PCR 39
2.2.6 Agarose Gel Electrophoresis 39
2.2.7 Restriction Enzyme mediated digestion Construction of Mutant fragments 39
2.2.7.1 Upstream and downstream fragments 40
2.2.7.2 Gentamicin resistance cassette 40
2.2.7.3 Construction of Gateway compatible knockout vector (excluding Stk1) 40
2.2.8 Ligation 40
2.2.9 Gibson Assembly 40
2.2.10 Miniprep 40
2.2.11 Transformation of *E. coli* 41
2.2.12 Transformation of *P. aeruginosa* strains 41
2.2.13 Selection of Deletion Mutants 41
2.2.14 FLP Recombinase Mediated Marker Deletion 41
2.3 Results and Discussion 42
2.3.1 BLASTP search and AlphaFold structural analysis reveals that proteins with conserved Hanks type serine/threonine kinase domains exist in *P. aeruginosa* PAO1 and PA2192 42
2.3.2 Individual deletion mutants 45
2.3.3 Multiple deletion mutants 47

Chapter 3 Phenotypic characterisation of the eSTK deletion mutant strains of *Pseudomonas aeruginosa* 49

3.1 Introduction 49
3.2 Materials and Methods 50
3.2.1 Construction of Knockout mutants 50
3.2.2 Growth curves 50
3.2.3 Minimum Inhibitory Concentration and Minimum Bactericidal Concentration of planktonic bacteria 50
3.2.4 96 well plate crystal violet assay 50
3.2.5 Microfluidic flow cell setup Coverslip and device preparation 51

3.2.5.1 Connecting the syringe pump to the device 51
3.2.5.2 Preparing the inoculum 51
3.2.5.3 Disinfecting, inoculating, and flowing media through the device 51
3.2.5.4 Staining the biofilm with Baclight Live/Dead stain 52
3.2.6 Confocal 52
3.2.7 Live and dead cell quantification 52
3.2.8 Mean fluorescent intensity quantification 52
3.2.9 Biofilm antibiotic susceptibility 52
3.3 Results 53
3.3.1 Growth curves of the mutant and wild type strains in LB media 53
3.3.2 Planktonic antibiotic susceptibility assays of stationary phase cultures of the wild type and mutant strains to tobramycin 55
3.3.3 Crystal violet Assay shows no significant difference in biofilm formation between the mutants and wild type strains 55
3.3.4 Confocal microscopy and IMARIS analysis of the wild type and knockout strains 57
3.3.4.1 Viabilty 58
3.3.4.2 Biofilm matrix 60
3.3.4.3 Differentiation 62
3.3.4.4 Filamentation in the PpkA and QKO mutant 63
3.3.5 Antibiotic susceptibility to tobramycin of the WT and QKO biofilms at 96 hours 64
3.4 Discussion 65
Chapter 4 Investigating the proteome of the QKO mutant relative to wildtype PAO1 69
4.1 Introduction 69
4.2 Materials and methods 70
4.2.1 Construction of mutants for SILAC 70
4.2.2 Strains used for this chapter 71
4.2.3 Primers used for this chapter 72
4.2.4 Growth curves for SILAC strains 72

4.2.5 Growth curves for validation of planktonic growth conditions in M9 media with serine hydroxamate 72
4.2.6 Growth conditions for microfluidic biofilms 72
4.2.7 Growth conditions for planktonic cultures 72
4.2.8 Protein extraction 73
4.2.9 Protein precipitation 73
4.2.10 Protein digestion 73
4.2.11 Quantification of extracted proteins and peptides 73
4.2.12 Phosphopeptide enrichment 74
4.2.13 Labelling of peptides using TMT 74
4.2.14 Liquid chromatography Mass spectrometry 74
4.2.15 Analysis of raw files for whole proteome and phosphoproteome analysis using MaxQuant 74
4.2.16 Statistical analysis 75
4.3 Results 75
4.3.1 Deletion of the ArgH gene of *Pseudomonas aeruginosa* results in a death phase upon entry into stationary phase of planktonic growth 75
4.3.1.1 Addition of exogenous L-arginine leads to significantly increased biofilm formation 76
4.3.2 Characterisation of the planktonic growth of the wildtype and quadruple KO mutant of PAO1 in M9 media with and without SHX 77
4.3.3 DirectDetect quantification of extracted protein, peptide and phospho-peptide 78
4.3.4 Preparing and normalising the data 79
4.3.5 Checking for batch effects using principal component analysis 80
4.3.6 Identifying differentially expressed proteins 81
4.3.7 Networks established via differential expression analysis 83
4.3.7.1 Pathways differentially expressed when comparing QKO to the wild type 84
4.3.8 Weighted Gene Co-expression Analysis (WGCNA) 95
4.3.8.1 Analysis of modules that significantly link to a trait 101

4.3.8.2 MEblack 103
MEblue 108
4.3.8.3 108
MEgreen 113
4.3.8.4 113
4.3.9 Phosphoproteomics 115
4.3.9.1 Iron storage 117
4.3.9.2 Central metabolism 117
4.3.9.3 Reactive oxygen species detoxification 118
4.4 Discussion 120
Chapter 5 Conclusion and Outlook 129
5.1 Different effects are observed when deleting YeaG from an acutely virulent strain, compared to a chronic strain 129
5.2 eSTK's are important in regulating key processes that impact the adaptability of *P. aeruginosa* PAO1 130
5.3 Deletion of eSTK's does not affect the antibiotic susceptibility of PAO1 relative to the wild type in planktonic or biofilm culture when treated with tobramycin 130
5.4 Follow on research 131
Appendix A 133
List of References 181

Table of Tables

Table 1: Comparison between Bacterial and Eukaryotic translation initiation 17

Table 2: Identity matrix of EF-Tu from model pathogenic bacteria and Eukaryotic eEF-1 from Homo sapiens 20

Table 3: identity matrix of EF-G from model pathogenic bacteria and Eukaryotic eEF-2 from Homo sapiens 20

Table 4: Strains and plasmids used during this study 37

Table 5: The primers used to create and confirm the deletion mutants used during this study 38

Table 6: Homologous proteins identified in *Pseudomonas aeruginosa* after a BLASTP search against PknB from Mycobaterium tuberculosis, a Hanks type consensus sequence, and PrkA from *Bacillus subtilis* *Pstk is short for "Probable serine/threonine protein kinase" **PA2727 was not studied further.....43

Table 7: Tobramycin Minimum Inhibitory Concentrations and Minimum Bactericidal Concentrations of stationary phase planktonic *Pseudomonas aeruginosa* PAO1 WT and the eSTK mutant strains 55

Table 8: Strains and plasmids used in this chapter.....71

Table 9: Primers used in this chapter 72

Table 10: Differentially expressed proteins identified from the biofilm, planktonic and serine hydroxamate treated planktonic samples. Protein network data is from the PseudoCYC and KEGG databases..... **Error! Bookmark not defined.**

Table 11: Proteins found in the MEblack module with corresponding network/pathway data from PseudoCYC and KEGG ..... **Error! Bookmark not defined.**

Table 12: Proteins found in the MEblue module with corresponding network/pathway data from PseudoCYC and KEGG ..... **Error! Bookmark not defined.**

Table 13: Proteins found in the MEgreen module with corresponding network/pathway data from PseudoCYC and KEGG ..... **Error! Bookmark not defined.**

Table of Tables

Table 14: Phosphoproteins identified in the biofilm and planktonic samples, showing the position of the phosphorylation and on which residue. Network/pathway data are from the PseudoCYC and KEGG databases ..... **Error! Bookmark not defined.**

Table of Figures

Figure 1: The life cycle of a biofilm. Firstly, the bacterial cells adhere to the surface. This is followed by population growth and biofilm formation, resulting in nutrient fluctuations that trigger dispersal pathways in some cells (Red cells). Lastly, the small group of cells break out of the biofilm and disperse. The cycle would then repeat resulting in diversification and microcolony formation. 3

Figure 2: Bacteria encased in a biofilm, where the grey cells are metabolically active and red cells are metabolically inactive. The change in colour from the outer edge to the centre simulates the chemical gradient caused by rapidly proliferating cells on the outer edge of the biofilm.....5

Figure 3: (p)ppGpp induction in response to nutrient starvation. RelA is activated when a deacetylated tRNA binds to the ribosome and results in (p)ppGpp production, whereas, (p)ppGpp production as a result of other stressers is controlled by SpoT 8

Figure 4: A bacterial biofilm where grey cells are metabolically active and red cells are metabolically inactive (Persisters). Treatment with antibiotic results in only tolerant persisters remaining, which then become metabolically active and repopulate when the stress is removed. Upon repopulation, different cells may become persisters. 10

Figure 5: The stages of translation elongation in bacteria. I) EF-Tu:GTP:tRNA binds to the ribosomal A-site ii) EF-Tu:GTP is hydrolysed to EF-Tu:GDP, facilitating translocation of tRNA to the ribosomal P-site iii) EF-G:GTP binds the 30s subunit of the ribosome, is digested to EF-G:GDP, resulting in translocation of tRNA to the ribosomal E-site, where it is ejected iV) The ribosome is now ready for another round of translation elongation.....18

Figure 6: The potential mechanism of kinase induced dormancy and how this benefits the survival of cells in response to stress. The red cells are metabolically inactive and the grey cells are metabolically active. 24

Figure 7: Summary of the steps used to create the construct. i) Sequences flanking the gene of interest and the gentamicin resistance cassette were amplified ii) These were digested with EcoRI and HindIII, then ligated with T4 or T7 ligase iii) The resulting

Table of Figures

fragment was amplified iv) The fragment and pEX100T vector were digested with SmaI, then ligated with T4 ligase 31

Figure 8: pEX100T plasmid developed by Herbert Schweizer and used to create the deletion mutants in this study 33

Figure 9: Gentamicin resistance cassette flanked by FRT sequences from pFGM1 plasmid developed by Herbert Schweizer, which was used to create the markerless deletion mutants in this study 34

Figure 10: pFLP3 plasmid used for FLP mediated removal of the FRT flanked gentamicin resistance marker 35

Figure 11: Alignment of the four serine/threonine kinases from *Pseudomonas aeruginosa* selected for study, with PknB from *Mycobaterium tuberculosis* being used a root. The Alignment shows less similarity between YeaG and the other kinases, however there is still homology at the regions corresponding to the ATP binding site and the active site 44

Figure 12: Structure predictions from AlphaFold show conserved and overlapping regions of their protein secondary structures. A) Pstk B) PpKA C) Stk1 D) YeaG E) Super-imposed image of all the kinases selected for study in *Pseudomonas aerugionosa*, and PknB of *Mycobaterium tuberculosis* as a root/reference (orange). The overlapping regions are mostly linked to the ATP binding sites and active sites of the kinases..... 45

Figure 13: Gel showing the size differences of the amplified genomic area between the wild type and mutant strains, confirming that individual knockouts were achieved for PAO1. The ladder used was the '1Kb ladder' from Promega 46

Figure 14: Gel showing the size differences of the amplified genomic area between the wild type and mutant strains, confirming that individual knockouts were achieved for PA2192, except for PpkA. The ladder used was the '1Kb ladder' from Promega 46

Figure 15: Gel showing the size differences of the amplified genomic regions of the quadruple deletion mutant of PAO1 compared to the wild-type strain, confirming that the deletions had been achieved in the desired location. The ladder used was the '1Kb ladder' from Promega 47

Figure 16: Absorbance readings of planktonic growth in LB media of *Pseudomonas aeruginosa* PAO1 and eSTK mutants over 24 hours to measure growth kinetics. There is no difference observed in the growth kinetics. Error bars show standard deviation 53

Figure 17: Absorbance readings of planktonic growth in LB media of *Pseudomonas aeruginosa* PA2192 and eSTK mutants over 24 hours to measure growth kinetics. There is an observable difference in the maximum turbidity of the sample for the YeaG mutant (b). The large standard deviation is possibly a result of mucoidy 'clumps' passing through the absorbance path at time of measuring. Error bars show standard deviation.....54

Figure 18: Absorbance readings from 96-well crystal violet staining assays to measure total biofilm formation of the *Pseudomonas aeruginosa* PAO1 strain and eSTK deletion mutants. No significant difference were observed. Error bars show standard deviation 56

Figure 19: Absorbance readings from 96-well crystal violet staining assays to measure total biofilm formation of the *Pseudomonas aeruginosa* PA2192 strain and eSTK deletion mutants. No significant differences were observed. Error bars show standard deviation 57

Figure 20: 3D render of the PDMS flow cell device used for growth of continuous culture biofilms. Media is flowed through at a rate of 5 µl per minute while the device is heated at 37^{o}C 58

Figure 21: Longitudinal IMARIS analysis showing the Live cell count compared to the dead cell count of *Pseudomonas aeruginosa* PAO1 WT and the mutant strains in biofilms produced under flow 58

Figure 22: IMARIS analysis showing the ratio of Dead:Live biomass for *Pseudomonas aeruginosa* PAO1 WT, QKO, and PpkA. P<0.05. Error bars show SEM.....59

Figure 23: Viable cell counts of 96-hour biofilms of PAO1 produced under flow show no significant difference despite seeing more dead cells in the biofilm of the QKO mutant under confocal. Error bars show standard deviations.....59

Figure 24: Confocal microscopy images of PAO1 biofilms attached to a PDMS surface and stained with BACLIGHT Live/Dead stain (Green = Live, Red = Dead). All images were taken from the outlet of the device. 60

Table of Figures

Figure 25: Confocal microscopy images of PA2192 biofilms attached to a PDMS surface and stained with BACLIGHT Live/Dead stain (Green = Live, Red = Dead). Highlighting the difference in matrix formation between the wild-type and the ΔYeaG mutant at 48 hours (left) and 96 hours (right). All images were taken from the outlet of the device 61

Figure 26: IMARIS analysis showing the mean fluorescent intensity values of 48-hour and 96-hour biofilms from the outlet of the device of the PA2192 wildtype and PA2192 ΔYeaG strain. Error bars show standard deviation 62

Figure 27: Differentiation down the channel of *Pseudomonas aeruginosa* PA01 biofilms on the PDMS flow cell at 96-hours. There appears to be increased differentiation with increased distance along the channel, likely due to reduced nutrient availability 63

Figure 28: Filamentation of the PpkA and QKO flow cell biofilms of PAO1. Filamentation is usually the result of a stressful environment and is hypothesised to be a mechanism for a cell to occupy as many niches as possible simultaneously 63

Figure 29: The antibiotic susceptibility to tobramycin of 96-hour QKO biofilms relative to the WT. There was no significant difference observed at any concentration of tobramycin despite seeing an increased amount of potentially membrane compromised cells in the QKO mutant. Error bars show standard deviation..... 64

Figure 30: Planktonic growth of lysine and arginine auxotrophic mutants in LB. The lysine auxotrophic mutant shows regular growth kinetics when compared to the wild type, however the arginine auxotroph shows a significantly increased death phase that is restored when additional L-arginine is added. Error bars shows standard deviaiton 76

Figure 31: Lysine + arginine double auxotrophic mutant 96-well crystal violet biofilm formation assay with exogenous 12mm L-arginine. A significant increase in biofilm formation is observed at all time points, likely due to increased growth of anaerobic parts of the biofilms. Error bars show standard deviation 77

Figure 32: Planktonic growth kinetics of PAO1 (WT) and the QKO deletion mutant with and without SHX in M9 growth media. Cessation of growth is induced in response to SHX treatment in both QKO and the wild type. Error bars show standard deviation..... 78

Figure 33: DirectDetect read outs of the protein and peptide concentrations to show that protein extraction and peptide purification had been successful. There is particularly large variation in the results of the phosphor-peptide purification. Error bars show standard deviation 79

Figure 34: Histograms of the Log_2 transformed and quantile normalised data of the biofilm, planktonic and SHX treated samples. They show a normal distribution confirming that a parametric t-test would be suitable for calculating significance 80

Figure 35: Principal component analysis by sample and mass spec run. This shows that the samples in each mass spec run are highly similar, but that there are large amounts of variation between runs on the mass spec 81

Figure 36: The total number of proteins identified by MaxQuant compared to the number of proteins found to be differentially expressed in each sample 82

Figure 37: Volcano plots showing the relative proportion of proteins that are not significant (grey), significant but don't meet the fold change cut-off (blue), not significant but meet the fold change cut-off (green), and are significant and meet the fold change cut-off (red).....83

Figure 38: The number of proteins linked to each pathway/network for the biofilm, planktonic and SHX treated planktonic samples. The red part of the bar corresponds to proteins that are downregulated in that pathway, and the blue to upregulated proteins 93

Figure 39: The workflow for Weighted gene co-expression analysis. Firstly, data are increased by a power determined by soft-thresholding, followed by identification of highly interconnected genes which are then linked to an external characteristic/trait96

Figure 40: Data adjusted by the R package COMBAT principal component analysis by strain shows that all batch effects have been removed and that the data is suitable to carry forward into the next step of the analysis.....97

Figure 41: Sample dendrogram and heatmap used to determine if there are any significant outlier samples that should be removed before performing the correlation analysis98

Figure 42: Soft thresholding (left) vs connectivity/interconnectedness (right). A soft thresholding power of 10 was selected in order to meet the minimum level of scale free

topology required for WGCNA analysis. The Mean connectivity graph shows that this substantially lowers the interconnectedness of the data set. 99

Figure 43: Cluster dendrogram of eigengenes produced using a signed Nowick TOM. The different colours represent clusters of co-expressed genes 100

Figure 44: Module-trait relationship heatmap of a signed Nowick network. The top number in the boxes show how strongly positively or negatively correlated the module is to the characteristic, with the bottom number showing how significant the correlation is. MEgreen, MEblack and MEblue are significantly correlated to the Mutant phenotype 101

Figure 45: MEblack proteins by number in each network/pathway. All pathways are negatively correlated with the mutant phenotype in this module 107

Figure 46: MEblue proteins by number in each network/pathway. All pathways are negatively correlated with the mutant phenotype in this module 112

Figure 47: MEgreen proteins by number in each network/pathway. All pathways are positively correlated with the mutant phenotype in this module 115

Figure 48: Pathway network analysis of phosphoproteins identified in the biofilm 119

Figure 49: Pathway network analysis of phosphoproteins identified in Planktonic culture 120

Figure 50: Unprocessed confocal images of PpkA (Top) and TKO (Bottom) Filamentation 133

Research Thesis: Declaration of Authorship

Print name:	Conor Patrick William Graham

Title of thesis:	The Role of Serine/Threonine Kinases in Translation Machinery Regulation and Antibiotic Susceptibility in Response to Nutrient Starvation in *Pseudomonas aeruginosa*

I declare that this thesis and the work presented in it are my own and has been generated by me as the result of my own original research.

I confirm that:

1. This work was done wholly or mainly while in candidature for a research degree at this University;
2. Where any part of this thesis has previously been submitted for a degree or any other qualification at this University or any other institution, this has been clearly stated;
3. Where I have consulted the published work of others, this is always clearly attributed;
4. Where I have quoted from the work of others, the source is always given. With the exception of such quotations, this thesis is entirely my own work;
5. I have acknowledged all main sources of help;
6. Where the thesis is based on work done by myself jointly with others, I have made clear exactly what was done by others and what I have contributed myself;
7. None of this work has been published before submission

Signature:		Date:	

Acknowledgements

I've had a lot of support and understanding from lots of people along the way, and I would like to thank them all for everything they have done. In particular, I would like to thank the whole microbiology group, my supervisor Professor Jeremy Webb and my parents whom this would not have been possible without.

Definitions and Abbreviations

EPS = Extracellular Polymeric Substances

ecDNA = Extracellular DNA

PMN = Polymorphonuclear leukocytes

RMF = Ribosome Hibernation Factors

HPF = Hibernation Promoting Factors

MBC = Minimum Bactericidal Concentration

MIC = Minimum Inhibitory Concentration

QS = Quorum Sensing

ppGpp = Guanaosine Tetraphosphate

TA = Toxin Anti-toxin

SHX = Serine Hydroxymate

Ppx = Exopolyphosphate

eSTK = Hanks type Serine/ Threonine Kinase

Gm cassette = Gentamicin Resistance Cassette

T6SS = Type VI secretion system

Chapter 1 **Introduction**

Biofilms were first discovered by Van Leeuwenhoek when examining the dental plaque on his own teeth in the 17th century. However, it wasn't until 1978 that biofilm theory was properly established. Investigations into marine ecosystems showed that bacteria are surrounded by polysaccharide fibres which allow them to tenaciously adhere to surfaces and form matrix enclosed biofilms that are very different to their planktonic counterparts (Costerton, Geesey and Cheng, 1978). Since this discovery over 40 years ago our appreciation and understanding of the nature, architecture and clinical relevance of biofilms has substantially increased, with research into anti-biofilm therapeutics being an area of intense research.

1.1 Hallmarks of a biofilm

Biofilm formation constitutes an alternative lifestyle that enables planktonic cells to assume a multicellular structure in which co-operation facilitates and prolongs survival in adverse environments (Kostakioti, Hadjifrangiskou and Hultgren, 2013).

1.1.1 Adhesion

The first step in the aggregation of these cells is surface attachment which can be further subdivided into three stages (Figure 1):

Formation of the conditioning layer:

Many inert surfaces such as glass or painted metal will not provide sufficient attachment surfaces for biofilm formation. However, a layer composed of many organic and inorganic particles present in a bulk fluid can settle onto a substrate. This layer favourably modifies the substrata for bacterial adhesion by providing greater scope for cellular interactions that will result in adhesion (Hermansson, 1999; O'Toole, Kaplan and Kolter, 2000; Tolker-Nielsen, 2015).

Reversible adhesion:

Initially, planktonic cells move from the liquid media to the attachment surface by physical forces or bacterial appendages such as flagella. A small portion of these cells reversibly adsorb to the surface (Hermansson, 1999; O'Toole, Kaplan and Kolter, 2000; Tolker-Nielsen, 2015). (Marshall, Stout and Mitchell, 1971) described reversible adhesion of bacteria to a surface as a balance of repulsive forces and attractive van der Waals forces. Together these can be called the DVLO forces.

Irreversible adhesion:

The switch from reversible to irreversible adhesion is considered a time dependent process. This was shown by (Marshall, Stout and Mitchell, 1971), who reasoned this was due to the production of polymeric bridges between the bacteria and the surface. They observed that polymeric fibrils were made by an irreversibly adhered *Pseudomonas* strain.

This study was further proved by (O'Toole and Kolter, 1998) who used genetic analysis, and knock-out strains of *Pseudomonas fluorescens,* to identify the pathways involved in biofilm development. One process found to be important is protein synthesis. Inhibiting this pathway by using tetracycline to inhibit the ribosome caused biofilm formation to decrease but did not reduce planktonic cell viability. This effect can only be seen during biofilm development, as treating a fully established biofilm with tetracycline shows no consequence. Thus, providing evidence that the bacterial interaction with a surface requires protein synthesis.

To find out whether the newly synthesised proteins were extracytoplasmic, the protease Pronase E was used. A significant decrease in attached cells was observed in the presence of Pronase E, and again there was no effect on planktonic viability. This suggests that extracytoplasmic proteins are involved in bacterial attachment. (O'Toole and Kolter, 1998).

1.1.2 Binary population growth and matrix formation

After adhesion, binary population growth occurs and genes that promote sessility are upregulated. This includes genes that are responsible for the formation of the extracellular matrix that surrounds the population leading to the definition of a biofilm, “Matrixenclosed microbial populations that adhere to each other and to surfaces or interfaces” (Prigent-Combaret *et al.*, 1999) (Figure 1).

1.1.3 Dispersal

Biofilm dispersal provides a mechanism for escape as the biofilm matures and a planktonic lifestyle becomes more advantageous. In many biofilms, including *P. aeruginosa* biofilms, c-di-GMP acts as a nutrient sensor and has been extensively implicated in the shift between sessility and motility. Generally, an increase in c-di-GMP promotes sessility and a decrease promotes motility (Barraud et al., 2009), usually in response to fluctuating levels of carbon and nitrogen

sources (Sauer et al., 2002). *P. aeruginosa* has a plethora of other mechanisms that contribute to biofilm dispersal, namely alginate lyase production for degradation of the EPS, increased rhamnolipid/surfactant production and programmed cell death which creates a void that aids dispersal (Kostakioti, Hadjifrangiskou and Hultgren, 2013 2003). The dispersed planktonic cells ultimately reinitiate the process of biofilm formation when they encounter a suitable environment, resulting in an overall biofilm population that will be more likely to survive an unfavourable change in environmental conditions (Kostakioti, Hadjifrangiskou and Hultgren, 2013) (Figure 1).

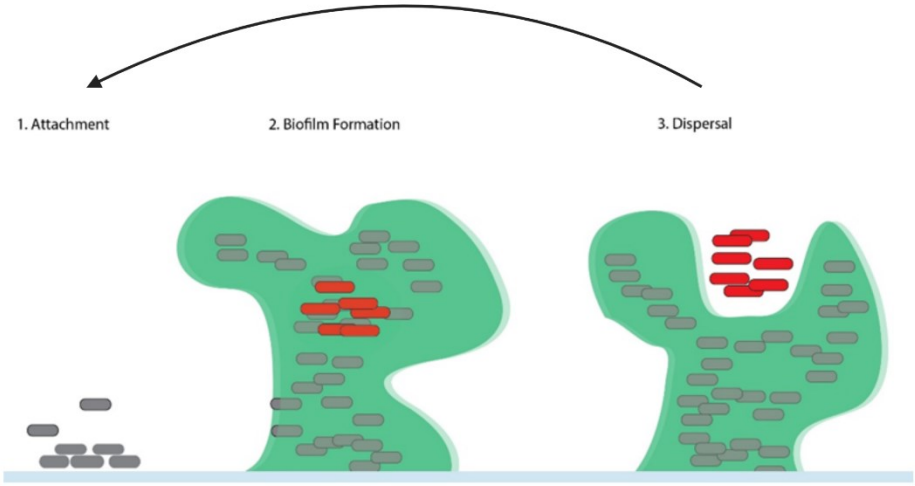

Figure 1: The life cycle of a biofilm. Firstly, the bacterial cells adhere to the surface. This is followed by population growth and biofilm formation, resulting in nutrient fluctuations that trigger dispersal pathways in some cells (Red cells). Lastly, the small group of cells break out of the biofilm and disperse. The cycle would then repeat resulting in diversification and microcolony formation.

1.1.4 Characteristics of the EPS

Bacteria in a biofilm only make up about 10% of the mass, the other 90% is contributed by extracellular polymeric substances (EPS) produced by the bacteria (Flemming and Wingender, 2010). The exact composition of the EPS varies with the species of bacteria and environmental conditions, resulting in differing biofilm phenotypes. However, the EPS of a biofilm is usually a mixture of polysaccharides, extracellular DNA (ecDNA), and proteins. These components contribute to the overall structure and tolerance of biofilms (Wei and Ma, 2013). In *P. aeruginosa*

in vitro it results in the formation of mushroom-like microcolonies protruding out of the biofilm surface. This is thought to allow nutrients to reach more of the biofilm (Flemming and Wingender, 2010).

A study by Davies and colleagues in 1998 revealed how important the biofilm matrix is for its inherent tolerance. They performed an experiment which knocked out genes required for the las quorum sensing network, implicated in the upregulation of genes required for biofilm formation. They found that the signalling mutant formed flat, undifferentiated biofilms, due to issues in formation of the extracellular matrix. In fact, they shared physiology to that of their planktonic counterparts, and as a result were significantly more susceptible to the surfactant sodium dodecyl sulphate (Sauer et al., 2002). No conclusions were drawn about this at the time, but more recent studies attributed the lack of ecDNA release, and therefore reduced mechanical protection from harmful compounds, as a potential reason for susceptibility (Allesen-Holm et al., 2006).

Another critical aspect of biofilm EPS is the production of virulence factors that interfere with the host innate immune response. In particular, rhamnolipid production via the Rhl quorum sensing network has been shown to cause necrotic death of polymorphonuclear leukocytes (PMN's) in vitro. In 2009, Van Gennip et al induced an inactivating mutation in the quorum sensing controlled gene rhlA, usually responsible for rhamnolipid production. They found that the inactivating mutation resulted in severely inhibited rhamnolipid production, reduced necrosis of PMN's in vitro, and increased clearance in comparison to the wild type in vivo (Van Gennip et al., 2009).

Furthermore, the EPS immobilises biofilm cells allowing rapid and strong cell-cell communication, providing a mechanism for the cells in the biofilm to synchronise behaviours in response to environmental stimuli, and a high level of DNA exchange/ conjugation, increasing the spread of antibiotic resistance and other useful genes. This ultimately serves to benefit the population (Flemming and Wingender, 2010). The matrix also contributes towards different cellular phenotypes as a result of differing nutrient availability. Rapidly proliferating cells at the edge of the biofilm will receive more nutrients than the metabolically less active cells in the centre (Macia, Rojo-Molinero and Oliver, 2014). The idea that bacteria grow preferentially in a matrix enclosed biofilm was not immediately accepted, however, more advanced imaging techniques such as confocal microscopy soon revealed the clinical importance of biofilms. Biofilms were found to be a cause of persistent/chronic infection and occur commonly on inert and biological surfaces (Costerton, Stewart and Greenberg, 1999 1998). For this reason, biofilm related nosocomial infections in American hospitals alone account for an estimated 1.7 million infections and 99,000 associated deaths each year:

- 32% of all healthcare-associated infection are urinary tract infections

- 22% are surgical site infections
- 15% are lung infections
- 14% bloodstream infections (Klevens et al., 2007).

1.2 Chemical gradients and physiological heterogeneity in biofilms contribute to multi-drug tolerance and persistence

It is well established that cells in a biofilm are physiologically different to their planktonic counter parts, and that most biofilms consist of microcolonies with an EPS that contributes to a structurally complex, channelled architecture that is thought to allow nutrients to reach the whole biofilm. Despite this, mature biofilms contain concentration gradients of both metabolic substrates and products (Figure 2), and also have noticeably different proteomes to their planktonic counter parts (Sauer et al., 2002; Stewart et al., 2015; Wood, Knabel and Kwan, 2013).

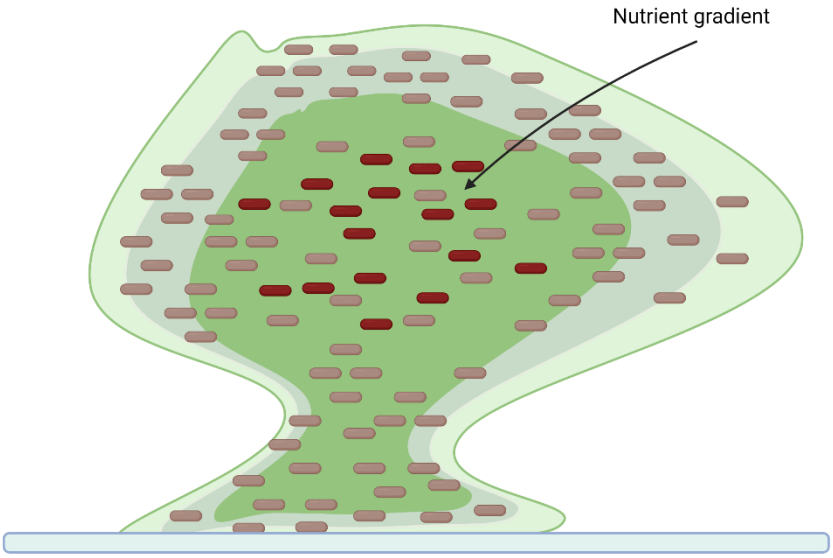

Figure 2: Bacteria encased in a biofilm, where the grey cells are metabolically active and red cells are metabolically inactive. The change in colour from the outer edge to the centre simulates the chemical gradient caused by rapidly proliferating cells on the outer edge of the biofilm

The efficacy of antimicrobials in vitro is rarely representative of the efficacy in vivo. Numerous studies indicate that environmental conditions that lead to nutrient starvation could be responsible for this marked difference in susceptibility (Field et al., 2005; Hill et al., 2005; King et al., 2010). A leading hypothesis is that nutrient deprivation leads to reduced metabolic activity,

which in turn inactivates many processes such as translation, transcription and cell wall synthesis that are targeted by antibiotics.

1.2.1 Biofilm induced hypoxia

Cells in bacterial biofilms are often starved of nutrients due to the rapidly proliferating, and therefore rapidly metabolising, cells on the outer edge of the biofilm preventing effective nutrient penetration into the centre of the biofilm (Figure 2). This creates a nutrient gradient that leads to a well characterised state of nutrient deprivation (Nguyen et al., 2011). Oxygen depletion in biofilms is by far the most studied, and there have now been numerous reports showing the effect of this in vitro (King et al., 2010; Field et al., 2005; Hill et al., 2005).

A study by Boriello and colleagues showed that *P. aeruginosa* in 48 hour old biofilms were incompletely killed when exposed to tobramycin, ciprofloxacin, carbenicillin, ceftazidime, chloramphenicol or tetracycline for 12 hours. Using oxygen microelectrodes, it was shown that the biofilms contained large anoxic regions, and that oxygen only penetrated roughly 50 µm into a 210 µm thick biofilm. Furthermore, the regions of active protein synthesis were visualised using an inducible GFP protein. They found that the regions of active protein synthesis only extended roughly 30 µm deep into the biofilm from its interface with the air. Interestingly, the tolerance to antibiotics was only found to exist in 48h-old biofilms, with 4 hour, mostly aerobic biofilms still being susceptible (Borriello et al., 2006). It could be argued, that poor antibiotic penetration was a leading contributor to this tolerance, rather than nutrient limitation and metabolic inactivity. However, a similar article showed that there was no acceleration in killing in *P. aeruginosa* biofilms treated with tobramycin and ciprofloxacin, even after antibiotic penetration. This was determined by a diffusion cell bioassay, and oxygen limitation was again correlated with antibiotic tolerance (Walters et al., 2003) showing the significance of gradients in biofilms.

A recent study by Williamson et al showed that ribosome hibernation factors (RMF) are upregulated in slow growing, antibiotic tolerant sub populations of PA biofilms in response to hypoxia. This was done via microarray analysis of the transcriptome of isolated biofilm subpopulations. It was demonstrated that cells at the top of the biofilm i.e. nutrient wealthy, had high mRNA abundances for genes involved in general metabolic functions, while the mRNA abundance of housekeeping proteins were much lower at the bottom of the biofilm. Interestingly, ribosomal rRNAs were abundant throughout the biofilm, but were inactivated in the anoxic/ tolerant subpopulations. This is likely due to their inhibition via the RMF's and hibernation promoting factors (HPF), which are upregulated in this group (Williamson et al., 2012). RMF's ultimately inhibit binding at the ribosomal A-site, whereas HPF's cause the dimerization of

ribosomes into an inactive state. Critically, they only act on non-translating ribosomes, allowing for the present round of translation to finish (Polikanov, Blaha and Steitz, 2012). Another study showed that a minimum number of functional ribosomes is required for resuscitation of the slow growing, tolerant populations. This was found to require the hibernation promoting factor PA4463 in *P. aeruginosa*, which preserves ribosomes (Akiyama et al., 2017).

1.2.2 Amino acid and carbon starvation in antibiotic tolerance

While oxygen depletion is clearly a factor in physiological heterogeneity, there are also other well characterised mechanisms of heterogeneity correlated with depletion of other nutrients. One of the best characterised is amino acid/ carbon starvation and the stringent response (Figure 3).

An experiment designed by Bernier et al used Escherichia coli auxotroph mutants unable to synthesise the amino acids leucine, cysteine and lysine. The auxotrophic mutants were isolated from tolerant subpopulations of *E. coli* biofilms and showed significantly greater survival and recalcitrance than their wild type counter parts when treated with ofloxacin and ticarcillin in media lacking the amino acid they were deficient in. Furthermore, the susceptibility of the mutants was restored when grown in LB media supplemented with the amino acid that the *E. coli* was unable to synthesise, highlighting the importance of nutrient deprivation. Ofloxacin is a second-generation quinolone that works by inhibiting DNA gyrase, halting DNA replication, and leading to cell death. This is interesting as cells do not need to be metabolically active to be targeted, suggesting that a specific mechanism, rather than growth arrest is responsible.

Further experimentation by Bernier et al revealed that in addition to the stringent response, the SOS response is invoked upon nutrient starvation and is indispensable for ofloxacin tolerance (Bernier et al., 2013). However, they were unable to identify the specific genes/ proteins that contributed to this tolerance. The SOS response was first observed in starved *E. coli* cells, which implies a link between the SOS response, cellular metabolism and cellular adaptation (Erill, Campoy and Barbe, 2007). The SOS response is induced upon DNA breakage when RecA-dependent cleavage of the SOS gene repressor LexA occurs. This allows the transcription of roughly 40 genes that co-ordinate multiple cellular processes that include DNA repair and cell division arrest (Erill et al., 2016).

Another more recent study by Kwan et al mimicked the role of cellular inhibition of certain processes in *E. coli* such as, i) Transcription, by pre-treating with rifampin which inhibits mRNA synthesis by binding and inactivating RNA polymerase ii) Translation, by pre-treating with tetracycline and iii) ATP synthesis by pre-treating with carbonyl cyanide 3-chlorophenylhydrazone.

All of these treatments showed a significant increase (1000 – 10,000 fold) in persistence to ciprofloxacin and ampicillin over untreated cultures (Kwan et al., 2013).

The mechanisms above along with the fact that spontaneous, stochastic formation of persister cells is extremely rare (Balaban et al., 2004; Kwan et al., 2013) demonstrate the importance of environmental stresses in leading to enhanced antibiotic tolerance and persistence.

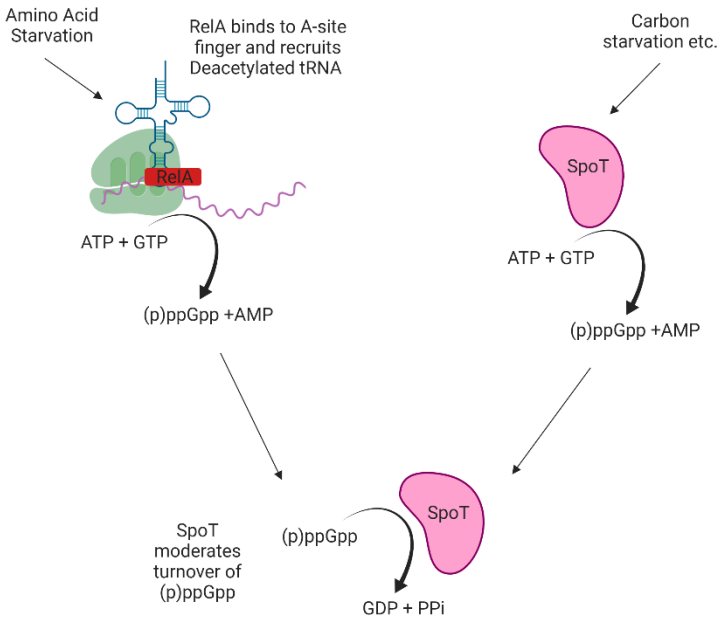

Figure 3: (p)ppGpp induction in response to nutrient starvation. RelA is activated when a deacetylated tRNA binds to the ribosome and results in (p)ppGpp production, whereas, (p)ppGpp production as a result of other stressers is controlled by SpoT

1.3 Persister cells

The mechanisms above show the potential importance of environmental stresses, and the ability of bacteria to adapt to these stresses, in multidrug tolerance and persister formation. These cells were first observed in 1944 by Joseph Bigger when penicillin would not sterilize flask cultures of *Staphylococcus aureus*, instead 1% of the cells would remain and repopulate the flask. These cells were aptly named persisters (Bigger, 1944).

1.3.1 Defining a persister cell: A historical perspective

The persister phenomenon has been poorly defined for a long time, however, the field is now coming to a consensus on what a persister cell is and isn't(Wood, Knabel and Kwan, 2013; Wood, Song and Yamasaki, 2019; Brauner et al., 2016).

Originally, the general consensus was that persistence existed as cells that were either not growing or were growing very slowly (Brauner et al., 2016; Balaban et al., 2004). This was when Balaban et al coined the term type I and type II persisters, where type I were not growing and type II were slow growing (Balaban et al., 2004).

This theory was accepted for a long time, and led to the study of the mechanisms of slow growing cells to help study persistence (Kim and Wood, 2017). However, type II persister cells were obtained after several treatments of cells with ampicillin, had an inherited phenotype, and were growing before addition of antibiotics (Balaban et al., 2004). This is in direct contradiction of two of the key hallmarks of a persister cell, they must not have an inherited phenotype and must be dormant. This confusion on exactly what a persister is has led to the publication of studies that have thought they were studying persisters, but in fact were studying tolerant, slow growing cells (Kim and Wood, 2017). However, a more unified stance on exactly what a persister is has now been obtained (Kim and Wood, 2017; Kim et al., 2018; Wood, Song and Yamasaki, 2019). A persister cell must be dormant, must not have an inherited phenotype, and must be able to be resuscitated (Wood, Song and Yamasaki, 2019). This has also lead to a set of "Guidelines" published by Kim and Wood (Kim and Wood, 2017) that should be adhered to when directly studying persister cells:

- The number of putative tolerant cells should not increase prior to antibiotic treatment and should not change rapidly during treatment.
- The number of putative tolerant cells should be measured above the MIC, ensuring that the cell number does not change as a function of antibiotic concentration.
- The number of putative persister cells should not be increasing in the absence of antibiotics and nutrients.
- At no point should the putative persister cells come into contact with a high nutrient medium that will cause them to resuscitate (Kim and Wood, 2017).Hopefully these new guidelines, along with a unified consensus on what a persister is, will allow for the accurate study of potential mechanisms leading to their formation.

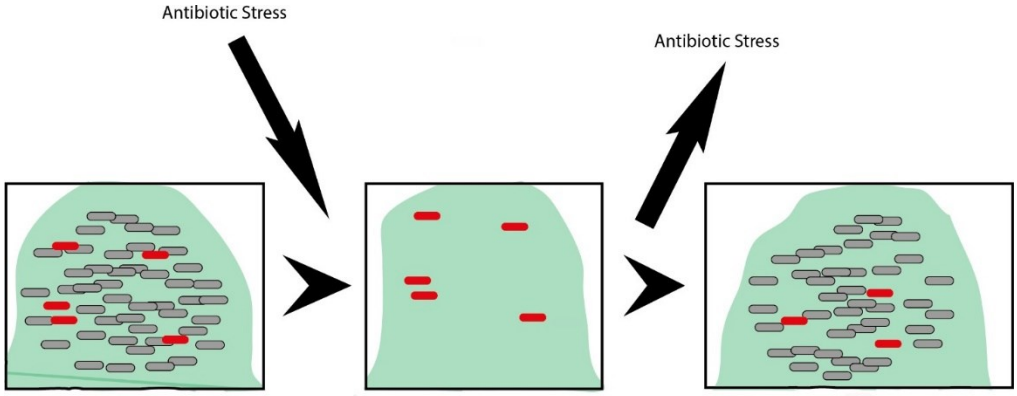

Figure 4: A bacterial biofilm where grey cells are metabolically active and red cells are metabolically inactive (Persisters). Treatment with antibiotic results in only tolerant persisters remaining, which then become metabolically active and repopulate when the stress is removed. Upon repopulation, different cells may become persisters.

1.4 The role of the stringent response and toxin anti-toxin systems in translation inhibition

Before talking about the potential genes and mechanisms involved in persister formation as a result of nutrient deprivation, it is important to understand the transcriptome of a cell during the stringent response.

A study by Durfee and colleagues induced the stringent response in a wild type strain of *E. coli* K12 and a RelA mutant using the compound, serine hydroxamate (SHX), which inhibits serine-tRNA synthetase and therefore mimics amino acid starvation. This revealed that almost 500 genes were differentially expressed as a result of the stringent response. Interestingly, more genes were up-regulated than down-regulated. Among the up-regulated genes were Toxins of TA systems and exopolyphosphate (Ppx), which activates Lon protease (Durfee et al., 2008).

Lon protease is essential to TA system mediated induction of the stringent response as it degrades anti-toxins e.g. RelB of the RelEB TA module, and free ribosome proteins. This leads to activation of the auto-toxic toxins of the TA modules and protein synthesis inhibition. Furthermore, activation of ribosome dependent mRNA endonucleases, such as RelE, rescues ribosomes from stalling, critical during amino acid starvation (Durfee et al., 2008).

TA systems are small genetic elements composed of a toxin gene and its cognate antitoxin. These systems are grouped into five classes, depending on their interaction with its anti-toxin. The most well studied, and most relevant TA systems to this project are Type II TA systems. Within this class both the toxin and the anti-toxin are small proteins that form a neutral protein-protein complex. The toxin is usually more stable, but the anti-toxin is produced at a much greater rate. When the

cells environment changes e.g. nutrient deprivation, the anti-toxin is rapidly degraded by Clp or Lon proteases, allowing the toxin to act on its cellular target (Unterholzner, Poppenberger and Rozhon, 2013). Interestingly, studies have shown that TA systems very effectively induce a non-growing state from which cells can easily be resuscitated by addition of the cognate anti-toxin, showing that they could be extremely relevant in persister formation and multi-drug tolerance (Maisonneuve and Gerdes, 2014).

Type II TA systems are known to have an effect on a variety of cellular targets, these include DNA replication machinery, mRNA, tRNA, 30S ribosomes, 50S ribosomes and cytoskeletal proteins. Interestingly, mRNA is the most frequent target in *E. coli*, possibly due to the fact that inhibition of protein synthesis at the mRNA level is arguably less severe than direct inhibition of a protein. As these proteins cleave cellular mRNAs, they are termed mRNA interferases. These can then be further classified into ribosome-dependent or ribosome independent mRNA interferases (Maisonneuve et al., 2011; Maisonneuve, Castro-Camargo and Gerdes, 2013; Yamaguchi and Inouye, 2011).

1.4.1 Ribosome-independent mRNA interferases

Ribosome-independent mRNA interferases, like their name's sake, cleave free floating mRNA independently of any translation machinery. The MazF, ChpBK, MqsR, YhaV, HicA and RnlA TA systems all fall into this category, however the MazF system is by far the best characterised (Yamaguchi and Inouye, 2011). In the MazF system, ppGpp results in the activation of Lon or Clp protease which ultimately breaks down the anti-toxin MazE. MazF is then activated and able to cleave single strands of mRNA specifically at ACA sites and halt protein synthesis (Zhang et al., 2003). Interestingly, rRNAs and tRNAs are protected from MazF by ribosomal proteins and secondary structures (Yamaguchi and Inouye, 2011).

1.4.2 Ribosome-dependent mRNA interferases

Ribosome-dependent mRNA interferases associate with mRNAs at the ribosomal A-site ultimately resulting in cleavage. The RelE, YoeB, YafQ, YafO and HigA TA systems are all part of this sub group, with RelE being the most characterised (Yamaguchi and Inouye, 2011).

The RelEB TA system consists of the RelE toxin and its cognate anti-toxin RelB. RelE itself has no endoribonuclease activity, however it is thought to activate the endogenous ribonuclease activity of ribosomes and preferentially cleaves mRNA encoding stop codons at the ribosomal A-site (Starosta et al., 2014). RelE has been shown to act on its cellular target in response to nutritional stress, due to the degradation of the anti-toxin by Lon protease (Christensen et al., 2001).

1.4.3 Other TA systems

Another TA system, HipAB, was originally thought to phosphorylate Elongation FactorTu (EF-Tu) causing inhibition of translation (Schumacher et al., 2009). This conclusion was made using in vitro experimentation by cloning both genes into an expression vector and using mass spec to determine if phosphorylation had occurred. However, recent evidence has suggested this may not be the only mechanism by which HipA induces stasis. GltX, an aminoacyl-tRNA synthetase that catalyses the transfer of glutamate to tRNA, prepares or "charges" Glutamyl tRNA for translation. HipA was found to phosphorylate a serine residue on Gltx and therefore induce strong inhibition of translation and induction of ppGpp. This mechanism was confirmed by adding saturating amounts of GltX to cells over expressing HipA, significantly reducing the toxicity (Germain et al., 2013).

Interestingly, there is a TA system that uses phosphorylation of EF-Tu as a mechanism of translation inhibition. The prophage P1 of *E. coli* encodes doc toxin of the doc-phd TA system and was originally thought to block the ribosomal A-site (Liu et al., 2008b).

However, later studies showed that doc phosphorylates a highly conserved threonine residue (Thr-382) on EF-Tu in *E. coli* which is critical for function. This inhibits the formation of the EF-Tu:GTP:tRNA complex and therefore induces stasis (Castro-Roa et al., 2013; Cruz et al., 2014).

While TA systems can clearly result in cellular stasis, they are mostly found in clinical strains and are likely the result of evolutionary selection and advantage. Bacteria lacking TA operons almost certainly still need to tightly regulate their rate of protein synthesis, suggesting undiscovered, alternative mechanisms to the ones above exist. This was further demonstrated when a hipAB deletion mutant did not result in the reduction of persister cell formation (Korch, Henderson and Hill, 2003).

1.4.4 Controversy surrounding Toxin Antitoxin Systems

A study by Maisonneuve et al revealed that TA operon transcription was turned on in a stochastic manner at low frequencies in exponentially growing *E. coli* cells. The frequency at which this occurred was similar to the frequency of persister formation in *E. coli*. With this information they concluded that TA systems are the final effectors of bacterial persister formation (Maisonneuve, Castro-Camargo and Gerdes, 2013). However, this study has sparked controversy with issues in reproducibility, and does not fit in with other recent debates in the field. The authors used their previous work as a model to critically examine common experimental procedures in an attempt to overcome the inconsistencies in results produced by other laboratories. The results showed that

seemingly simple assays are very sensitive to alterations in culture conditions and growth phase. Furthermore, and most importantly, the *E. coli* strain being used in the study was found to be infected by bacteriophage 80. Lysogenisation of this bacteriophage was shown to be the cause of many of the phenotypes reported in this study, in particular, the role of TA modules in *E. coli* persister formation under unstressed conditions i.e. stochastic induction of TA modules was no longer supported. The importance of ppGpp and Lon (Which degrades antitoxins of toxin antitoxin modules) are still supported (Harms et al., 2017).

1.5 The mechanisms and advantages of eukaryotic translation inhibition in response to cellular stress in the tumour microenvironment

The studies mentioned earlier serve to show the critical importance of elucidating the biochemical mechanisms by which biofilm induced nutrient deprivation can lead to persister formation in bacteria. While biofilms are exclusive to bacteria, there are other examples of acute nutrient deprivation in response to poor nutrient utilisation, such as the often nutrient deprived and hypoxic tumour microenvironment (Leprivier et al., 2015). Translational regulation in nutrient deprived tumour cells is well characterised, and the mechanisms employed may provide an insight into similar and conserved mechanisms in bacteria.

The tumour microenvironment and a biofilm are homologous in the sense that rapidly proliferating cells can result in severe nutrient deprivation and acute hypoxia, necessitating the tight and rapid regulation of energy consuming processes such as protein synthesis. There are a plethora of mechanisms that tumour cells utilise to regulate their translation in response to nutrient deprivation, and range from selectively translating certain mRNA transcripts, to direct inhibition of translation machinery (Leprivier et al., 2013; Leprivier et al., 2015; Koromilas, 2015). The direct inhibition of translation machinery is primarily controlled by four different Serine/ Threonine kinases; PERK, HRI, Gcn2 and eEF2k. PERK, HRI and Gcn2 all act on eIF-2, while eEF2k inhibits eEF-2. Briefly, PERK has been found to be activated as a result of reactive oxygen species (ROS) and the unfolded protein response (UPR), HRI is activated as result of oxidative stress, Gcn2 is directly activated by uncharged tRNA and eEF2k by severe nutrient deprivation.

1.5.1 Direct inhibition of translation machinery

Hypoxia in the tumour microenvironment is commonplace and must be managed for the tumour to progress. Hypoxia exerts a selective pressure on the tumour cells, favouring the emergence of hypoxia-resistant, and therefore chemo and radio-therapy resistance (Hochachka et al., 1996;

Thomas, 1996; Leprivier et al., 2015). Overall translation inhibition is primarily at the initiation stage, and is facilitated by the phosphorylation of eukaryotic initiation factor two alpha (eIF2) by PERK. This prevents the recruitment of methionyl-initiator tRNA to the 40S subunit of the ribosome. Under severe hypoxia eIF2 is phosphorylated extremely rapidly (less than 1 hour) (Koritzinsky et al., 2006). PERK is a type I trans-membrane protein that is usually associated with the UPR and acts as a quality control mechanism (Chakrabarti, Chen and Varner, 2011). The PERK-eIF2 pathway is thought to be induced by ROS created during hypoxia. Indeed, treatment of hypoxic cells with antioxidants resulted in the inhibition of this pathway (Liu et al., 2008a). In addition to this pathway, the eEF2k-eEF-2 pathway is strongly induced under hypoxia, leading to the inactivation of eEF-2 and inhibition of translation elongation (Connolly et al., 2006).

Nutrient deprivation is also a major contributor to global translation arrest and a key component of tumour expansion. Usually, nutrient deprivation acts as barrier against tumour development, as oncogenic mutations dramatically sensitise them to this. This is due in part to the inability of oncogenic cells to restrict anabolic processes or upregulate catabolic processes in nutrient deprived environments (Buzzai et al., 2005; Leprivier et al., 2015). A relatively recent paper by Leprivier and colleagues showed that the eukaryotic elongation factor two (eEF-2) is phosphorylated by eukaryotic elongation factor two kinase (eEF-2k) in severely nutrient starved tumour cells. In a murine model this ultimately resulted in translation elongation inhibition and therefore halting of protein synthesis, protecting the cells against starvation stress (Leprivier et al., 2013). Additionally, Leprivier and colleagues determined that HeLa cells (the first successfully cloned human cell line frequently used in research today) that were knocked down for eEF-2 showed reduced cell death in comparison to siRNA controls under nutrient deprivation, and that over expression of eEF-2k increased HeLa cell survival. Furthermore, it was reported that increased expression of eEF-2k correlated with a reduced survival rate in glioma.

Arguably the most interesting part of the study by Lepriver et al was that *Caenorhabditis elegans* deficient in efk-1, an eEF-2k orthologue, had a markedly reduced life span compared to the wild type in a low nutrient environment. This ultimately serves to show that elongation factor inhibition may be a highly conserved mechanism.

Gcn2 is another Serine/ Threonine kinase that phosphorylates and inactivates eIF2. Gcn2 is directly activated by uncharged tRNA i.e. tRNA without an attached amino acid, allowing the tight regulation of translation during amino acid stress (Leprivier et al., 2015; Castilho et al., 2014). This mechanism is absolutely conserved in eukaryotes and is found to provide tumours with a protective effect against amino acid starvation. The targeted disruption of Gcn2 and eIF-2

inhibition was found to severely compromise cell survival (Ye et al., 2010). Furthermore, Gcn2 inhibition was shown to prevent growth of tumour xenografts in immunocompromised mice.

The action of many anti-cancer drugs and antibiotics involve the induction of oxidative stress (Belenky et al., 2015). In cancer, the build-up of damaged biomolecules can then lead to the activation of the apoptotic pathway, or the production of antioxidants by p53 (Zhu et al., 2009; Levine, 1997). Tumour cells can hijack this mechanism to protect against oxidative stress, and therefore chemo therapeutics (Rotblat et al., 2013). Upon oxidative stress HRI is activated and phosphorylates eIF2, resulting in global translation arrest and a protective effect. Indeed, deletion of HRI dramatically compromises the survival of tumour cells under Arsenite exposure (McEwen et al., 2005).

Another critical step is the inactivation of mTORC1 (Leprivier et al., 2015). mTOR is a catalytic subunit of the TOR complex and functions as a Serine/ Threonine protein kinase. The mTOR subunit is further composed of two subunits mTORC1 and mTORC2, which are defined by their regulatory unit RAPTOR or RICTOR respectively (Zoncu, Efeyan and Sabatini, 2011). mTORC1 promotes cap-dependent translation initiation by preventing the inhibition of eIF4E, furthermore, it acts a nutrient sensing subunit that becomes inhibited by AMPK (Or other mechanisms) during severe hypoxia, nutrient deprivation and genotoxic stress. AMPK is activated during many cellular stress responses, however, the most well characterised mechanism of activation is by the relative ratios of AMP:ATP and ADP:ATP. This provides a very intimate link between cellular stress and global translation inhibition (Leprivier et al., 2015).

1.5.2 Selective mRNA translation

The inhibition of eIF2 and mTORC1 inhibits cap-dependent translation, promoting cap independent (eIF5B) and therefore, selective mRNA translation.

The advantages of these mechanisms is clear, phosphorylation is a robust and rapid method of inhibiting global translation. Allowing the cell to quickly adapt to unfavourable conditions promoting survival, not unlike the role of persister formation in biofilms. Therapeutically, targeting these mechanisms would be very attractive, and could result in improved clearance of cancerous cells. If similar mechanisms existed in prokaryotes, targeting these mechanisms could reduce persister formation, improve treatment and ultimately quality of life.

1.6 Bacterial and eukaryotic translation: a comparison

Before determining whether a mechanism similar to the ones above may exist in bacteria, it is necessary to compare the mechanistic themes involved in translation of mRNA in both eukaryotes and bacteria.

1.6.1 Initiation

Initiation involves a significantly more complex mechanism in eukaryotes and archaea than it does in bacteria, however, there are similarities between them. Both bacteria and eukaryotes use AUG as the initiating codon. However, while bacteria use the addition of a formyl group to determine between initiating methyl tRNA and internal methyl tRNA, eukaryotes usually just use the AUG codon closest to the 5' end of the mRNA sequence. Eukaryotic mRNA usually only has one start site, and is therefore likely to only code for one protein (monocistronic). Whereas bacterial mRNA may contain multiple start sites, allowing for the simultaneous coding of many different proteins (Polycistronic) Lac operon *E. coli*. The way initiation codons are identified is also different in bacteria, a specific sequence called a Shine-Delgarno sequence (after the discoverers) aligns the mRNA via specific base pairing near the 3' terminus of 16S rRNA. Contrasting to most eukaryotic mRNAs that have a ribosome binding 7-methylguanosine cap at their 5' terminus, where the ribosome then scans from to find a start codon. This is consistent with the polycistronic and monocistronic nature of the translation machinery. Briefly, translation initiation in bacteria involves:

- The binding of three initiation factors to the 30S subunit; IF-1, IF-2 and IF-3
- The initiator F-met tRNA sequence binding to IF-2 associated with GTP, and the release of IF-3 to allow the recruitment of the 50S subunit
- This then triggers the hydrolysis of GTP bound to IF-2, resulting in the dissociation of IF-1 and IF-2 (Bound to GDP). The ribosome is now prepared for the elongation stage of translation

Translation initiation in eukaryotes requires a minimum of ten initiation factors and is therefore significantly more involved. In summary:

- The eukaryotic initiation factors eIF-1, eIF1A and eIF-3 bind to the 40S sub unit
- eIF-2 associates with the initiator methionyl tRNA
- The eIF-4 group of initiation factors recognise the 5' cap of the mRNA and recruit it to the 40S subunit.

- The 40S subunit (With eIF's attached) then scan the mRNA for an AUG initiation codon. When this is located, eIF-5A triggers the hydrolysis of eIF-2:GTP to eIF2:GDP, resulting in the release of the initiation factors and the binding of the 60S subunit to create the 80S complex.

In terms of functionality, only eIF-2 and IF-2 have similar roles in initiation of translation. Which is interesting considering IF-2 has greater homology to eIF5B (That helps to join the two ribosomal subunits together) than to eIF-2 (Lee et al., 2002). For a side-by-side comparison see Table 1.

Table 1: Comparison between Bacterial and Eukaryotic translation initiation

BACTERIA	EUKARYOTES
Three initiation factors bind to the 30s subunit: IF-1, IF-2 and IF-3	Initiation factors eIF-1, eIF1A and eIF-3 bind to the 40S subunit
The initiator F-met tRNA sequence binds to IF-2 associated with GTP	eIF-2 associates with the initiator methionyl tRNA
IF-3 is released to allow the recruitment of the 50s subunit	The eIF-4 group of initiation factors recognise the 5' cap of the mRNA and recruit it to the 40S subunit
This triggers the hydrolysis of GTP bound to IF-2	The 40S subunit (With eIF's attached) then scan the mRNA for an AUG initiation codon.
This results in the dissociation of IF-1 and IF-2 (bound to GDP).	eIF-5A triggers the hydrolysis of eIF-2:GTP to eIF-2:GDP
	The Initiation factors are released
	The 60S subunit binds to create the 80S complex.

1.6.2 Elongation

The elongation step of translation is highly similar between bacteria and eukaryotes (Figure 5):

- Firstly, EF-Tu in bacteria or eEF-1 in eukaryotes complexed with GTP binds to the aminoacyl tRNA and escorts it the ribosomal A-site
- The GTP is then hydrolysed to GDP, causing EF-Tu/eEF-1 to dissociate and facilitate the translocation of the aminoacyl tRNA to the ribosomal P-site. The hydrolysis of GTP to GDP is the rate limiting step in translation elongation, and provides a period of time for incorrectly, and therefore weakly associated tRNA to dissociate from the ribosome. Making this step critical for translation accuracy.
- The next step is translocation of the now uncharged tRNA to the ribosomal E-site for ejection. This requires either eEF-2 in eukaryotes or EF-G in bacteria coupled with GTP. EF-G binds to the 30s subunit of the ribosome and results in hydrolysis of GTP to GDP, facilitating the translocation of the tRNA to the E-site, and movement of three new nucleotides into the ribosomal A-site, ready for another round of translation elongation (Cooper, 2000).

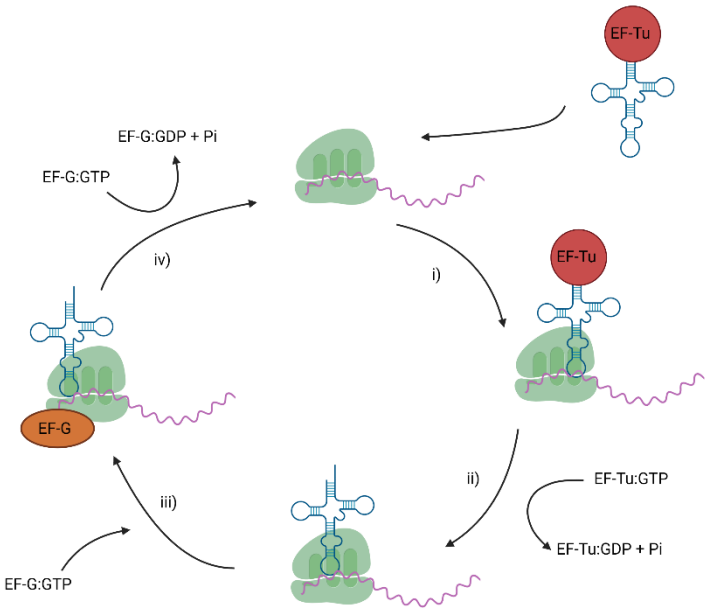

Figure 5: The stages of translation elongation in bacteria. I) EF-Tu:GTP:tRNA binds to the ribosomal A-site ii) EF-Tu:GTP is hydrolysed to EF-Tu:GDP, facilitating translocation of tRNA to the ribosomal P-site iii) EF-G:GTP binds the 30s subunit of the ribosome, is digested to EF-G:GDP, resulting in translocation of tRNA to the ribosomal E-site, where it is ejected iV) The ribosome is now ready for another round of translation elongation.

1.7 Ubiquitous nature of translation machinery and the evolution of protein synthesis regulation

Protein synthesis is a necessity for life and is therefore conserved to some extent across all phylogenetic domains. However, some translation machinery is more highly conserved than others, particularly between eukaryotes and bacteria. This needs to be investigated further in order to reliably ascertain which mechanisms of translation regulation could be conserved.

1.7.1 Translation initiation factors

Translation initiation varies significantly in complexity, with bacteria only needing three initiation factors, and eukaryotes needing ten (Cooper, 2000). There is structural homology between IF-1 and eIF-1, and also IF-2 and eIF5B. There is arguably functional homology between IF-2 and eIF-2 (As they both ultimately recruit the initiating tRNA), however, there is no homologue for bacterial IF-3 (Benelli, La Teana and Londei, 2017). This suggests that any mechanism employed by eukaryotes to regulate initiation factors, principally the phosphorylation of the eIF-2 subunit, is unlikely to be conserved in bacteria.

It has been suggested that divergent evolution is responsible for this change. Eukaryotes evolved significantly more complex translational apparatus to match their more sophisticated and accurate protein synthesis regulation. Whereas, bacteria use the bare minimum of accessory factors for initiation, furthermore, transcription and translation are simultaneous in bacteria, meaning there is not much scope for sophistication of regulating mRNA translation at the initiation stage (Benelli, La Teana and Londei, 2017).

1.7.2 Translation elongation factors

Translation Elongation Factors are found in every known organism on the planet and are very highly conserved between these organisms, serving to highlight how critical translation elongation is to life as we know it.

To gain an understanding of how well conserved elongation factors are, it is necessary to firstly compare the percentage identity of EF-Tu and EF-G of different bacterial species, and to their human orthologues (Table 2).

Table 2: Identity matrix of EF-Tu from model pathogenic bacteria and Eukaryotic eEF-1 from Homo sapiens

Species	Identity%					
Homo sapiens	100.00	18.61	18.12	17.52	20.80	20.58
Mycobacterium tuberculosis	18.61	100.00	70.96	72.96	75.26	73.21
Streptococcus pneumoniae	18.12	70.96	100.00	75.13	73.35	69.29
Staphylococcus aureus	17.52	72.96	75.13	100.00	74.87	73.86
Escherichia coli	20.80	75.26	73.35	74.87	100.00	85.03
Pseudomonas aeruginosa	20.58	73.21	69.29	73.86	85.03	100.00

It is clear that there is very high homology between all the bacterial elongation factors listed in this table. However, there does not appear to be a very high level of homology between the eukaryotic elongation factor 1 (eEF-1) and EF-Tu (Table 2), or eEF-2 and EF-G (Table 3). While this information shows that a conserved and regulated mechanism of translation elongation in response to nutrient deprivation across the bacterial domain is certainly possible, it would also suggest that any conserved mechanism of translation elongation factor inhibition in humans, such as the one described by Leprivier and colleagues, would not be likely to be present in bacteria.

Table 3: identity matrix of EF-G from model pathogenic bacteria and Eukaryotic eEF-2 from Homo sapiens

Species	Identity%					
Homo sapiens	100.00	27.79	29.93	27.91	28.70	29.15
Mycobacterium tuberculosis	27.79	100.00	69.13	59.28	60.06	59.83
Streptococcus pneumoniae	29.33	69.13	100.00	57.12	59.71	58.61
Staphylococcus aureus	27.91	59.28	57.12	100.00	59.83	60.89
Escherichia coli	28.70	60.06	59.71	59.83	100.00	76.59
Pseudomonas aeruginosa	29.15	59.83	58.61	60.89	76.59	100.00

However, percentage identity only tells a small portion of the story. The function and basic mechanism of elongation factors is ubiquitously conserved, suggesting that eukaryotic and bacterial elongation factors could be subject to similar mechanisms of regulation.

The functional regions of elongation factors are so well conserved that they are already the targets for some bacteriostatic antibiotics and secreted toxins. Kirromycin and Fusidic acid target EF-Tu, and EF-G respectively. Kirromycin mostly affects the release of GDP from EF-Tu, whereas, Fusidic acid works by ultimately stalling the ribosome (Borg et al., 2015; Wolf, Chinali and Parmeggiani, 1974). Tse6 secreted by *P. aeruginosa* induces stasis and also associates with and inhibits all bacterial EF-Tu, however, the inhibition of EF-Tu is not thought to be the primary mechanism of Tse6. The authors suggest that Tse6 targets EF-Tu because of its ubiquitous nature, which then causes Tse6 to activate and drastically reduce cyclic di-GMP levels in the cell (Whitney et al., 2015).

Eukaryotic elongation factor targeting by bacteria is also known to occur with exotoxin A from *P. aeruginosa* and diphtheria toxin from Corynebacterium diphtheria both targeting a ubiquitously conserved residue, Diphthamide, on eEF-2. This ultimately halts protein synthesis and induces cell death and necrotic tissue via apoptosis (Michalska and Wolf, 2015; Murphy, 2011).

There is approximately 900 million years between the first bacterial and eukaryotic cell (Cooper, 2000). This suggests that bacteria would have had to regulate protein synthesis in response to stress well before the first eukaryotic cell, and therefore the first eukaryotic translation regulation mechanism came into existence. Regulation of translation is primarily controlled by Hanks-type serine/ threonine kinases in eukaryotic cells, probably due to the robustness, speed and reversibility of phosphorylation as a post translational modification (Leprivier et al., 2013 2015; Leprivier et al., 2015 2015). Since the genomes of bacteria such as *P. aeruginosa*, *Mycobacterium tuberculosis* and *S. aureus* have been sequenced, many Hanks-type serine/ threonine kinases have been discovered in the bacterial phyla. The potential importance of these kinases have been mostly ignored, due to originally thinking that bacterial signalling was totally controlled by histidine kinases. However, recent studies are starting to show their importance in cell regulation (Canova and Molle, 2014; Kant et al., 2017; Klein et al., 2008; Krupa and Srinivasan, 2005; Prisic and Husson, 2014). It could be possible that regulation of translation machinery by Hanks-type serine/ threonine kinases was a prokaryotic invention that was ultimately conserved in eukaryotes.

1.8 The bacterial vs human kinome

The difference between the kinomes of bacteria and humans is vast, with humans understandably having a significantly larger and more complex kinome. A survey completed in 2002 predicted that humans have 518 protein kinase genes, roughly 2.3% of the whole genome (Manning et al., 2002). Since then, the number has further increased to give a total of at least 568 kinases. Nearly all of these are serine/ threonine kinases, a smaller portion are tyrosine kinases, and a smaller portion again are atypical protein kinases (Lai, Safaei and Pelech, 2016). Of these, 175 have been directly implicated in disease via mutation, mis-expression or copy number changes. This is particularly true for cancer where 121 protein kinases are implicated, 51 of these being tyrosine kinases (Manning and Hunter, 2010). In general, protein kinases seem to make up approximately 2% (+/0.2%) of all eukaryotic genomes including *Saccharomyces cerevisiae* and *C. elegans*. The protein kinases of higher eukaryotes also all belong the Hanks-type (HT) family. This is ultimately characterised by a unifying two lobe architecture and conserved motifs, namely a small N-terminal lobe forming a -sheet and a larger C-terminal lobe composed of -helices (Nguyen et al., 2017).

Bacterial kinomes are diverse across the phyla, although in a stark contrast to their eukaryotic counterparts, have very few Hanks-type serine/threonine kinases (Nguyen et al., 2017). It is for this reason that signalling by these kinases has generally been overlooked and the focus put onto the two-component system (TCS). TCS's usually consist of a membrane bound histidine kinase that transduces a signal as a result of an environmental stimulus and an effector molecule inside the cell. The number of these systems encoded in the genome varies significantly with *P. aeruginosa* having 127 TCS's, *E. coli* having 60 and *Bacillus subtilis* having 70 (Balasubramanian et al., 2013).

While, in general, there are very few Hanks-type serine/threonine kinases in bacterial genomes, the ones that are present have recently been shown to be play essential roles in many cellular processes (Dworkin, 2015). Furthermore, some bacterial species are shown to have significantly more Hanks-type kinases, such as *M. tuberculosis* which has 11 and *Myxococcus xanthus* which has over 100 (Nguyen et al., 2017).

The difference between the eukaryotic and bacterial kinome is clear, however, there are distinct similarities in the way the kinases are utilised. In particular, the way they regulate intracellular process such as protein synthesis.

1.9 Translation machinery phosphorylation in response to nutrient deprivation in bacteria

There are multiple confirmed roles of Hanks type serine/threonine kinases (eSTK's) in bacteria ranging from virulence and secretion to cell wall metabolism (Dworkin, 2015) (For a comprehensive list see (Pereira, Goss and Dworkin, 2011)). For the purpose of this review I will be discussing the roles of eSTK's in the regulation of protein synthesis.

As discussed earlier the Doc toxin can phosphorylate a threonine on EF-Tu leading to its inactivation. However, there isn't any strong evidence to show that this mechanism is induced in response to nutrient deprivation, and this mechanism is only found in *E. coli*. Protein synthesis is one of the most energy demanding processes in the cell and so needs to be regulated under conditions where nutrients are not abundant. Proteins, such as EF-Tu, which mediate these processes are often found in the phosphoproteomes of diverse organisms, suggesting that they could be regulated this way (Macek and Mijakovic, 2011). However, EF-Tu is the most abundant protein in the cell, and only 10% is found to be phosphorylated. Suggesting that phosphorylation alone is therefore unlikely to be what induces stasis (Sandro F. F. Pereiraa, 2015).

In 2015 Pereiraa and colleagues used *Bacillus subtilis* as a model organism to investigate whether phosphorylation of EF-Tu inhibited its GTPase activity, preventing its release from the ribosomal A-site and inducing stalling (Pereira, Gonzalez and Dworkin, 2015). *B. subtilis* responds to nutrient deprivation by forming a highly resistant, proteinaceous endospore. During this sporulation process, cells undergo an asymmetric division that generates two compartments, a fore spore and the mother cell. *B. subtilis* therefore allows the study of two genetically identical, but differently metabolising cells. Indeed, they found that a Threonine residue conserved across all translational GTPases was being phosphorylated by a Ser/Thr kinase expressed selectively during sporulation, YabT. Furthermore, EF-Tu was found to elute in the ribosome fraction when using ultracentrifugation and a sucrose cushion, more so in the endospore than the mother cell. This suggests that the GTPase of EF-Tu was being inhibited, preventing the release from the ribosomal A-site and inducing stalling. This was thought to have a dominant negative effect and so explains why a relatively small proportion of phosphorylated EF-Tu could induce cellular stasis (Sandro F. F. Pereiraa, 2015). However, there is conflicting evidence to the mechanism of EF-Tu phosphorylation induced stasis described above. A very recent paper showed that phosphorylation of EF-Tu by Doc toxin traps it in the open conformation (Almost identical to EF-Tu bound to GDP), preventing ternary complex formation with the ribosome and halting translation (Talavera et al., 2018). The authors also observed that phosphorylation of EF-Tu drastically

reduces its solubility and aggregates, potentially explaining why EF-Tu was found in the ribosome fraction by Pereiraa et al (Talavera et al., 2018).

A previous study by Macek and colleagues compared the phosphoproteomes of the gram positive *B. subtilis* and the gram negative bacteria *E. coli*. They found that between the two phosphoproteomes there were 14 direct orthologous proteins, with EF-Tu being included in this. Furthermore, a recent study showed that EF-Tu and EF-Ts both appear in the phosphoproteome of *P. aeruginosa* during the planktonic state and during biofilm development (Petrova and Sauer, 2009). This could suggest a conserved mechanism across different species of bacteria.

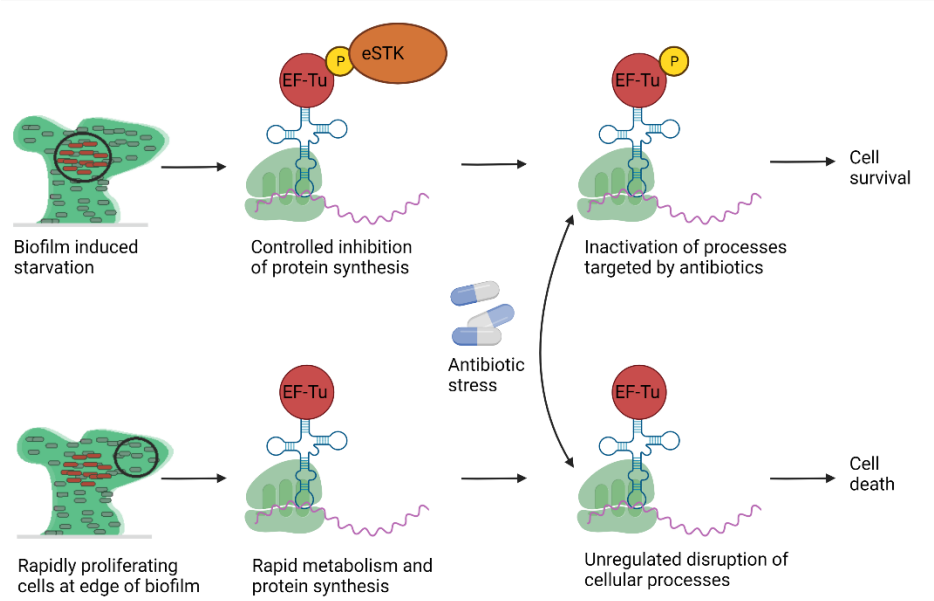

Figure 6: The potential mechanism of kinase induced dormancy and how this benefits the survival of cells in response to stress. The red cells are metabolically inactive and the grey cells are metabolically active.

1.10 The structure and activation of Hanks type serine/threonine kinases

Hanks-type serine/threonine kinases share 12 conserved subdomains that ultimately fold into the typical two-lobe catalytic core with the active site in the cleft between the two lobes. (Krupa and Srinivasan, 2005; Janczarek et al., 2018; Hanks, Quinn and Hunter, 1988). The two lobes have different functions, the N-terminal lobe takes on the job of binding and correctly orienting the ATP molecule, whereas the C-terminal lobe is essential for binding to the substrate and transfer of the donated phosphate group (Hanks, Quinn and Hunter, 1988; Janczarek et al., 2018). These lobes ultimately control the switch between the active and inactive state of the kinases. The C-

terminal and N-terminal lobe undergo numerous conformational changes that are essential for the transition between these states. Upon phosphorylation, the C-helix is directed towards the active site, allowing multiple interactions between the two lobes required for activation (Huse and Kuriyan, 2002; Pereira, Goss and Dworkin, 2011; Hanks, Quinn and Hunter, 1988; Janczarek et al., 2018). The activation loop is clearly the most important part of kinase regulation, within this loop are the conserved DFG and APE motifs that define the activation segment (Nolen, Taylor and Ghosh, 2004). The magnesium binding loop, activation loop, and the P+1 loop are contained within this segment and is ultimately responsible for substrate specificity (Huse and Kuriyan, 2002; Nolen, Taylor and Ghosh, 2004; Pereira, Goss and Dworkin, 2011; Janczarek et al., 2018). They are usually activated by phosphorylation of at least one Serine or Threonine residue in the activation loop via either trans or auto-phosphorylation, stabilising the activation loop.

Unlike phosphorylation on histidine and aspartate residues, phosphorylation by eSTK's results in a highly stable interaction between the serine/threonine and the phosphate. This ultimately means that a specific phosphatase is required to reverse the action of the kinase, and also to switch the kinase to the inactive conformation. These phosphatases usually have significant homology to their eukaryotic counterparts and are therefore termed eukaryote-like serine/threonine phosphatases (Pereira, Goss and Dworkin, 2011).

There are two Hanks-type serine/threonine kinases that have been formally identified previously in *P. aeruginosa*, Stk1 and PpkA. Another kinase, YeaG, has been studied in other bacteria in some detail and exists in the *P. aeruginosa* genome, but at the time of reading has not been formally identified.

1.10.1 Stk1

Stk1 has been characterised from a biochemical standpoint and has had some phenotypic analysis performed (Mukhopadhyay *et al.*, 1999; Zhu *et al.*, 2021b). The protein was first identified as being a Hanks type kinase by developing an 800 bp probe from the conserved regions of serine/threonine kinases conserved in Mycobacteria. After the protein was identified, it was cloned into the pGEX-4T1 plasmid and expressed in *E. coli*. After purification, an in vitro kinase assay showed that Stk1 is able to autophosphorylate, and is capable of phosphorylating eukaryotic histone H1, a commonly used substrate for kinases of this type (Mukhopadhyay et al., 1999; Sarg et al., 2006).

A phenotypic and proteomic analysis by zhu et al showed that a stk1 deletion mutant of *P. aeruginosa* PAO1 had significant downregulation of type IV pilus-related proteins and upregulation of T6SS-H1-related proteins. This was linked to a reduction in type IV pilus mediated

twitching motility and an increase in growth competition advantage, likely moderated by the T6SS-H1-related proteins (Zhu *et al.*, 2021b).

1.10.2 PpkA

PpkA has been characterised extensively in terms of Type six secretion (T6SS) mediated virulence, however, there is very little on its role in adaptation to changing environmental conditions (Goldova et al., 2011; Pan et al., 2017a; Mougous et al., 2007; Hsu, Schwarz and Mougous, 2009).

In 2007, Mougous et al identified that PpkA post translationally regulates Hcp secretion island-I-encoded type VI secretion system of *P. aeruginosa* (Mougous et al., 2007). The T6SS consists of a membrane and tail complex that are equivalent to contractile phage tails and the Hcp secretion island is responsible for Hcp1 secretion, believed to form nanotubes on the bacterial surface which may allow transport of other T6SS effectors (Depluverez, Devos and Devreese, 2016). PpkA was found to catalyse this activity by acting on a FHA domain containing protein named Fha1. It was later found that Fha1 is a core scaffolding protein of the Hcp island T6SS (Mougous et al., 2007). It was postulated that the post translational regulation of this system by threonine phosphorylation likely reflects its requirement to rapidly respond to change in environmental conditions (Goldova et al., 2011; Pan et al., 2017a; Michalska and Wolf, 2015; Mougous et al., 2007).

More recently, in 2017 Pan et al broadly examined the potential roles of PpkA in regulation of cellular processes including: biofilm formation, pyocyanin production, oxidative and osmotic stress response, cell invasion and plant virulence (Pan et al., 2017a). They found that biofilm formation was significantly reduced in the PpkA deletion strain compared to the wild type, however, although complementation of the mutant restored biofilm formation to that of the wild type, this data is not supported by our study. It is possible that this is due to the different experimental procedures used, in particular the media. Our study uses a nutrient deficient M9 medium, whereas, Pan et al used a nutrient rich LB broth which may be more likely to support planktonic growth. It was also found that the PpkA deletion mutant was also significantly more sensitive to hydrogen peroxide induced oxidative stress, as well as NaCl induced osmotic stress. Furthermore, the mutant strain was found to have decreased pyocyanin production and significantly reduced ability to invade HeLa cells and lettuce leaf (Pan et al., 2017a). While this study is certainly informative in terms of the potential roles of PpkA, it does not provide any detail on the potential mechanistic pathways by which these phenotypes are produced.

The paper by Pan et al does however seem quite redundant when looking at the paper released by Goldova et al six years prior (Goldova et al., 2011). Goldova et al discovered through a global

transcriptome analysis that genes regulating oxidative stress and iron metabolism were down regulated, providing a potential mechanism for the effect that was seen by Pan et al. However, Goldova et al were examining the effect of a Ppka-PppA double knockout mutant, making it difficult to assume that PpkA was solely responsible for regulating these processes.

1.10.3 YeaG

YeaG has been shown to be essential for long term nitrogen starvation survival *E. coli*, as well as being required for full induction of the stringent response via RpoS. This has been linked to its role in the denitrification pathway via the nitrogen starvation protein ntrc and the anaerobic regulator anr (Figueira et al., 2015).

1.10.4 The role of adjacent phosphatases

Both PpkA and Stk1 have adjacent phosphatases. This is likely due to the highly stable bond formed when a serine or threonine residue is phosphorylated, necessitating a specific phosphatase to remove the phosphate group from the residue (Dworkin, 2015). Furthermore, Mougous et al showed that PppA is critical for attenuating PpkA moderated secretion of Hcp1 (Mougous et al., 2007).

1.11 Which translation factors are the most effective targets for cellular protein synthesis inhibition?

It is clear looking at the discussed literature that direct and indirect Translation factor inhibition in response to cellular stress is a utilised, and relatively conserved mechanism from humans to bacteria (Pereira, Gonzalez and Dworkin, 2015; Leprivier et al., 2013) . While this certainly shows that this mechanism may exist in *P. aeruginosa*, there is still no hard evidence. It is therefore important to consider which factor is likely to be inhibited and cause cellular quiescence.

1.11.1 Initiation Factors

As shown earlier, eukaryotic organisms have a comparatively complex mechanism for initiation of translation using at least 10 discrete initiation factors (Lee et al., 2002). Furthermore, transcription and translation do not occur simultaneously in eukaryotes. This provides a lot of scope for inhibition of initiation factors by eSTK's such as Gcn2 (Castilho et al., 2014). This makes a lot of sense as recruitment of the initiating Fmet tRNA to the ribosomal A-site is the rate determining step (RDS) in eukaryotic translation (Koromilas, 2015). Theoretically, inhibiting IF-2 in

bacteria would also result in inhibition of recruitment of initiator tRNA to the ribosome. However, IF-2 does not appear in the phosphoproteome of *P. aeruginosa* (Ravichandran et al., 2009). It could be further argued that bacteria do not require inhibition of translation initiation due to translational control by operons and attenuation. This is where the rate of translation alters the structure of the RNA, which influences the rate of transcription (Brantl, 2004). This information suggests that translational regulation in response to nutrient deprivation is likely controlled at the elongation stage.

1.11.2 Elongation Factors

Most characterised mechanisms that inhibit translation elongation factors in bacteria, do so by inactivating EF-Tu (Pereira, Gonzalez and Dworkin, 2015; Cruz et al., 2014; Germain et al., 2013). This is the bacterial orthologue of eEF-1, and so differs to the mechanism characterised by Leprivier and colleagues where eEF-2, the orthologue of EF-G, is inhibited (Leprivier et al., 2013).

The serine/threonine protein kinases PrkC of *B. subtilis* has been shown to phosphorylate a threonine residue of EF-G in vitro, and that PrpC regulates this activity (Gaidenko, Kim and Price, 2002). The authors hypothesised that this served a regulatory role in stationary phase B.subtilis cells, and that disruption of this mechanism affected the cell density at stationary phase (Gaidenko, Kim and Price, 2002). It had also been previously stated that EF-G was possibly related to regulation of sporulation in *B. subtilis* (Mitchell, Morris and Vary, 1992).

EF-P is another ubiquitous, ribosome dependent translation elongation factor that is critical for virulence and high stress survival in bacteria. EF-P alleviates ribosome stalling at polyproline stretches and has been associated with production of CadC, which induces an appropriate stress response to abnormal pH levels. The ability of EF-P to alleviate ribosome stalling is dependent on its lysinylation by YjeK and YjeA. Interestingly, YjeA uses a similar mechanism as an aminoacyl-tRNA synthatase and catalyses the transfer of RBeta-lysine to K34 on EF-P and activates it with ATP. In fact, it is homologous to lysine tRNA synthetase, with the exception of the codon recognising N-terminal domain. Genomic analysis has revealed that there is an abundance of polyproline stretch-containing proteins not only in bacteria, but also archaea and eukaryotes. Therefore, high stress conditions that result in the expression of polyproline peptides will require EF-P, YjeK and YjeA. The absence of any of these genes has resulted in defects in the stress response, sporulation and critically antibiotic sensitivity (Ude et al., 2013; Starosta et al., 2014; Navarre et al., 2010). A deletion mutant of a protein homologous to YjeA, PoxA, in Salmonella was found to persistently respire under nutrient-poor conditions, whereas wild type cells would cease. The explanation put forward by the authors is that the mutant resulted in translational errors of

membrane proteins that respond to environmental ques and became “Stress-Blind”. Further respiration under these conditions potentially lead to the formation of radicals and therefore, increased general antibiotic sensitivity (Navarre et al., 2010). Interestingly, this is an example of where an elongation factor is induced in response to nutrient deprivation, but inhibiting either PoxA or EF-P via pharmaceuticals could help reduce persistence.

The final ubiquitous and essential elongation factor is EF-Ts. When an EF-Tu-GTP:tRNA complex interacts with the ribosome, the GTPase activity of EF-Tu is activated and results in its dissociation from the ribosome. EF-Tu is now associated with GDP and currently is inactive. The role of EF-Ts is to catalyse the removal of GDP from EF-Tu, allowing for another round of elongation. When EF-Tu:GDP and EF-Ts from Heliobacter pylori were pre-incubated in a 1:2 molar ratio the EF-Tu:GDP levels dropped by 15.6%, highlighting the effectiveness of this mechanism. Furthermore, EF-Ts and EF-Tu were found to have a synergistic effect on molecular chaperoning. The information suggests that inhibition of EF-Ts would indeed prevent GDP release/ EF-Tu turnover and inhibit translation elongation and induce stasis. However, the presence of 1 molar equivalent of EF-Ts was found to completely inhibit the GTPase activity of EF-Tu, preventing further translation. This mechanism is mimicked by the therapeutic, Bismuth. Bismuth was found to increase turnover of EF-Tu via GDP release, but inhibited the intrinsic GTPase activity of the enzyme. In this manner, cellular inhibition of this elongation factor to induce persistence seems unlikely due to the “double edged sword” effect and the presence of functional alternatives (Wang et al., 2013). However, EF-Ts does appear in the phosphoproteome of *P. aeruginosa* (Petrova and Sauer, 2009). This suggests that both EF-Tu and EF-Ts are inhibited simultaneously.

This information certainly suggests that EF-Tu and EF-Ts are the most likely targets for cellular inhibition.

1.12 Aims and Hypothesis

The overall aim of this project is to investigate the role of multiple Hanks Type serine/threonine kinases in *P. aeruginosa.* Specifically, to investigate the formation of metabolically inactive cells, biofilm development and viability, and the ability to adapt to nutrient starvation. At the time of writing, there are no studies in this area for *P. aeruginosa*. This affords the opportunity for discovery of new mechanisms and ultimately next generation anti-biofilm therapeutic.

Chapter 2 Creation of the eSTK deletion mutants identified in *Pseudomonas aeruginosa*

2.1 Introduction

With recent advances in long read gene sequencing complementing shotgun sequencing (Tyson et al., 2018), and the whole genome sequence of *P. aeruginosa* PAO1 (and other strains) being revealed with fewer and fewer contigs, it has become easier than ever to identify and delete targets in *P. aeruginosa* with the help of high throughput techniques. These techniques allow a robust method for elucidating the function, and downstream effectors of a specific gene.

To facilitate the study of the eSTK's identified in PAO1, it was necessary to first identify them, delete them from the genome individually and sequentially to account for any redundancy between the kinases targets (Pereira, Goss and Dworkin, 2011).

The general methodologies and theories used to create the deletion mutants in this study will be reviewed and summarised below. The same methodologies were used for PA2192, but the genes were only deleted individually due to time constraints.

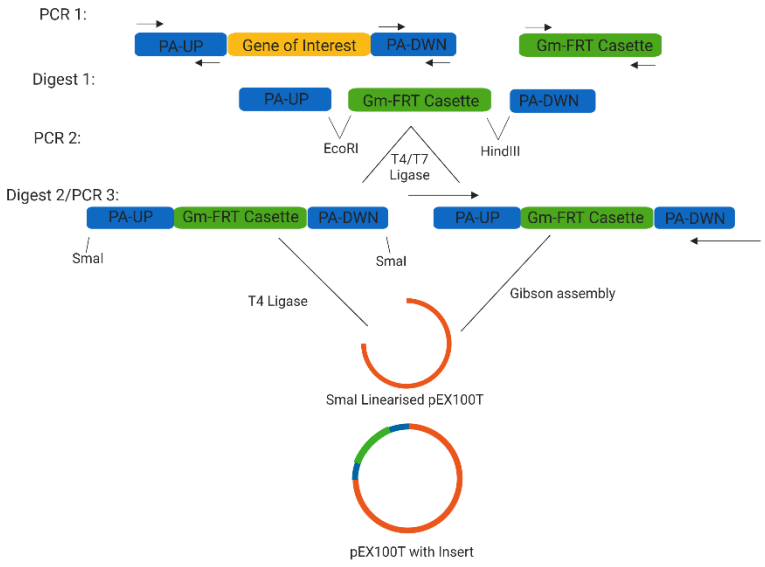

Figure 7: Summary of the steps used to create the construct. i) Sequences flanking the gene of interest and the gentamicin resistance cassette were amplified ii) These were digested with EcoRI and HindIII, then ligated with T4 or T7 ligase iii) The resulting fragment was amplified iv) The fragment and pEX100T vector were digested with SmaI, then ligated with T4 ligase

2.1.1 Rationale for selecting the plasmid vector and marker to facilitate gene deletions in *P. aeruginosa*

Many different methods have been developed to allow transfer of recombinant plasmids to *P. aeruginosa*, such as transformation of chemically competent, or electroporated cells. However, conjugation is the most frequently used due to the reduced need for specialist equipment (required for electroporation), comparatively simple manipulation procedures, and that the resulting conjugally transferred DNA is less susceptible to host restriction (Schweizer, 1992). Therefore, it is necessary for the selected plasmid to be maintained and to be able to replicate in *E. coli* and conjugate into *P. aeruginosa*, as well as containing a sufficient number of restriction sites and selectable markers (Schweizer, 2004 1992; Schweizer, 1992 1992). The method used in this study was developed by Herbert Schweizer, however was simplified and streamlined in our lab by Yuming Cai (Cai, 2018) as part of previous project and used the pEX100T plasmid developed by Herbert Schweizer (Schweizer, 1992).

Figure 8: pEX100T plasmid developed by Herbert Schweizer and used to create the deletion mutants in this study

The pEX100T (Figure 8) vector is a derivative of the original pUC19 vector (Schweizer, 1992) and has the following features that are relevant to this gene deletion method:

- ori is a high copy number ColE1/pMB1 origin of replication that can only be induced in *E. coli*. In *P. aeruginosa*, the plasmid cannot replicate and so must undergo allelic exchange of to obtain the resistance encoded by the marker on the plasmid (Schweizer, 1992)
- bla is a beta lactamase that will degrade any beta-lactam antibiotic, such as ampicillin or carbenicillin. This allows for the selection of the plasmid in *E. coli*, and for counter selection in *P. aeruginosa* (Schweizer, 1992)
- oriT is the origin of transfer that allows the conjugation of the plasmid to *P. aeruginosa* from the conjugative *E. coli* strain (S-17) iv) sacB from *Bacillus subtilis* results in secretion of levansucrase which renders bacterial growth sensitive to sucrose. This allows for selection of double crossover mutants, as opposed to the more common merodiploids (Steinmetz et al., 1985; Schweizer, 1992)

- Unique cloning sites for SmaI and I-SceI (Rare meganuclease site) to allow greater access to cloning sites

To facilitate the actual deletion, and the selection of the deletion mutant in *P. aeruginosa*, a gentamicin resistance cassette flanked by the upstream and downstream sequences that were adjacent to the gene to be deleted were used (Figure 7). This allows for allelic exchange to occur after conjugation, chromosomal deletion mutants rely on host recombination systems to facilitate allelic exchange between the plasmid vector and the host chromosome (Hmelo et al., 2015).

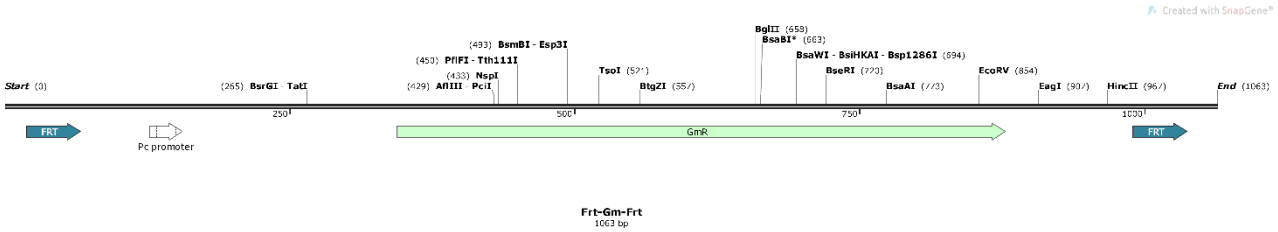

Figure 9: Gentamicin resistance cassette flanked by FRT sequences from pFGM1 plasmid developed by Herbert Schweizer, which was used to create the markerless deletion mutants in this study

The Gentamicin resistance cassette (Figure 9) contains a gentamicin acetyl transferase which inactivates gentamicin. The sequence was obtained from the pFGM1 plasmid developed by Herbert Schweizer and is flanked by FRT sites on each side, which allow the removal of the marker from the genome by FLP recombinase (Barekzi et al., 2000; Schweizer, 2003) (Discussed in detail in 2.1.3).

2.1.2 Methodologies used to create recombinant constructs in plasmids

Many protocols require that the fragments immediately upstream and downstream of the gene are amplified and ligated to a selectable marker, followed by integration into a plasmid to facilitate the deletion of the gene (Choi et al., 2005; Hmelo et al., 2015; Schweizer, 1992). During this study a restriction-ligation method (Figure 7), and Gibson assembly were used to accomplish this (Gibson et al., 2009). Briefly, the restriction-ligation method involves amplifying the upstream and downstream fragments using primers that introduce specific restriction sites to the end of these sequences. The DNA is the digested using the specific restriction enzymes and ligated to the appropriate fragment using a DNA ligase e.g. T4 or T7 (Figure 7).

Gibson assembly is a relatively new method that, instead of using restriction enzymes, relies on overlapping sequences. In short, the upstream and downstream fragments are amplified using long primers that are designed so that they create an overlap with the fragment that they are to

be annealed to. The fragments are then mixed into a single vessel, Gibson assembly master mix added, and incubated at 50°C. The 5' T5 exonuclease then "Chews back" the DNA and generates a sticky end, followed by ligation by a DNA ligase to join the fragments. Gaps are then filled in by a DNA polymerase (Gibson et al., 2009). A major advantage of this method is that it is, relatively speaking, sequence independent. Normally, with a restriction ligation method it is necessary to ensure that the upstream and downstream sequences do not contain any restriction sites that will otherwise be used to ligate the fragments together. However, as Gibson assembly negates the use for restriction sites (Gibson et al., 2009) there is no need for this.

2.1.3 Method used to create a markerless deletion

The FLP recombinase mediated system developed by (Choi and Schweizer, 2005) was used for the removal of the gentamicin resistance marker from the *P. aeruginosa* genome after homologous recombination.

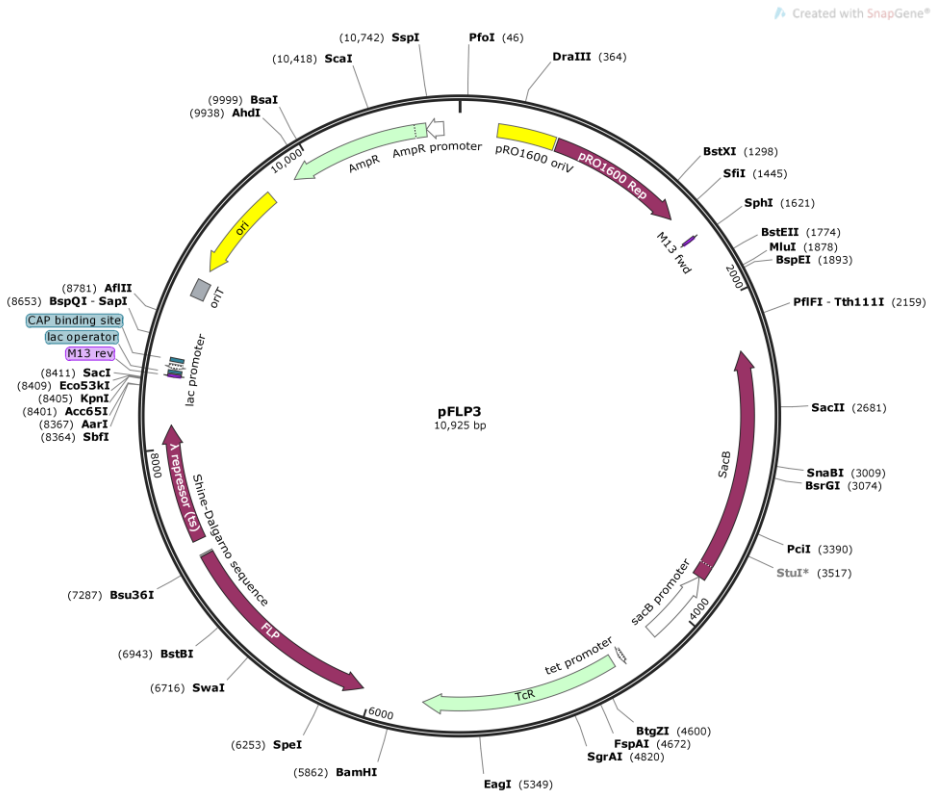

Figure 10: pFLP3 plasmid used for FLP mediated removal of the FRT flanked gentamicin resistance marker

The FLP recombinase system is native to *Saccharomyces cerevisiae* and is found on a 2 µm plasmid (Gronostajski and Sadowski, 1985)(Figure 10). It has been shown that this system promotes efficient recombination between two identical FLP recombination sites on the plasmid. When the FRT sites are inverted there is an inversion event, and a deletion event when the sites

are in a direct orientation. This confers no advantage to *S. cerevisiae*, however is still conserved (Gronostajski and Sadowski, 1985, Schweizer, 2003).

When using a resistance marker that is flanked by FRT sites, this system can be exploited to remove the marker that would otherwise be permanently part of the genome. Firstly, an appropriate plasmid expressing the FLP recombinase must be chosen. For this study the pFLP3 plasmid developed by (Choi and Schweizer, 2005) was used in combination with the gentamicin FRT cassette described in 2.1.1. The key features of the pFLP3 plasmid are:

The pRO1600 oriV origin of replication, and the pRO1600 REP protein, this origin of replication allows the plasmid to replicate when the REP protein is present (S.E.H. West, 1994)

- TcR, encodes a tetracycline efflux protein
- FLP, encodes the FLP recombinase
- SacB, ori, bla (Discussed in 2.1.1.)

2.2 Materials and Methods

2.2.1 Blast search, conserved domain search and multiple sequence alignment

The BLASTP search against the PAO1 reference strain and PA2192 was conducted on pseudomonas.com with all settings on default. The protein sequences used for the alignment were a Hanks type consensus sequence (Stancik et al., 2018), PknB from *M. tuberculosis*, and PrkA from *B. subtilis*.

The multiple sequence alignment was performed using the Clustal Omega algorithm on the ebi website.

2.2.2 Strains and plasmids relevant to this chapter

The pEX100T plasmid was kindly donated by Herbert Schweizer. The PpkA mutant strain and the wild type were donated by the Mougous Lab (Mougous et al., 2007), and pFLP3 and pFGM1 were purchased from AddGene.

Table 4: Strains and plasmids used during this study

Strains/ Plasmids		Characteristics/reference	Source
Pseudomonas aeruginosa			
PAO1		Reference strain with moderate drug Resistance (Mougous et al., 2007)	Mougous lab
	ΔPA1782	Referred to as Pstk	This Study
	ΔPpkA	(Mougous et al., 2007)	Mougous lab
	ΔStk1	This Study	
	ΔYeaG	This Study	
	ΔPstkΔPpkAΔStk1ΔYeaG	Referred to as QKO	This Study
PA2192		Cystic fibrosis isolate with a mucoid mutation	ATCC
	ΔPA1782	Referred to as Pstk	This Study
	ΔYeaG	This Study	
	ΔStk1	This Study	
Escherichia coli			
	DH5-α	sup E44, ΔlacU 169(ΔlacZΔM 15), recA1, endA1, hsdR17, thi1, gyrA96, relA1, Δpirphagelysogen.	
	S-17	TpR, SmR, recA, thi, pro, hsdR-M+RP4: 2Tc:Mu: Km Tn7 Δpir.	
Plasmids			
	pEX100T	Gateway compatible gene replacement Vector with ampicillin resistance (Quenee, Lamotte and Polack, 2005)	Donated by Herbert schweizer
	pFLP3	Expresses FLP recombinase	Purchased from Addgene
	pFGM1	Encodes a Gm cassette with FRT sites (Choi and Schweizer, 2005)	

2.2.3 Primers used in this study

Table 5: The primers used to create and confirm the deletion mutants used during this study

Oligo name	Sequence	Bases
Gm-Frt-F	ATGC GAATTC AGCTCGAATTGGGGATCTT	29
Gm-Frt-R	ATGC AAGCTT CTCGAATTAGCTTCAAAAGCGC	32
Pstk-Up-F	ATGC CCCGGG TATTTCCACGACCAGTACG	29
Pstk-Up-R	ATGC GAATTC CAGCGCGTCCTGGTTTT	27
Pstk-Dwn-F	ATGC AAGCTT TCCTGGT CTGGCTGAA	26
Pstk-Dwn-R	ATGC CCCGGG GGAGCTT GATGCCGTT	26
Pstk-Up-F (S)	TTCTTCTACAGCGTCAC CTT	20
Pstk-Dwn-R (S)	TCGATCTGCACCACCTT	17
Stk1-Up-F	CCTGTTATCCCTACCCATCGTCACCAGCCTGG	32
Stk1-Up-R	ATGC GAATTC GACAGCG GTTCGTTCAT	27
Stk1-Dwn-F	ATGC AAGCTT CGTTCTT GCCCGTTGA	26
Stk1-Dwn-R	GATAACAGGGTAATCCCTCGATCCGCTCGGTTTCG	35
Stk1-Fwd (S)	AACGAGGATGCCTTCCT	17
Stk1-Rev (S)	TCGCATGAATTCATTCG CC	19
PpkA-Up-F (S)	TTCGTCAGCAGCCTGAT	17
PpkA-Dwn-R (S)	ACATCGAGGAACTCGAG C	18
YeaG-Up-F	ATGC CCCGGG GCACATC GACAACCACTC	28
YeaG-Up-R	ATGC GAATTC ACGTCTC CTCGCTCGAT	27
YeaG-Dwn-F	ATGC AAGCTT AGTTGGC TGTCCTACGAGA	29
YeaG-Dwn-R	ATGC CCCGGG GCACCG GTTCGTCGATAT	28

2.2.4 DNA extraction

Whole genome extraction from PAO1 was performed using the Wizard Genomic DNA Purification Kit as per manufacturer's instructions. Overnight cultures were made by inoculating 4 ml of Luria-Bertani medium with PAO1 from a glycerol stock. This was then aliquoted into 1.5 ml Eppendorf tubes which were centrifuged at 16,000 x g for 2 minutes to pellet the cells. Once the cells were pelleted, the supernatant was poured off and 600 µl of Nuclei Lysis Solution was added to resuspend the pellet. This was followed by incubation at 80°C for 5 minutes to lyse the cells.

Once the solution had returned to room temperature, RNA contamination was avoided by adding 3 µl of RNase Solution to the cell lysate, mixing, and then incubating at 37°c for 45 minutes. The sample was again allowed to return to room temperature and 200 µl of Protein Precipitation solution was added to precipitate any contaminating proteins, followed by vortexing vigorously for 20 seconds. The vortexed cell lysate was then cooled on ice for 5 minutes and centrifuged at 16,000 x g for 3 minutes. Contaminating protein was precipitated and pelleted at the bottom of the microcentrifuge tube. The supernatant, which contains the DNA, was transferred to a clean

microcentrifuge tube containing 600 µl of isopropanol to precipitate the DNA. The solution was gently mixed until thread-like strands of DNA formed a visible mass, this was then centrifuged at 16,000 x g for 2 minutes to pellet the DNA. The supernatant was then poured off and 600 µl of room temperature ethanol added and mixed to wash the DNA pellet. This was then centrifuged again at 16,000 x g for 2 minutes and the supernatant poured off. The pellet was then air dried for 15 minutes and 100 µl of DNA Rehydration solution was added. The DNA was incubated at 65°c for 1 hour to facilitate rehydration.

2.2.5 PCR

DNA in the samples were denatured by heating to 98°C for 30 seconds, or 5 minutes for colony PCR. This was followed by 35 cycles of 98°C for 5 seconds to denature the DNA, 15 seconds of a temperature determined by the annealing Tm of the primers, and 72°C for a length of time determined by how long the fragment in question was for elongation. Immediately after the 35 cycles, a final elongation stage was done at 72°C for 2 minutes. The PCR reaction was then cooled to 4°C as a holding temperature. All fragments were amplified with 12.5 µl of 2x Q5 high fidelity polymerase from NEB, 1.25 µl of each relevant primer at 10 µM, 2.5 µl of DNA at 10 ng/µl for plasmid DNA and 100 ng/µl for genomic DNA and molecular grade water up to 25 µl. NEB Q5 polymerase is known to work at approximately 30s per Kb, so elongation times were worked out accordingly. All PCR purification was carried out using the QIAquick PCR Purification Kit. All centrifugation steps were at 17,900 x g for 60 seconds.

2.2.6 Agarose Gel Electrophoresis

Agarose gels were composed of High Molecular Grade Agarose from Bioline with no detectable DNase or RNase activity, 100 ml of 1x Tris-Acetate-EDTA (Crabbe et al.) and 10 µl of SYBR safe DNA stain from Invitrogen. Gels were composed of <1% agarose i.e. <1 g in 100 ml of TAE to facilitate DNA purification via gel extraction to facilitate good band separation and gel extraction. All Gels were run at 90 volts, 300 mA and 10 watts and all gel extraction was carried out using the QIAquick Gel Extraction kit with centrifugation steps carried out at 17,900 x g for 60 seconds.

2.2.7 Restriction Enzyme mediated digestion Construction of Mutant fragments

All restriction endonucleases were supplied by New England Bioloabs. Digestion of the gene fragments and the Gentamicin resistance cassette (Gm cassette) was performed in a thermocycler at 37°C for 2 hrs to facilitate digestion, followed by 30 minutes of heat inactivation at 80°C.

2.2.7.1 Upstream and downstream fragments

The upstream fragments were cleaved with 1 µl EcoRI, while the downstream fragments were cleaved with HindIII. In addition, 2 µl of Cutsmart buffer, 500 ng of DNA, and water to make up to 20 µl were added.

2.2.7.2 Gentamicin resistance cassette

The Gm cassette was digested with two restriction endonucleases, EcoRI and HindIII. As above, 1 µl of each restriction endonuclease, 2 µl of Cutsmart buffer, and water to make up to 20 µl were added.

2.2.7.3 Construction of Gateway compatible knockout vector (excluding Stk1)

The reactions contained 500 ng of KO fragment and the pEX100T vector, which were digested with 1 µl of SmaI. In addition, 2 µl of buffer and water up to 20 µl were added. The digest was performed in a thermocycler at 25°C for 2 hours, this was followed by the addition of 1 µl of rSAP and an hour at 37°C to dephosphorylate the ends and prevent self-ligation. rSAP and SmaI were then heat inactivated at 80°C for 30 minutes.

2.2.8 Ligation

All ligations were performed using a temperature gradient. A water bath was heated to 37°C and the ligation reaction placed into it. This was then placed in a fridge at 4°C overnight. The reactions contained the relevant DNA, 0.5 µl of T4 ligase, 1 µl of T4 buffer and water to make up to 10 µl.

2.2.9 Gibson Assembly

The Stk1 Knock out fragment was ligated to the pEX100T vector by means of Gibson assembly. Briefly, the pEX100T Vector was linearised by digestion with SmaI, following this, approximately 0.25 pmols of vector and 0.25 pmols of the Stk1 Knock out fragment were mixed. To this, 10 µl of 2x Gibson assembly master mix (NEB) and a volume of Deionized H2O up to 20 µl were added. This mixture was then incubated in a thermocycler at 50°C for 1 hour to facilitate ligation of the fragments and stored at -20°C for subsequent transformation.

2.2.10 Miniprep

All Miniprep's were carried out using the QIAquick Miniprep kit with centrifugation steps carried out at 17,900 x g for 60 seconds

2.2.11 Transformation of *E. coli*

E. coli DH5and *E. coli* S-17 were both transformed using the high efficiency protocol developed by NEB. Briefly, the cells were thawed on ice until the last ice crystals melted. This was then followed by adding 40 µl of the relevant *E. coli* cells to 4 µl of plasmid DNA and gently mixing. After allowing to cool on ice for 30 minutes, the mixture was heat shocked at 42°C for 30 seconds and then placed back on ice for 5 minutes. 950 µl of LB broth was then added to the mixture and incubated at 37°C in a shaking incubator at 180 rpm for at least 60 minutes. These were then plated on the appropriate selective media.

2.2.12 Transformation of *P. aeruginosa* strains

P. aeruginosa was grown overnight at 42°C to reduce expression of restriction systems that severely limit the introduction of foreign DNA. The following day, 500 µl of *E. coli* S-17 and 500 µl of *P. aeruginosa* are mixed in an Eppendorf. This mixture is then filtered through 0.45 µm filter paper (Millipore), which allows the liquid to pass through, while the cells remain on the filter disc. The filter paper is then incubated on LB agar for 4 hours at 37°C, allowing for conjugation and growth to occur. The bacteria were then re-suspended in 1 ml of sterile PBS and plated on the appropriate selection media

2.2.13 Selection of Deletion Mutants

For plasmid maintenance in *E. coli* DH5-α, the media was supplemented with 15 µg/ml of gentamicin and 100 µg/ml of ampicillin simultaneously for selection, and for *E. coli* S-17, 50 µg/ml of streptomycin was also present. Deletion mutants of *Pseudomonas aeruginosa* PAO1 were initially selected for by plating onto cetrimide agar (Sigma Aldrich) containing 30 µg/ml of gentamicin. The resulting colonies were then stabbed into cetrimide agar containing 30 µg/ml of gentamicin and 10% sucrose, to select for double crossover mutants and cure the plasmid. All strains were grown aerobically in an incubator at 37°C. The same procedure was used for PA2192, but with 60 µg/ml of gentamicin.

2.2.14 FLP Recombinase Mediated Marker Deletion

FLP mediated recombination was achieved via transformation of the pFLP3 plasmid into the ΔPAXXXX PAO1 strain. After this, the strain containing the plasmid is selected for on certrimide agar supplemented with 200 µg/ml Tetracycline, colonies are picked, and are then stabbed into certrimide agar containing Tet 200 µg/ml or Gentamicin 30 µg/ml. Colonies that grew on Tetracycline plates, but not gentamicin plates, were picked and stabbed onto 15% sucrose agar

until the plasmid had diluted out. This was confirmed by counter selection by 400 µg/ml carbenicillin.

2.3 Results and Discussion

2.3.1 BLASTP search and AlphaFold structural analysis reveals that proteins with conserved Hanks type serine/threonine kinase domains exist in *P. aeruginosa* PAO1 and PA2192

BLASTP analysis revealed a total of five genes that contain regions homologous to the Hanks type serine/threonine kinase templates that we used (Table 6). The templates were PknB from *M. tuberculosis*, a Hanks type serine/threonine kinase consensus sequence (Stancik et al., 2018), and PrkA from *B. subtilis*. BLASTP against PknB revealed three homologous proteins, PpkA, Stk1 and a probable serine/threonine protein kinase, hereafter referred to as Pstk (Table 6). The conserved domain search of these proteins revealed that all three contain a specific area of homology linked to PknB, and that Pstk also contains a region homologous to PTC1 (a phosphatase), leading to the annotation of bifunctional serine/threonine kinase/phosphatase.

When compared to the hanks type consensus sequence (Stancik et al., 2018), four proteins were identified, the same three as above and PA2727 (Table 6). PA2727 has a conserved PkC super family region, however, did not have any specific hits on the conserved domain search. The ATP binding domain of DNA helicases were also found on the sequence, and PA2727 was found to bare homology to other putative DNA helicases in other bacteria. It was decided that there would be no further study of this protein due to being unable to determine whether PA2727 was a kinase or helicase. However, this could be an interesting avenue for future work if the function could be determined by an in vitro kinase assay.

PA0588, hereafter referred to as YeaG, was identified when compared to PrkA from *B. subtilis*. PrkA family eSTK's are more enigmatic than their PknB counterparts, so the conserved domain search simply revealed that YeaG has homology to PrkA family serine protein kinases.

The Alignment (Figure 11) shows homology between the eSTK's of *P. aeruginosa* PAO1 at the ATP binding site and active sites of the kinases, but no homology in other areas. The binding site and active site are within the conserved Hanks-type regions of the kinases.

Table 6: Homologous proteins identified in *Pseudomonas aeruginosa* after a BLASTP search against PknB from Mycobaterium tuberculosis, a Hanks type consensus sequence, and PrkA from *Bacillus subtilis* *Pstk is short for "Probable serine/threonine protein kinase" **PA2727 was not studied further

Blast Search Query sequence	Homologous Proteins Identified in PAO1	Homologous Proteins Identified in PA2192	Conserved Domains
PknB (*Mycobaterium tuberculosis*)			
	PA0074/PpkA	PA2G_03986	STKc_PknB_like
	PA1671/Stk1	PA2G_00652	STKc_PknB_like
	PA1782/Pstk*	PA2G_00764	STKc_PknB_like + PTC1 Bifunctional serine/threonine kinase/phosphatase
Hanks Type Consensus Sequence			
	PA0074/PpkA	PA2G_03986	STKc_PknB_like
	PA1671/Stk1	PA2G_00652	STKc_PknB_like
	PA1782/Pstk*	PA2G_00764	STKc_PknB_like + PTC1 Bifunctional serine/threonine kinase/phosphatase
	PA2727/Hypothetical Protein PA2G_01841	PkC Superfamily Kinase + Putative DNA helicase	
PrkA (*Bacillus subtilis*)			
	PA0588/YeaG	PA2G_04508	PrkA Family serine protein kinase

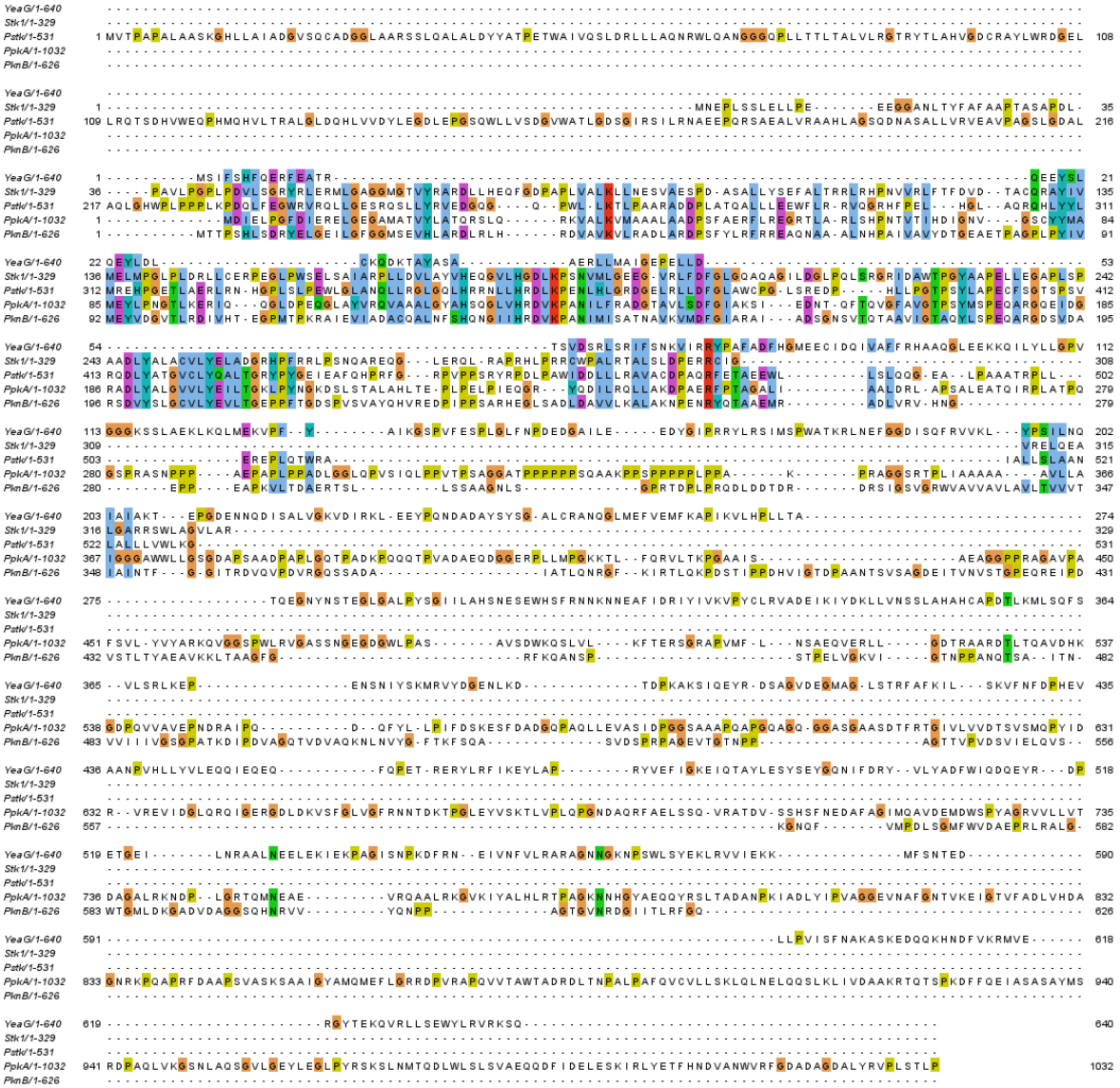

Figure 11: Alignment of the four serine/threonine kinases from *Pseudomonas aeruginosa* selected for study, with PknB from *Mycobaterium tuberculosis* being used a root. The Alignment shows less similarity between YeaG and the other kinases, however there is still homology at the regions corresponding to the ATP binding site and the active site

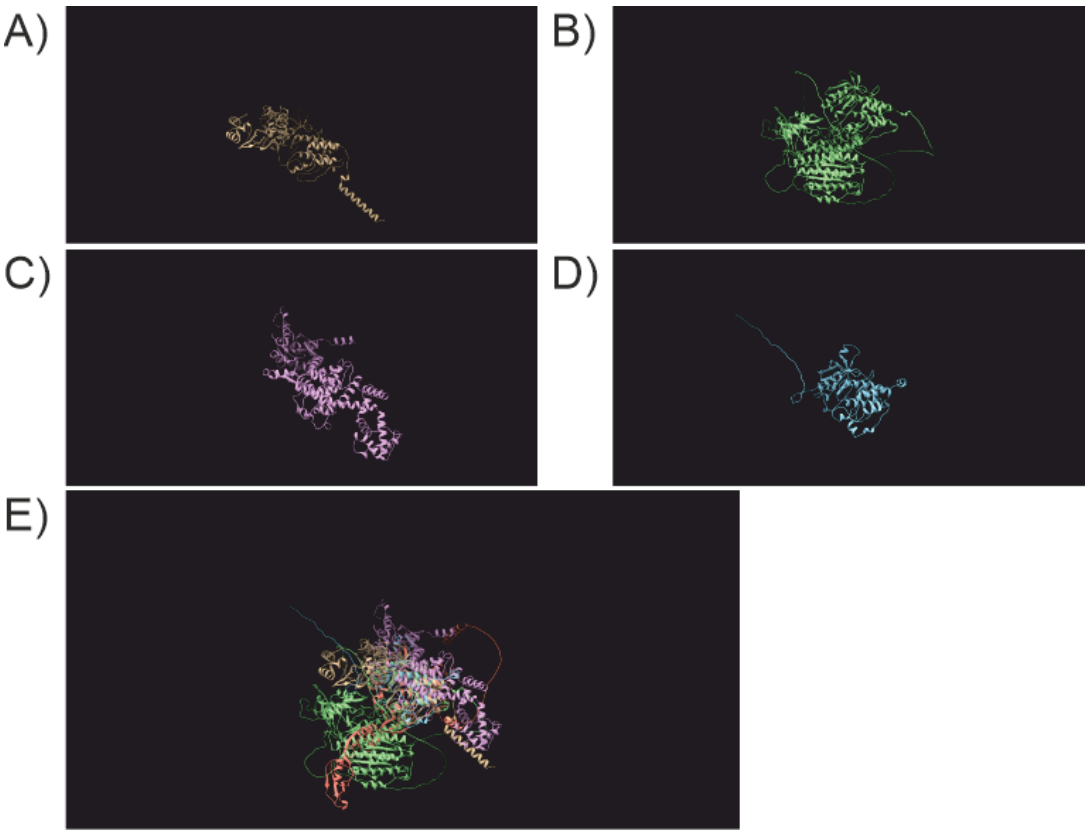

Figure 12: Structure predictions from AlphaFold show conserved and overlapping regions of their protein secondary structures. A) Pstk B) PpKA C) Stk1 D) YeaG E) Super-imposed image of all the kinases selected for study in *Pseudomonas aerugionosa*, and PknB of *Mycobaterium tuberculosis* as a root/reference (orange). The overlapping regions are mostly linked to the ATP binding sites and active sites of the kinases.

The AlphaFold structural analysis (Figure 12) also shows homology between the secondary structures of the Hanks-type domains of the kinases, with no homology in any of the other regions. It is possible that the lack of homology in the sequence and secondary structures of the kinases outside of the Hanks-type domains are what infers their specificity to their substrates.

The combined results of the alignment (Figure 11), conserved domain search and the AlphaFold analysis (Figure 12) show that the proteins/genes selected for study all have a conserved serine/threonine kinase catalytic domain that is strongly linked to a Hanks-type catalytic domain, and that they are promising targets to study for the role of translation inhibition and metabolic adaptation in *P. aeruginosa.*

2.3.2 Individual deletion mutants

Individual mutants were constructed as described in the methods section (Section 2.2). Figure 13 shows that all the gene deletions were achieved and that all PCR amplification products are the

expected size. The PpkA deletion band is much smaller due to the deletion being markerless (Mougous et al., 2007). The PpkA mutant was not achieved for PA2192 due to time constraints.

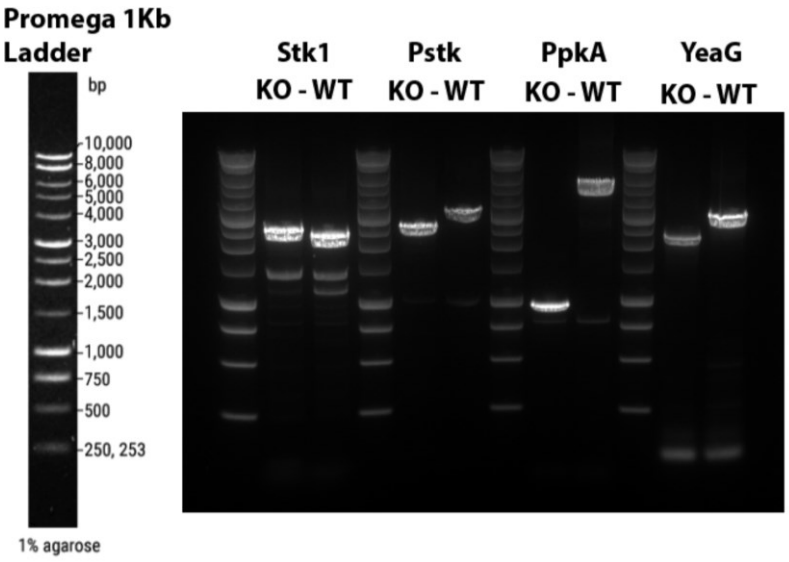

Figure 13: Gel showing the size differences of the amplified genomic area between the wild type and mutant strains, confirming that individual knockouts were achieved for PAO1. The ladder used was the '1Kb ladder' from Promega

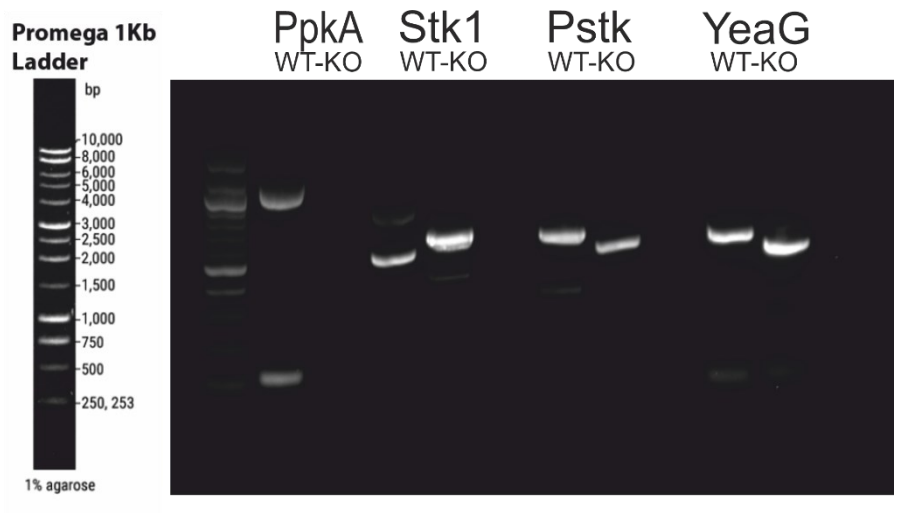

Figure 14: Gel showing the size differences of the amplified genomic area between the wild type and mutant strains, confirming that individual knockouts were achieved for PA2192, except for PpkA. The ladder used was the '1Kb ladder' from Promega

2.3.3 Multiple deletion mutants

All multiple deletion mutants were constructed as described in the method section (Section 2.2). All PCR amplification products were the expected size (Figure 15). The Stk1, PpkA and Pstk strains are markerless in the QKO mutant.

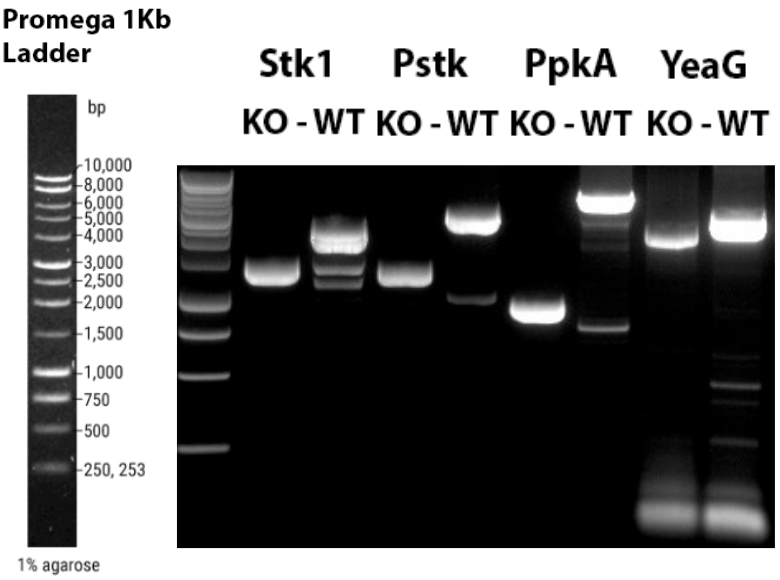

Figure 15: Gel showing the size differences of the amplified genomic regions of the quadruple deletion mutant of PAO1 compared to the wild-type strain, confirming that the deletions had been achieved in the desired location. The ladder used was the '1Kb ladder' from Promega.

In conclusion, the work in this chapter has identified four eSTK's in the genomes of *P. aeruginosa* PAO1 and PA2192 via a blast search (Table 6), multiple sequence alignment and conserved domain analysis (Figure 11) and through structural predictions provided by alphafold (Figure 12). This was followed the construction of multiple chromosomal deletion mutants of *P. aeruginosa* PAO1 and PA2192. For PAO1, all the eSTK's identified have been deleted both individually and sequentially, whereas for PA2192, it was not possible within the time frame of this project to construct the Δ*ppka* deletion mutant due to difficulties preparing the knockout fragment i.e. the flanking genomic regions and the gentamicin resistance cassette. Therefore, for PA2192 the individual mutants for the other three kinases were constructed.

Chapter 3 Phenotypic characterisation of the eSTK deletion mutant strains of *Pseudomonas aeruginosa*

3.1 Introduction

Reversible phosphorylation is a key mechanism that allows robust and rapid responses to changes in environmental conditions such as nutrient availability (Pereira, Gonzalez and Dworkin, 2015; Janczarek et al., 2018; Bhagirath et al., 2019). This is controlled by various protein kinases in bacteria, including: Histidine kinases, Tyrosine kinases, Arginine kinases, and Hanks-type (or eukaryote-like) serine/threonine kinases (eSTK's) (Janczarek et al., 2018). In *P. aeruginosa*, Sensor histidine kinases and two component systems (TCS's) are the most well studied. *P. aeruginosa* has over 60 different TCS's and have been shown to regulate several cellular functions in response to an environmental stimulus such as hypoxia or nutrient deprivation (Bhagirath et al., 2019). This is partly how *P. aeruginosa*'s metabolic versatility can be explained (Sivaneson et al., 2011). For example, the GacS/GacA TCS has been shown to regulate biofilm formation and the switch to a chronic infective phenotype (Ali-Ahmad et al., 2017; Sivaneson et al., 2011).

However, in recent years the role of hanks type serine/threonine kinases in the regulation of physiological processes in bacteria have become apparent (Cruz et al., 2014; Pereira, Gonzalez and Dworkin, 2015; Chawla et al., 2014; Sajid et al., 2011). For example, *Mycobaterium tuberculosis* has 11 eSTK's that regulate a broad range of processes. PknB alone has been found to regulate several proteins involved in physiological processes such as: Heat shock (GroEL1), Cell wall synthesis (GlmU), Oxidative stress response (SigH), and Glycogen recycling (GarA) (Janczarek et al., 2018). In particular, we are interested in the role of eSTK's in the regulation of metabolic adaptability, with particular relation to the stringent response in the nutrient deprived biofilm environment. We believe that chromosomally deleting eSTK's identified in *P. aeruginosa* will potentially prevent the regulation of metabolic processes that would usually facilitate the ability of the biofilm to be highly metabolically plastic, occupy multiple niches and form dormant cells.

In this study, we focus on elucidating the roles of four eSTK's identified via a BLAST search in *P. aeruginosa* PAO1 and PA2192, with a particular focus on biofilm development, viability and susceptibility (more details in 3.3).

3.2 Materials and Methods

3.2.1 Construction of Knockout mutants

The PAO1 PpkA mutant was generously donated by the Mougous lab (Univeristy of Washington), and the other knockouts were prepared as stated in Chapter 2.

3.2.2 Growth curves

An overnight culture of bacteria was diluted 1000-fold in LB broth (LB broth lennox Formedium). This was then aliquoted into a 96 well plate and placed in a plate reader (FLUOstar OPTIMA BMG LabTech). Measurements were taken up to every 30 minutes at 584 nm.

3.2.3 Minimum Inhibitory Concentration and Minimum Bactericidal Concentration of planktonic bacteria

The antibiotic was first prepared in a sterile water solution, diluted to a concentration in the first row of a 96 well plate and serially diluted 7 times, with the last well as a sterile water control. 20 µl from each well was transferred to a fresh 96 well plate, with 280 µl of 1:1000 overnight culture (Mueller Hinton Broth – Sigma Aldrich) of the bacteria being added to that. This was incubated statically at 37°C for 24 hours. The wells were visually inspected for growth to determine the Minimum Inhibitory Concentration. For the Minimum Bactericidal Concentration, viable cell counts were performed on the two wells with the lowest concentration showing no visible growth, and were compared to the viable cell counts of the inoculum.

3.2.4 96 well plate crystal violet assay

An overnight culture of bacteria (LB broth) was diluted 100-fold into a defined M9 medium containing 1x M9 salts (Formedium), 20 mM Glucose, 100 µM CaCl2 and 2mM MgSO4 (M9 media mix). This was then aliquoted into a 96 well plate and water added to the outer wells of the plate to help reduce evaporation. The plate was then incubated at 37°C for 24 hours and rinsed with sterile M9 salts to remove planktonic cells. If a biofilm longer than 24 hours was required, M9 media mix was added into the rinsed wells and left to incubate for another 24 hours. If the biomass of the biofilm was to be measured, 0.1% Crystal Violet (Sigma Aldrich) (CV) was added. The wells were then emptied, rinsed with water, and allowed to dry for at least overnight. Following this, the biofilm was dissolved with 30% acetic acid and absorbance of the wells measured on a plate reader at 584 nm.

3.2.5 Microfluidic flow cell setup Coverslip and device preparation

The glass coverslips were washed with 0.3% RBS 35 soap (Prepared in dH2O), rinsed with water, and then immersed in 100% ethanol for 5 minutes. This was followed by another water rinse step, 5 minutes incubation in 100% methanol, rinsing with water, then autoclaving at 121°C for 15 minutes. The microfluidic device (Channel dimensions 3 cm x 2mm x 200 µm) was constructed from PDMS, specifically, Sylgard 184 and RT cure at a ratio of 10:1. Using a 1 mm biopsy punch, holes were created at the inlet and outlet of the device channels. The device was then naturally adhered onto the glass coverslip.

3.2.5.1 Connecting the syringe pump to the device

The device was placed on a hot plate at 37°C, two needles (0.5 x 16 mm) were then broken approximately in half ensuring that the core remained intact. The sharp end of this needle was inserted into LDPE tubing (internal diameter – 0.38 mm/ external diamater – 1.09 mm), and the blunt end into either the inlet or outlet hole. The outlet tubing was then placed into a 50 ml falcon tube to collect the flow through. The inlet tubing had an intact needle inserted into it, the other end of this needle was then ultimately connected to a syringe containing the appropriate solution.

3.2.5.2 Preparing the inoculum

A Mueller-Hinton broth overnight culture is prepared from a glycerol stock and grown for 16 hours at 37°C. The overnight culture is used to inoculate M9 medium at a ratio of 1:100, containing 1x M9 salts, 5 mM Glucose, 100 µM CaCl2 and 2mM MgSO4. After growth for 16 hours at 37°C, the M9 overnight culture is centrifuged at 4000 xg for 10 minutes to pellet the cells, the supernatant poured off, and the pellet re-suspended in PBS. This is repeated, followed by diluting the solution to approximately 108 CFU's ml-1 in PBS.

3.2.5.3 Disinfecting, inoculating, and flowing media through the device

The device was disinfected by flowing through 70% ethanol at 50 µl min-1 for 5 minutes. This was followed by a wash step with sterile PBS at 50 µl min-1 for 5 minutes, then a priming step where the M9 medium (3.2.5.3) is flowed through at 50 µl min-1 for 5 minutes. The inoculum is then flowed through the device at 5 µl min-1 for 1 hour, followed by M9 media being flowed through at 5 µl min-1 for the remainder of the experiment.

3.2.5.4 Staining the biofilm with Baclight Live/Dead stain

3 µl of Propidium iodide and 3 µl of Syto 9 (BacLight Live/Dead kit) were added to 1ml of PBS. This was flowed through the device at 50 µl min-1 until the device had filled with the stain, then flow reduced to 5 µl min-1 for 15 minutes. The biofilm was then destained with PBS flowed through the device at 50 µl min-1 until the device had filled, then flow reduced to 5 µl min-1 for 15 minutes.

3.2.6 Confocal

Confocal microscopy was conducted on a Leica SP-8 confocal system using the 63x oil immersion objective. Images were taken using the Leica LasX software and firmware. The DPSS and Argon lasers were used, with initial laser power being set to 2%. Syto-9 was imaged at a wavelength of 488 nm, and propidium iodide at 561 nm. All images were taken with a resolution of 1024x1024 and each z-slice was 1 µm apart.

3.2.7 Live and dead cell quantification

The biofilm images had the background fluorescence subtracted using the background subtraction option on IMARIS (Rolling ball method). The surfaces tool was then used to identify and quantify live and dead cells in the biofilm.

3.2.8 Mean fluorescent intensity quantification

Images from 50% along the length of the channel were taken and mean fluorescent intensity calculated using IMARIS

3.2.9 Biofilm antibiotic susceptibility

Antibiotics were suspended in M9 minimal media and ran through the flow cell at 5 µl/min for six hours. Bacteria were then scraped from the channel and resuspended in PBS, followed by plating on LB for counting of viable cells.

3.3 Results

3.3.1 Growth curves of the mutant and wild type strains in LB media

96 well plate planktonic growth curve assays were used to determine the growth kinetics of the mutant strains compared to the wild type (Figure 16). Importantly, this ensures that we are inoculating with cultures that are at the correct stage of growth, and that any perceived change in the antibiotic susceptibility or biofilm phenotype of the mutant is not simply due to the bacteria growing more slowly than the wild type planktonically.

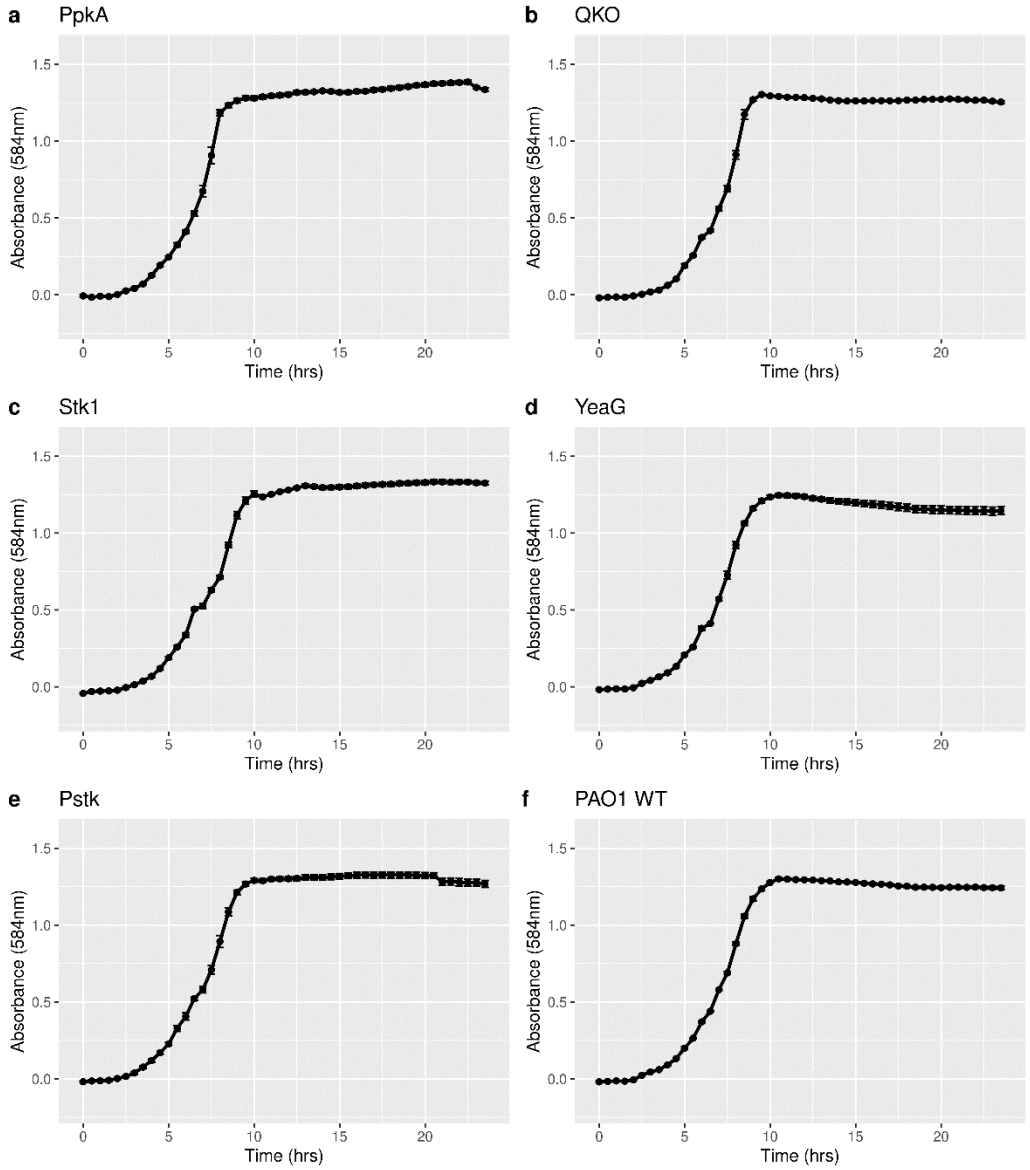

Figure 16: Absorbance readings of planktonic growth in LB media of *Pseudomonas aeruginosa* PAO1 and eSTK mutants over 24 hours to measure growth kinetics. There is no difference observed in the growth kinetics. Error bars show standard deviation. Three replicates were performed on different days

The data (Figure 16) shows no noticeable difference in the planktonic growth kinetics of the mutants compared to the wild type in nutrient rich media with PAO1. This is not necessarily unexpected in nutrient rich media with an acutely infectious strain like PAO1 due to a lack of environmental pressure.

Interestingly, the YeaG mutant of PA2192 (Figure 17) shows a delayed entry into stationary phase compared to the WT and the other mutants. WT PA2192 readily forms aggregates when growing in LB overnight cultures with shaking at 180 rpm, the YeaG mutant did not seem to form aggregates under these conditions, leading to an increase in planktonic growth.

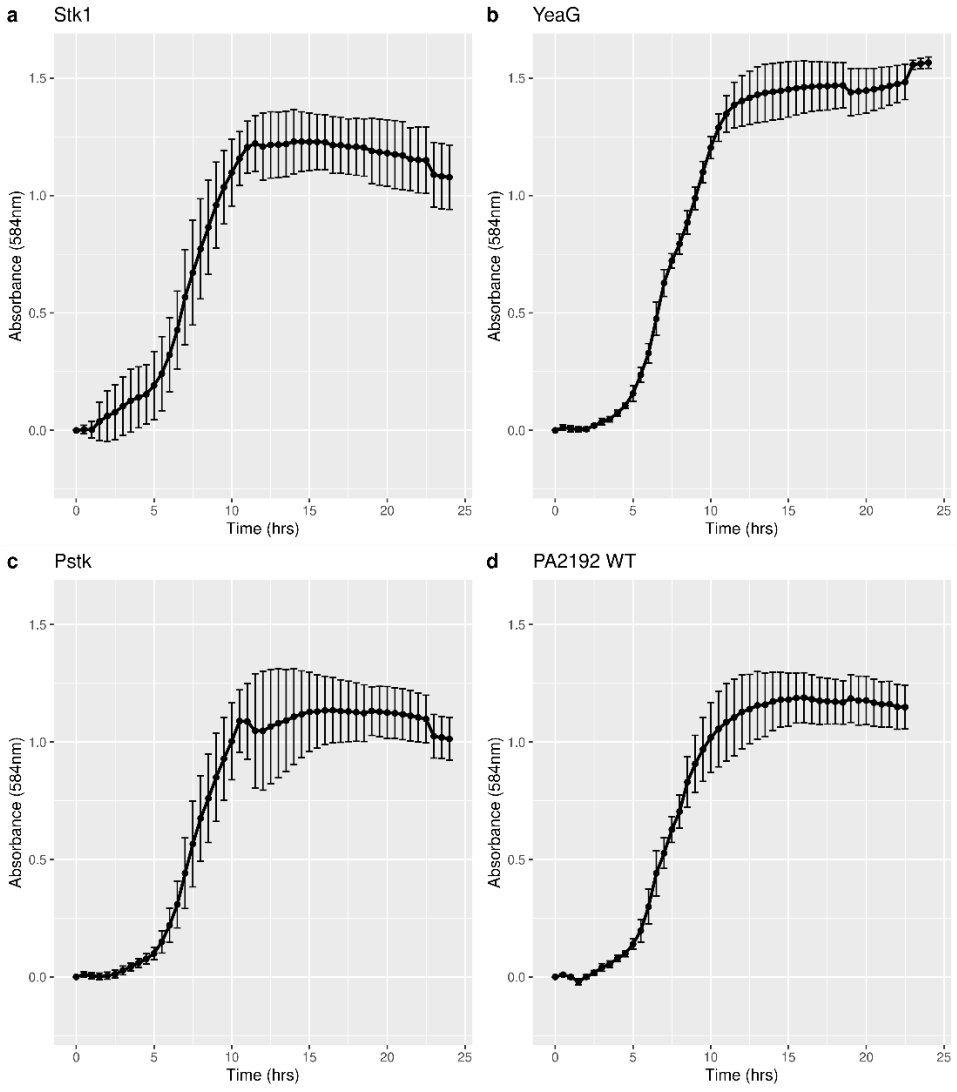

Figure 17: Absorbance readings of planktonic growth in LB media of *Pseudomonas aeruginosa* PA2192 and eSTK mutants over 24 hours to measure growth kinetics. There is an observable difference in the maximum turbidity of the sample for the YeaG mutant (b). The large standard deviation is possibly a result of mucoidy 'clumps' passing through the absorbance path at time of measuring. Error bars show standard deviation. Three replicates were performed on different days

3.3.2 Planktonic antibiotic susceptibility assays of stationary phase cultures of the wild type and mutant strains to tobramycin

MIC's and MBC's with tobramycin were performed in order to determine if there are any differences in the planktonic antibiotic susceptibility of mutants compared to the wild type (Table 7). For PAO1 the results showed that there is no change in the MIC value for the mutants compared to the wild type, and that there are no major changes in the MBC values. The Pstk and Stk1 deletion mutants show a very slight increase in the MBC, however, is not enough to say that the tolerance has increased. For PA2192 (Table 7), there were no differences at all in the planktonic susceptibility of the mutants compared to the WT. As with the planktonic growth curves, this is not necessarily unexpected as the experiment is performed in nutrient rich media that does not result in environmental stress.

Table 7: Tobramycin Minimum Inhibitory Concentrations and Minimum Bactericidal Concentrations of stationary phase planktonic *Pseudomonas aeruginosa* PAO1 WT and the eSTK mutant strains

Strain	MBC Value PAO1	MIC Value PAO1	MBC Value PA2192	MIC Value PA2192
	(µg/ml)	(µg/ml)	(µg/ml)	(µg/ml)
Wild Type	0.25	0.25	0.25	0.25
ΔPpkA	0.25	0.25	N/A	N/A
ΔPstk	0.5	0.25	0.25	0.25
QKO	0.25	0.25	N/A	N/A
ΔStk1	0.5	0.25	0.25	0.25
ΔYeaG	0.5	0.25	0.25	0.25

3.3.3 Crystal violet Assay shows no significant difference in biofilm formation between the mutants and wild type strains

96 well plate crystal violet assays were used to determine total biofilm formation of the wild type and mutant strains over 96 hours to see if there are any major outliers before moving onto more precise biofilm detection methods such as CLSM

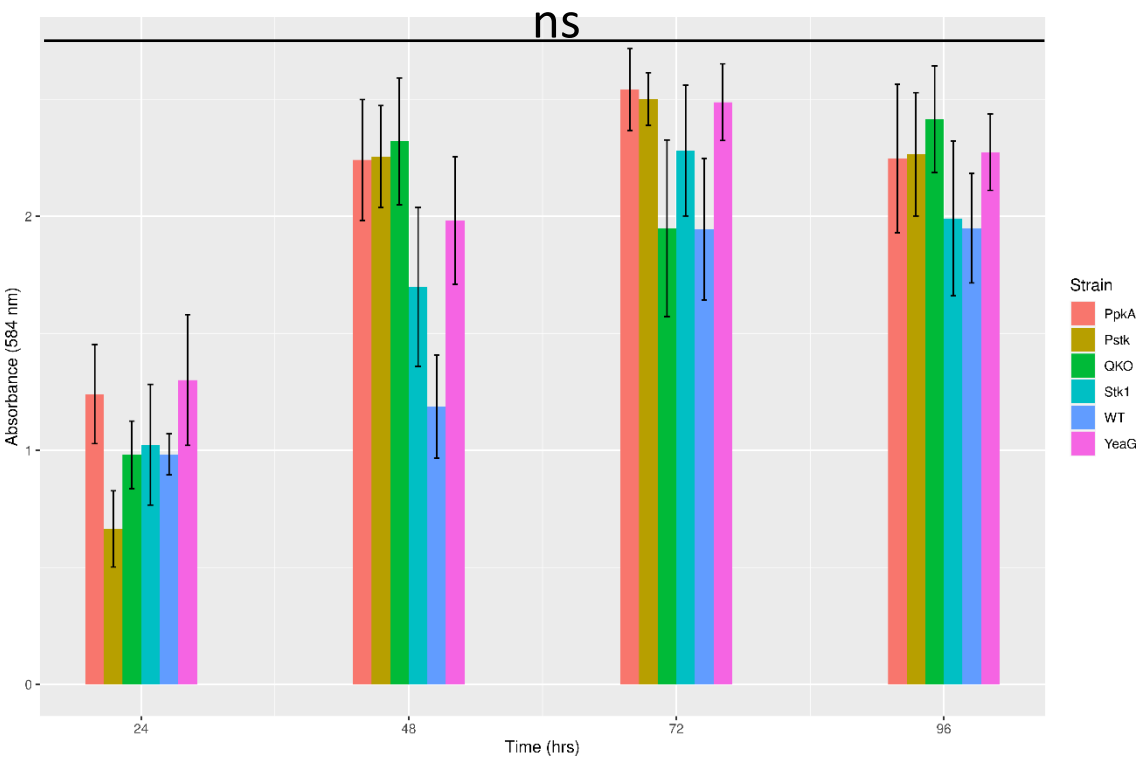

Figure 18: Absorbance readings from 96-well crystal violet staining assays to measure total biofilm formation of the *Pseudomonas aeruginosa* PAO1 strain and eSTK deletion mutants. No significant difference were observed. Error bars show standard deviation. Three replicates were performed on different days. $P < 0.05$

No significant differences were found between the strains for PAO1 (Figure 18), however, there is a significant difference at 24 hrs with the YeaG mutant for PA2192 (Figure 19). Interestingly there was no significant difference after the first 24 hrs. This makes sense when looking at the planktonic growth data in the previous section (Figure 17), it could be hypothesised that increased planktonic growth and reduced initial aggregation would result in less biofilm formation in the first 24 hours, which could be followed by a recovery. Crystal violet staining is not a sensitive assay and does not provide any information on the structure or viability of the biofilm, and as a result should only be used for screening for large differences in biofilm formation and shouldn't be the only biofilm assay used.

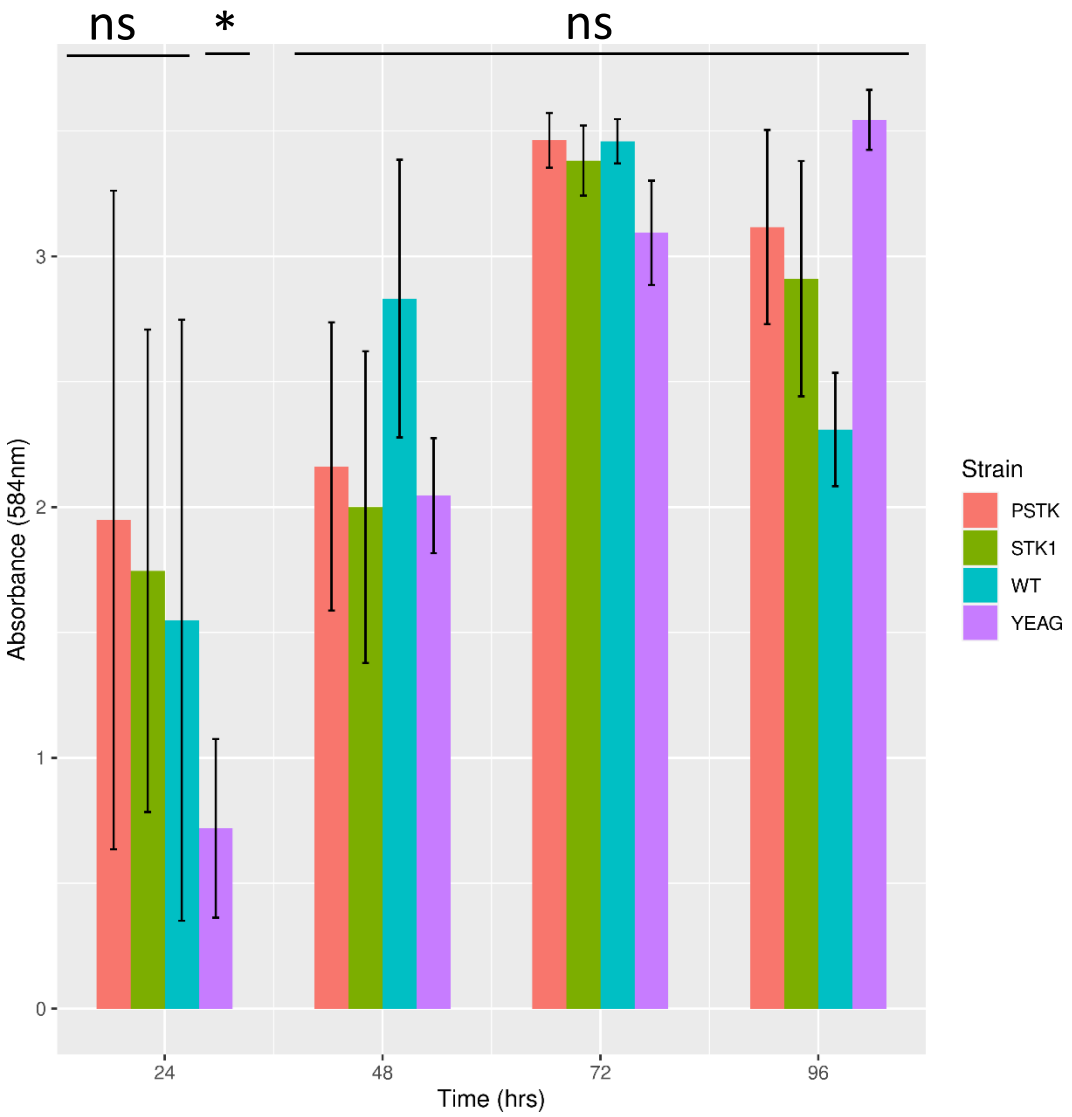

Figure 19: Absorbance readings from 96-well crystal violet staining assays to measure total biofilm formation of the *Pseudomonas aeruginosa* PA2192 strain and eSTK deletion mutants. No significant differences were observed. Error bars show standard deviation. Three replicates were performed on different days. $P < 0.05$

3.3.4 Confocal microscopy and IMARIS analysis of the wild type and knockout strains

Microfluidic PDMS devices (Figure 20) were used to grow either 24, 48, 72 and 96 hour biofilms for PAO1, or 48 + 96 hour biofilms for PA2192 for visualisation via BacLight Live/Dead stain (Green = Live, Red = Dead) and confocal microscopy. Biofilms were imaged at five points along the device, the inlet, 25%, 50%, 75% and the outlet.

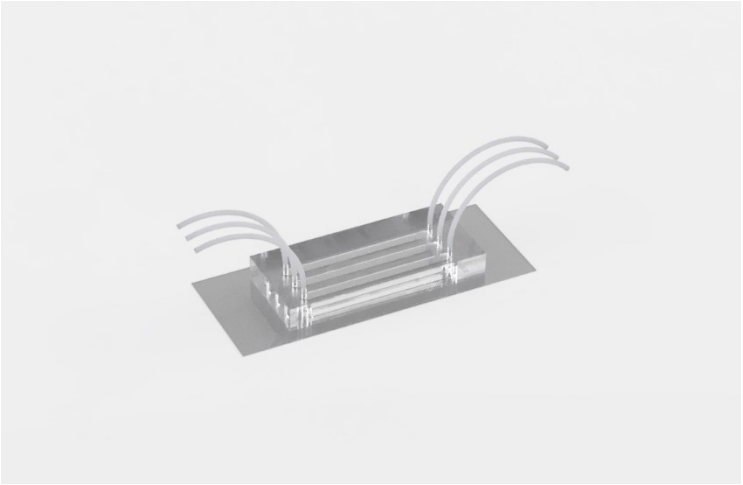

Figure 20: 3D render of the PDMS flow cell device used for growth of continuous culture biofilms. Media is flowed through at a rate of 5 µl per minute while the device is heated at 37^{o}C

3.3.4.1 Viabilty

Analysis with IMARIS shows that for the PpkA and QKO mutant of PAO1 there is a clear increase in the number of dead cells in the centre of the biofilm (Figure 24), and furthermore this phenotype becomes more evident as the age of the biofilm increases (Figure 21, Figure 22). This could be the result of the mutant biofilms being unable to respond to an induced nutrient gradient. This would normally trigger the stringent response and would have a protective effect on the cells, which may not be able to happen in the mutant strains.

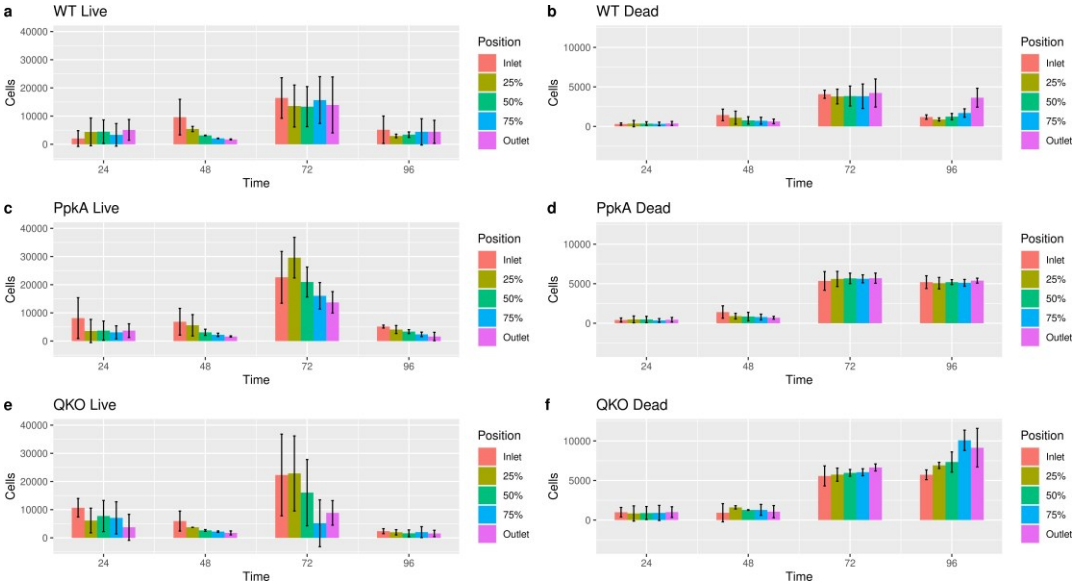

Figure 21: Longitudinal IMARIS analysis showing the Live cell count compared to the dead cell count of *Pseudomonas aeruginosa* PAO1 WT and the mutant strains in biofilms produced under flow. Three replicates were performed on different days

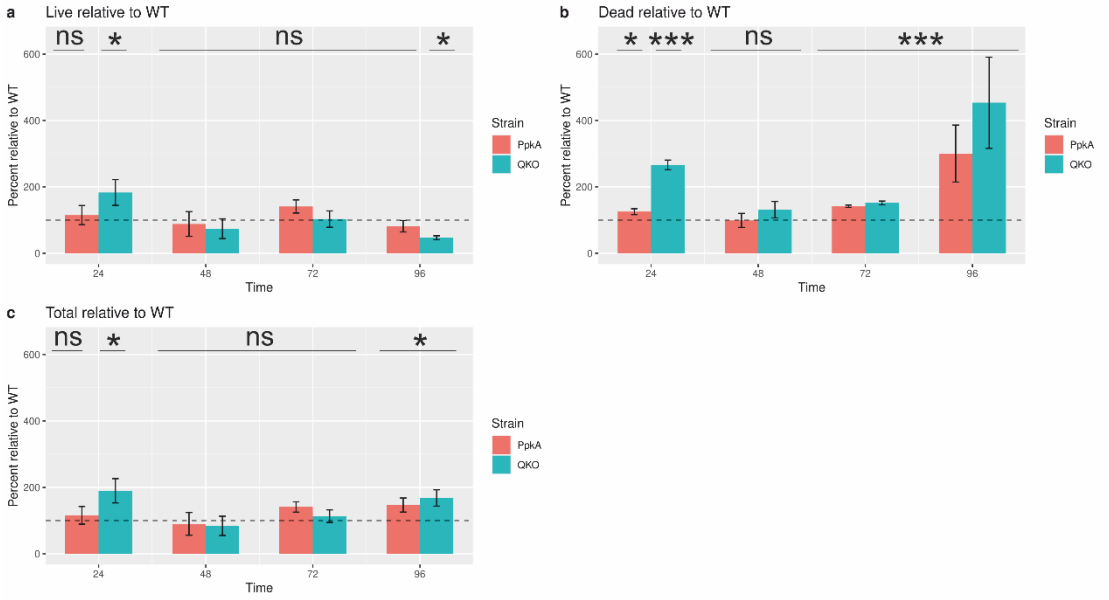

Figure 22: IMARIS analysis showing the ratio of Dead:Live biomass for *Pseudomonas aeruginosa* PAO1 WT, QKO, and PpkA. P<0.05. Error bars show SEM

The Live/Dead ratios could not be determined reliably for PA2192 due to the volume of EPS causing autofluorescence and staining of the extracellular DNA in the EPS. This is due to an issue with the thresholding, where the imaging software cannot reliably determine what information from the image needs to be subtracted. However, it is fairly clear from the images that there is no significant differences in the viability of the ΔStk1, ΔPstk and ΔYeaG mutants of PA2192.

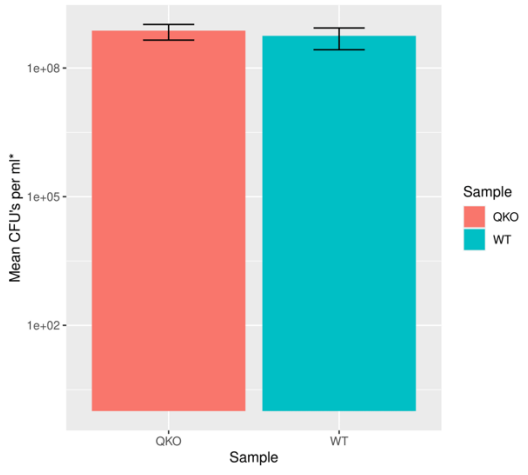

Figure 23: Viable cell counts of 96-hour biofilms of PAO1 produced under flow show no significant difference despite seeing more dead cells in the biofilm of the QKO mutant under confocal. Error bars show standard deviations. Three replicates were performed on different days

Interestingly, despite there being a significant difference in the dead and live populations of QKO at 96 hours relative to the wildtype, there is no significant difference observed when measuring the CFU's per ml (Figure 23). The lack of difference in the viability of the biofilms shown by CFU's compared to the large amount of stained dead cells reported by the confocal suggests that the cells that are stained as 'dead' are only membrane compromised. It is possible that reintroducing the membrane compromised cells to nutrient rich media such as an LB plate that was used to grow the CFU's would have a rescuing effect, preventing the compromised membrane from being terminal.

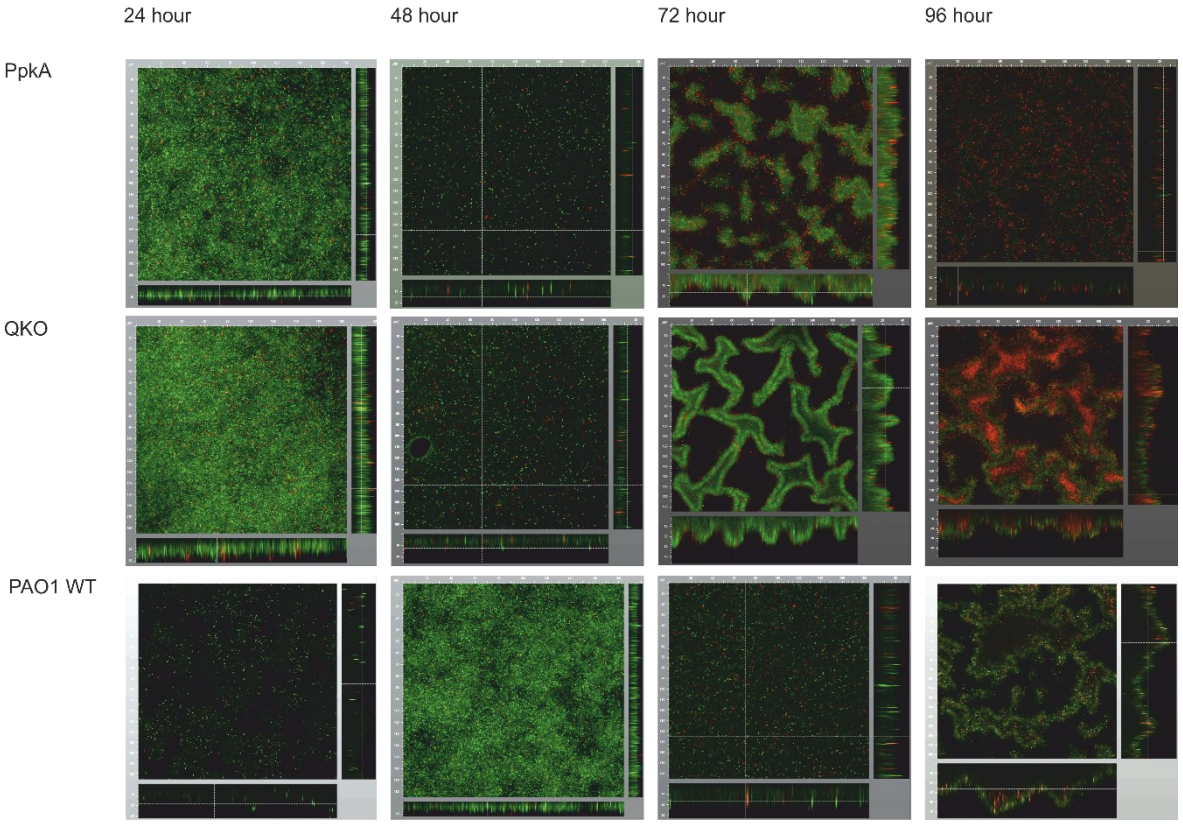

Figure 24: Confocal microscopy images of PAO1 biofilms attached to a PDMS surface and stained with BACLIGHT Live/Dead stain (Green = Live, Red = Dead). All images were taken from the outlet of the device. Three replicates were performed on different days

3.3.4.2 Biofilm matrix

For PA2192, there seems to be a reduction in the size of the thickness of the matrix in the ΔYeaG mutant (Figure 25). When this is combined with the planktonic growth curve data, it could suggest a potential decrease in the production of mucoid compounds such as alginate and psl.

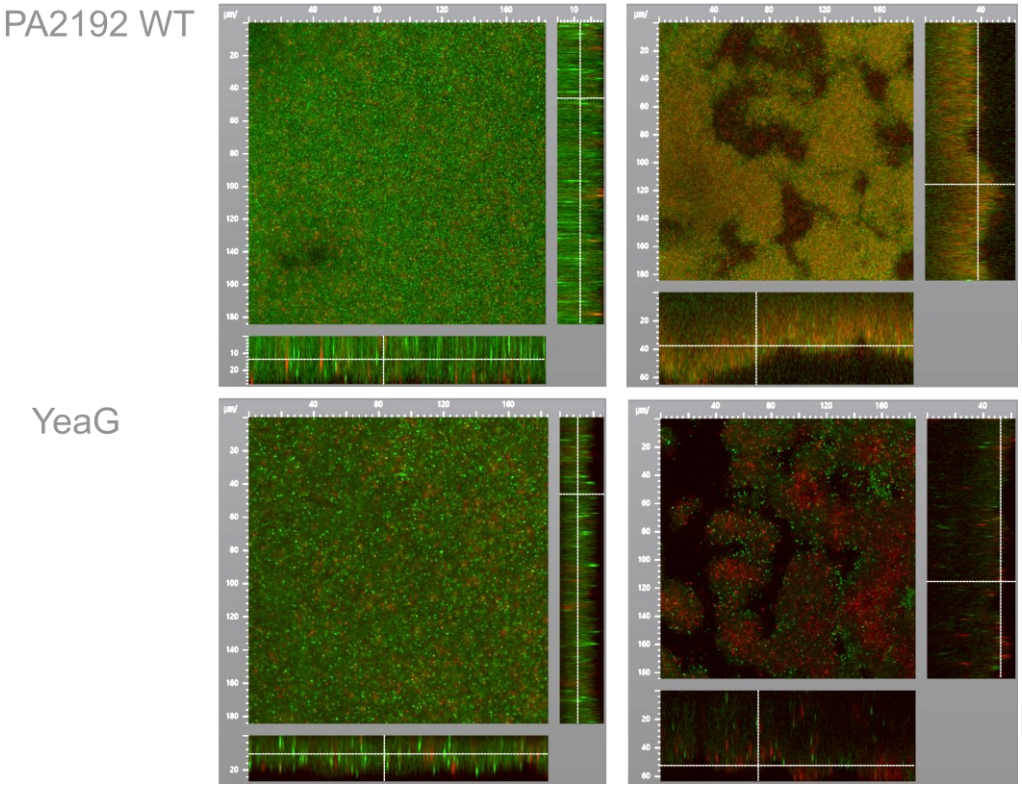

Figure 25: Confocal microscopy images of PA2192 biofilms attached to a PDMS surface and stained with BACLIGHT Live/Dead stain (Green = Live, Red = Dead). Highlighting the difference in matrix formation between the wild-type and the ΔYeaG mutant at 48 hours (left) and 96 hours (right). All images were taken from the outlet of the device. Two replicates were performed on different days

This data is supported to an extent when looking at the mean fluorescent intensities of the confocal images (Figure 26). Although the data is non-significant, this is possibly a combination of the inherent variation of biofilms and not enough replicates due to time constraints.

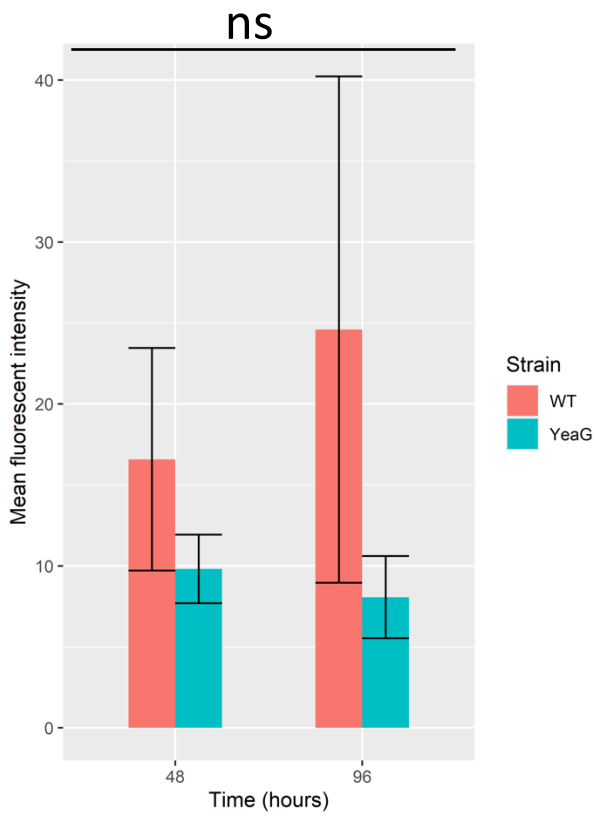

Figure 26: IMARIS analysis showing the mean fluorescent intensity values of 48-hour and 96-hour biofilms from the outlet of the device of the PA2192 wildtype and PA2192 ΔYeaG strain. Error bars show standard deviation. $P < 0.05$. Two replicates were performed on different days

3.3.4.3 Differentiation

The differentiation of the biofilm increases significantly with age in all strains, evidenced by the thickness of the biofilms, and by the water channels (Figure 27). This is to be expected, as the biofilm becomes thicker with age, it would be optimal to create more channels for nutrient uptake. Furthermore, microcolony formation would result in increased differentiation with age.

There is also a clear increase in differentiation as the distance from the inlet of the channel increases (Figure 27). This becomes more evident as the age of the biofilm increases, as this likely acts as a 'doubling up' of differentiation. The increase in differentiation is likely a result of reduced nutrient availability as moving away from the inlet, and microcolonies that have dispersed naturally from the centre of the biofilm attaching further down the channel and becoming differentiated.

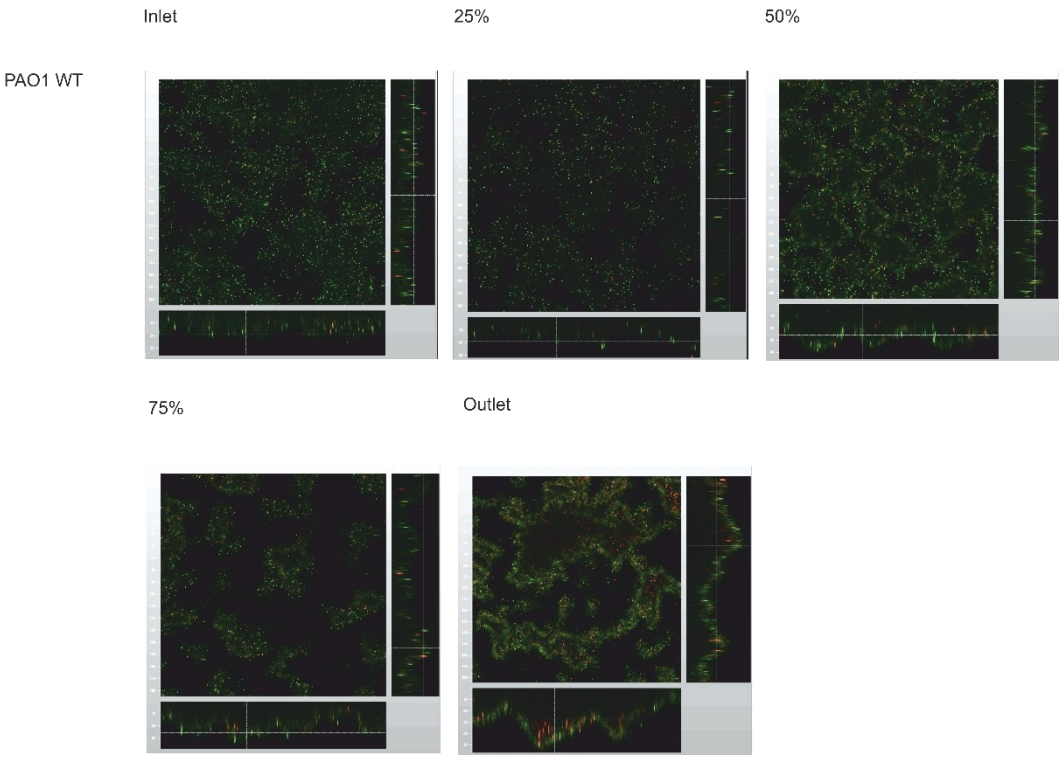

Figure 27: Differentiation down the channel of *Pseudomonas aeruginosa* PA01 biofilms on the PDMS flow cell at 96-hours. There appears to be increased differentiation with increased distance along the channel, likely due to reduced nutrient availability

3.3.4.4 Filamentation in the PpkA and QKO mutant

In the QKO and PpkA mutant, but not in the wild type strain, there are cells that have undergone filamentation (Figure 28). This is usually a stress response in bacteria and has been shown to be induced by nutritional stress, ROS and DNA damage/SOS response (Justice et al., 2008; Justice et al., 2006).

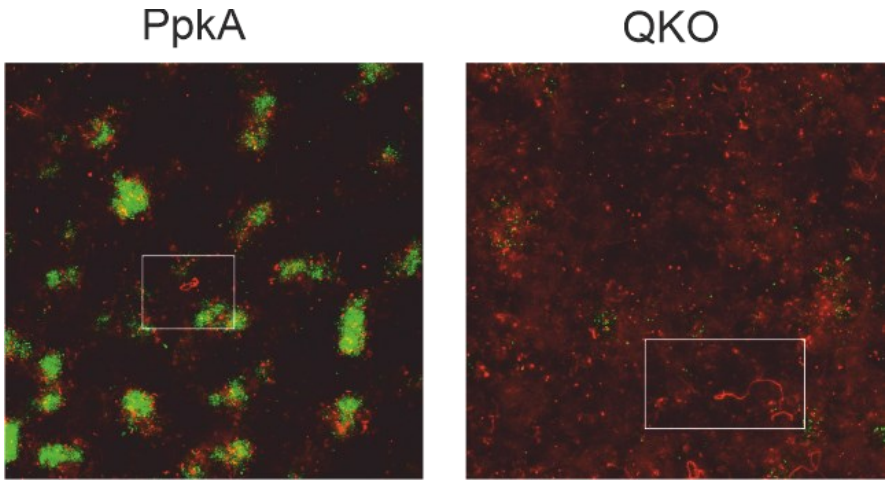

Figure 28: Filamentation of the PpkA and QKO flow cell biofilms of PAO1. Filamentation is usually the result of a stressful environment and is hypothesised to be a mechanism for a cell to occupy as many niches as possible simultaneously

3.3.5 Antibiotic susceptibility to tobramycin of the WT and QKO biofilms at 96 hours

The antibiotic susceptibility of the QKO mutant is unchanged relative to the wild type strain at all concentrations of tobramycin used (Figure 29). This is unusual when there is such a strong phenotype suggesting that the permeability of the membrane has increased. This is especially true as one of the difficulties of using tobramycin is that it usually has to be actively transported into the cell, however with a semi-permeable membrane this effect should be reduced and allow more tobramycin into the cytoplasm. It is feasible that not enough tobramycin was used to generate a significant response in the thick biofilms facilitated by the PDMS flow cells. However, there does seem to have been a 3-log reduction in the number of viable bacteria at 80 µg/ml tobramycin relative to the control, suggesting that there should be an enough of an effect to see any difference between the wildtype and QKO if there was one.

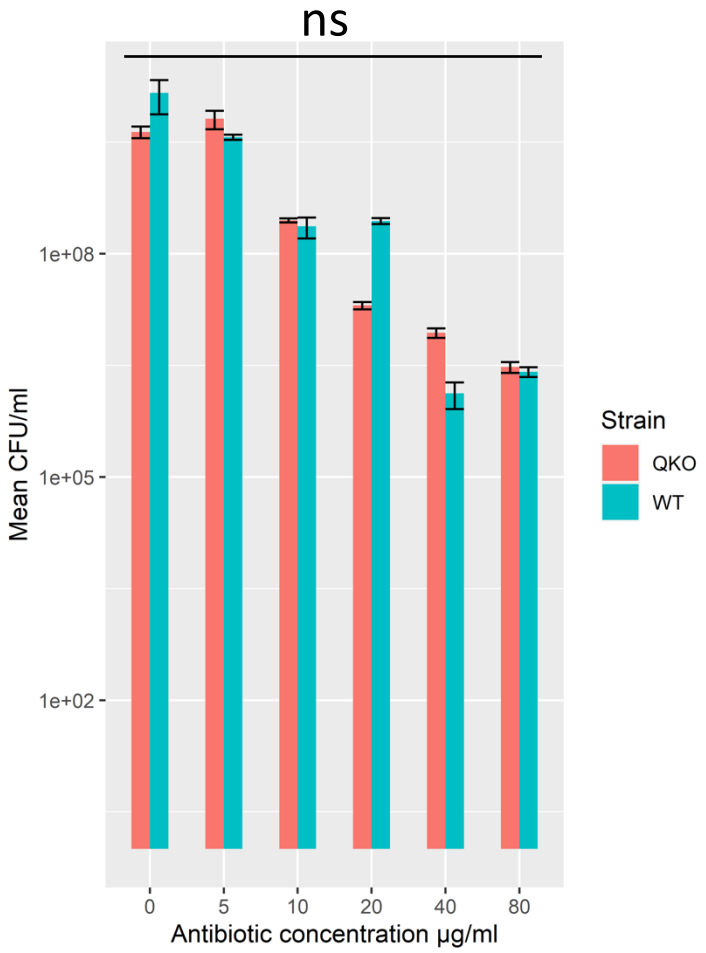

Figure 29: The antibiotic susceptibility to tobramycin of 96-hour QKO biofilms relative to the WT. There was no significant difference observed at any concentration of tobramycin despite seeing an increased amount of potentially membrane compromised cells in the QKO mutant. Error bars show standard deviation. $P < 0.05$. Three replicates were performed on different days

3.4 Discussion

The role of eSTK's in environmental adaptability of bacteria has only fairly recently started to become elucidated (Pereira, Gonzalez and Dworkin, 2015; Pereira, Goss and Dworkin, 2011; Figueira et al., 2015), and have barely been studied in *P. aeruginosa* (Goldova *et al.*, 2011; Pan *et al.*, 2017b; Zhu *et al.*, 2021a; Mougous *et al.*, 2007). It is therefore difficult to confidently infer any function to the kinases based on the phenotypes seen at this stage, however, it is possible to make some suggestions on the mechanisms based on the role of eSTK's in other bacteria.

There were no significant differences in the planktonic growth kinetics (Figure 16, Figure 17) or the planktonic antibiotic susceptibilities (Table 7) between the wildtype and mutant strains of PAO1 or PA2192. This suggests that either the kinases are only relevant in the biofilm phenotype, or that they are only relevant in environmentally harsh conditions, as opposed to the high nutrient Mueller Hinton or LB broth. While it has been shown that eSTK's can respond to environmental triggers in bacteria, such as YabT in *B. subtilis* which has shown to be part of a trigger in sporulation from the mother cell in harsh environmental conditions (Pereira, Gonzalez and Dworkin, 2015) and YeaG in *E. coli* which adapts to sustained nutrient deprivation (Figueira et al., 2015), and that they can be upregulated in the biofilm (Varadarajan et al., 2020) there is also significant evidence to show that eSTK's are relevant in regulating processes that are critical for normal planktonic survival (Chawla et al., 2014; Janczarek et al., 2018; Gaidenko, Kim and Price, 2002) such as cell wall synthesis by PknB (Chawla et al., 2014). Because no differences were seen in the planktonic data, it may suggest that eSTK's have a smaller role to play in the planktonic phenotype in *P. aeruginosa* than in other bacteria. However, there is a difference in the planktonic growth kinetics of the YeaG mutant in PA2192 (Figure 17). This could be due to a difference in the essential genes of acute and chronic strains, such as PAO1 and PA2192 respectively. It is possible that a chronic strain that relies less on being virulent, and more on biofilm formation and longevity would be more reliant on the genes controlled by YeaG to tightly regulate planktonic growth.

Furthermore, it is notable that no significant differences were seen in the crystal violet assay for PAO1 (Figure 18), despite previous studies linking the PpkA mutant to reduced biofilm formation (Pan et al., 2017a). This is possibly due to the different methods employed by Pan et al to produce the biofilms. They used LB media and no shaking in their assay, whereas we used a defined M9 medium and shaking at 50 rpm. For PA2192 there only seems to be a difference at 24 hrs for the YeaG mutant (Figure 19). This is likely the result of reduced aggregation of cells and a slower switch into the biofilm phenotype. This conclusion is supported by the growth curve data which shows an increase in planktonic growth relative to the wildtype strain (Figure 17).

The confocal images combined with IMARIS analysis show that there is a greater ratio of Live/Dead biomass in the ΔPpkA mutant and QKO mutant than in the wildtype for PAO1 (Figure 22). It is likely that the PpkA deletion is responsible for the greater dead biomass in the QKO mutant, however, it is possible that there is a stronger phenotype in the QKO mutant due to the theoretical redundancy of targets of eSTK's (Pereira, Goss and Dworkin, 2011). This could mean that a single deletion mutant would simply result in the upregulation of another kinase to counter act this deletion, and that therefore, the QKO mutant would potentially result in the bacterium not being able to sufficiently upregulate another kinase.

For PA2192, there does not appear to be a change in the viability of the mutant biofilms relative to the wildtype. However, based on the images (Figure 25) and mean fluorescence intensity (Figure 26) there appears to be a reduced thickness of the biofilm matrix. This could be a result of reduced mucoid compounds that promote adhesion and the biofilm phenotype, such as alginate. This is supported in principle as non-clinical isolates such as PAO1 usually rely on PSL as the main component of their matrix, whereas clinical isolates, especially from CF, have been shown to upregulate alginate production (Franklin et al., 2011; Irie et al., 2017). Seeing as there is no phenotype in the ΔYeaG mutant of PAO1, but there is a reduction in initial aggregation of ΔYeaG in PA2192, it is sensible to assume that this could be linked to alginate production.

There is no difference in the antibiotic susceptibility to tobramycin of the 96-hour biofilms of the QKO mutant relative to the wildtype at all the concentrations tested (Figure 29). This does not seem to be reflective of the clearly stressed biofilm culture and suggests that either the compromised membrane phenotype that has been observed is not relevant to the increased uptake of tobramycin, or that there are other mechanisms that are counteracting the potentially increased uptake of tobramycin. Tobramycin is an aminoglycoside that ultimately targets the 30S ribosome, so it is possible that ribosomal proteins have been downregulated in response to severe nutrient starvation, reducing the effectiveness of tobramycin. This would be counter to the hypothesis that eSTK's would prevent the downregulation of translational machinery via preventing the induction of the stringent response due to nutrient starvation.

The filamentation in the PpkA and QKO deletion mutant (Figure 28) is likely to also be primarily the result of the single PpkA deletion. Previous studies have shown PpkA to be critical in the adaptation and resistance of *P. aeruginosa* to oxidative stress and osmotic stress (Goldova et al., 2011; Pan et al., 2017a), oxidative stress in particular has been shown to induce DNA damage and the SOS response, which can in turn lead to filamentation (Justice et al., 2008; Justice et al., 2006). While the role of PpkA in oxidative stress resistance is likely responsible for the increased dead cells and filamentation, it is tempting to consider that these may be due in part to *P. aeruginosa* not being able to effectively regulate starvation responses, as a result of reduced metabolic

plasticity due to dysregulation of intracellular signalling. However, this would need to be proven experimentally and will be discussed in Chapter 4.

In conclusion, it has been shown that eSTK's are relevant to biofilm formation in both PAO1 and PA2192. In PA2192 there appears to be a reduction in the production of mucoidy compounds such as alginate that make up the biofilm matrix, reducing initial biofilm formation and potentially reducing mature biofilm matrix thickness. In PAO1, a degenerative membrane compromised phenotype has been observed that suggests significant dysregulation of intracellular processes over time, alluding to our hypothesis of eSTK's being essential for metabolic adaptability in mature biofilms being correct.

Chapter 4 Investigating the proteome of the QKO mutant relative to wildtype PAO1

4.1 Introduction

After determining that in PAO1 there was a strong phenotype showing significantly more dead cells in the centre of the biofilm of the PpkA and QKO mutant (Figure 24), it was decided that proteomics and phosphoproteomics would be employed to attempt to determine which biological pathways were causing this phenotype. Due to the significant cost involved with this type of analysis, only QKO and the wildtype strain were studied.

Nanoflow liquid chromatography tandem mass spectrometry (LC-MS/MS)-based quantitative proteomics and phosphoproteomics has facilitated major new discoveries in cell biology. This is driven in part by improvements in MS instruments, phosphoproteomic enrichment protocols, and computational tools and algorithms used to determine protein identity and phosphopeptide sites (Hogrebe et al., 2018; Altelaar et al., 2013). However, another important aspect of proteomics and phosphoproteomics is which labelling strategy you use. There are three approaches that can be used for labelling proteins or peptides for mass spec purposes (Altelaar et al., 2013; Hogrebe et al., 2018):

- Stable isotopic labelling with amino acids in culture (SILAC)
- Label free quantification (LFQ)
- Isobaric labelling (TMT/ITRAQ)

The simplest of these methods is LFQ, which involves no labelling of the sample. LFQ is arguably the most common choice for standard shotgun proteomics as it can relatively easily be performed by amateurs and the data analysis is simple. However, it has been found that even with recent advancements in LFQ, it is the least suitable method for phosphoproteomics due to lower precision and no possibility for multiplexing (Hogrebe et al., 2018; Altelaar et al., 2013).

SILAC has been the most used approach for phosphoproteomics over the last decade. This is mostly due to the enhanced sensitivity you get over LFQ which allows for easier identification of phosphopeptides. It involves metabolically labelling certain samples with heavy labelled lysine or arginine in culture. There is an argument that labelling as early as possible reduces variation in the labelling of the samples (Altelaar et al., 2013), however metabolic labelling can be a complex

process. In order to use SILAC effectively, you must remove the ability of the host cell to create its own lysine and arginine. This prevents mixing of light and heavy amino acids in the proteins you are trying to analyse. There are fundamental issues with this, mainly that you must first construct knockouts of at least either the lysine or arginine pathway, and that doing this may alter the phenotype of the organism you are trying to study (Altelaar et al., 2013; Hogrebe et al., 2018; Chua et al., 2016).

While the most used method for proteomics is LFQ and for phosphoproteomics is SILAC, isobaric labelling strategies such as ITRAQ and TMT have recently risen in popularity for both (Altelaar et al., 2013; Chahrour, Cobice and Malone, 2015). Isobaric labelling is performed on peptides (i.e. after protein extraction and digestion) and so there is no need to delete genes to use this method. Furthermore, TMT has been shown to have the lowest deviation in labelling efficiency of the three techniques (Hogrebe et al., 2018) and has the highest capacity for multiplexing (11-plex for TMT compared to 7-plex for SILAC at time of writing). Samples that are multiplexed will not suffer from mass-spec run variation as opposed to LFQ samples.

No studies have been done on the proteome and phosphoproteome of mutants of eukaryote-like serine/threonine kinases in *P. aeruginosa*. Of particular interest is stringent response and translation proteins, and proteins that are linked to antibiotic resistance or tolerance. This chapter will show that dual SILAC labelling with *P. aeruginosa* is not advisable due to the disruption of that arginine pathway and its effect on growth and biofilm formation, and that using TMT analysis to analyse the proteomes of biofilm, planktonic, and planktonic cultures treated with serine hydroxamate (to induce the stringent response), it was possible to begin to allude to the mechanism leading to the phenotype that we saw in chapter 3.

4.2 Materials and methods

4.2.1 Construction of mutants for SILAC

Mutants were constructed using the methodology described in chapter 2

4.2.2 Strains used for this chapter

Table 8: Strains and plasmids used in this chapter

	Strains/ Plasmids	Characteristics/reference	Source
Pseudomonas aeruginosa			
PAO1		Reference strain with moderate drug Resistance (Mougous et al., 2007)	Mougous lab
	ΔPstkΔPpkAΔStk1ΔYeaG	Referred to as QKO	This Study
	ΔLysA	Auxotrophic for lysine	This study
	ΔArgH	Auxotrophic for arginine	This study
	ΔLysAΔArgH	Double auxotrophe for arginine and lysine	This study
Escherichia coli			
	DH5-α	sup E44, ΔlacU 169(ΔlacZΔM 15), recA1, endA1, hsdR17, thi1, gyrA96, relA1, Δpirphagelysogen.	
	S-17	TpR, SmR, recA, thi, pro, hsdR-M+RP4: 2Tc:Mu: Km Tn7 Δpir.	
Plasmids			
	pEX100T	Gateway compatible gene replacement Vector with ampicillin resistance (Quenee, Lamotte and Polack, 2005)	
	pFLP3	Expresses FLP recombinase	

4.2.3 Primers used for this chapter

Table 9: Primers used in this chapter

Oligo name	Sequence	Bases
Gm-Frt-F	ATGC GAATTC AGCTCGAATTGGGGATCTT	29
Gm-Frt-R	ATGC AAGCTT CTCGAATTAGCTTCAAAAGCGC	32
LysA-Up-F	ATG CCC CGG GTC CAG GTC GCT GTC ATC	27
LysA-Up-R	ATG CGA ATT CGG CGC TCT CTC AGA AAC	27
LysA-Dwn-F	ATG CAA GCT TCC CAG ACC ATG CTT TTG	27
LysA-Dwn-R	ATG CCC CGG GCA CGC CAT GGG GAT T	25
ArgH-Up-F	ATG CCC CGG GGA TAC AGA TTG ACC TCG CC	29
Argh-Up-R	ATG CGA ATT CGG TAT CTC TCG CTG CAA C	28
ArgH-Dwn-F	ATG CAA GCT TTT TCT CCA CCG CCA	24
Argh-Dwn-R	ATG CCC CGG GAT CGA AGC CTA TTA CCG	27

4.2.4 Growth curves for SILAC strains

Growth curves for the validation of the SILAC strains were identical as in Chapter 2, with the exception of adding exogenous L-arginine in some instances.

4.2.5 Growth curves for validation of planktonic growth conditions in M9 media with serine hydroxamate

Mueller-Hinton broth overnight cultures were washed and resuspended in PBS. A 1:100 dilution of this was used to create a 20 ml culture in minimal M9 medium (the same recipe used in feeding the biofilm (see chapter 2)). Cultures were allowed to grow for 26 hours, with relevant cultures treated with SHX at a final concentration of 200 µ m at 6 hours. Absorbance reading were taken using a manual spectrophotometer at 600 nm.

4.2.6 Growth conditions for microfluidic biofilms

Biofilms were grown for 96 hours. The exact culture conditions were identical as previously described in chapter 2 for flow cell biofilms

4.2.7 Growth conditions for planktonic cultures

Mueller-Hinton broth overnight cultures were washed and resuspended in PBS. A 1:100 dilution of this was used to create a 20 ml culture in minimal M9 medium (the same recipe used in feeding the biofilm (see chapter 2)). Cultures were allowed to grow for 26 hours, with relevant cultures treated with SHX at a final concentration of 200 µ m at 6 hours.

4.2.8 Protein extraction

For the biofilm the microfluidic PDMS chip was removed from the glass coverslip and the biofilm scraped into 990 µl HBSS + 10 µl Phosphatase inhibitor using a sterile tip. The planktonic cultures were spun at 4,000 xg for 10 mins, supernatant removed, and resuspended in 990 µl HBSS + 10 µl Phosphatase inhibitor.

The samples were then washed twice by spinning at 10,000 xg for 5 minutes, then resuspending in 990 µl HBSS + 10 µl Phosphatase inhibitor. The bacteria were then lysed using a combination of chemical lysis and freeze/thaw by resuspending in 990 µl 7 M urea, 2 M thiourea, 35 mM CHAPS, 20 mM DTT, 1M NaCl, 10 µl phosphatase inhibitor, and freezing at -80°C for 30 minutes followed by thawing at 34°C for 20 minutes.

4.2.9 Protein precipitation

The following were combined in a 1:8:1 ratio:

- 1 mL cell lysate
- 8 mL 100% ice-cold acetone
- 1 mL 100% trichloroacetic acid (100% TCA w/v)

This was then kept at -20°C for 1 hour, before being centrifuged at 20,000 xg for 10 minutes at 4°C. The supernatant was then discarded, and the pellet washed twice with ice-cold acetone using the same conditions as above. After this, the pellet was allowed to air dry at room temperature and was ultimately resuspended in 500 µl of 100 mM TEAB + 0.1% Rapigest and 5 µl phosphatase inhibitor.

4.2.10 Protein digestion

Dithiothreitol was added to the extracted proteins at a final concentration of 2 mM, this was then incubated at 60°C for 45 minutes. After being allowed to cool to room temperature, iodoacetamide was added at a final concentration of 6 mM and was incubated in the dark for 45 minutes at room temperature. Trypsin was added at a ratio of 1/50 of the sample weight, and then incubated overnight at 37°C.

4.2.11 Quantification of extracted proteins and peptides

Proteins and peptides were quantified using the direct detect spectrophotometer.

4.2.12 Phosphopeptide enrichment

Phosphopeptides were enriched using pierce TiO2 spin tips following manufacturers instruction.

4.2.13 Labelling of peptides using TMT

Peptides were labelled using the TMT 10-plex kit following manufacturer's instructions, with the exception of only using 10 µl of TMT reagent to label 25 µg of peptide for whole proteome analysis, and 2 µl of TMT reagent for labelling of phosphopeptides to save costs. Up to 8 samples were then combined and cleaned up using the Oasis PRIME HLB µElutionPlate to carry forward into LC MS/MS.

4.2.14 Liquid chromatography Mass spectrometry

Peptide extracts (1 µg on column) were separated on an Ultimate 3000 RSLC nano system (Thermo Scientific) using a PepMap C18 EASY-Spray LC column, 2 µm particle size, 75 µm x 75 cm column (Thermo Scientific) over a 240 min (single run) linear gradient of 3–25% buffer B (0.1% formic acid in acetonitrile (v/v)) in buffer A (0.1% formic acid in water (v/v)) at a flow rate of 300 nL/min. Peptides were introduced using an EASY-Spray source at 2000 V to a Fusion Tribrid Orbitrap mass spectrometer (Thermo Scientific). Each analysis was performed using the MultiNotch MS3-based TMT acquisition method (McAlister et al., 2014). The ion transfer tube temperature was set to 275°C. Full MS spectra were recorded from 300 to 1500 m/z in the Orbitrap at 120,000 resolution with an automatic was performed using TopSpeed mode at a cycle time of 3 s. Peptide ions were isolated using an isolation width of 1.6 amu and trapped at a maximal injection time of 120 ms with an AGC target of 300,000. Higher-energy collisional dissociation (HCD) fragmentation was induced at an energy setting of 28 for peptides with a charge state of 2–4. Fragments were analysed in the orbitrap at 30,000 resolution. Following acquisition of each MS2 spectrum, MS3 spectra were collected using the MultiNotch MS3 acquisition strategy.

4.2.15 Analysis of raw files for whole proteome and phosphoproteome analysis using MaxQuant

Raw files were analysed using MaxQuant. The group-specific settings were setup to quantify peptides that were identified through MS3 10-plex TMT labelling. The group settings used were:

Type: MS3

Digestion: trypsin/P

Modifications: oxidation, N-terminal acetylation

Match between runs was also switched on which improves the number of peptides identified. The PAO1 reference strain fasta file was obtained from Uniprot.

4.2.16 Statistical analysis

Data were first normalised using the quantile normalisation function inside perseus (using R backend) and were then log2 transformed. The rest of the analysis then varied depending on the next step.

Differential expression analysis

The proteins were then compared by doing a fold change analysis (dividing one condition by the other) and performing individual t-tests on all proteins that were present in both samples. A false discovery rate was not used. Proteins that had a greater than a 1.5 log2 fold change and P-value of >0.05 were selected for further study

WGCNA

WGCNA analysis was carried out using the WGCNA package in R

4.3 Results

4.3.1 Deletion of the ArgH gene of *Pseudomonas aeruginosa* results in a death phase upon entry into stationary phase of planktonic growth

In order to use SILAC effectively as a labelling strategy, it was first necessary to disrupt the arginine and lysine synthesis by deleting the terminal genes from their respective biosynthesis pathways.

Deleting LysA (the terminal gene in lysine biosynthesis) was well tolerated by the cell, provided that lysine was present in the media. However, when deleting ArgH (the terminal gene in arginine biosynthesis), instead of the culture going into stationary phase, there is a significant drop in optical density seen that is likely caused by cell death (Figure 30). This is possibly caused by the switch from aerobic into anaerobic respiration as the culture moves into the anoxic stationary phase. L-arginine can be fermented to use as a carbon source in anoxic conditions (Borriello et al., 2006). Stationary phase can be recovered by supplementing the media with 12mM arginine, re-enforcing the importance of arginine as an energy source in stationary phase. This phenotype was also demonstrated in the ΔLysA + ΔArgH double mutant as this is the strain that would have been used as part of the proteomics experiment.

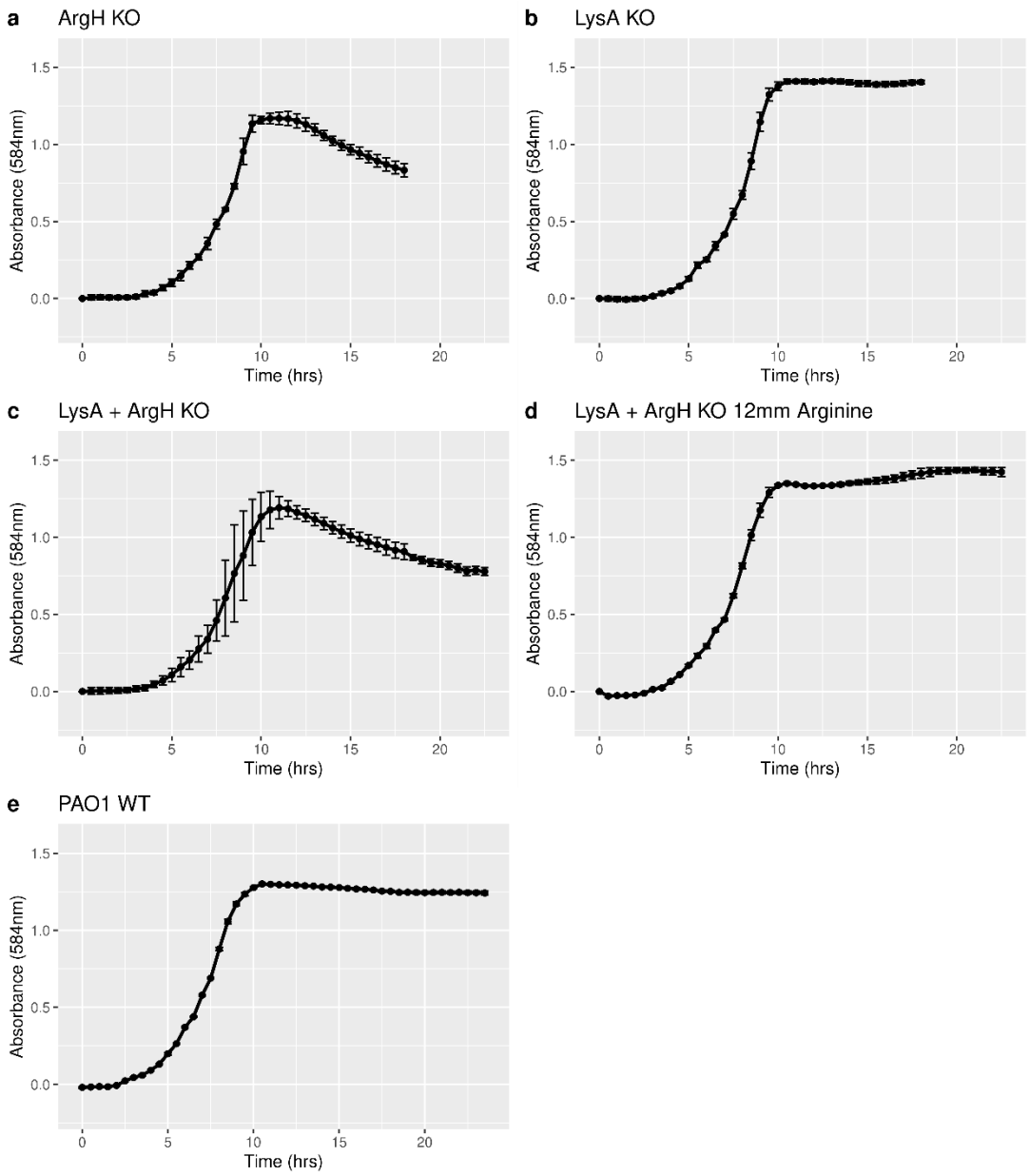

Figure 30: Planktonic growth of lysine and arginine auxotrophic mutants in LB. The lysine auxotrophic mutant shows regular growth kinetics when compared to the wild type, however the arginine auxotroph shows a significantly increased death phase that is restored when additional L-arginine is added. Error bars shows standard deviation. Three replicates were performed on different days

4.3.1.1 Addition of exogenous L-arginine leads to significantly increased biofilm formation

After determining that it is possible to planktonically grow a dual LysA + ArgH deletion mutant, it was necessary to see how the mutant would respond to growing as a biofilm with the amino acids added exogenously. There is a clear phenotype showing that the addition of exogenous L-lysine and L-arginine greatly increases biofilm formation (Figure 31). This is likely due to providing a carbon source to the anoxic parts of the biofilm through fermentation of L-arginine, resulting in significantly increased growth in those areas (Borriello et al., 2006)

Due to the phenotypes seen when adding exogenous amino acids, it was decided that dual labelled SILAC would not be a suitable way forward with *P. aeruginosa*. Instead, TMT 10-plex labelling was used, which does not require genetically altering the strains in any way.

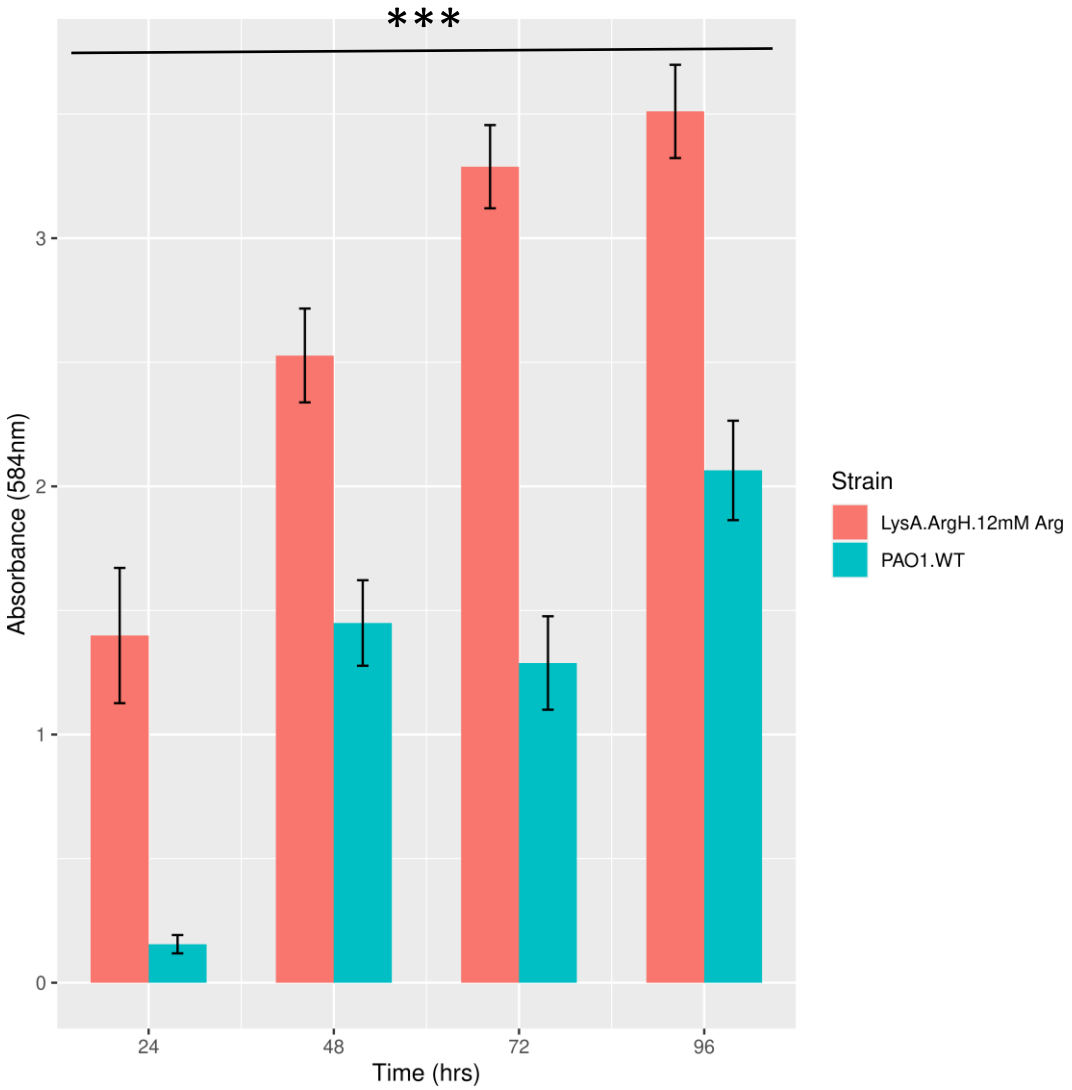

Figure 31: Lysine + arginine double auxotrophic mutant 96-well crystal violet biofilm formation assay with exogenous 12mm L-arginine. A significant increase in biofilm formation is observed at all time points, likely due to increased growth of anaerobic parts of the biofilms. Error bars show standard deviation. $P < 0.05$. Three replicates were performed on different days

4.3.2 Characterisation of the planktonic growth of the wildtype and quadruple KO mutant of PAO1 in M9 media with and without SHX

In order to validate that serine hydroxamate would induce stationary phase in both strains planktonic growth kinetics were examined (Figure 32).

P. aeruginosa wild type and QKO were grown in M9 minimal media for 26 hours, with the SHX being introduced at 6 hours when necessary. There is a clear reduction in growth when treated with SHX in both strains.

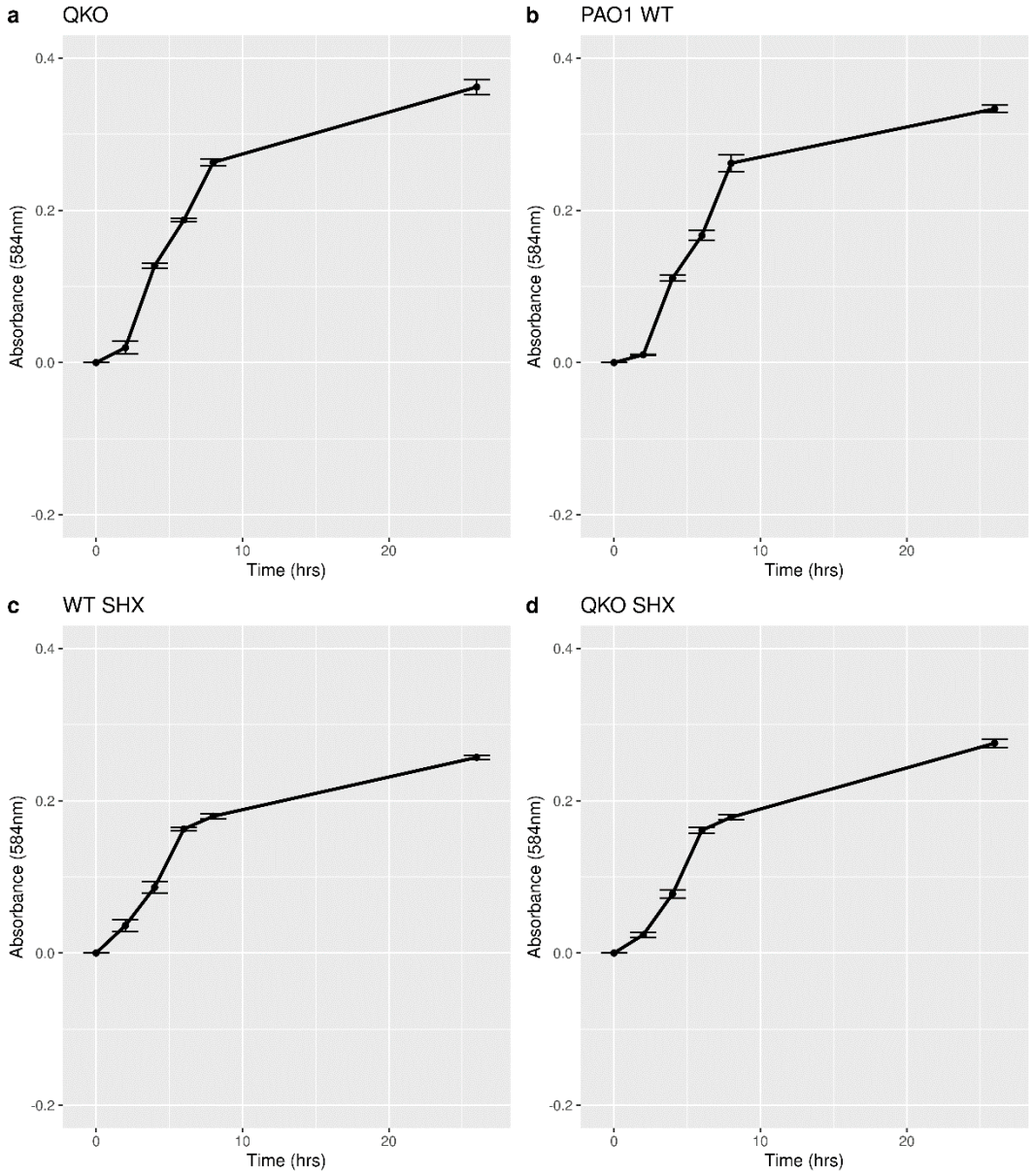

Figure 32: Planktonic growth kinetics of PAO1 (WT) and the QKO deletion mutant with and without SHX in M9 growth media. Cessation of growth is induced in response to SHX treatment in both QKO and the wild type. Error bars show standard deviation. Three replicates were performed on different days

4.3.3 DirectDetect quantification of extracted protein, peptide and phospho-peptide

DirectDetect shows that protein extraction and digestion into peptides was successful (Figure 33). It is difficult to determine at this stage whether the phospho-peptide enrichment was successful, however you would normally expect to enrich roughly 1% of the total amount of starting peptide.

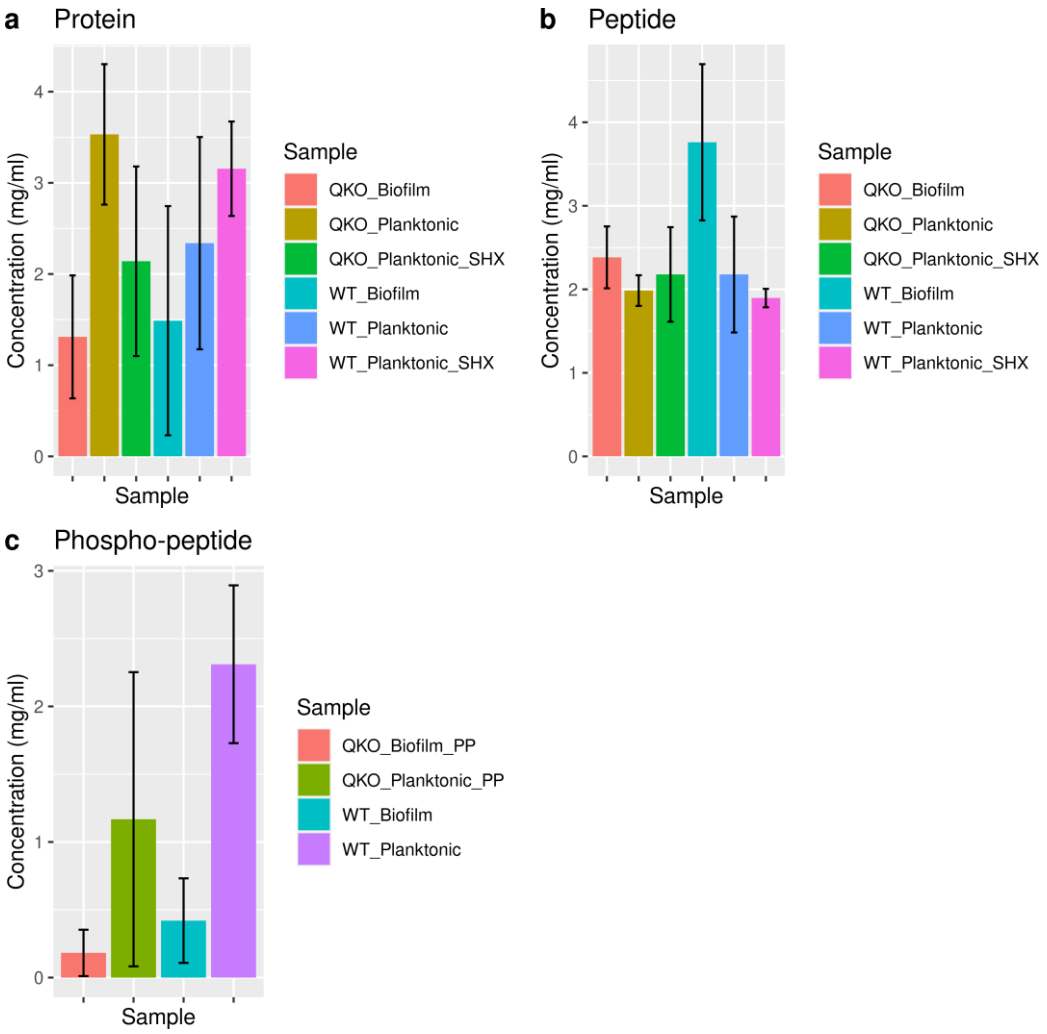

Figure 33: DirectDetect read outs of the protein and peptide concentrations to show that protein extraction and peptide purification had been successful. There is particularly large variation in the results of the phosphor-peptide purification. Error bars show standard deviation

4.3.4 Preparing and normalising the data

After the RAW files were processed using MaxQuant, the data was log2 transformed and normalised using the quantile normalisation function in R. Histograms were then plotted to visually examine the data and check for a normal distribution (Figure 34). All of the histograms show a roughly normal distribution, so multiple t-tests can be used to examine differential expression.

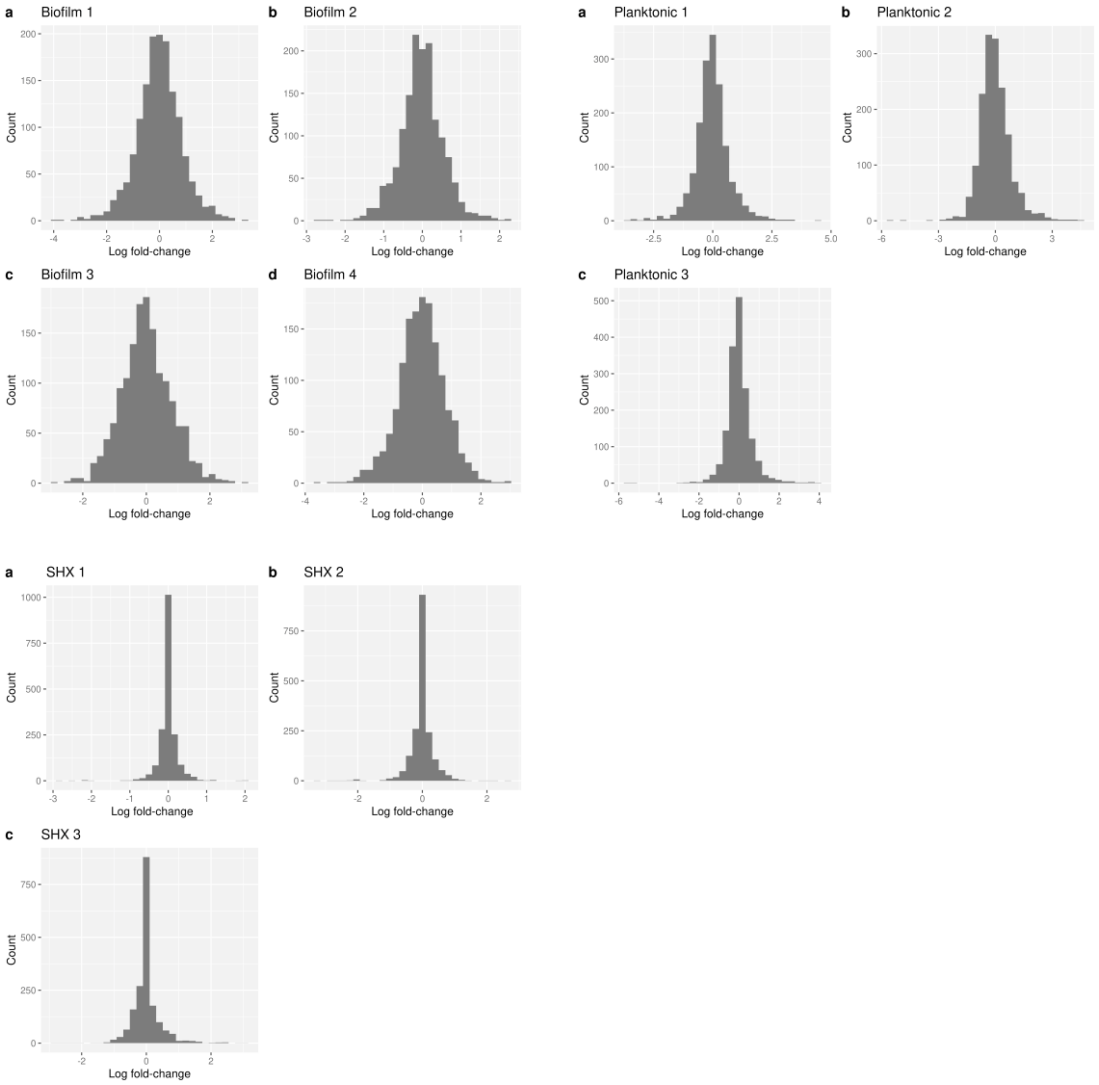

Figure 34: Histograms of the Log_2 transformed and quantile normalised data of the biofilm, planktonic and SHX treated samples. They show a normal distribution confirming that a parametric t-test would be suitable for calculating significance

4.3.5 Checking for batch effects using principal component analysis

After checking for a normal distribution, it was important to check for batch effects that could have been introduced. Principal component analysis determines what the main sources of variation are between the samples and can then be plotted to clearly see if there are any batches. There are three clear batches that seem to correspond to the different mass spec runs (Figure 35). This makes comparing between samples of different mass spec runs difficult, but there is a very tight grouping within runs which means that we can be very confident in those comparisons.

This batch effect could have been reduced if the sample conditions were split equally within each mass spec run, making it easier to normalise between the runs.

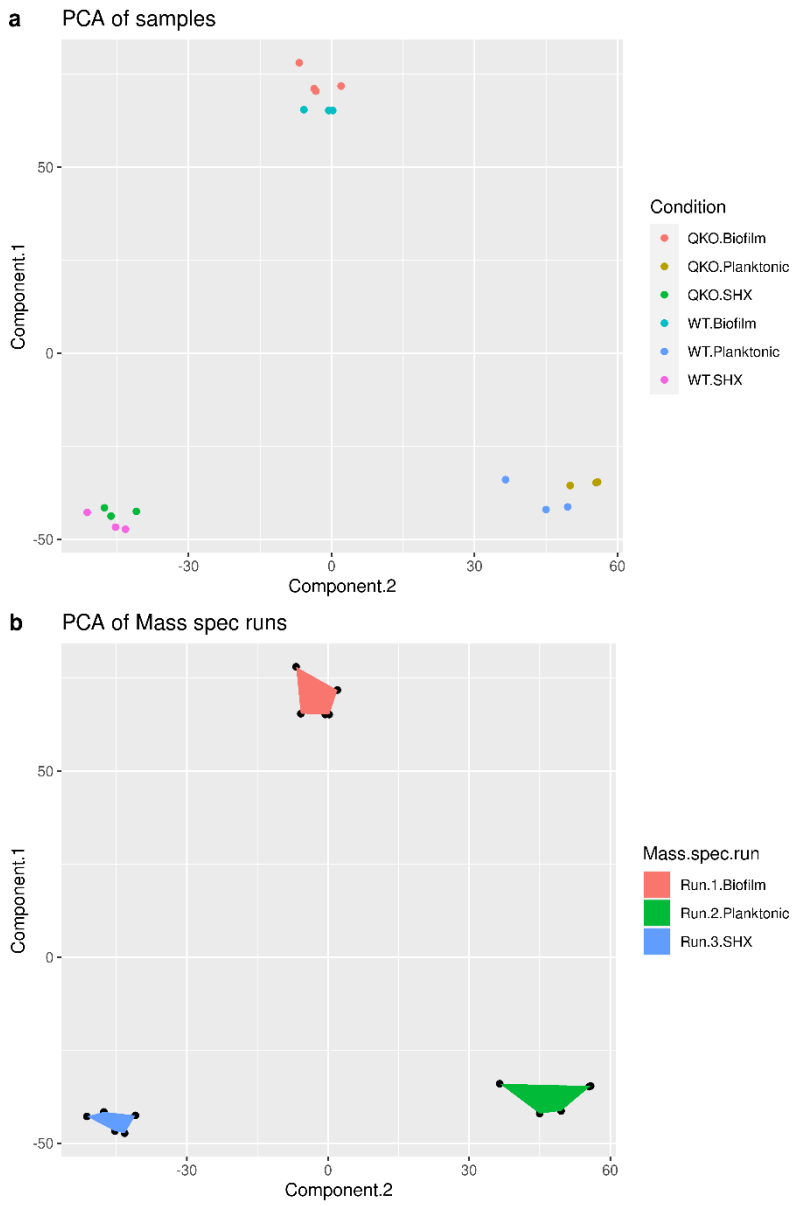

Figure 35: Principal component analysis by sample and mass spec run. This shows that the samples in each mass spec run are highly similar, but that there are large amounts of variation between runs on the mass spec

4.3.6 Identifying differentially expressed proteins

In order to determine which proteins were differentially expressed the log2 fold change was calculated, and t-tests performed on each protein across the replicates. For the purpose of this work, differentially expressed refers to proteins that have a log2 fold change of >0.58 or <-0.58 (equivalent to a 1.5-fold change), and also have a p-value of less than <=0.05. Figure 36 shows a side by side comparison of the data and which conditions have the most differentially expressed proteins. It can be seen that the biofilm and planktonic conditions seem to show a similar level of proteins that are differentially expressed, whereas the SHX condition shows far fewer differentially expressed proteins.

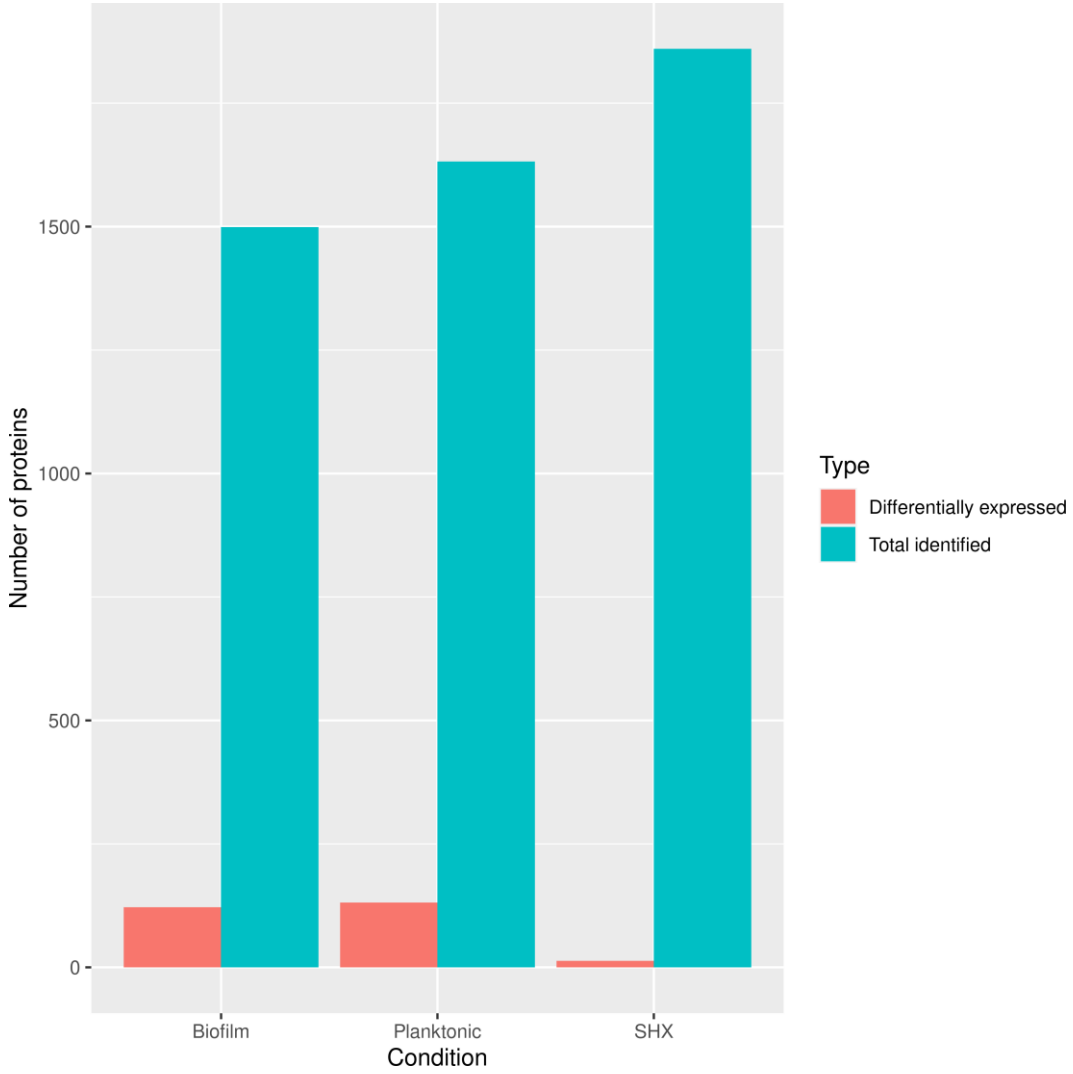

Figure 36: The total number of proteins identified by MaxQuant compared to the number of proteins found to be differentially expressed in each sample

Volcano plots can also be used to visualise the proteins that are differentially expressed (Figure 37). The x-axis show the log2 fold change, and the y-axis shows the -log10 p-value. The red dots show proteins that have both a sufficiently different log2 fold change, and a sufficiently significant p-value. When looking at the plots we can see that although the biofilm and planktonic conditions have similar numbers of differentially expressed proteins, the planktonic condition seems to have proteins that are more differentially expressed in terms of both significance and fold change.

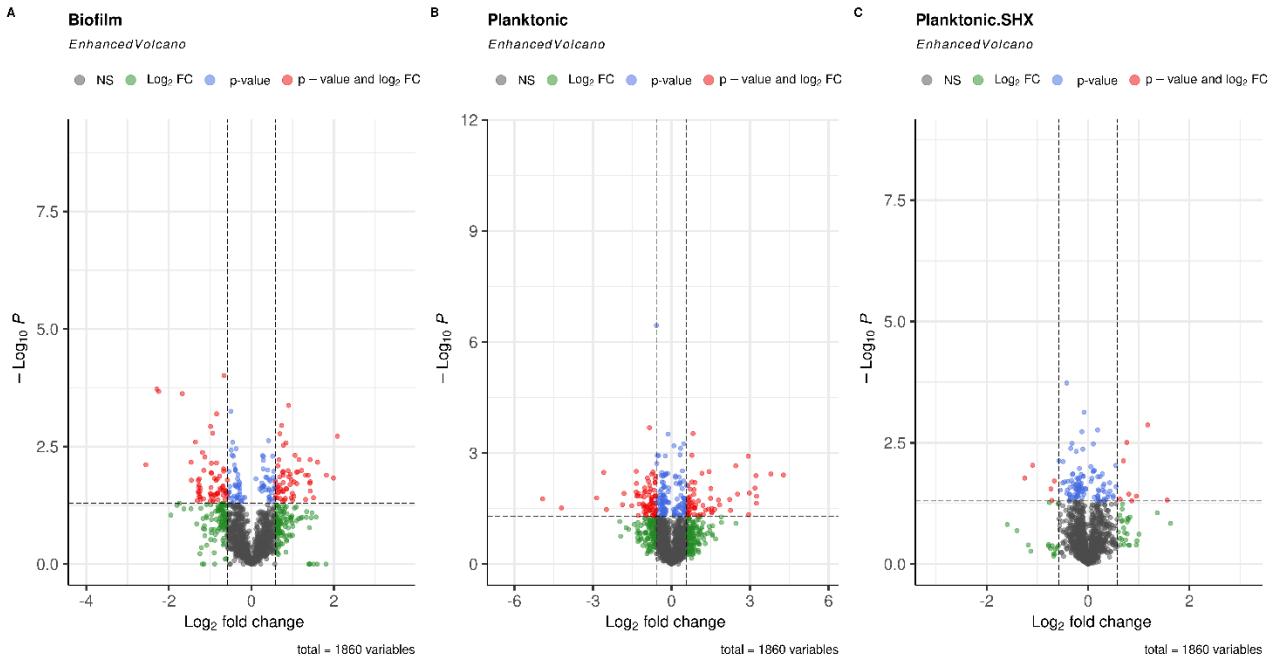

Figure 37: Volcano plots showing the relative proportion of proteins that are not significant (grey), significant but don't meet the fold change cut-off (blue), not significant but meet the fold change cut-off (green), and are significant and meet the fold change cut-off (red)

4.3.7 Networks established via differential expression analysis

When the differentially expressed proteins in each sample have been determined, it is possible to use networking tools like KEGG, PseudoCYC, String-db and QuickGO to group proteins into pathways and networks. This can be helpful in determining what the overall effect of the gene deletions are on the organism, and whether the biofilm phenotype in Chapter 3 can be explained.

There is significant overlap between the biofilm and planktonic conditions in terms of protein differential expression of the QKO mutant relative to the wild type. This is surprising as no visible phenotype was demonstrated in planktonic culture in chapter 3, and the growth curves in M9 minimal media shown in this chapter show no significant differences. This is likely a result of the mutations generating such a strong phenotype, that the usual phenotypic differences that would be visible between a planktonic culture and a biofilm are overshadowed. Interestingly, the serine hydroxamate treated planktonic cultures show very few differentially expressed proteins(data in appendix) (Table 10).

4.3.7.1 Pathways differentially expressed when comparing QKO to the wild type

Due to the fact the biofilm and planktonic conditions show broadly very similar mechanistic variations, and that the SHX treated samples show very few differences, the mutant and the wild type will be compared generally across the samples.

It is tempting to make conclusions based solely on the differential expression of individual proteins, and to not look at the networks overall. However, this can give a warped perspective of the data and analysis in this way should be done carefully.

4.3.7.1.1 Iron acquisition and utilisation

Iron is used by many bacteria as it is an ideal candidate for many oxido-reduction reactions due to its ability to exist in two oxidation states, Fe2+ and Fe3+. Fe3+, the dominant form in oxygenated environments, has extremely low solubility and requires dedicated mechanisms to be taken up by the cell. Whereas Fe2+ is soluble and is most abundant under anaerobic conditions (Nguyen et al., 2014; Bonneau, Roche and Schalk, 2020; Lin et al., 2017).

P. aeruginosa uses multiple strategies to acquire iron:

- The production of the siderophores pyoverdine and pyochelin that chelate Fe3+ and their uptake via TonB-dependent receptors (Hancock and Brinkman, 2002; Luscher et al., 2018)
- The uptake of siderophores of other bacteria (xenosiderophores) (Luscher et al., 2018)
- Via uptake of host haem (Bonneau, Roche and Schalk, 2020; Cornelis and Dingemans, 2013)
- By reduction of extracellular Fe3+ to Fe2+ via phenazine compounds, and their uptake by the Feo system

Whether pyoverdine, pyochelin, or both are secreted is thought to depend partly on its autoregulation, but mostly on the iron starvation level of the cell. Pyochelin is less energy intensive to produce but has a significantly lower affinity for iron than pyoverdine. As a result, pyochelin is released when intracellular iron levels are low, and pyoverdine when iron levels are severely low (Bonneau, Roche and Schalk, 2020; Cornelis and Dingemans, 2013). There are likely other factors that influence the iron acquisition strategy of *P. aeruginosa*. Pyochelin and phenazines can redox cycle, potentially causing oxidative stress to the cell, and pyoverdine is linked with expression of acute virulence factors such as exotoxin A and with mature biofilm formation (Cornelis and Dingemans, 2013; Xie et al., 2013).

In the biofilm and planktonic conditions, proteins that control the biosynthesis of Iron acquisition siderophores pyoverdine and pyochelin are upregulated in the QKO strain. In the biofilm, protein

TonB3 is upregulated, however, this protein has been linked more to twitching mobility than iron transport, explaining how a TonB-dependent receptor potentially involving iron transport is simultaneously downregulated (Huang et al., 2004). This seemingly counter intuitive decision to upregulate Fe3+ iron chelation while simultaneously reducing iron transport across the membrane could be a mechanism of oxidative stress protection via reduction of hydroxyl radicals from Fenton chemistry (da Cruz Nizer et al., 2021). In addition, this is likely why PhzS that is involved in phenazine biosynthesis is downregulated in the QKO.

4.3.7.1.2 Detoxification of reactive oxygen species

Oxidative stress derived from reactive oxygen species (ROS) (i.e. superoxide O2-, H2O2, and hydroxyl radicals HO-) is a major challenge for all living organisms. In bacteria, examples of where ROS are produced include as part of normal aerobic respiration, through Fenton chemistry and by phagocytes during infection. Even at relatively low intracellular levels, ROS can cause damage to important biomolecules such as DNA, RNA and proteins (da Cruz Nizer et al., 2021; Xie et al., 2013; Wongsaroj et al., 2018; Ochsner et al., 2000).

The potential damage caused by ROS necessitates specific mechanisms to protect against them, and due to the vastness of the challenge this is controlled by several adaptive responses to either detoxify or repair the damage caused by ROS, such as production of siderophores to chelate free iron, transcriptional regulators that are activated by oxidation such as OxyR, Fur and SoxR, protein repair via chaperones, detoxifying enzymes such as super oxide dismutase, the glyoxylate shunt, and the mucoid phenotype (da Cruz Nizer et al., 2021; Xie et al., 2013; Wongsaroj et al., 2018; Ochsner et al., 2000). This section will focus on proteins that detoxify ROS and their transcriptional regulators, as opposed to reduce their formation, or repair the damage they cause.

In the QKO mutant strain, an equal number of genes linked to ROS detoxification are upregulated and downregulated. Although slightly different proteins are significantly differentially expressed in the planktonic and biofilm conditions, this is almost certainly due to stochastic heterogeneity as opposed to a meaningful difference as all the proteins differentially expressed are controlled by the same transcription factors. The upregulated proteins are alkyl hyperoxide reductase (ahpF), thiol peroxidase (tpx) and glutathione synthetase (gshB), which are all involved in networks that catalyse the formation of H2O from H2O2 (da Cruz Nizer et al., 2021; Xie et al., 2013). The downregulated proteins are superoxide dismutase (SOD) B (sodB), glutathione peroxidase PA2826, and 1-cys periredoxin lsfA. SOD's are periplasmic enzymes that catalyse the conversion of O2- into H2O2 and are the first line of defence against superoxide radicals, while PA2826 and lsfA both detoxify H2O2 (da Cruz Nizer et al., 2021).

P. aeruginosa has two SOD's, sodB which has an Fe core and is expressed when iron is replete, and sodM which has a manganese core that is expressed under iron starvation conditions. At first, this shows a potential reasoning for the downregulation of sodB, as based on the expression of iron chelating siderophores it can be assumed that cell is experiencing iron starvation, however, it would be expected that this would be accompanied by an increase in the expression of sodM. As an increase of expression of sodM is not observed, it suggests an alternative reason for the downregulation of sodB. The large upregulation of ahpF, tpx and gshB suggest that cell is suffering from acute ROS stress from H_2O_2, the product of sodB and sodM mediated superoxide radical detoxification. It is plausible that the accumulation of H_2O_2 is leading to reduced activity of the SOD enzymes until sufficient H_2O_2 has been cleared. It is difficult to be sure of the reason for the downregulation of PA2826 and lsfA, when highly similar enzymes are upregulated. However, it could be linked to a lack of reducing power in the cell due to low levels of NADPH that enzymes such as glutathione reductase use to replenish the ability of H_2O_2 detoxifying enzymes.

4.3.7.1.3 Type VI secretion machinery

Bacteria are in a constant state of competition against multiple organisms, and therefore require mechanisms that allow them to be dominant in an ecological niche. Type VI secretion systems (T6SS) of gram-negative bacteria resemble an inverted bacteriophage puncturing device and can participate in several functions such as virulence, antibacterial activity and metal ion uptake (Li et al., 2018; Goldova et al., 2011; Mougous et al., 2007; Hachani et al., 2011).

P. aeruginosa has at least three gene clusters that code for T6SS machinery, H1-T6SS to H3-T6SS. The proteins secreted by these systems broadly fall into two families, Hcp and VgrG. Hcp is thought to form nanotube structures on the surface of bacteria that allow transport of other T6SS effectors into the cell, while VgrG proteins form puncturing devices that bare homology to bacteriophage tails, and perforate membranes to allow protein or macromolecular complex transport (Mougous et al., 2007).

Critically, deletion of T6SS systems from *P. aeruginosa* have been shown to have attenuated virulence in murine models, and they are shown to be upregulated in chronic infections of CF patients (Gallique, Bouteiller and Merieau, 2017).

Two proteins linked to type VI secretion are downregulated in the QKO mutant, VgrG1b and clpV3. VgrG1b is co-expressed with the H1-T6SS, however, does not rely on or regulate this system. It is secreted independently to any know T6SS in *P. aeruginosa*. VgrG1b has also been shown to be required for the delivery of Tse7, the expression of which induces the SOS response, growth arrest and ultimately DNA degradation. The activity of this toxin is attenuated by Tsi7 through a protein-protein interaction so specific that it will only bind to Tse7 from the same

isolate (Hachani et al., 2011; Gallique, Bouteiller and Merieau, 2017; Pissaridou et al., 2018). clpV proteins are cytoplasmic AAA+ ATPase's essential in recycling T6SS machinery, with clpV3 being shown to be essential to the H3-T6SS. Furthermore, the T3SS which is involved in the secretion of various virulence factors such as pyocyanin, and other cellular processes such as swimming motility and biofilm formation is downregulated in a clpV3 mutant. Interestingly, this deletion was also shown to downregulate the H2-T6SS and the H3-T6SS but upregulate the H1-T6SS (Li et al., 2020).

These genes are almost certainly downregulated as a result of the deletion of PpkA. It has been shown previously that PpkA controls assembly of the H-T6SS via phosphorylation of threonine 362 of Fha1. The mechanism was proposed by mougous et al, stating that when an environmental signal is received, PpkA autophosphorylates and stimulates Fha1 binding, phosphorylated Fha1 then eventually reaches a sufficient level to trigger the H-T6SS. The environmental sensor was thought to be the periplasmic VWA region of PpkA, and very importantly shows that the T6SS and *P. aeruginosa* in general is capable of rapid response to environmental cues (Mougous et al., 2007).

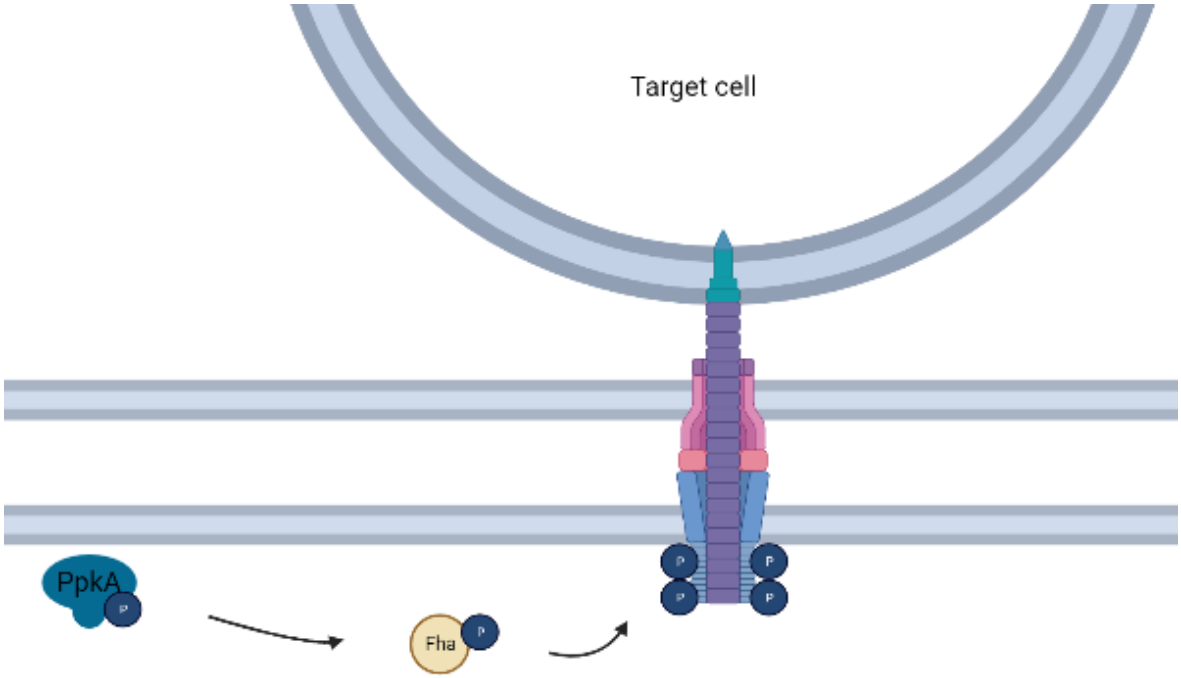

Figure 38: The basic mechanism of the type VI secretion machinery and how it links to the eSTK PpkA in *Pseudomonas aeruginosa*

4.3.7.1.4 Protein synthesis, central metabolism, respiration and NADPH production

P. aeruginosa is highly metabolically plastic and is able to thrive in a variety of environmental conditions. This plasticity allows for rapid changes of the central metabolism, in particular, the source of oxidiser for generating NAD(P)H. NAD(P)H is used in numerous catabolic reactions such as in the electron transport chain and as a reducing agent when detoxifying ROS (da Cruz Nizer et al., 2021). *In-vitro*, this usually comes from a carbon source such as glucose and a combination of several pathways:

- Peripheral pathways that encompass the oxidative transformation of glucose, acetate and glycerol
- The pentose phosphate pathway (PPP)
- The Entner-Doudoroff pathway (EDP)
- The TCA cycle and glyoxylate shunt
- The gluconeogenic reaction

P. aeruginosa can also use the process of denitrification which uses nitrite or nitrate as the terminal electron acceptor in respiration, usually in response to anoxia (Dolan et al., 2020; Figueira et al., 2015).

The MEP pathway and isoprenoid production are another important aspect of respiration. Isoprenoids are ubiquitous in the three domains of life and are involved in a wide variety of biological functions. In bacteria, they are involved in the production of ubiquinone and menaquinone, which are part of the electron acceptors of the shuttles involved in the electron transport chain. The electron shuttles couple the redox reaction to proton translocation and conserves the redox energy in a proton gradient (Heuston et al., 2012).

In the QKO mutant, there are numerous proteins that are differentially expressed that are involved in central metabolism. Glukokinase (glk) and glyceraldehyde-3-phosphate dehydrogenase (GapA) are highest up the carbon utilisation pathway and are both up regulated. Broadly, these proteins are responsible for metabolising glucose into pyruvate so that it can enter the TCA cycle. Phosphoenolpyruvate carboxylase (ppC) is also upregulated and catalyses the conversion of phosphoenolpyruvate to oxaloacetate (Dolan et al., 2020).

There are three genes from the MEP pathway that are differentially expressed Dxs, Dxr, Hpd and ExaA. All three are downregulated and are involved in the biosynthesis of isoprenoids from glyceraldehyde-3-phosphate and pyruvate. This directly links to the downregulation of NuoB, SenC, CoxB and CycB that are involved in the electron transport chain.

Interestingly, despite the central metabolism seeming to be overall downregulated, oxidoreductases and dehydrogenases are generally upregulated which both reduce NAD(P)+ to NAD(P)H. This also links to the upregulation of renalase that converts beta-NAD(P) to NAD(P)+, preparing for another round of reducing.

Being able to tightly regulate protein synthesis is also a key component of surviving in various ecological niches. Protein synthesis is the most energy expensive process in the cell and so must be able to adapt to varying nutritional availability. In the QKO biofilm, six ribosomal proteins were downregulated. This is linked to acute nutrient starvation and reduced protein synthesis (Starosta et al., 2014).

4.3.7.1.5 Fatty acid synthesis

Bacterial fatty acids primarily serve as the hydrophobic element of the cell membrane, however they are also used as storage lipids, the most prevalent of these being polyhydroxyalkanoic acids. Storage lipids are usually formed as a result of exogenous acyl chains as opposed to de novo synthesis, so are not relevant in the differential expression of fatty acid biosynthesis proteins (Cronan and Thomas, 2009).

Gram negative bacteria generally use type II fatty acid synthesis. This system relies on acetyl-CoA as a precursor and malonyl-CoA during the elongation step, with the intermediates covalently bound to ‘acyl carrier protein’, a highly structurally plastic protein that allows the acyl groups to slide in and out of the hydrophobic cavity. This achieves a compromise between shielding the acyl chain from any solvents and allowing access thioester acyl carbons on the proximity such that fatty acid synthesis can proceed (Cronan and Thomas, 2009).

There are three main fatty acid biosynthesis proteins that are upregulated in the QKO mutant FabD, FabG and PA1736. PA1736 is involved in the formation of octanoyl-coA, whereas FabD is involved in the conversion of malonyl-CoA into a-malonyl-[acp]. Both of these compounds then move into saturated fatty acid elongation, with FabG catalysing the first reaction. Interestingly, enzymes such as AccD involved in the formation of fatty acid intermediates from acetyl-CoA are generally downregulated. This could be linked to a downregulation of the TCA cycle and a lack of acetyl-CoA being produced.

4.3.7.1.6 Biofilm formation

There are several important proteins for biofilm formation that are differentially expressed in the QKO mutant. These range from protruding proteins such as pili and flagella, to alginate production and intracellular signalling. Many of the differentially expressed proteins have more than one role in biofilm formation, so sections will be presented separately.

The first step in biofilm formation is initial attachment to a surface, whether it be host epithelial cells, other bacteria or an abiotic surface. The irreversible attachment of bacteria to a surface is often mediated by appendages that anchor the bacteria in place, such as flagella and pili. In the QKO mutant, fliC, fliD and LecA are all downregulated, fliC is a type B flagellin, fliD a mucin adhesion flagellar cap that promotes the attachment of bacteria to surfaces, and LecA a cytoxin lectin and adhesin that binds hydrophobic galactosides and aids attachment (Diggle et al., 2006; Arora et al., 1998). On top of this, flp, a type IV pilin, and PilV, that is required for type IV fimbrial assembly are both downregulated. Interestingly, PilR, which belongs to the PilRS two component system is upregulated. PilR has been shown to stimulate the production of type IV fimbriae through transcriptional regulation, however it is possible that the downregulation of the other proteins is tied to a different mechanism that is preventing PilR from having the desired effect, or that the effect of PilR is not stochiometric i.e. more PilR doesn't necessarily mean more signal (Hobbs et al., 1993; Burrows, 2012).

The production of EPS is arguably the defining feature of a biofilm. It provides mechanical protection and a mechanism for the safe passage of communal goods. There are three major polysaccharides involved in *P. aeruginosa* EPS production, PEL, alginate and the PSL polysaccharide. Usually alginate and PSL are inversely regulated, and most non-CF isolates do not express high levels of alignate (Franklin et al., 2011). Whereas, PSL is expressed by most environmental and clinical isolates. Despite PSL and alginate usually being inversely regulated, both the pathways are downregulated in the QKO mutant (Irie et al., 2017; Mann, 2015). PslCFG are all downregulated and are required for PSL production, with AlgW (a protease that cleaves MucA and allows the transcription factor algU to stimulate alginate production) being downregulated from the alginate pathway simultaneously (Cezairliyan and Sauer, 2009).

Twitching motility has been shown to be essential for biofilm differentiation and microcolony formation. One of the significant factors controlling this are the type IV pili (Burrows, 2012). Deletion mutants of genes relating to pili form thick, undifferentiated biofilms which would surely inhibit their ability to occupy different ecological niches. The downregulation of flp and PilV suggest that twitching may be inhibited to a degree in the QKO mutant.

The biofilm is associated entirely with the chronic phenotype. There are several mechanisms that are employed to start the phenotypic switch from the acute to chronic state, however only the GacS signalling cascade is differentially expressed in the QKO mutant. GacS is heavily downregulated and is part of the GacS/GacA two-component-system to control expression of virulence related genes in response to extracellular environmental signals. GacA modulates the activity of RsmB, that binds to and sequesters RsmA. RsmA has been shown to indirectly modulate the transcription of a significant portion of the *P. aeruginosa* genome through the regulation of

QS and controls the reciprocal expression of acute and chronic virulence determinants via GacS/GacA (Perez-Martinez and Haas, 2011; Brencic et al., 2009; Ali-Ahmad et al., 2017).

4.3.7.1.7 Stress response regulators

Bacteria exist in highly dynamic and often nutritionally replete environments that result in various stressors being applied. To counter this, bacteria have evolved numerous and sophisticated stress responses to survive and quickly adapt to changing environmental conditions.

One of the major limiting nutrients for aerobic and facultative anaerobic bacteria is oxygen. Oxygen is used as the final electron acceptor during aerobic respiration/the electron transport chain, and so is critical in the formation of the proton motive gradient and energy production. A lack of oxygen triggers the dimerisation of the transcription factor Anr. Anr's ability to sense oxygen comes from its iron-sulphur cluster, under anaerobic conditions the cluster is [4Fe-4S]2+ that can dimerise and bind to DNA, whereas when the cluster is bound to oxygen it becomes [2Fe-2S] that leads to protein monomerization and loss of DNA binding ability(Trunk et al., 2010; Tribelli et al., 2019) . A recent study by tribelli et al., showed that there are at least 11 Anr-boxes that are common to most pseudomonas genomes, and that collectively across several species of pseudomonas it was responsible for controlling 253 genes. In particular, genes related to denitrification, arginine fermentation, high affinity cytochrome oxidases, and CupA fimbriae have been shown to be regulated by Anr. Anr is upregulated in the QKO mutant, suggesting a more oxygen deprived state than compared to the wildtype. Usually, Anr would be able to trigger the upregulation of denitrification genes, so that nitrogen can replace oxygen as the terminal electron acceptor in respiration (Tribelli et al., 2019). However, the YeaG deletion of the QKO mutant seems to negatively regulate nitrogen metabolism pathways, preventing this effect from being seen (Figueira et al., 2015).

Another major component of cell survival in stressful conditions is induction of the RpoS sigma factor (Stewart et al., 2015; Snyder, Gordon and Stoebel, 2012; Durfee et al., 2008). This is often referred to as the general stress response and can be triggered by various environmental stressors such as oxidative stress, nutrient starvation, and entry into stationary phase. The synthesis of RpoS is governed by multiple factors, including by the transcription factor DksA and the ppGpp (Kanjee, Ogata and Houry, 2012; Lemke et al., 2011). Usually, as nutrients are used up and the cell becomes starved, ppGpp will accumulate and in conjunction with DksA will mobilise a global transcriptional response via altering the binding kinetic of RNAP to combat the stress (Kanjee, Ogata and Houry, 2012; Lemke et al., 2011). DksA is upregulated in the QKO mutant, however there is no significant induction of proteins related with the RpoS transcription factor. This may suggest that ppGpp is being synthesised in lower quantities in the mutant strain.

4.3.7.1.8 The lack of differential expression when treated with serine hydroxamate

Relative to the biofilm and planktonic conditions, there are very few differentially expressed proteins in the SHX treated condition. There are still around 1,800 proteins identified in the mass spec run for these samples, and the histograms show generally very low divergence from zero for all three samples, suggesting that an issue with extraction, purification, or running on the mass spec is unlikely to have caused this.

This suggests that stringent response induction via SHX is effectively 'rescuing' the QKO mutant from the phenotype that is shown in the planktonic and biofilm samples. One theory is that the stringent response induction is so strong that it circumvents the need for the activation of the other pathways that result in the phenotype. It is also possible that the mutant is unable to effectively produce ppGpp through natural mechanisms, so the addition of a toxin that forces its induction may rescue certain elements of the intracellular state. However, the most likely reason for lack of differentially expressed proteins is due to treating the cells with SHX at approximately mid-exponential phase. At mid-exponential, it can be assumed that the nutritional status of the cell is good, and that the cell is generally unstressed. The addition of SHX at this stage may induce an effective non-growing state that therefore protects the nutritional status of the cell.

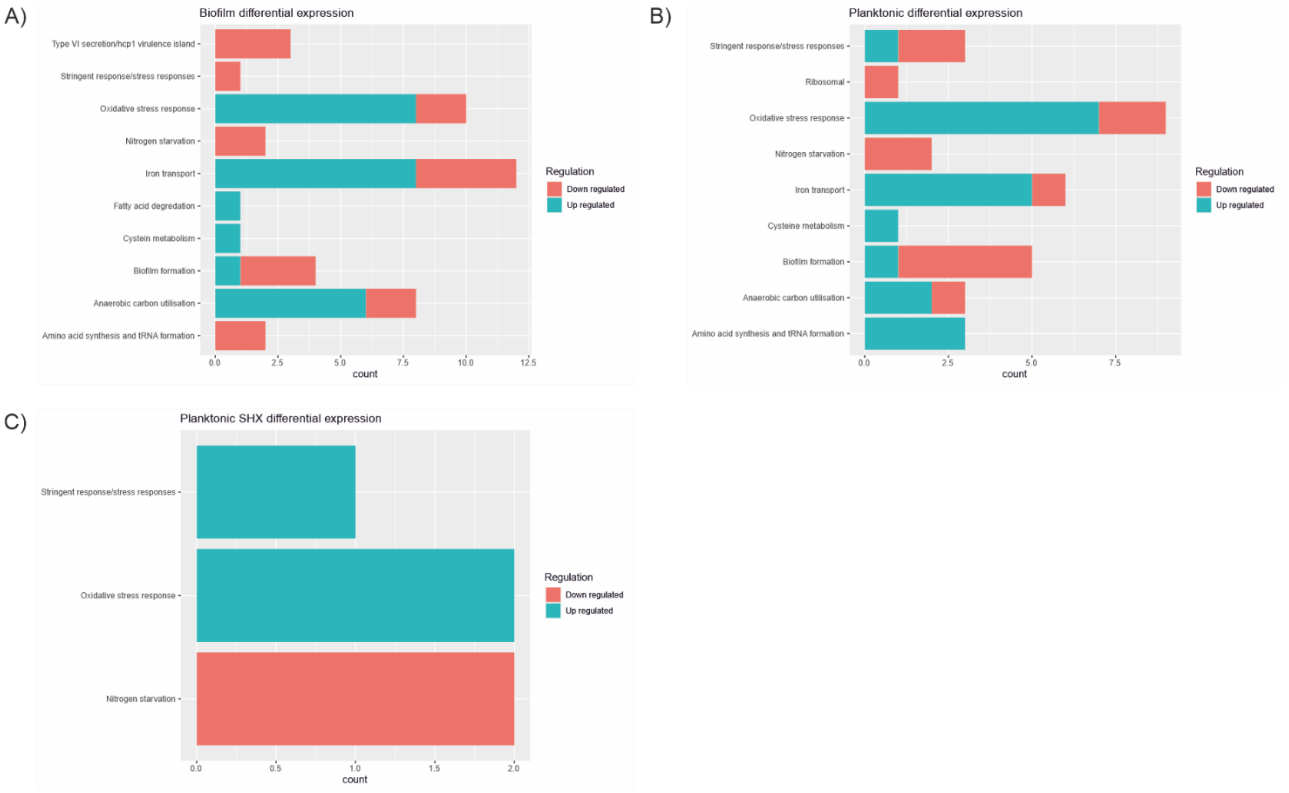

Figure 39: The number of proteins linked to each pathway/network for the biofilm, planktonic and SHX treated planktonic samples. The red part of the bar corresponds to proteins that are downregulated in that pathway, and the blue to upregulated proteins

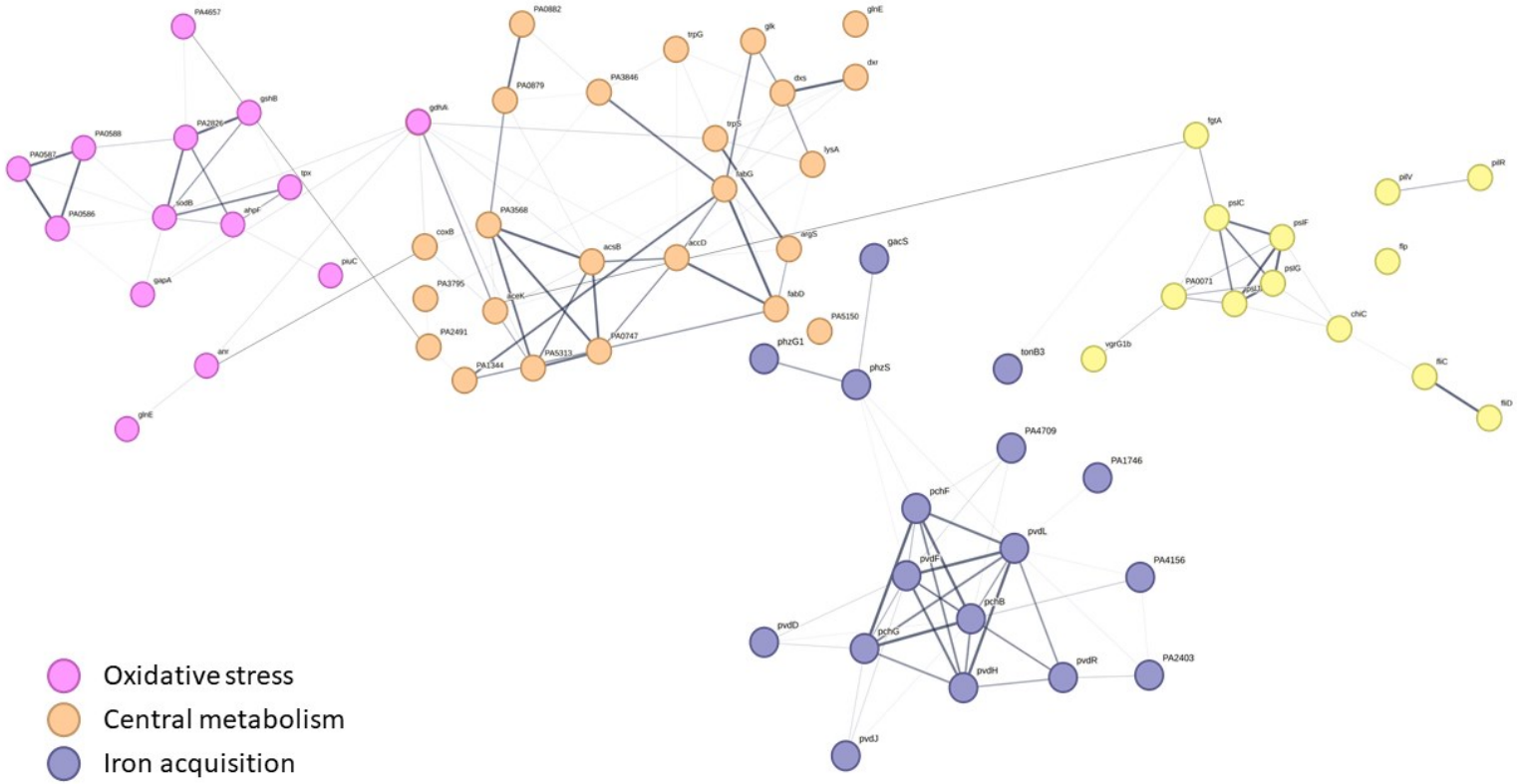

Figure 40: Protein network interactions as provided by String-db (string-db.org). Proteins were uploaded to string-db in individual clusters based on there function as determined by literature and structural review, these groups were then linked together manually using using the same technique. Proteins linked to oxidative stress are in pink, central metabolism in orange, iron acquisition in Blue/grey, and biofilm formation in yellow. The interactions shown are not exhaustive and more highlight the key findings of the differential expression analysis.

4.3.8 Weighted Gene Co-expression Analysis (WGCNA)

Differential expression is the most common way to find proteins of interest in a proteomics dataset. However, there are other unsupervised methods such as weighted gene co-expression network analysis (WGCNA) that find potentially interesting groups of proteins that may not have shown up in the differential expression analysis. WGCNA can be used for finding clusters (modules) of co-expressed genes, for summarizing such clusters using the module eigengene or an intramodular hub gene, for relating modules to one another and to external sample traits (using eigengene network methodology), and for calculating module membership measures. Correlation networks facilitate network-based gene screening methods that combine gene significance information and module membership information to identify candidate biomarkers or therapeutic targets (Zhang and Horvath., 2005) (Horvath et al., 2006) (Langfelder et al., 2007).

WGCNA works on the assumption that the information captured during microarray experiments is significantly more than can be shown by a list of differentially expressed genes. Instead, microarray data are better represented by considering the relationships between measured protein groups (proteins), which can be assessed using pair-wise correlations between gene expression profiles. WGCNA starts at the whole matrix level which usually consists of thousands of proteins, identifies modules relevant to a particular phenotype, and finally looks at intramodular connectivity and gene significance to identify the key drivers in a particular phenotype or pathway.

An advantage of WGCNA over differential expression analysis is that it alleviates the multiple testing problem that is inherent in microarray analysis. The multiple testing problem relates to how testing for significance is performed in differential expression analysis. Usually, a t-test is done on each protein, which in the case of our dataset means approximately 1,800 t-tests are being performed. The issue arises from the $p <= 0.05$ cutoff that is classically used to determine if a protein is significantly differentially expressed, as it is effectively being assumed that 5% of the significant proteins will only be shown as significant due to stochastic variation or ‘chance’. This can be offset to an extent using a false discovery rate (FDR) algorithm such as Benjamini-Hochberg that alters the p-values determined during a t-test, resulting in fewer significant hits being found. However, this method has been shown to be far too extreme for our proteomics data set and resulted in no significant proteins being discovered in any of the conditions. Instead of relying on this, WGCNA focuses on the relationship between a few modules and the phenotypic trait, with the eigengene significance and corresponding p-values being calculated for each module, instead of thousands of genes. The modules do not make use of predefined protein sets (is unsupervised), rather the modules are constructed using hierarchical clustering. After the formation of these

modules, they can be linked to the biological trait and candidate biomarkers can start to be elucidated.

Unprocessed data can be very noisy, so networks may appear random.

Biological systems are not random and proteins interact in a co-ordinated manner i.e. are scale free

Correlations values can be increased to a power determined by soft thresholding to achieve scale free topology

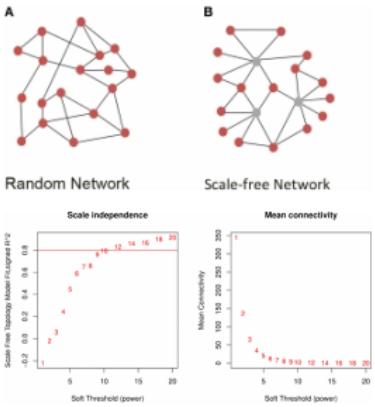

Correlation adjacency matrix is produced

Then this is used to identify modules of highly connected genes

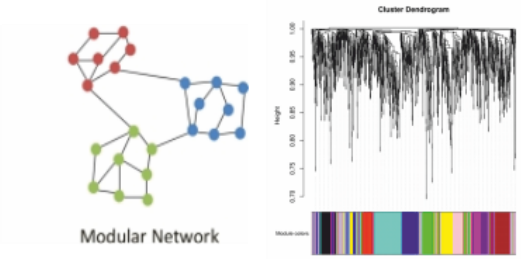

The modules can then be linked to external characteristics or traits

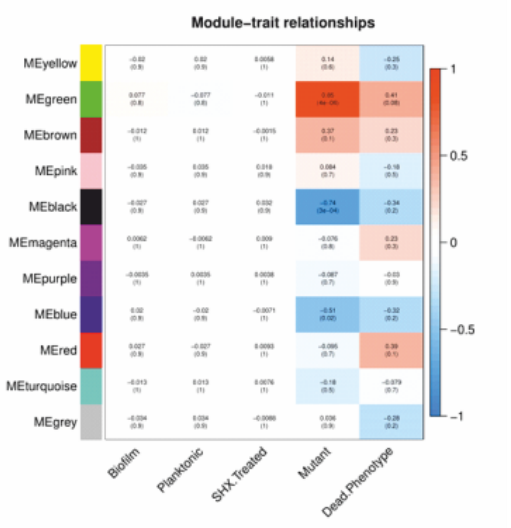

Key drivers can be identified using the gene signifcance and module membership meaures

Figure 41: The workflow for Weighted gene co-expression analysis. Firstly, data are increased by a power determined by soft-thresholding, followed by identification of highly interconnected genes which are then linked to an external characteristic/trait

The first step is to remove any batch effects from the data using the R package COMBAT. Figure 35 shows that the data is 3 batches that relate to the different mass spec runs. Because WGCNA looks at all the proteins together from every condition in a single matrix, it is important that these batches are removed as best as possible to prevent skewing of the data. The PCA plot (Figure 42) shows that the batch effect resulting from the different mass spec runs has successfully been removed.

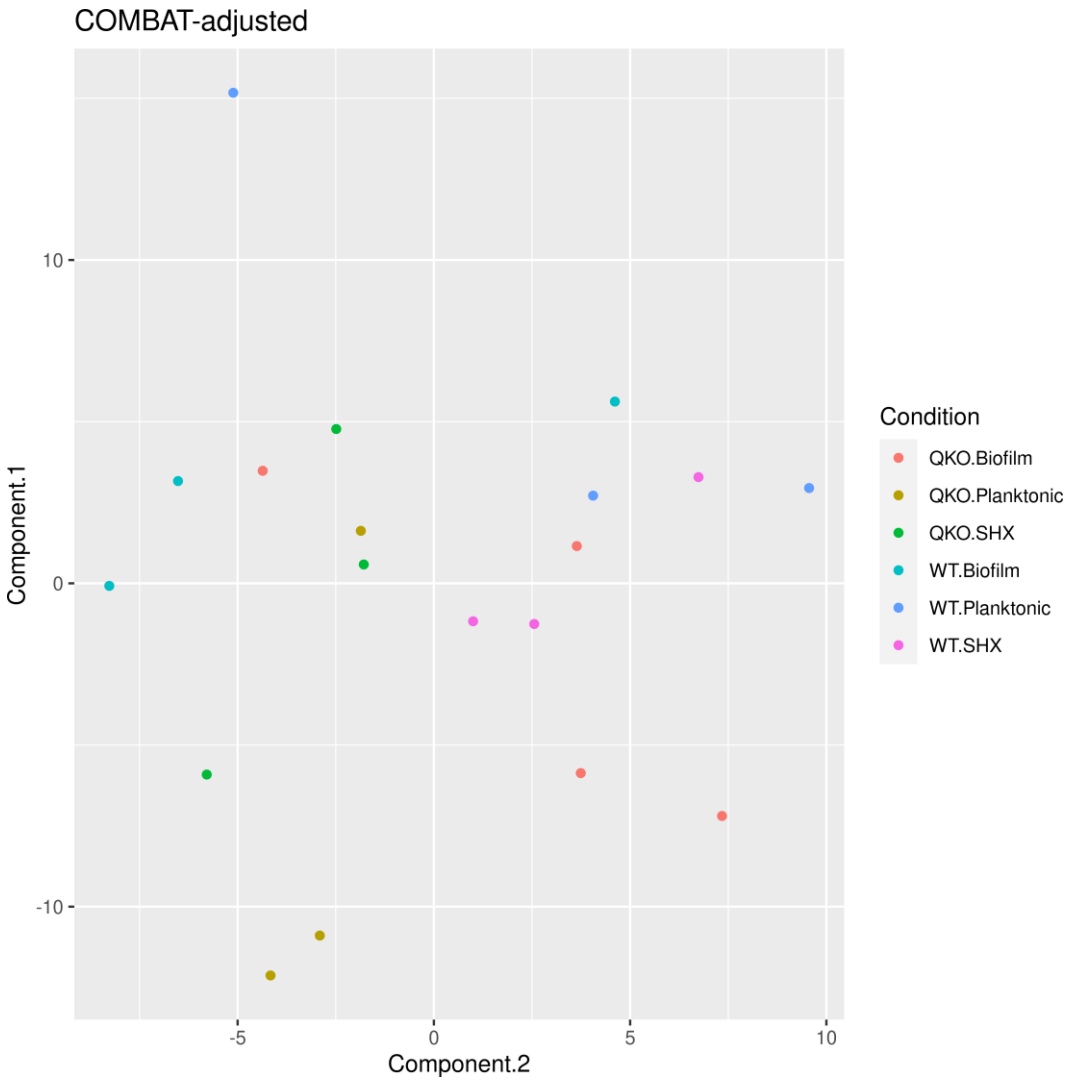

Figure 42: Data adjusted by the R package COMBAT principal component analysis by strain shows that all batch effects have been removed and that the data is suitable to carry forward into the next step of the analysis

The next step is constructing a sample dendrogram (Figure 43) to see if there are any outlier samples that should be excluded from the analysis, and then showing which traits these samples correspond to. If an outlier sample is included in the analysis, it could have a detrimental effect on the significance calculation and make the whole process defunct. In this case, there were no samples that were significant outliers, so were all carried forward into the network construction.

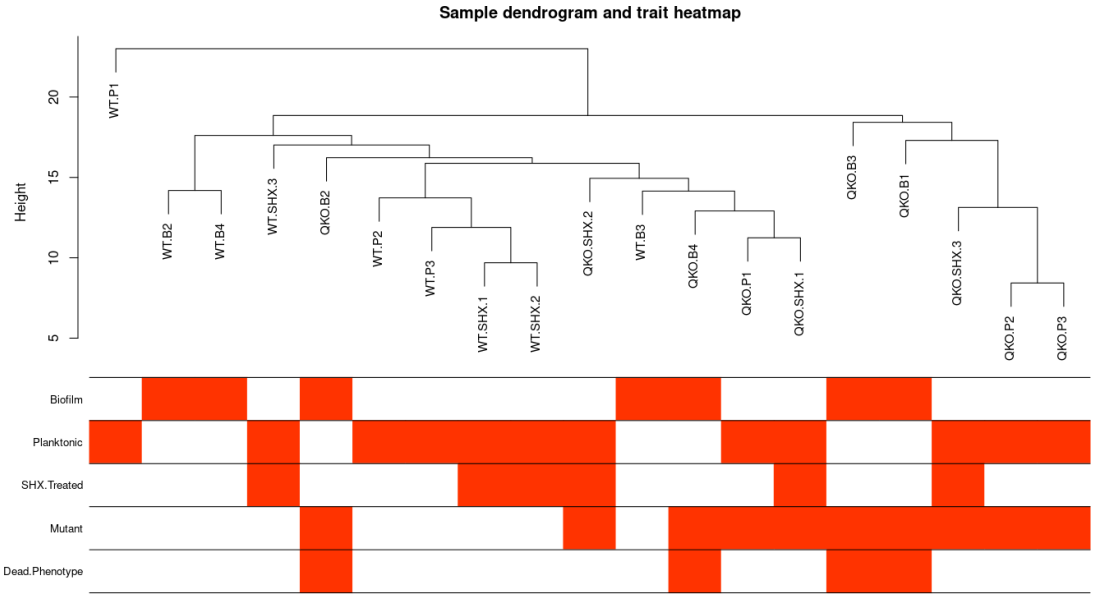

Figure 43: Sample dendrogram and heatmap used to determine if there are any significant outlier samples that should be removed before performing the correlation analysis

The soft threshold value required to get a sensible level of scale free topology (SFTR), while maintaining connectivity is calculated. This is necessary as the WGCNA network is constructed by calculating the Pearson correlations for all pairs of genes in the network, however, microarray data is often noisy and the number of samples per condition is usually low. In order to combat this, the Pearson correlations are weighted by taking their absolute value and raising them to the power β. This ultimately serves to punish the weak and emphasize the strong correlations on an exponential scale. The weighted Pearson values represent the strength of the connectivity between each gene in the network.

The minimum value of SFTR recommended for WGCNA is 0.8, in order to get this level of SFTR a soft thresholding power of 10 is required. The connectivity graph (Figure 44) shows that this significantly reduces the random interconnectedness of the genes, while still maintaining an element of connectivity required for module construction

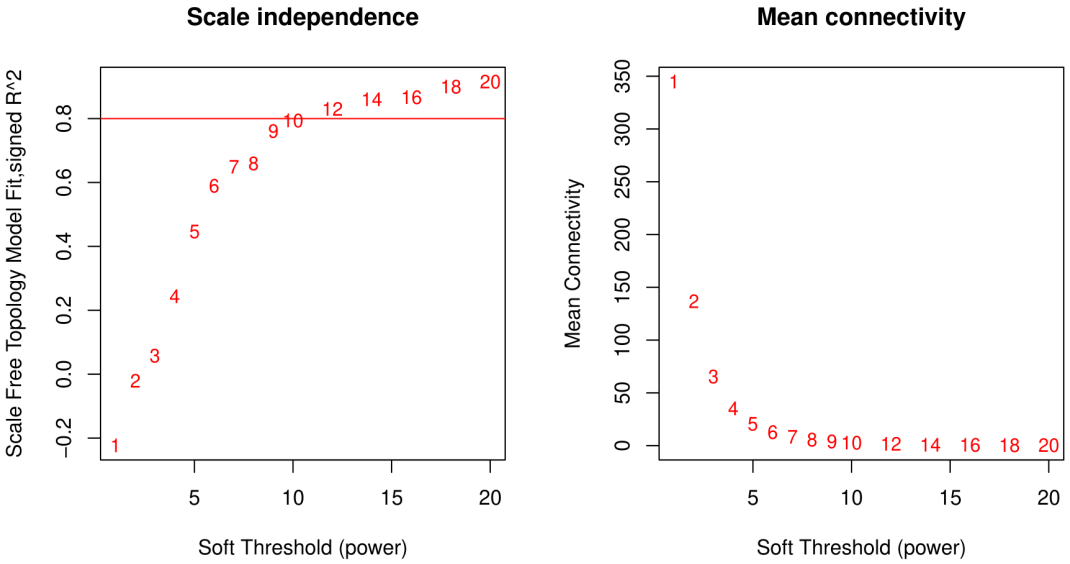

Figure 44: Soft thresholding (left) vs connectivity/interconnectedness (right). A soft thresholding power of 10 was selected in order to meet the minimum level of scale free topology required for WGCNA analysis. The Mean connectivity graph shows that this substantially lowers the interconnectedness of the data set.

When the connection strengths for each gene pair has been established, they can be added together to produce a single value of connectivity (k) that describes how strongly the gene is connected to all other genes in the network. This is where the weighted gene co-expression analysis begins, where the k of all gene pairs in the microarray is calculated, and then ultimately transformed into an adjacency matrix using a topological overlap matrix (TOM) based dissimilarity measure i.e. a matrix of connection strengths determined after raising the correlations to the power β (Zhang and Horvath 2005, Horvath et al 2006).

There are different types of TOM provided by the WGCNA package that provide slightly different results. The two main types are ‘signed Nowick’ and ‘unsigned’. The unsigned analysis looks purely at the Pearson correlation between gene pairs and ignores if that correlation is positive or negative, whereas a signed network of any kind will take into account the direction of the correlation. Peter Langfelder (one of the software developers) suggests using a signed network variation as generally speaking the direction does matter and mixing them together makes analysis more complicated. Secondly, because negatively and positively correlated genes usually come from biologically different categories e.g. they are under the control of separate transcription factors. With this in mind, a signed Nowick TOM was chosen that groups positively correlated and negatively correlated genes into separate modules. This TOM is then used in module eigengene (ME) identification and a dendrogram is constructed (Figure 45).

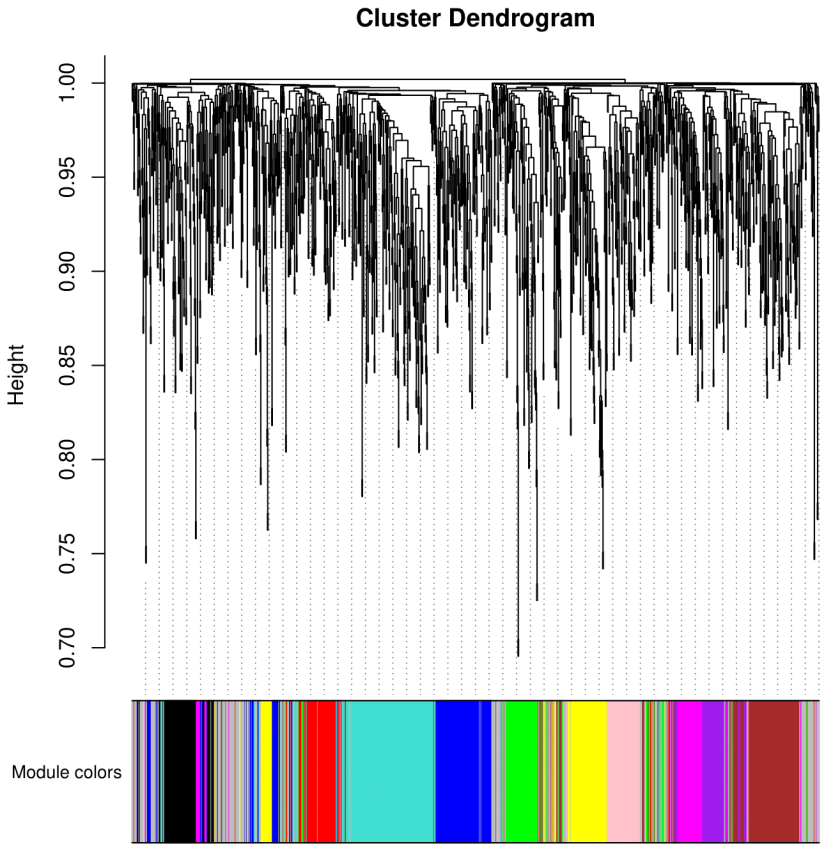

Figure 45: Cluster dendrogram of eigengenes produced using a signed Nowick TOM. The different colours represent clusters of co-expressed genes

The modules can then be related to traits to show module-trait relationships in a heatmap (Figure 46). Five traits/conditions were chosen to relate the modules to, samples that were grown as a biofilm, samples grown planktonically, samples that were treated with SHX, samples that have had the kinase genes deleted (Mutant), and samples that exhibit the 'dead' biofilm phenotype shown in Chapter 3. The heat map below shows the correlation (top number) and significance (bottom number) of each module in relation to the traits.

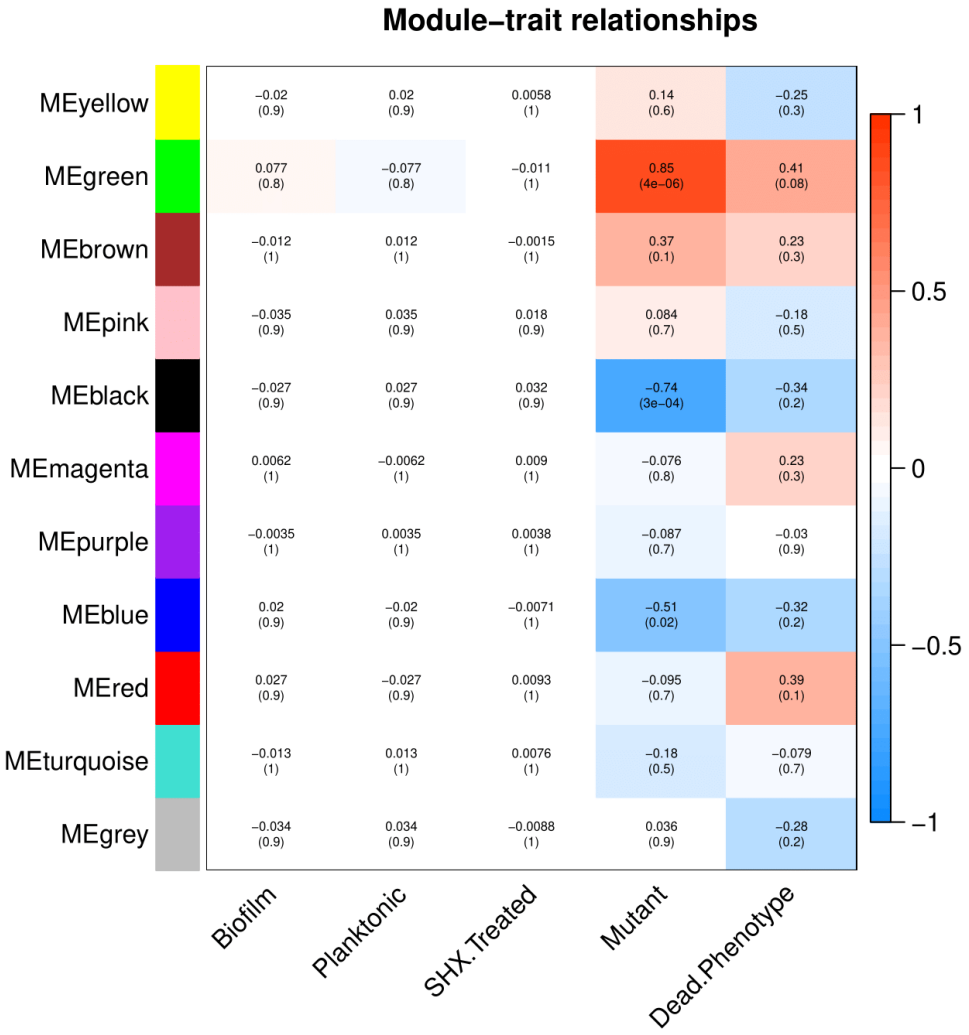

Figure 46: Module-trait relationship heatmap of a signed Nowick network. The top number in the boxes show how strongly positively or negatively correlated the module is to the characteristic, with the bottom number showing how significant the correlation is. MEgreen, MEblack and MEblue are significantly correlated to the Mutant phenotype

4.3.8.1 Analysis of modules that significantly link to a trait

There are three significant modules that all relate to the QKO mutant phenotype, MEgreen, MEblack and MEblue. MEblack and MEblue are negatively correlated with the mutant phenotype, while MEgreen is positively correlated. The fact that there are no significant modules for the other conditions confirms how strong a driver the gene knockouts are for creating the phenotype observed in this dataset.

The gene significance relates to the total strength of the pairwise comparisons for that gene i.e. the further away from zero the gene significance is, the more biologically important it is. The

module membership describes how relevant the protein is to the Module Eigengene it has been assigned to and is ranked from 0 – 1. It is important to consider both of these values when determining how important a particular protein is. Interestingly, this is more complicated with the modules that consist of genes that are negatively correlated with the mutant phenotype. The correlation between module significance and gene significance is very strong for MEgreen, however for MEblue and MEblack the correlation is much weaker

4.3.8.2 MEblack

MEblack is the module most negatively correlated with the mutant phenotype, with an average gene significance score of -0.74 and a p-value of 3E-04. The module seems to mostly consist of genes linked to central metabolism and outer membrane proteins, however there are also interesting proteins linked to stringent response induction.

4.3.8.2.1 Topoisomerases

Topoisomerases are essential enzymes that control DNA topology, specifically supercoiling and decatenation that allow the effective nucleic acid packing and cell dynamics (Sissi and Palumbo, 2010). Every organism must have at least one type I and type II topoisomerase to maintain effective levels of supercoiling and prevent chromosomal entanglements. Bacterial topoisomerase I, prevents hypernegative supercoiling of DNA during transcription and plays an important role of transcription of stress genes during stress responses. Type IIA topoisomerases such as Gyrase and Topoisomerase IV are crucial regulators of bacterial cell cycle progression and synergistically allow control of chromosome packing and functional transcription and replication(Sissi and Palumbo, 2010).

The type IIA topoisomerases, Topoisomerase IV (parEC) and DNA gyrase (gyrB), and the type I topoisomerase (topA) are all found in this module. parEC and topA have both a high gene significance (GS) and module membership (MM) score, showing that they are important biologically and are important proteins in the module. While gyrB does have good GS and MM scores, the data suggests that it is less relevant than the other topoisomerases.

4.3.8.2.2 Central metabolism, aerobic and anaerobic respiration, fatty acid synthesis

There are several genes of the superpathway of glycolysis, pyruvate dehydrogenase, TCA, and glyoxylate bypass found in this module. Broadly, this is quite similar to the proteins identified as part of the differential expression analysis, however the lack of a hard cutoff and stronger correlations when using WGCNA allows a much clearer picture of how downregulated the TCA cycle is in particular. On top of this, cytochrome oxidase proteins such as NuoBLG, MqoB, and ccoN2 that are involved in electron transport are in this module, which ties into AtpA, which is used to create ATP using the proton motive force generated as a result of electron transport.

The denitrification protein nirS has also been identified in this module, which is partly responsible for metabolizing nitrogen to nitric oxide for use as a terminal electron acceptor during anaerobic respiration and for dispersal.

There is only one gene associated with fatty acid synthesis in this module (FadD1), however, due to its very high module score and gene significance it is worth considering the role of fatty acids in the module.

4.3.8.2.3 Biofilm formation

The proteins linked to biofilm formation stem from the same networks as the ones found in the differential expression analysis. This consists of PSL proteins, proteins involved in the formation of pili and alginate production proteins.

4.3.8.2.4 Detoxification of reactive oxygen species

The sodB gene is found in this module, as in the differential expression analysis. However, the KatA gene that encodes catalase and is responsible for the detoxification of H2O2 is novel to this module (da Cruz Nizer et al., 2021; Xie et al., 2013). This is consistent with the data seen in the differential expression that shows a paradoxical downregulation of some proteins that detoxify H2O2, despite showing a phenotype consistent with severe oxidative stress.

4.3.8.2.5 Transcription and translation

rpoBC forms the DNA directed RNA polymerase that is essential for transcription of DNA into RNA and ultimately in the expression profile of the bacteria.

The genes fusA1 and fusA2 that both encode for the translation elongation EF-G, and the translation initiation factor infB are all found in this module. This is consistent with the downregulation of ribosomal proteins seen in the differential expression analysis and suggests significant nutritional stress.

4.3.8.2.6 Membrane proteins

P. aeruginosa is a gram-negative bacterium, and so has a cytoplasmic membrane with a symmetrical phospholipid bilayer and an asymmetric outer membrane with a phospholipid inwardly facing and a lipopolysaccharide outer layer, which ultimately creates a permeability barrier. To overcome this barrier, the outer membrane of *P. aeruginosa* contains several β-barrel proteins that produce water-filled channels that allow the diffusion of nutrients into the cell or contribute to membrane integrity, generally termed as porins (Malinverni and Silhavy, 2011; Hancock and Brinkman, 2002; Chevalier et al., 2017). In gram-negative bacteria there are two classes of outer membrane porin, non-specific general porins and substrate specific channels. *P. aeruginosa* broadly lacks general porins such as OmpFC, which contributes to its very low membrane permeability relative to other bacteria e.g. the permeability is only about 8% that of *E. coli*. This, the fact that *P. aeruginosa* has specific porins from the oprD family that uptake a

plethora of small molecules specifically, and the expression of broadly specific outer membrane efflux proteins such as mexB results in part to its high intrinsic resistance to antibiotics (Chevalier et al., 2017; Schweizer, 2012).

There are several porins and porin related proteins contained within this module. The iron and calcium regulated OprH, which is the smallest porin in *P. aeruginosa* and has been suggested to strengthen the outer membrane by interacting directly with LPS. The glucose specific porin oprB, that is transcribed as part of the gltBFGKoprB operon, has been shown to be important for type III secretion and virulence, and is usually downregulated in the biofilm relative to planktonic cultures (Chevalier et al., 2017). The more recently discovered Opr86 that has been shown to be essential for viability, plays a key role in OMP assembly and biofilm formation in some strains of *P. aeruginosa* (Tashiro et al., 2008). BamB, part of the BAM complex, is also thought to be responsible for OMP assembly by allowing insertion of β-sheets into the membrane (Malinverni and Silhavy, 2011).

On top of this there are more general membrane proteins that encode sodium transporters, iron transporters, and hypothetical proteins that are predicted to be localised to the outer membrane and play a role in its integrity.

4.3.8.2.7 Type VI secretion

The type VI secretion proteins tagR and icmf are both found in this module. This is almost certainly linked to the PpkA deletion and are required for full expression of the hcp-1 secretion island virulence factors (Hsu, Schwarz and Mougous, 2009; Mougous et al., 2007).

4.3.8.2.8 The stringent response, toxin anti-toxin systems and multidrug resistance

The induction of the stringent response has multiple regulators and has been discussed on much greater detail in Chapter 1. Broadly, most types of nutritional starvation can result in the induction of the stringent response, with arguably the most powerful inducer being uncharged tRNA entering the ribosomal A-site due to amino acid starvation. This stimulates the production of the far reaching alarmone ppGpp by relA (Starosta et al., 2014; Brown et al., 2014a; Kanjee, Ogata and Houry, 2012; Potrykus et al., 2011). Interestingly, relA is found in this module and suggests a reduced induction of the stringent response despite some clear indicators of nutrient stress. This is especially unexpected as the growth kinetics of the mutant and wildtype strain are indistinguishable when treated with SHX. One of the effectors of ppGpp induction, lon protease, is found in this module and is primarily associated with the release of toxins from their cognate antitoxin in TA systems (Maisonneuve, Castro-Camargo and Gerdes, 2013). However, in *P. aeruginosa* it has been suggested that lon proteases have more specialised roles and can be

involved in DNA replication, transcription, membrane fusion, proteolysis and protection from nitric oxide. *P. aeruginosa* also has an alternative to lon proteases, asrA, that responds to heat shock and tobramycin induced stress is also downregulated (Kindrachuk et al., 2011).

4.3.8.2.9 Chemotaxis and response to environmental stimuli

P. aeruginosa has the ability to sense environmental stimuli such as changes in chemical gradients and alter its movement behavior in response to this. This is normally mediated through flagella or pili-based motility, with the former being significantly more characterized (Sampedro et al., 2015; Burrows, 2012). Both mechanisms effectively function in the same way, a sensor module detects the chemical change, followed by a transduction module launching a signaling cascade that results in the movement of the bacteria.

There are several genes associated with type IV pili-based chemotaxis found in this module. Pili proteins already described above are obviously key to this movement. However, there are also three chemotaxis transducers identified, and two proteins that are responsible for the methylation of pili. The methylation of pili is a key mechanism to control twitching motility (Sampedro et al., 2015).

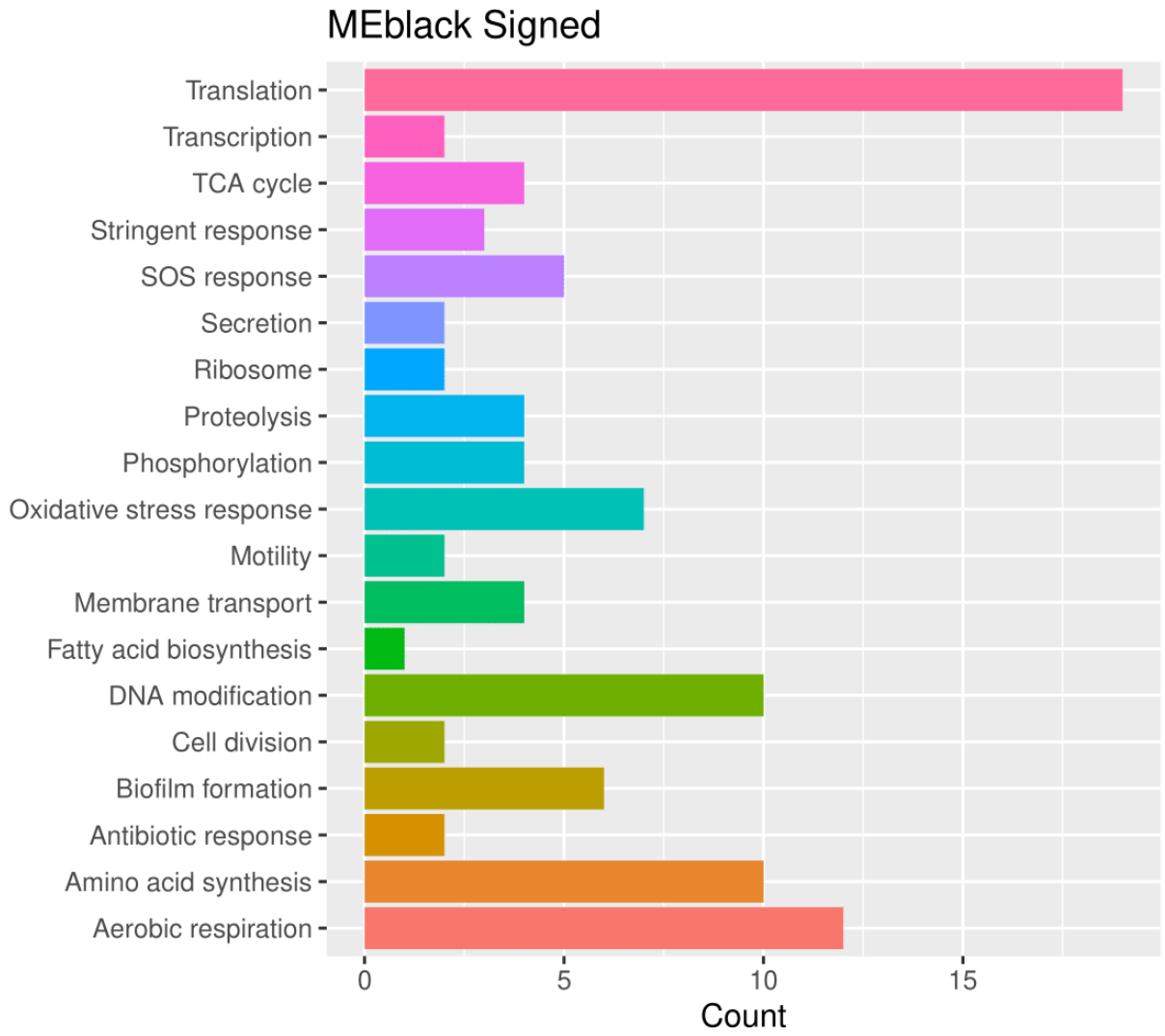

Figure 47: MEblack proteins by number in each network/pathway. All pathways are negatively correlated with the mutant phenotype in this module

4.3.8.3 MEblue

MEblue is another module that is negatively correlated the mutant phenotype. The gene significance score of 0.5 is still fairly high, however, the p-value of 0.02 is much higher relative with the other negatively correlated module, MEblack. As with MEblack, the majority of the negatively correlated proteins are in the central metabolism and membrane protein sections. However, there are more genes linked to translation and DNA repair in this module.

4.3.8.3.1 Central metabolism

There are several proteins linked to the central metabolism found in this module. Most of them being cytochrome oxidases or enzymes in the TCA cycle. Some of these proteins, such as isocitrate dehydrogenase (idh), have extremely low gene significance scores, but a relatively high module membership score. It is important to understand that while this does not make the protein irrelevant, it does mean that it is highly unlikely that it contributed significantly to the expression profile of the bacteria.

We also see more proteins that would classically be involved in denitrification, such as ntrc and narX. Both are part of a two-component system, with ntrc being a transcriptional regulator that is usually upregulated under anaerobic conditions to increase denitrification, and narX a sensor of nitrate that upregulates its metabolism (Brown et al., 2014a; Brown et al., 2014b; Petrova and Sauer, 2009; Fowler and Hanson, 2015). These proteins are novel to this module and contribute significantly to the nitrogen starvation aspect of the proteome.

4.3.8.3.2 Translation

There is a cluster of ribosomal proteins found in this module, consistent with the differential expression analysis and suggests that acute nutrient starvation is occurring. IF-1 is also found but has a very low gene significance score.

4.3.8.3.3 Quorum sensing regulation

The Las and Rhl quorum sensing systems of *P. aeruginosa* regulate the production of several virulence factors and many other proteins that are important for cell survival. The Las system positively regulates the Rhl system due to their hierarchical organization. In addition to this, several other proteins have been shown to involved in the regulation of QS, such as GacAS, MvfR, Hfq, RpoN, RpoS and RsmA (Sonnleitner et al., 2006; Perez-Martinez and Haas, 2011).

Hfq is found in this module and has been found to strongly stimulate the Rhl QS system at high cell densities. However, instead of Hfq directly inducing the upregulation of Rhl, it was found to stabilize the small regulatory RNA RsmY that sequesters RsmA (Sonnleitner et al., 2006).

The gene significance of Hfq is low, however it should be considered that proteins with low levels of stoichiometry such as RNA binding proteins and transcriptional regulators may have their significance underestimated by WGCNA.

4.3.8.3.4 Nutrient starvation and the stringent response

spoT which both synthesizes and metabolises ppGpp under different conditions is found in this module, as well as the nitrogen starvation protein ntrc that has already been mentioned in the central metabolism section (Nguyen et al., 2011; Starosta et al., 2014).

4.3.8.3.5 Membrane proteins

There are numerous membrane proteins in this module that have a variety of different functions. OprF is the most abundant non-lipoprotein OMP of *P. aeruginosa* and has been shown to have a variety of functions, such as: being a non-specific channel, providing structural integrity due to its interaction with peptidoglycan, biofilm formation and quorum sensing. There are also three OMP's that are responsible for metal ion transport in the cell, FvbA and PfeA that transport iron, and oprC that transports copper (Bonneau, Roche and Schalk, 2020; Hancock and Brinkman, 2002; Chevalier et al., 2017; Luscher et al., 2018; Minandri et al., 2016). Interestingly, opdQ is also found and seems to be linked to the NarXL two-component system, that regulates denitrification and is also shown to be negatively correlated with the mutant phenotype (Fowler and Hanson, 2015). There is also lptF that has been linked to alginate production and membrane integrity. lolB is partly responsible for localizing these proteins to the outer membrane, and so could also be a key driver (Tanaka, Narita and Tokuda, 2007).

There are three OMP's that all correspond to different multidrug resistance mechanisms, mexH, mexE and PmpM. They are all multidrug efflux pumps that are 'broadly specific' and allow the selective entry/removal of particular chemicals to/from the cytoplasm. This plays a role in *P. aeruginosa*'s inherent resistance to antibiotics (He et al., 2004; Schweizer, 2012).

In addition, there are also several membrane bound ABC transporters identified in this module.

4.3.8.3.6 Haem biosynthesis

Haem is an iron-containing group found in many essential proteins such as cytochromes and haem binding globins. hemF and hemN are both found in this module and are both responsible for the production of protoporphyrinogen IX, an intermediate in the ferrohaem production pathway. This downregulation of haem biosynthesis is reflected in the downregulation of several cytochromes that use ferrohaem as an electron acceptor that are involved in the central metabolism of *P. aeruginosa* (Boynton et al., 2009).

4.3.8.3.7 Type VI secretion

Fha1 is a forkhead-associated domain protein that is required for hcp-1 virulence island secretion. It is usually phosphorylated by PpkA, however in the mutant phenotype this is of course not possible. It is therefore not surprising that it is found in this module (Mougous et al., 2007).

4.3.8.3.8 Biofilm formation and motility

There are numerous proteins that are associated with biofilm formation networks found in this module. Some have already been discussed and link to PSL formation, pili associated motility/attachment and flagellar based attachment. However, the regulatory protein typA, a ribosome binding GTPase, is novel to this module. TypA has been shown to play a role in swarming motility and biofilm formation, and virulence factor expression (Neidig et al., 2013).

4.3.8.3.9 Detoxification of reactive oxygen species

The H2O2 detoxifying enzyme glutathione peroxidase has been identified in this module, consistent with the data seen in the differential expression analysis.

4.3.8.3.10 Chaperones and proteases

Chaperones help to ensure that proteins that become misfolded due to exogenous stressors such as metal ions and heat can be refolded and maintain their normal function. As well as this, they allow access to cut sites for proteases when a damaged or redundant protein needs to be degraded (Jakob et al., 1999; Kumar et al., 2021).

There are several proteins linked to this. HtpG that is a heat shock protein, clpA that is the chaperone part of clpAP protease responsible for breaking down protein aggregates, pfpI which has been linked to antibiotic resistance and swarming, and PA2725 that is a probable chaperone.

4.3.8.3.11 DNA repair

DNA repair is critical for long term survival of all organisms (Oliver, Baquero and Blazquez, 2002). DNA damage can be caused by several factors such as oxidative stress and from mismatches during DNA replication or homologous recombination. DNA that is damaged as a result of a mismatch is repaired using the mismatch repair system (MMR). This pathway consists of three proteins that recognize and then cleave the DNA: mutS, mutL and mutH. The DNA is made accessible and split from its opposing strand via DNA helicase, uvrD (Oliver, Baquero and Blazquez, 2002). mutS and UvrD are both found in this module. This could just be reflective of a decreased transcription rate, as the replicative DNA helicase dnaB is also found in this module, as well as a probable ATP dependent DNA helicase PA3950.

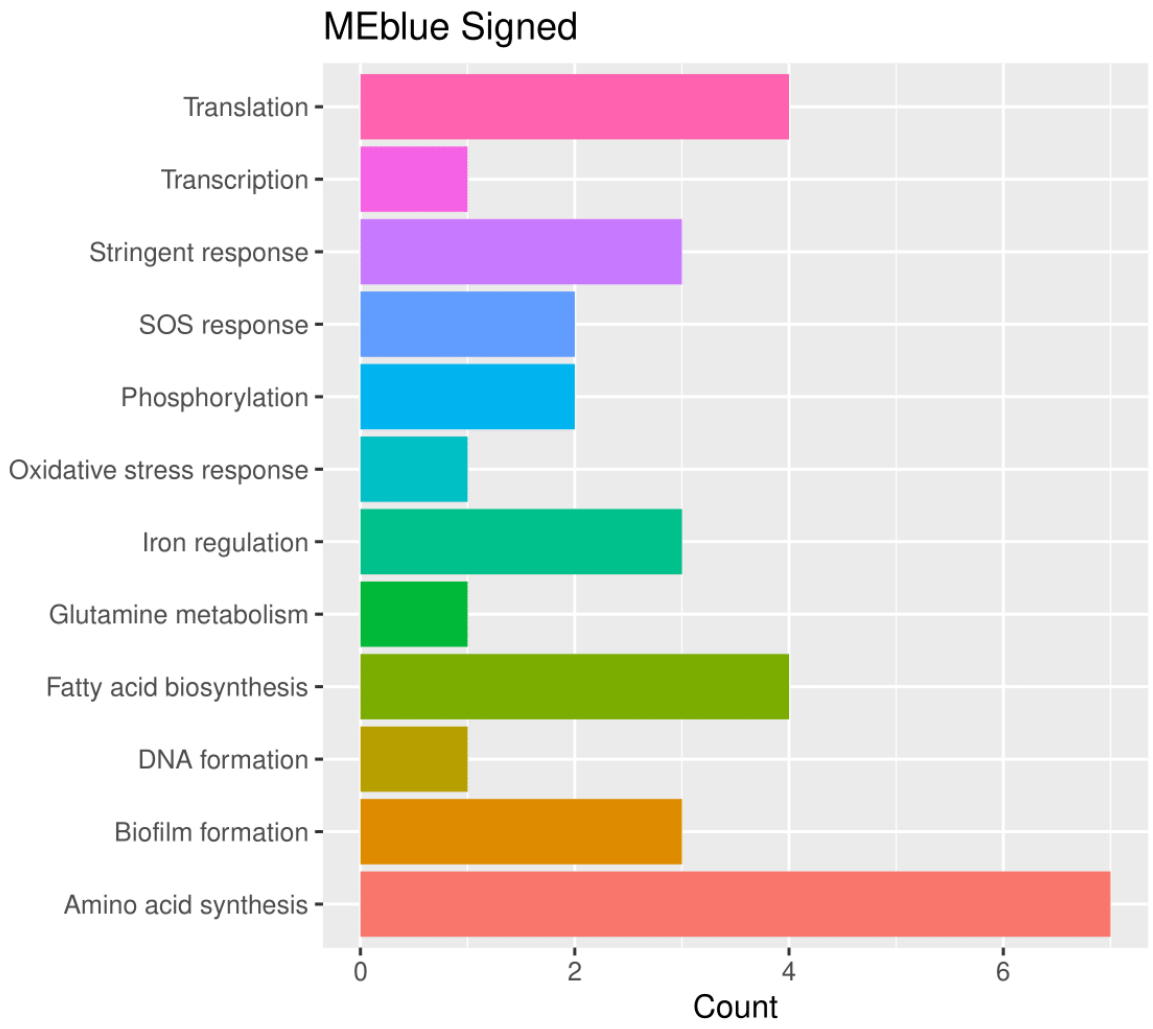

Figure 48: MEblue proteins by number in each network/pathway. All pathways are negatively correlated with the mutant phenotype in this module

4.3.8.4 MEgreen

MEgreen is the only module that is positively correlated with the mutant phenotype. It is also the strongest correlation and most significant module in general with an average gene significance score of 0.85 and p-value of 4E-06. The gene significance is also much more strongly correlated with the module membership score in this module.

There is arguably a weak correlation to the dead phenotype i.e. mutant biofilm, with this module as well. However, as the p-value is >0.05 this will not be discussed further.

4.3.8.4.1 Detoxification of reactive oxygen species

There are several genes that are linked to the oxidative stress response found in this module. Some of these are directly or indirectly involved in detoxifying hydrogen peroxide, such as thiol peroxidase, alkyl hyperoxide reductase and glutathione synthetase. Interestingly, super oxide dismutase M is found in this module, and was not found in the differential expression analysis. It is likely that sodM is positively correlated as it has a manganese core instead an iron core, unlike sodB which has been shown to be negatively correlated with the mutant phenotype, reflective of the apparent iron starvation level of the cell (da Cruz Nizer et al., 2021; Xie et al., 2013). This positive correlation of sodM provides a potential mechanism for where all the H2O2 is coming from and why the detoxifying enzymes are necessary. Another interesting protein found in this module is the chaperonin yrfI, which although classed as a heatshock protein, is actually regulated by redox (Jakob et al., 1999). Oxidising conditions such as H2O2 stress cause the formation of disulfide bonds to form in yrfI, presumably causing it to activate and prevent the aggregation of proteins due to oxidative stress.

Renalase is also found in this module, and while it is not directly involved in the oxidative stress response, it prevents the ‘clogging up’ of dehydrogenase enzymes that provide NAD(P)H for the reduction of reactive oxygen species.

4.3.8.4.2 Central metabolism

There is a plethora of proteins that are involved in the central metabolism of *P. aeruginosa* found in this module. Two of these proteins, fructose bisphosphate and gapA, are involved in the early steps of glycolysis II that produces pyruvate for entry into the TCA cycle. However, as all the other proteins of the TCA cycle are negatively correlated with the mutant phenotype, it is probably one of the intermediates that is important. There are proteins linked to tryptophan biosynthesis (trpEG), that catalyse the conversion of chorismate to anthranilate, with pyruvate and L-glutamate being produced during the reaction, potentially providing an alternative mechanism for

pyruvate production. There are also genes linked to glutamate synthesis (gdha) and cysteine synthesis (cysM, PA0399), which is probably linked to the synthesis of glutathione for reactive oxygen species detoxification, which starts with L-glutamate and L-cysteine.

On top of this there are numerous dehydrogenase proteins that are responsible for NAD(P)H production, explaining why renalase is the most significant protein in this module.

4.3.8.4.3 Siderophore production

Several pyoverdine any pyochelin siderophores are found in this module, consistent with the differential expression analysis.

4.3.8.4.4 Stress responses

There are two stress response proteins, Anr which is a transcriptional regulator that mediates the anaerobic stress response, and a cold shock protein cspA. Csp's have also been shown to contribute to osmotic, oxidative, starvation, pH and ethanol stress tolerance (Keto-Timonen et al., 2016; Derman et al., 2015). While cspA hasn't been well characterised in *P. aeruginosa*, due to the growth conditions of this experiment (37^{o}C) it seems highly unlikely that the protein would be induced as a result of cold shock.

4.3.8.4.5 Biofilm formation and motility

There are some proteins linked to biofilm formation found in this module. Three of which correspond to pili or flagella, and one which corresponds to the transcriptional activator algB that results in the increased expression of alginate protein (Wood, Leech and Ohman, 2006). This is unusual, as algW which positively regulates with increased alginate production has already been found to be downregulated in the differential expression analysis.

4.3.8.4.6 Transcription

The RNA polymerase subunit RpoZ is found in this module. RpoZ is mostly linked to the induction of spoT during nutrient starvation to help induce the stringent response. However, spoT has already been shown to negatively correlated with the mutant phenotype in MEblue, potentially suggesting another biologically interesting role for this protein.

4.3.8.4.7 Fatty acid biosynthesis

There are three proteins found that are linked with fatty acid biosynthesis, consistent with the differential expression analysis.

Figure 49: MEgreen proteins by number in each network/pathway. All pathways are positively correlated with the mutant phenotype in this module

4.3.9 Phosphoproteomics

Phosphoproteins are post-translationally modified and so usually are of very low abundance in the cell and tend to co-exist with their non-modified isoforms. The importance of phosphoproteins are not normally reflected by their abundance due to their very low stoichiometry, so to combat the low abundance of phosphoproteins in the cell, phosphoproteomics involves the enrichment of phosphopeptides from a trypsin digested cell lysate using strategies such as TiO2 affinity chromatography columns. The principle being that

only phosphorylated proteins remain in your sample, making them easier to quantify and to find biologically important differences in phosphorylation.

For the phosphoproteomics experiment in this study, phosphopeptides were enriched using TiO2 columns from 1 mg of starting peptides. It would usually be expected that 1% of the sample would be enriched for phosphopeptides. Unfortunately, the enrichment for this study was very poor and so only a very small fraction of the starting peptides were enriched. This could be the result of many factors, however most likely it will be due to human error in the enrichment protocol, or a lack of phosphopeptides in the staring peptide sample.

While phosphopeptides were identified, the quantification of the reporter ion by the mass spec that would normally be used to calculate the log fold change seems to be incorrect. This can be shown by presence of proteins in the enrichment such as vgrG1b (**Error! Reference source not found.**) showing no significant difference, despite a significant difference almost certainly being expected based on previous studies (Hsu, Schwarz and Mougous, 2009; Mougous et al., 2007), and also by the fact that several phosphoproteins were identified that had no reporter ion value.

Because of this, it is impossible to make any conclusions from the phosphoproteomics data. However, careful assumptions will be made based on what is seen in the phosphoproteomics and standard proteomics data, in the hope that future work can look to confirm or deny these assumptions.

As with the differential expression analysis, the biofilm and planktonic conditions will be discussed together as there is significant crossover between the two.

A fundamental issue that arises when studying phosphoproteins of *P. aeruginosa* and most gram-negative bacteria is that because there has been so little prior research, it is very rare that you'll be able to reliably determine what effect the phosphorylation is having on the protein. It is more complicated still, as phosphoproteins usually have multiple phosphosites that can be phosphorylated in different combinations, leading to different effects.

The focus of this section will be on identifying key drivers that, if were phosphorylated on a serine or threonine residue could lead to the difference seen between the proteomes of the WT and QKO mutant.

4.3.9.1 Iron storage

Bacterial ferritin (ftnA) is a non-haem binding iron storage protein that functions as a bet-hedging strategy for when iron sources become depleted (Yao et al., 2011). Furthermore, they help to protect the cell from oxidative stress due to fenton chemistry by oxidising Fe2+ to Fe3+ using O2 or H2O2 as an acceptor and internalise the mineral. Then when iron starvation occurs, the iron is reduced and ready for incorporation into cell metabolism (Yao et al., 2011).

The ferroxidation step takes place in the ferroxidase centres of the protein, located in the middle of each subunit (Yao et al., 2011). ftnA is phosphorylated at Threonine residues 80 and 81, which are located in the ferroxidase core. It is possible, that in the QKO mutant this phosphorylation is unable to occur, preventing the conformational change that allows the ferroxidation to take place. If this were to be the case, the lack of iron storage could explain the upregulation of pyoverdine which chelates Fe3+ iron. This also links to the upregulation of certain oxidative stress proteins, as it's also possible that the lack of an ability to detoxify and store Fe2+ could lead to more reactive oxygen species formation via fenton chemistry.

4.3.9.2 Central metabolism

There are a few proteins that are involved in central metabolism. PtsP and PpsA are both involved in the production of pyruvate via glycolysis II. If phosphorylation of these proteins regulates their activity and is not possible in the QKO mutant, this could prevent the adequate production of pyruvate for the TCA cycle. Isocitrate dehydrogenase is also phosphorylated and catalyses the formation of 2-oxoglutarate, which can continue through the cycle or be used for L-glutamate biosynthesis. Both of these mechanisms give potential reasoning for the significant downregulation of the TCA cycle in the QKO mutant.

4.3.9.3 Reactive oxygen species detoxification

The main phosphoprotein of interest in relation to the oxidative stress response is the transcriptional regulator oxyR. OxyR is a LysR type redox sensitive transcriptional regulator that responds to high levels of intracellular H2O2. It is responsible for the induction and regulation of approximately 122 genes, including major H2O2 detoxifiers KatA and ahpF (Nguyen et al., 2011; da Cruz Nizer et al., 2021; Xie et al., 2013). This is interesting as ahpF is significantly positively correlated with the mutant phenotype, while KatA is negatively correlated. OxyR is phosphorylated at threonine residues 2 and 4, which are both located in the LysR like helix turn domain that enables DNA binding. It could be possible that phosphorylation at these residues is required for effective DNA binding and therefore transcriptional upregulation at the KatA binding site.

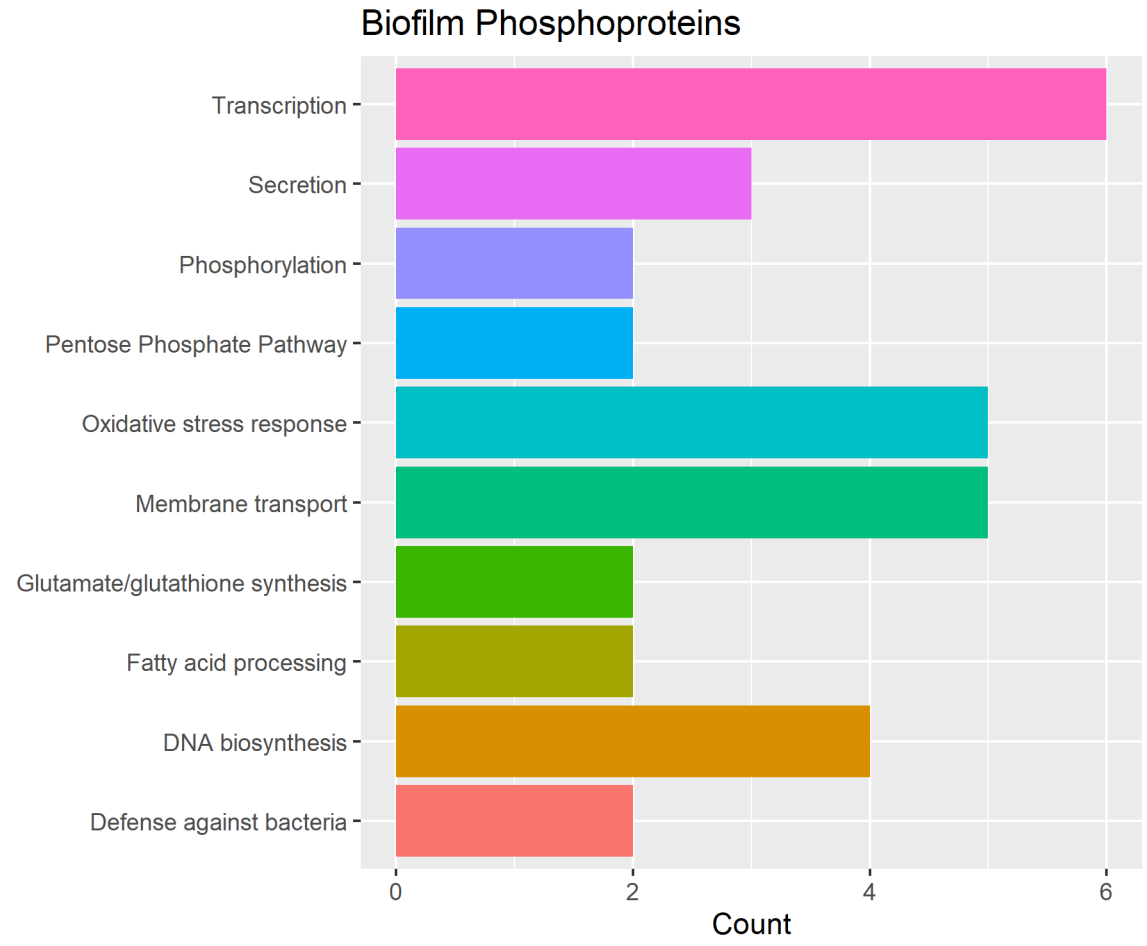

Figure 50: Pathway network analysis of phosphoproteins identified in the biofilm

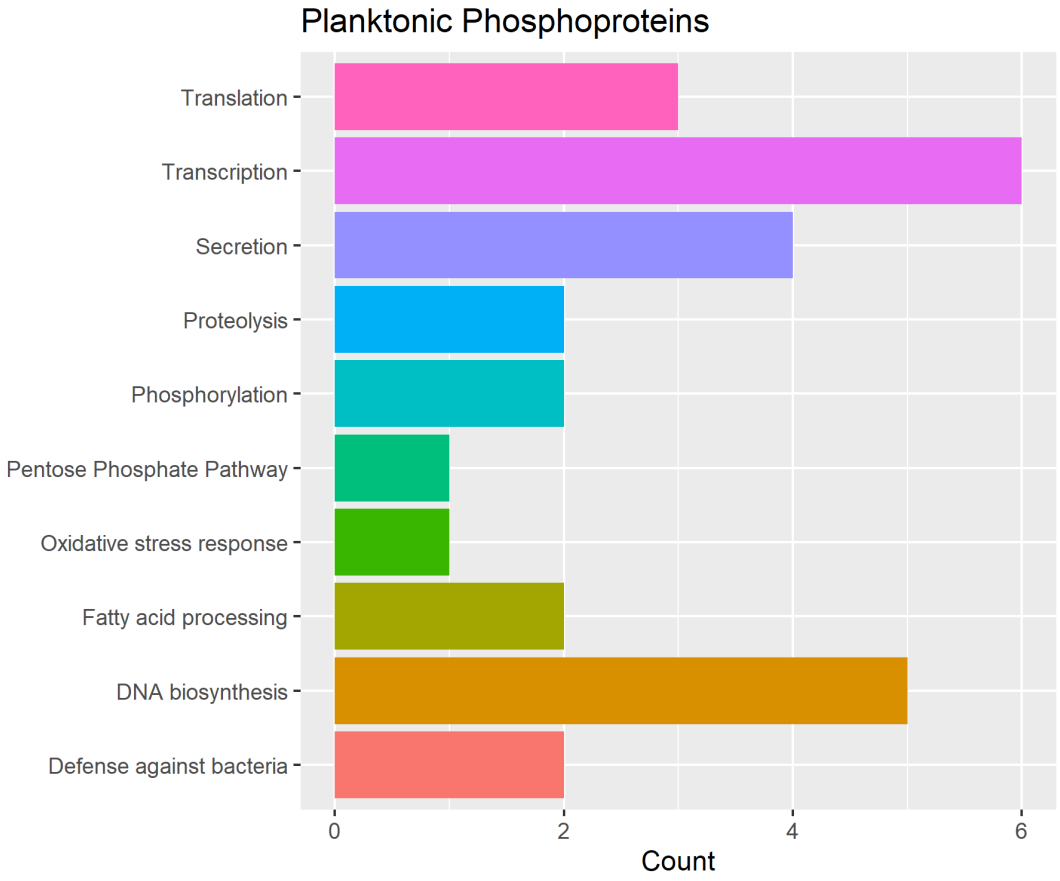

Figure 51: Pathway network analysis of phosphoproteins identified in Planktonic culture

4.4 Discussion

In Chapter 3 there was a clear phenotype identified for the QKO and ΔPpkA mutants of PAO1, that showed a significant increase in the proportion of membrane compromised cells in the centre of the biofilm (Figure 24). This effect increased with the maturity of the biofilm and with the sequential deletion of the kinases i.e. the effect was more severe for QKO than it was for ΔPpkA. Interestingly there was no phenotype observed when studying the planktonic cultures of QKO and ΔPpkA, suggesting that this was a biofilm specific phenotype. It was hypothesised that nutrient limitation in the centre of mature biofilms was leading to the increased number of membrane compromised cells, due to the bacteria being unable to effectively regulate its metabolism, perhaps through lack of stringent response induction. In order to elucidate the potential mechanisms for the membrane compromised phenotype, a proteomic analysis comparing the QKO strain to the wildtype would be performed using three separate testing conditions:

- 96-hour flow cell biofilm in minimal media
- 26-hour planktonic culture in minimal media
- 26-hour serine hydroxamate treated planktonic culture in minimal media

On top of this phosphoproteomics would be performed for the 96-hour flow cell biofilm and the 26-hour planktonic culture. Dual labelled SILAC was initially chosen to be the mechanism by which we labelled the samples, due to the fact that it is incorporated metabolically, it does not require an additional labelling step as with TMT. However, after deleting the terminal gene in the arginine biosynthesis pathway ArgH, there was a sharp drop in the ability of *P. aeruginosa* to survive in the stationary phase of planktonic cultures (Figure 30). This could be circumvented by the addition of exogenous L-arginine, however this resulted in significantly increased biofilm formation (Figure 31) and a reduced MIC to tobramycin. It was proposed that this was due to arginine providing nutrients to the anoxic parts of the culture, increasing its metabolic rate and making it more susceptible to antibiotics (Borriello et al., 2006). It would still have been possible to use SILAC by only labelling the lysine residue, however it was determined that TMT would be more effective than this, and due to its high multiplexing potential would also reduce cost.

Two strategies were used to identify proteins of interest in the whole proteome samples. Firstly, differential expression analysis was utilised by performing one t-test per protein with a p-value cut off of <=0.05 and a fold change cut off of <1.5 or >1.5 (Table 10). After this, WGCNA was used to identify modules of genes that highly correlate with a particular testing condition (Figure 46). The results were broadly very similar for both analysis pathways when looking at the whole network level. However, the unsupervised method utilised by WGCNA avoids multiple testing bias and hard cut offs, which ultimately led to a more sensitive and thorough look at the pathways that are differentially correlated. Both systems identified proteins that were not in the other, showing the importance of performing more than one type of analysis.

With the exception of the SHX treated planktonic cultures there appears to be a complete dysregulation of several important and highly interconnected pathways in the QKO mutant, such as type VI secretion, Iron transport, OMP's, reactive oxygen species detoxification, the central metabolism and nitrogen utilisation, and the stringent response (Table 10). Cultures were treated with SHX at mid-exponential phase when nutrients were replete, suggesting that eSTK's may play an important role in the metabolic plasticity of *P. aeruginosa* in nutrient depleted conditions such as in the biofilm and in stationary phase planktonic cultures.

The differential expression of type VI secretion machinery was expected as a result of the initial characterisation of the role of PpkA in hcp-1 virulence island secretion (Mougous et al., 2007). This is particularly true of the VgrG proteins of the T6SS that form the puncturing tip of the spike that injects the toxin into the bacteria (Hsu, Schwarz and Mougous, 2009; Mougous et al., 2007). However, based on the current knowledge available, deletion of eSTK's involved in T6SS has not shown a differential expression of the two-component GacS/GacA system until this study. The

GacSA system is induced with the T6SS and is thought to regulate the activity of approximately 500 genes via RsmA and quorum sensing. The sensor domain GacS is downregulated log2 -2 fold and is almost certainly linked to the observed phenotype. GacSA has also been shown to control the switch to the chronic phenotype through retS and LadS (Perez-Martinez and Haas, 2011; Brencic et al., 2009).

The Fe3+ chelators pyoverdine and pyochelin were both upregulated in the QKO mutant. The upregulation of pyoverdine in particular suggests acute iron starvation is occurring, as usually *P. aeruginosa* will default to pyochelin as it much less costly to produce (Cornelis and Dingemans, 2013; Minandri et al., 2016). Interestingly, phenazine proteins were downregulated in the differential expression analysis. Phenazines ultimately work to reduce the insoluble and non-biologically active Fe3+ to the soluble Fe2+ that can be integrated into enzyme cores. However, excess free-floating Fe2+ could cause the production reactive oxygen species through fenton chemistry (da Cruz Nizer et al., 2021). Paradoxically, TonB dependent membrane proteins that are involved in the transport of ferri-siderophores into the cell such as PfeA, FvbA and TonB are negatively correlated with the mutant phenotype. This suggests a dysregulation of the iron gathering mechanism in the QKO mutant, as it seems unlikely that the cell would upregulate pyoverdine unless intracellular iron levels were depleted. This is consistent with the regulation of iron uptake by the fur regulon, that is co-repressed by intracellular Fe2+. When Fe2+ levels are low, fur stops repressing iron uptake genes such as pyoverdine (Troxell and Hassan, 2013). This seemingly counterintuitive downregulation of iron uptake membrane proteins is likely linked to a defect in the assembly of OMP's and will be discussed in more detail below.

The central metabolism and other core pathways such as translation appear to be completely dysregulated in the QKO mutant. In particular, the links between glycolysis, the TCA cycle, oxidative phosphorylation and denitrification are interesting, as there is an increase in expression of some proteins of the glycolysis pathway such as GapA, Fbp and glk, which ultimately are involved in pyruvate production, but a significant downregulation in the dehydrogenases of the TCA cycle that initiates from pyruvate, and a reduction in the ubiquinones that are involved in oxidative phosphorylation. This could be linked to several factors, a potential lack of oxygen for use as a final electron acceptor, feedback inhibition of the TCA cycle due to upregulation of non-TCA dehydrogenases providing sufficient NADPH, and a lack of Fe2+ iron being available for the electron accepting cores of the ubiquinone proteins (Trunk et al., 2010; Tribelli et al., 2019). The potential of oxygen starvation being the key driver for this phenomenon is backed up by the upregulation of the anaerobic response regulator Anr. Usually, the induction of Anr leads to a swap from using oxygen as a terminal electron acceptor to denitrification (Trunk et al., 2010). However, the denitrification pathway is also dysregulated in the QKO mutant, leading to a down

regulation of proteins such as nitrite reductase. This is almost certainly linked to the deletion of YeaG from the genome, which has previously been shown to be required for survival under sustained nitrogen starvation in *E. coli* (Figueira et al., 2015). The TCA cycle is inhibited when a sufficient level of NAD(P)H is detected intracellularly, a significant upregulation of non-TCA dehydrogenases in the QKO mutant suggests that there would be an equal increase in the amount of NAD(P)H produced as a result of these reactions, potentially leading to a downregulation of the TCA cycle while not impacting glycolysis. The lack of iron being available for the enzymes involved in oxidative phosphorylation is supported by the significant upregulation of iron chelating siderophores.

The detoxification of reactive oxygen species is also dysregulated in the QKO mutant. ROS are produced as a result of numerous processes, such as oxidative phosphorylation, fenton chemistry in reaction with Fe2+ and from non-respiratory flavin dehydrogenases (da Cruz Nizer et al., 2021). The superoxide dismutase proteins SodB and SodM that produce hydrogen peroxide from oxygen radicals are both regulated as expected, as the sodB protein is downregulated under iron limiting conditions and sodM is upregulated to take over (da Cruz Nizer et al., 2021; Xie et al., 2013), however the hydrogen peroxide response is not what would be expected when comparing to previous literature. There are several upregulated proteins that detoxify H2O2 such as ahpF, glutathione peroxidase and thiol peroxidase that use NAD(P)H to reduce H202 to 2 H2O. However, KatA that encodes catalase and is usually the main H2O2 detoxifying enzyme in *P. aeruginosa* is negatively correlated with the QKO mutant. KatA expression is regulated by numerous pathways such as QS, iron levels, Anr, OxyR and IscR, (da Cruz Nizer et al., 2021) potentially explaining the paradoxical downregulation of this protein despite signs of significant H2O2 stress. The link to the iron levels is controlled by the fur regulon, which allows the transcription of certain genes when iron levels in the cell become depleted as appears to be the case in the QKO mutant (Troxell and Hassan, 2013). Anr is also found to be positively regulated in the QKO mutant and would usually elevate KatA expression, despite H2O2 not being produced during anaerobic respiration (Trunk et al., 2010; Tribelli et al., 2019). Anr is closely linked with denitrification and nitrite reductase through the transcriptional regulator DNR (Trunk et al., 2010), and the regulation of nitrite reductase has been shown to be impacted as a result of deleting YeaG from the genome (Figueira et al., 2015). A recent study showed that nirS deletion mutants produced approximately 50% the KatA of WT PAO1, suggesting that potentially a basal level of NO is required for full KatA activity (Su et al., 2014).

Translation apparatus such as elongation and initiation factors, and ribosomal proteins are generally downregulated in the QKO mutant. Generally, this suggests acute nutrient deprivation and therefore reduced protein synthesis is occurring. However, the stringent response proteins

SpoT, RelA and Lon that would normally induce rapid growth arrest via induction of ppGpp or TA-systems are all strongly negatively correlated with mutant phenotype. These proteins are normally upregulated as a result of the RpoS sigma factor that has been shown to require YeaG for full expression (Figueira et al., 2015), providing a mechanism for why these proteins are negatively correlated with the mutant. This could mean that the cell is unable to rapidly and effectively react to nutrient starvation via the controlled inhibition of protein synthesis. Furthermore, the nitrogen starvation response regulator ntrC is downregulated and is likely the result of deleting the YeaG eSTK (Figueira et al., 2015). This demonstrates that a significant proportion of the starvation response mechanisms that *P. aeruginosa* relies on are dysregulated. The downregulation of these proteins fits nicely with the hypothesis that eSTK's are essential for metabolic adaptation and stringent response induction, and that inhibiting eSTK's may prevent a reduction in metabolic activity that would otherwise reduce the effectiveness of antibiotics.

Numerous OMP's are downregulated in the QKO mutant. OMP's contribute to a large number of processes that are important in regulating intracellular homeostasis and nutrient acquisition, such as the efflux of antibiotics via the MexOMP's and siderophore uptake by TonB OMP's (Hancock and Brinkman, 2002; Fowler and Hanson, 2015; Chevalier et al., 2017; Luscher et al., 2018; Schweizer, 2012). On top of this, they are a crucial component in the stability of the outer membrane. This has been demonstrated using a knockdown mutant of BamA, that is responsible for insertion of proteins into the outer membrane, causing severe membrane stress and spurious firing of the T6SS as part of the 'tit for tat' attack strategy of *P. aeruginosa* i.e. *P. aeruginosa* perceives the membrane stress caused to be as a result of a hostile bacteria attacking using T6SS machinery (Malinverni and Silhavy, 2011; Stolle et al., 2021; Hews et al., 2019). This link to the T6SS suggests that the PpkA deletion is likely responsible for the downregulation of most of the outer membrane proteins either directly or indirectly. *P. aeruginosa* responds to T6SS attacks from other bacteria by upregulating and firing its own H1-T6SS and is thought to be in direct response to membrane stress. This membrane stress is detected by the sigma factor RpoE, which then leads to a cascade that ultimately results in outer membrane biogenesis (Malinverni and Silhavy, 2011; Stolle et al., 2021; Hews et al., 2019). It is feasible that this would result in the upregulation of proteins such as BamAB that work to insert proteins into the outer membrane and restore membrane integrity and replace damaged OMP's. However, BamB has been shown to be negatively correlated with the mutant phenotype suggesting dysregulation between the detection of outer membrane stress and outer membrane biogenesis.

All of the seemingly important phenotypes thus far have been associated to the deletion of PpkA or YeaG, however this more likely reflects the relative lack of research into Stk1 and Pstk than the kinases being redundant. A very recent study revealed that the proteome of a deletion mutant of

stk1 has a downregulation in type IV pili, as seen in the QKO mutant (Zhu *et al.*, 2021a). This could suggest that the deletion of Stk1 is the key driver for this, however type IV pili are generally linked to the T6SS and both Stk1 and PpkA are found on T6SS loci. The study also used an unusual fold change cut off of 1.3, which is certainly on the low end of what is actually biologically relevant. At the time of writing there does not seem to be any research on the PA1782/Pstk specifically, however one study did link it to initial biofilm maturation (Southey-Pillig, Davies and Sauer, 2005).

The phosphoproteomics was not successful in identifying any differentially phosphorylated proteins (**Error! Reference source not found.**), likely due to an issue with the enrichment or the labelling of the peptides with the TMT reporter ions. While some inferences were made based on the whole proteome datasets, they will not be discussed further as it is impossible to make any reliable conclusions based on the data. Future work should focus on repeating this experiment and will be discussed in more detail in Chapter five.

The overarching goal of the study of the proteome was to elucidate the mechanisms surrounding the phenotype of the biofilms in Chapter 3, where there are significantly more membrane compromised cells found in the centre of the QKO biofilms relative to the wild type (Figure 24). While this summarises the phenotype, the reality is significantly more complex. This is due to the fact that there was no observable phenotype in the planktonic cultures and that the membrane compromised cell phenotype is degenerative over time. The proteomic phenotypes that have been observed in this chapter are linked to the QKO mutant generally and not the QKO biofilm specifically, showing that the dysregulation happens in planktonic culture at stationary phase where nutrient starvation starts to occur. This would therefore suggest that the membrane compromised cell phenotype would be seen at approximately equal levels across all biofilm timepoints. As this is not the case, it must be assumed that the phenotype is occurring as a result of the proteome being dysregulated over time. If the membrane compromised phenotype is broken down even further, it must be assumed that the membrane compromised cells are still alive based on the CFU analysis showing comparable viable cells in the QKO and WT biofilms (Figure 23). In effect, the mechanism must therefore be linked to the ability for propidium iodide (the red stain used in Live/Dead analysis) to cross the membranes of live cells. Propidium iodide cannot usually cross the membranes of live cells due to its exposed positive charge and the polarisation of the cell membrane (Davey and Hexley, 2011; Kirchhoff and Cypionka, 2017; Rosenberg, Azevedo and Ivask, 2019). However, bacteria with an increased membrane potential have been shown to allow the passage of propidium iodide through the outer membrane while still being alive (Kirchhoff and Cypionka, 2017). In Chapter 3, it was hypothesised that the mechanism allowing for an increase in membrane potential was linked to an increase of intracellular ROS species, which is certainly supported by the proteomics in this chapter.

Therefore, the mechanism proposed for the compromised membrane phenotype in the centre of the biofilm is as follows, the deletion of PpkA from the genome dysregulates T6SS and OMP localisation both directly through the signalling system for membrane stress and indirectly via the GacSA/RsmA signalling pathway. This contributes to the iron starvation issue highlighted by the upregulation of pyoverdine and pyochelin by downregulating TonB OMP's that are essential for siderophore uptake. Iron starvation leads to a reduced ability of the cell to produce iron core groups that are essential in several reducing enzymes, as well as in the enzymes of the aerobic respiratory chain such as cytochromes. This leads to dysregulation of the oxidative phosphorylation pathway, potentially resulting in electron leakage and substantially increased superoxide radical production (da Cruz Nizer et al., 2021; Kussmaul and Hirst, 2006). The superoxide radicals are then detoxified by SodM into H2O2, which can lead to a vicious cycle whereby through Fenton chemistry H2O2 can damage iron containing proteins by catalysing the formation of ferric oxide and water from Fe2+, ferric oxide can then be converted to insoluble Fe3+ and a hydroxyl radical (da Cruz Nizer et al., 2021). The downregulation of phenazines then means that Fe3+ is not being efficiently converted back into Fe2+ for use in enzymes, so the cycle continues. Furthermore, as oxygen is being used up and converted into superoxide the transcriptional regulator Anr is upregulated and would usually signify a shift to anaerobic respiration via denitrification, where nitrogen is used as the final electron acceptor instead of oxygen (Trunk et al., 2010; Tribelli et al., 2019). However, the deletion of YeaG dysregulates this process and prevents the switch to anaerobic respiration via denitrification (Figueira et al., 2015). This could result in the excessive use of oxygen as a final electron acceptor and increase superoxide production via aerobic respiration. This would presumably eventually lead to a downregulation of the TCA cycle and oxidative phosphorylation as is supported by the proteomic data. The abundance of intracellular H2O2 then necessitates the upregulation of peroxidases such as ahpF, tpx and glutathione peroxidase to reduce the ROS to 2 H2O. A significant amount of reducing power in the form of NAD(P)H is required, leading to an increase in activity of non-TCA dehydrogenase enzymes that catalyse the formation of NAD(P)H from NAD+. The need for these enzymes is highlighted by the significant upregulation of renalase, that prevents dehydrogenases from being clogged with NAD+. It is plausible that over time ROS will not be able to be efficiently detoxified, and that membrane proteins will also start to become significantly damaged due to ROS attack. Potentially, this could then lead to a permeable membrane due to decreased membrane integrity, damaged or missing membrane proteins, and due to the membrane potential being reduced due to the significant intracellular levels of ROS. Ultimately allowing entry of propidium iodide into a viable cell.

The proteome also provides some clarity on why the antibiotic susceptibility of the QKO mutant biofilms to tobramycin is not reduced in Chapter 3 (Figure 29). Although it would be assumed that due to the apparent increased permeability of the membrane that more tobramycin would be transported into the cytoplasm of the QKO mutant, increasing its effectiveness. It is possible that due to the downregulation of translation proteins such as translation factors and ribosomes, that aminoglycosides such as tobramycin that attack the 30S subunit of the ribosome may have not as strong as an effect as would otherwise be possible with a semi-permeable membrane.

To conclude, there is very strong evidence that the metabolic adaptability of *P. aeruginosa* is significantly reduced when all of the eSTK's are deleted from the genome. This seems to link to a complete dysregulation of several core processes as opposed to one mechanism, which shouldn't be surprising as in other organisms eSTK's have been shown to be key regulatory proteins. This research shows the potential for creating anti-biofilm compounds that inhibit these systems and ultimately reduce *P. aeruginosa*'s ability to survive adverse conditions.

Chapter 5 **Conclusion and Outlook**

For immuno-compromised individuals, infection with *P. aeruginosa* can have serious implications, as due to rapid evolution and the numerous protective mechanisms of the *P. aeruginosa* biofilm, antibiotics cannot effectively combat the recalcitrance of this organism, that can ultimately result in mortality. This necessitates the discovery of novel, targeted adjunctive therapies that dysregulate the protective mechanisms of the biofilm and restore the effectiveness of golden-era antibiotics. Serine/threonine phosphorylation has been mostly overlooked in bacteria as it was originally assumed that the entirety of the intracellular signalling of prokaryotes was accomplished through histidine kinases and two-component systems. This study focused on elucidating the potential roles that four eukaryote-like serine/threonine kinases of *P. aeruginosa* have on the metabolic adaptability of the biofilm, with the goal of identifying a new target for drug discovery.

5.1 Different effects are observed when deleting YeaG from an acutely virulent strain, compared to a chronic strain

One of the questions we hoped to address within this study is if there would be a different phenotype observed when deleting eSTK's from the genome of an acutely virulent strain such as PAO1 and a chronic CF isolate such as PA2192. It was hypothesised that there may be a difference as chronic and acute strains are known to use different regulatory systems to exert their phenotype. There was no phenotype observed at all in PAO1 and PA2192 in the ΔStk1 and ΔPstk mutants. However, a visible phenotype was observed for ΔYeaG in PA2192 and not in PAO1. The planktonic growth curve of PAO1 shows no difference in a ΔYeaG background (Figure 16), whereas PA2192 shows a significant delay into stationary phase relative to the wildtype(Figure 17). It was observed that when growing PA2192 overnight in LB with shaking, clumps of biofilm would still form in the culture. This is likely the result of the alginate mutation that is characteristic of PA2192 enabling cells to easily clump together. In the PA2192 ΔYeaG mutant, overnight cultures would not show a clumping together of cells and would generally form a more turbid culture of planktonic cells, which is almost certainly the reason for the delayed entry into stationary phase during the growth curve experiment. It is hypothesised based on the proteomics dataset that showed a downregulation of alginate proteins in the QKO mutant, that YeaG may be responsible for this and in the PA2192 strain may facilitate an upregulation in the mucoid phenotype. Whereas PAO1 being an acute strain is unlikely to rely on alginate for biofilm formation and more likely to use PSL.

5.2 eSTK's are important in regulating key processes that impact the adaptability of *P. aeruginosa* PAO1

A critical element of this study was determining to what extent eSTK's regulate key processes that may provide protection from antibiotic attack due to driving biofilm adaptability. The presence of a membrane compromised phenotype in the QKO and ΔPpkA biofilms that was also degenerative based on time and based on the number of eSTK's deleted from the genome highlights that an important level of regulation that was originally being provided by eSTK's has now been removed. However, it was interesting that the viability of the biofilm was not affected.

When examining the proteomics dataset, it became clear how important these proteins are to the effective functioning of the cell. There appeared to be complete dysregulation of the central metabolism, iron sequestering and uptake, reactive oxygen species degradation, stringent response induction, and membrane maintenance and integrity. The majority of this dysregulation can likely be attributed to the deletion of PpkA and YeaG, as the key drivers of the mechanism seems to stem from a reduction in the capacity of the T6SS to respond to membrane stress and take up iron, and a lack of denitrification for anaerobic respiration. With this information a mechanism was proposed for the degenerative membrane compromised phenotype of the QKO biofilms. Broadly, it was hypothesised that dysregulation on T6SS lead to impaired iron uptake and increased membrane stress, which results in dysregulation of the TCA cycle and electron transport that ultimately leads to greatly increased superoxide radical production. This then leads to a vicious cycle of increased ROS production, membrane damage and oxygen utilisation that results in the upregulation of Anr to swap to the anaerobic phenotype. Dysregulation of denitrification by the deletion of YeaG prevents this happening, leading to ineffective adaptation to ROS that causes more membrane damage and membrane depolarisation that allows the passive entry of propidium iodide into the cells.

Even though the viability was unaffected, it is clear that the metabolic adaptability and presumably the ability of *P. aeruginosa* to occupy multiple niches has been reduced.

5.3 Deletion of eSTK's does not affect the antibiotic susceptibility of PAO1 relative to the wild type in planktonic or biofilm culture when treated with tobramycin

It is surprising when looking at the number of membrane compromised cells in the biofilm at 96 hours and at the proteome of the QKO mutant generally that it is not more susceptible to

treatment with tobramycin than the wildtype (Figure 29). This is especially true when considering that one of the major difficulties of treating with tobramycin is that it relies heavily on increased membrane permeability, which has been shown to be likely significantly increased relative to the WT strain. It is difficult to know the exact mechanism of why this is case, however it could possibly have been attributed to the downregulation of translation and ribosomal proteins observed in the proteomics analysis. Although the mechanism of tobramycin hasn't been fully elucidated, its major target is considered to be the 30S ribosome as with other aminoglycosides.

While this does of course call into question whether or not eSTK's are a worthwhile drug target for adjunctive therapies, it is worth considering that this is only testing one antibiotic on one strain of *P. aeruginosa in-vitro*. The effects of antibiotics *in-vivo* are rarely the same as seen in *in-vitro*, and as discussed above, inhibition of eSTK's in clinical isolates or generally more chronic strains may show a different effect and should be a focus of future work.

5.4 Follow on research

In this study we have shown that the eSTK's are required for the effective regulation of numerous key processes, and that the metabolic adaptability of *P. aeruginosa* is significantly perturbed when all four eSTK's are deleted from the genome. However, this does not translate to an increased susceptibility of *P. aeruginosa* to tobramycin (Figure 29). This is an extremely important point to consider before conducting further research, as nebulised and inhaled tobramycin is the major antibiotic used to treat *P. aeruginosa* infections in cystic fibrosis. With this in mind, it is the belief of the author that due to the extent of the dysregulation and the apparent lack of prior research into targeting eSTK's of *P. aeruginosa* that more work should be undertaken to further evaluate the potential for these proteins to be drug targets for adjunctive therapies.

In the first instance, there should be a focus on deleting PpkA from the genome of PA2192 and then creating a PA2192 quadruple eSTK knockout as with PAO1. Antibiotic susceptibility experiments should then be used to determine if there is the potential for an increased susceptibility to antibiotics of eSTK deletion mutants of CF isolates. Following this, proteomic and phosphoproteomic experiments should then be carried out on this strain, with the phosphoproteomics repeated for PAO1, to determine if there are major differences is the regulatory pathways controlled by eSTK's in a chronic CF isolate of *P. aeruginosa* relative to an acute strain. If there does appear to be a mechanism by which the antibiotic susceptibility of the bacteria is increased, work should focus on identifying a highly general eSTK inhibitor that can be used as a proof of concept to show that eSTK's can be inhibited in *P. aeruginosa* and that it's effective. If successful, a broadly specific inhibitor that can simultaneously inhibit all four of the

eSTK's identified in *P. aeruginosa* without being overly cytotoxic should be sought. Potential methods for this vary, as to develop a highly effective compound it would likely require a crystal structure of all the proteins first which is highly time consuming, however one of the most promising surrounds the use of bivalent kinase inhibitors that bind at the active site and one other site on the enzyme to increase specificity.

Another avenue of future research should be the use of tissue culture and model systems to determine to what extent the pathogenicity is being affected by the eSTK deletions. Mougous et al., have already released an excellent paper years ago that extensively characterises the attenuated virulence of a PpkA mutant, so research should focus on whether taking the biofilms out of an *in-vitro* environment may enhance their susceptibility to antibiotics. Current research in our lab uses a tissue culture model that uses CF primary cells to examine the virulence of *P. aeruginosa* quorum sensing mutants. While this is still *in-vitro*, in the first instance this would be an excellent place to start and would provide even more information about how appropriate a target eSTK's are for adjunctive therapies.

Appendix A

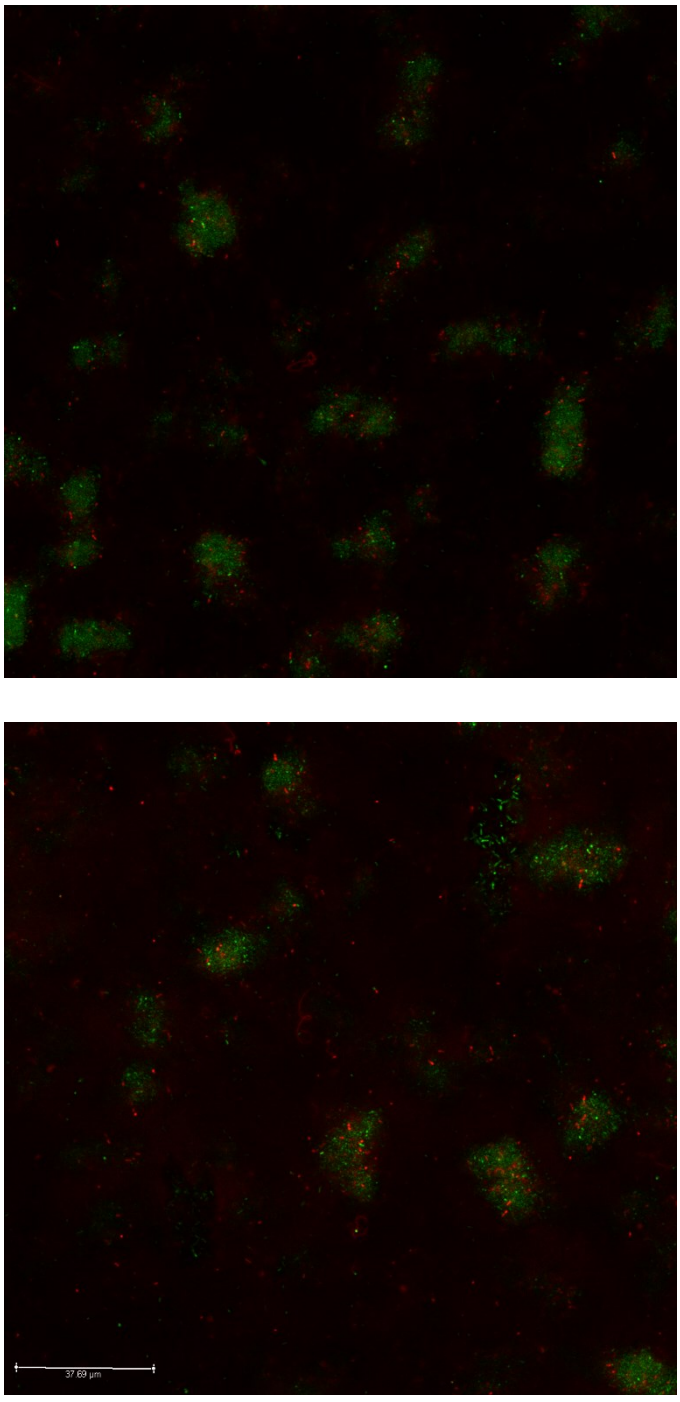

Figure 52: Unprocessed confocal images of PpkA (Top) and TKO (Bottom) Filamentation

Table 10: Differentially expressed proteins identified from the biofilm, planktonic and serine hydroxamate treated planktonic samples. Protein network data is from the PseudoCYC and KEGG databases

	Locus ID	Gene name	Protein	Log2 fold change	PseudoCYC	KEGG
Biofilm						
	PA0071	tagR1	hypothetical protein	-0.84	-	-
	PA0078	TssL1	hypothetical protein	0.68	-	Bacterial secretion system
	PA0095	vgrG1b	hypothetical protein	-0.96	-	Bacterial secretion system
	PA0140	ahpF	alkyl hydroperoxide reductase	0.59	-	-
	PA0282	cysT	sulfate transporter CysT	1.32	-	ABC transporters
	PA0359		hypothetical protein	1.42	-	-
	PA0406	tonB3	transporter TonB	0.7	-	-
	PA0536		hypothetical protein	1.43	-	-
	PA0558		hypothetical protein	1.31	-	-
	PA0586		hypothetical protein	-0.98	-	-
	PA0588		hypothetical protein	-2.29	-	-
	PA0649	trpG	anthranilate synthase component II	0.66	2-heptyl-3-hydroxy-4(1H)-quinolone biosynthesis	2-heptyl-3-hydroxy-4(1H)-quinolone biosynthesis
	PA0653		hypothetical protein	0.58	-	-
	PA0767	lepA	elongation factor 4	-0.63	-	-
	PA0878		hypothetical protein	1.04	-	C5-Branched dibasic acid metabolism

PA0879		acyl-CoA dehydrogenase	1.42	-	beta-Alanine metabolism
PA0881		hypothetical protein	1.51	-	-
PA0882		hypothetical protein	1.82	-	C5-Branched dibasic acid metabolism
PA0883		acyl-CoA lyase subunit beta	1.99	-	C5-Branched dibasic acid metabolism
PA0917	kup	potassium transport system protein kup	0.68	-	-
PA1053		hypothetical protein	0.77	-	-
PA1076		hypothetical protein	-1.25	-	-
PA1119	yfiB	Prokaryotic membrane lipoprotein lipid attachment site profile	-0.68	-	-
PA1249	aprA	alkaline metalloproteinase	-1.24	-	Cationic antimicrobial peptide (CAMP) resistance
PA1317	cyoA	cytochrome o ubiquinol oxidase subunit II	0.76	-	Metabolic pathways
PA1327		protease	-0.67	-	-
PA1344		short-chain dehydrogenase	0.69	-	-
PA1376	aceK	bifunctional isocitrate dehydrogenase kinase/phosphatase	0.99	-	-
PA1544	anr	transcriptional regulator Anr	0.73	-	-
PA1596	htpG	chaperone protein HtpG	-0.57	-	-
PA1618		esterase	0.64	-	-
PA1736		acetyl-CoA acetyltransferase	1.22	fatty acid salvage	Benzoate degradation
PA1746		hypothetical protein	-0.64	-	-

	PA1775	cmpX	hypothetical protein	1.16	-	-
	PA2236	pslF	biofilm formation protein PslF	-0.84	-	Biofilm formation - *Pseudomonas aeruginosa*
	PA2237	pslG	biofilm formation protein PslG	-0.62	-	Biofilm formation - *Pseudomonas aeruginosa*
	PA2240	pslJ	biofilm formation protein PslJ	0.76	-	Biofilm formation - *Pseudomonas aeruginosa*
	PA2300	chiC	chitinase	-1.46	-	-
	PA2389	pvdR	pyoverdine biosynthesis protein PvdR	0.89	-	-
	PA2399	pvdD	pyoverdine synthetase D	0.91	-	-
	PA2400	pvdJ	pyoverdine biosynthesis protein PvdJ	0.76	-	-
	PA2402		peptide synthase	0.69	-	-
	PA2403		hypothetical protein	-1.29	-	-
	PA2413	pvdH	diaminobutyrate--2-oxoglutarate aminotransferase	0.94	-	2-Oxocarboxylic acid metabolism
	PA2424	pvdL	peptide synthase	0.77	-	-
	PA2532	tpx	2-Cys peroxiredoxin	0.77	-	-
	PA2570	lecA	PA-I galactophilic lectin	-1	-	Biofilm formation - *Pseudomonas aeruginosa*
	PA2581		hypothetical protein	-0.97	-	-
	PA2626	trmU	tRNA-specific 2-thiouridylase MnmA	-0.92	-	Sulfur relay system
	PA2638	nuoB	NADH-quinone oxidoreductase subunit B	-0.69	-	Metabolic pathways
	PA2659		hypothetical protein	1.13	-	-

PA2794		hypothetical protein	0.86	-	-
PA2824		sensor/response regulator hybrid protein	0.8	-	Biofilm formation - *Pseudomonas aeruginosa*
PA2826		glutathione peroxidase	-0.61	-	Arachidonic acid metabolism
PA2832	tpm	thiopurine S-methyltransferase	-0.81	-	-
PA2871		hypothetical protein	0.83	-	-
PA2920		chemotaxis transducer	0.78	-	Bacterial chemotaxis
PA2967	fabG	3-oxoacyl-[acyl-carrier-protein] reductase FabG	0.94	-	Biosynthesis of unsaturated fatty acids
PA3082	gbt	glycine betaine transmethylase	-2.24	-	-
PA3112	accD	acetyl-CoA carboxylase carboxyltransferase subunit beta	-1.15	-	Biosynthesis of antibiotics
PA3121	leuC	3-isopropylmalate dehydratase large subunit	-0.97	L-leucine biosynthesis	2-Oxocarboxylic acid metabolism
PA3193	glk	glucokinase	0.58	glucose and glucose-1-phosphate degradation	Amino sugar and nucleotide sugar metabolism
PA3195	gapA	glyceraldehyde 3-phosphate dehydrogenase	0.67	aerobic glycerol degradation I	Biosynthesis of amino acids
PA3356		hypothetical protein	0.97	-	Alanine, aspartate and glutamate metabolism
PA3402		hypothetical protein	-0.67	-	-
PA3450	lsfA	1-Cys peroxiredoxin LsfA	-0.81	-	-

PA3554	arnA	bifunctional UDP-glucuronic acid decarboxylase/UDP-4-amino-4-deoxy-L-arabinose formyltransferase	1.1	-	Amino sugar and nucleotide sugar metabolism
PA3568		propionyl-CoA synthetase	0.64	acetate conversion to acetyl-CoA	Metabolic pathways
PA3650	dxr	1-deoxy-D-xylulose 5-phosphate reductoisomerase	-1.26	methylerythritol phosphate pathway I	Biosynthesis of antibiotics
PA3690		metal-transporting P-type ATPase	0.71	-	-
PA3728		hypothetical protein	-0.89	-	-
PA3742	rplS	50S ribosomal protein L19	-0.7	-	Ribosome
PA3746	ffh	signal recognition particle protein Ffh	-0.77	-	Bacterial secretion system
PA3798		aminotransferase	-1.13	-	-
PA3846		hypothetical protein	1.38	-	-
PA3919		hypothetical protein	0.97	-	-
PA3983		hypothetical protein	-0.75	-	-
PA3984	lnt	apolipoprotein N-acyltransferase	0.58	-	-
PA3999	dacC	D-ala-D-ala-carboxypeptidase	1	-	Metabolic pathways
PA4015		hypothetical protein	2.09	-	-
PA4044	dxs	1-deoxy-D-xylulose-5-phosphate synthase	-0.58	methylerythritol phosphate pathway I	Biosynthesis of antibiotics
PA4132		hypothetical protein	-2.56	-	-
PA4156		TonB-dependent receptor	-0.66	-	-
PA4180		acetolactate synthase	0.63	L-isoleucine biosynthesis I (from threonine)	2-Oxocarboxylic acid metabolism
PA4206	mexH	resistance-nodulation-cell division (RND) efflux membrane fusion protein	-0.76	-	Quorum sensing

	PA4216	phzG1	pyridoxamine 5'-phosphate oxidase	-1.18	Phenazine biosynthesis	Phenazine biosynthesis
	PA4217	phzS	hypothetical protein	-1.35	Phenazine biosynthesis	Phenazine biosynthesis
	PA4220	fptB	Pyochelin Fe(III) transport precursor	0.78	-	-
	PA4225	pchF	pyochelin synthetase	0.84	L-ornithine degradation II (Stickland reaction)	Biosynthesis of siderophore group nonribosomal peptides
	PA4244	rplO	50S ribosomal protein L15	-0.89	-	Ribosome
	PA4246	rpsE	30S ribosomal protein S5	-0.85	-	Ribosome
	PA4275	nusG	transcription antitermination protein NusG	-1.27	-	-
	PA4315	mvaT	transcriptional regulator MvaT	-1.27	-	-
	PA4366	sodB	superoxide dismutase	-1.23	superoxide radicals degradation	superoxide radicals degradation
	PA4385	groEL	molecular chaperone GroEL	-0.97	-	RNA degradation
	PA4390		hypothetical protein	-1.67	-	-
	PA4547	pilR	two-component response regulator PilR	0.58	-	Two-component system
	PA4551	pilV	type 4 fimbrial biogenesis protein PilV	-1.16	-	-
	PA4558		FkbP-type peptidyl-prolyl cis-trans isomerase	1.61	-	-
	PA4657		Renalase	1.06	-	-
	PA4661	pagL	lipid A 3-O-deacylase	-1.26	-	-
	PA4709		hemin degrading factor	0.84	-	-
	PA4729	panB	3-methyl-2-oxobutanoate hydroxymethyltransferase	-1.45	phosphopantothenate biosynthesis III (archaebacteria)	Biosynthesis of secondary metabolites

	PA4733	acsB	acetyl-CoA synthetase	-0.59	cis-genanyl-CoA degradation	Biosynthesis of antibiotics
	PA4739		hypothetical protein	-1.28	-	-
	PA4741	rpsO	30S ribosomal protein S15	-0.94	-	Ribosome
	PA4746	rimP	hypothetical protein	-0.81	-	-
	PA4758	carA	carbamoyl phosphate synthase small subunit	-0.82	L-arginine biosynthesis II (acetyl cycle)	Alanine, aspartate and glutamate metabolism
	PA4845	dipZ	thiol:disulfide interchange protein	0.9	-	-
	PA4875		hypothetical protein	1.42	-	-
	PA4948		hypothetical protein	-0.84	-	-
	PA4972		hypothetical protein	-0.58	-	-
	PA5028		hypothetical protein	-1.29	-	-
	PA5107	blc	outer membrane lipoprotein Blc	-0.94	-	-
	PA5150		short-chain dehydrogenase	1.1	-	-
	PA5172	arcB	ornithine carbamoyltransferase	-0.68	-	Arginine biosynthesis
	PA5201		hypothetical protein	-0.97	-	-
	PA5213	gcvP1	glycine dehydrogenase	0.6	-	Biosynthesis of antibiotics
	PA5300	cycB	cytochrome C5	-0.99	-	-
	PA5313		omega amino acid--pyruvate transaminase	1.03	-	beta-Alanine metabolism
	PA5343		hypothetical protein	-0.99	-	-
	PA5348	hupA	DNA-binding protein	-1.23	-	-
	PA5545		hypothetical protein	-0.88	-	-
	PA5570	rpmH	50S ribosomal protein L34	-1.31	-	Ribosome

Planktonic

PA0020		hypothetical protein	-0.96	-	-
PA0105	coxB	cytochrome C oxidase subunit II	-0.67	-	Metabolic pathways
PA0114	senC	cytochrome c oxidase assembly protein SenC	-0.64	-	-
PA0115		hypothetical protein	-1.05	-	-
PA0127		hypothetical protein	-0.57	-	-
PA0140	ahpF	alkyl hydroperoxide reductase	4.28	-	-
PA0171		hypothetical protein	0.78	-	-
PA0179		two-component response regulator	-1.24	-	Bacterial chemotaxis
PA0238		hypothetical protein	-0.83	-	-
PA0319		hypothetical protein	-0.64	-	-
PA0329		hypothetical protein	-1.33	-	-
PA0363	coaD	phosphopantetheine adenylyltransferase	0.66	coenzyme A biosynthesis I	coenzyme A biosynthesis I
PA0366	calB	coniferyl aldehyde dehydrogenase	-0.84	-	-
PA0381	thiG	thiazole synthase	1.54	-	Metabolic pathways
PA0387		non-canonical purine NTP pyrophosphatase	-0.77	-	Purine metabolism
PA0388		hypothetical protein	-1.27	-	-
PA0407	gshB	glutathione synthetase	3.24	glutathione biosynthesis	glutathione biosynthesis
PA0421		hypothetical protein	-0.65	-	Arginine and proline metabolism
PA0452		hypothetical protein	-0.8	-	-
PA0460		hypothetical protein	-1.35	-	-
PA0506		acyl-CoA dehydrogenase	0.92	-	-

	PA0577	dnaG	DNA primase	-0.88	-	DNA replication
	PA0586		hypothetical protein	-4.2	-	-
	PA0587		hypothetical protein	-2.86	-	-
	PA0588		hypothetical protein	-4.92	-	-
	PA0602		ABC transporter	-0.75	-	Quorum sensing
	PA0603	potA	ABC transporter ATP-binding protein	-0.71	-	Quorum sensing
	PA0660		hypothetical protein	1.49	-	Nitrogen metabolism
	PA0747		aldehyde dehydrogenase	-0.63	-	beta-Alanine metabolism
	PA0833		hypothetical protein	-1.05	-	-
	PA0865	hpd	4-hydroxyphenylpyruvate dioxygenase	-0.85	-	Metabolic pathways
	PA0902		hypothetical protein	0.86	-	Biosynthesis of amino acids
	PA0928	gacS	sensor/response regulator hybrid protein	-2.59	-	Biofilm formation - *Pseudomonas aeruginosa*
	PA0961		hypothetical protein	-0.92	-	-
	PA1010	dapA	4-hydroxy-tetrahydrodipicolinate synthase	0.82	L-lysine biosynthesis I	Biosynthesis of amino acids
	PA1045	dinG	ATP-dependent DNA helicase DinG	-0.83	-	-
	PA1091	fgtA	flagellar glycosyl transferase FgtA	0.72	-	-
	PA1092	fliC	B-type flagellin	-0.87	-	Flagellar assembly
	PA1094	fliD	B-type flagellar hook-associated protein	-1.52	-	Flagellar assembly
	PA1155	nrdB	ribonucleotide-diphosphate reductase subunit beta	2.52	-	Metabolic pathways
	PA1156	nrdA	ribonucleotide-diphosphate reductase subunit alpha	0.88	-	Metabolic pathways

PA1324		hypothetical protein	-1.87	-	-
PA1457	cheZ	protein phosphatase CheZ	0.63	-	Bacterial chemotaxis
PA1623		hypothetical protein	0.67	-	-
PA1678	prmB	50S ribosomal protein L3 glutamine methyltransferase	0.82	-	-
PA1687	speE1	polyamine aminopropyltransferase	0.58	ornithine spermine biosynthesis	Arginine and proline metabolism
PA1746		hypothetical protein	2.46	-	-
PA1829		hypothetical protein	-1.81	-	-
PA1930		chemotaxis transducer	-0.6	-	Bacterial chemotaxis
PA1982	exaA	quinoprotein ethanol dehydrogenase	-0.61	-	Biosynthesis of antibiotics
PA2001	atoB	acetyl-CoA acetyltransferase	0.63	Carnitine Catabolism to Glycine Betaine	Benzoate degradation
PA2233	pslC	biofilm formation protein PslC	-0.61	-	Biofilm formation - *Pseudomonas aeruginosa*
PA2247	bkdA1	2-oxoisovalerate dehydrogenase subunit alpha	-0.71	-	Biosynthesis of antibiotics
PA2249	bkdB	branched-chain alpha-keto acid dehydrogenase complex lipoamide acyltransferase	-0.63	-	Biosynthesis of antibiotics
PA2318		hypothetical protein	-0.95	-	-
PA2363		hypothetical protein	0.65	-	Biofilm formation - *Pseudomonas aeruginosa*
PA2371		ClpA/B-type protease	-2.48	-	Bacterial secretion system
PA2396	pvdF	pyoverdine synthetase F	3.25	-	-

PA2413	pvdH	diaminobutyrate--2-oxoglutarate aminotransferase	2.26	-	2-Oxocarboxylic acid metabolism
PA2464		hypothetical protein	-0.6	-	-
PA2491		oxidoreductase	1.1	-	-
PA2562		hypothetical protein	-0.71	-	-
PA2570	lecA	PA-I galactophilic lectin	-0.71	-	Biofilm formation - *Pseudomonas aeruginosa*
PA2633		hypothetical protein	-0.96	-	-
PA2727		hypothetical protein	-0.6	-	-
PA2796	tal	transaldolase B	0.64	pentose phosphate pathway	Biosynthesis of amino acids
PA2823		hypothetical protein	0.85	-	-
PA2840	deaD	ATP-dependent RNA helicase	-1.26	-	RNA degradation
PA2945	cobW	cobalamin biosynthesis protein CobW	1.44	-	-
PA2968	fabD	malonyl CoA-ACP transacylase	0.61	bryostatin biosynthesis	Fatty acid biosynthesis
PA3043	dgt2	deoxyguanosinetriphosphate triphosphohydrolase	0.61	-	Purine metabolism
PA3195	gapA	glyceraldehyde 3-phosphate dehydrogenase	3.19	aerobic glycerol degradation I	Biosynthesis of amino acids
PA3317		hypothetical protein	-0.84	-	-
PA3337	hldD	ADP-L-glycero-D-mannoheptose-6-epimerase	3.23	-	Lipopolysaccharide biosynthesis
PA3356		hypothetical protein	1.84	-	Alanine, aspartate and glutamate metabolism
PA3526		hypothetical protein	-0.63	-	-

PA3687	ppc	phosphoenolpyruvate carboxylase	0.65	biosynthetic metabolism	Carbon metabolism
PA3692	lptF	outer membrane porin F	-1.04	-	-
PA3736	hom	homoserine dehydrogenase	0.78	L-homoserine biosynthesis	Biosynthesis of amino acids
PA3795		oxidoreductase	0.87	-	-
PA3808		hypothetical protein	-0.98	-	-
PA3819		hypothetical protein	-0.92	-	-
PA3846		hypothetical protein	2.98	-	-
PA3858		amino acid-binding protein	-0.99	-	ABC transporters
PA3919		hypothetical protein	1.22	-	-
PA3924		long-chain-fatty-acid--CoA ligase	0.69	-	-
PA3925		acyl-CoA thiolase	1.65	fatty acid salvage	Benzoate degradation
PA3970	amn	AMP nucleosidase	0.9	-	Purine metabolism
PA4020	mpl	UDP-N-acetylmuramate	0.58	lipid A and peptidoglycan biosynthesis	lipid A and peptidoglycan biosynthesis
PA4180		acetolactate synthase	1.54	L-isoleucine biosynthesis I (from threonine)	2-Oxocarboxylic acid metabolism
PA4224	pchG	pyochelin biosynthetic protein PchG	2.22	pyochelin biosynthesis	Biosynthesis of siderophore group nonribosomal peptides
PA4230	pchB	isochorismate-pyruvate lyase	0.71	salicylate biosynthesis I	Biosynthesis of antibiotics
PA4283	recD	exodeoxyribonuclease V subunit alpha	-1.02	-	Homologous recombination

PA4306	flp	type IVb pilin Flp	-0.99	-	-
PA4327		hypothetical protein	-1.08	-	-
PA4328		hypothetical protein	2.95	-	-
PA4352		hypothetical protein	1.41	-	-
PA4362		hypothetical protein	-0.61	-	-
PA4373		hypothetical protein	-1.17	-	-
PA4439	trpS	tryptophan--tRNA ligase	0.59	tRNA charging	Aminoacyl-tRNA biosynthesis
PA4443	cysD	sulfate adenylyltransferase subunit 2	1.3	sulfate activation for sulfonation	Biosynthesis of antibiotics
PA4446	algW	AlgW protein	-0.73	-	-
PA4447	hisC1	histidinol-phosphate aminotransferase	0.75	phenylalanine biosynthesis, *Bacillus subtilis*	Biosynthesis of amino acids
PA4458		hypothetical protein	1	-	Lipopolysaccharide biosynthesis
PA4493	roxR	DNA-binding response regulator RoxR	0.78	-	Two-component system
PA4515	piuC	hydroxylase	3.79	-	-
PA4579		hypothetical protein	-0.72	-	-
PA4588	gdhA	glutamate dehydrogenase	2.93	glutamate degradation III	Alanine, aspartate and glutamate metabolism
PA4657		Renalase	1.8	-	-
PA4676		carbonic anhydrase	0.59	-	Nitrogen metabolism
PA4701		hypothetical protein	1.16	-	-
PA4717		hypothetical protein	-1.34	-	-

PA4723	dksA	suppressor protein DksA	0.9	-	-
PA4739		hypothetical protein	-0.88	-	-
PA4899		aldehyde dehydrogenase	1.03	-	Arginine and proline metabolism
PA4913		ABC transporter	-0.75	-	ABC transporters
PA4931	dnaB	replicative DNA helicase	-1.07	-	DNA replication
PA4952	rsgA	ribosome-associated GTPase	-0.77	-	Metabolic pathways
PA5014	glnE	bifunctional glutamine-synthetase adenylyltransferase/deadenyltransferase	-0.62	-	-
PA5051	argS	arginine--tRNA ligase	0.67	tRNA charging	Aminoacyl-tRNA biosynthesis
PA5060	phaF	polyhydroxyalkanoate synthesis protein PhaF	-0.77	-	-
PA5122		hypothetical protein	-0.78	-	-
PA5133		hypothetical protein	-0.78	-	-
PA5150		short-chain dehydrogenase	1.55	-	-
PA5161	rmlB	dTDP-D-glucose 4,6-dehydratase	0.72	dTDP-L-rhamnose biosynthesis I	Acarbose and validamycin biosynthesis
PA5178		hypothetical protein	1.2	-	-
PA5201		hypothetical protein	-0.66	-	-
PA5277	lysA	diaminopimelate decarboxylase	0.85	L-lysine biosynthesis II	Biosynthesis of amino acids
PA5278	dapF	diaminopimelate epimerase	-1.28	L-lysine biosynthesis I	Biosynthesis of amino acids
PA5304	dadA1	D-amino acid dehydrogenase small subunit	-1.04	D-arginine degradation	Phenylalanine metabolism
PA5335		hypothetical protein	1.5	-	-

	PA5359		hypothetical protein	-0.77	-	-
	PA5414		hypothetical protein	-1.35	-	-
SHX						
	PA0179		two-component response regulator	-0.66	-	Bacterial chemotaxis
	PA0586		hypothetical protein	-1.25	-	-
	PA0588		hypothetical protein	-1.09	-	-
	PA0920		hypothetical protein	-0.73	-	Cationic antimicrobial peptide (CAMP) resistance
	PA1151	imm2	pyocin-S2 immunity protein	0.95	-	-
	PA2021		hypothetical protein	0.7	-	-
	PA3049	rmf	ribosome modulation factor	0.63	-	-
	PA3440		hypothetical protein	0.81	-	-
	PA3768		metallo-oxidoreductase	-0.57	-	-
	PA4515	piuC	hydroxylase	1.18	-	-
	PA4588	gdhA	glutamate dehydrogenase	0.76	glutamate degradation III	Alanine, aspartate and glutamate metabolism
	PA4670	prs	ribose-phosphate pyrophosphokinase	-0.71	PRPP biosynthesis I	Biosynthesis of amino acids
	PA5214	gcvH1	glycine cleavage system protein H	0.86	-	Biosynthesis of antibiotics
	PA5252		ABC transporter ATP-binding protein	1.56	-	-

Table 11: Proteins found in the MEblack module with corresponding network/pathway data from PseudoCYC and KEGG

Locus ID	Gene name	Protein	Gene sig.	Mod Mem	PseudoCYC	KEGG
PA0004	gyrB	DNA gyrase subunit B	-0.43	0.58	-	-
PA0071		tagR1	-0.62	0.84	-	-
PA0077	icmF1	type VI secretion protein IcmF	-0.46	0.73	-	Bacterial secretion system
PA0426	mexB	multidrug resistance protein MexB	-0.5	0.72	-	beta-Lactam resistance
PA0519	nirS	nitrite reductase	-0.49	0.68	-	Microbial metabolism in diverse environments
PA0586		hypothetical protein	-0.87	0.74	-	-
PA0588		hypothetical protein	-0.94	0.72	-	-
PA0779	asrA	ATP-dependent protease	-0.39	0.73	-	-
PA0903	alaS	alanine--tRNA ligase	-0.54	0.83	tRNA charging	Aminoacyl-tRNA biosynthesis
PA0934	relA	GTP pyrophosphokinase	-0.66	0.55	ppGpp biosynthesis	ppGpp biosynthesis
PA0963	aspS	aspartate--tRNA ligase	-0.54	0.64	tRNA charging	Aminoacyl-tRNA biosynthesis
PA1032	quiP	acyl-homoserine lactone acylase QuiP	-0.5	0.74	-	-
PA1041		hypothetical protein	-0.62	0.77	-	-
PA1069		hypothetical protein	-0.62	0.72	-	-
PA1178	oprH	PhoP/Q and low Mg2+ inducible outer membrane protein H1	-0.56	0.75	-	-

PA1327		protease	-0.9	0.75	-	-
PA1557	ccoN2	cbb3-type cytochrome C oxidase subunit I	-0.34	0.65	-	Metabolic pathways
PA1562	acnA	aconitate hydratase	-0.79	0.74	acetyl-CoA assimilation	2-Oxocarboxylic acid metabolism
PA1580	gltA	citrate synthase	-0.45	0.75	acetyl-CoA assimilation	2-Oxocarboxylic acid metabolism
PA1583	sdhA	succinate dehydrogenase flavoprotein subunit	-0.49	0.8	superpathway of glycolysis, pyruvate dehydrogenase, TCA, and glyoxylate bypass	Biosynthesis of antibiotics
PA1585	sucA	2-oxoglutarate dehydrogenase subunit E1	-0.62	0.9	glutamate degradation III	Biosynthesis of antibiotics
PA1766		hypothetical protein	-0.65	0.54	-	-
PA1787	acnB	aconitate hydratase B	-0.36	0.69	acetyl-CoA assimilation	2-Oxocarboxylic acid metabolism
PA1794	glnS	glutamine--tRNA ligase	-0.46	0.7	tRNA charging	Aminoacyl-tRNA biosynthesis
PA1803	lon	Lon protease	-0.6	0.54	-	-
PA1805	ppiD	peptidyl-prolyl cis-trans isomerase D	-0.44	0.75	-	-
PA2071	fusA2	elongation factor G	-0.62	0.73	-	-
PA2234	pslD	biofilm formation protein PslD	-0.64	0.62	-	Biofilm formation - Pseudomonas aeruginosa
PA2638	nuoB	NADH-quinone oxidoreductase subunit B	-0.81	0.8	-	Metabolic pathways

PA2642	nuoG	NADH-quinone oxidoreductase subunit G	-0.54	0.76	-	Metabolic pathways
PA2644	nuoI	NADH-quinone oxidoreductase subunit I	-0.67	0.83	-	Metabolic pathways
PA2654	tipQ	chemotaxis transducer	-0.5	0.8	-	Bacterial chemotaxis
PA2732		hypothetical protein	-0.64	0.55	-	-
PA2735		restriction-modification system protein	-0.86	0.76	-	-
PA2744	thrS	threonine--tRNA ligase	-0.67	0.71	tRNA charging	Aminoacyl-tRNA biosynthesis
PA2788		chemotaxis transducer	-0.43	0.75	-	-
PA2815		acyl-CoA dehydrogenase	-0.18	0.57	-	Fatty acid degradation
PA2820	hypothetical protein		-0.58	0.79	-	-
PA2867		chemotaxis transducer	-0.14	0.52	-	-
PA2953		electron transfer flavoprotein-ubiquinone oxidoreductase	-0.51	0.87	-	-
PA2973		peptidase	-0.36	0.73	-	-
PA3011	topA	DNA topoisomerase I	-0.5	0.84	-	-
PA3141	wbpM	nucleotide sugar epimerase/dehydratase WbpM	-0.42	0.59	UDP-N-acetyl-alpha-D-fucosamine biosynthesis	UDP-N-acetyl-alpha-D-fucosamine biosynthesis
PA3152	hisH2	imidazole glycerol phosphate synthase subunit HisH	-0.42	0.68	glutaminyl-tRNA-gln-biosynthesis via transamidation	Biosynthesis of amino acids
PA3186	oprB	porin B	-0.57	0.81	-	-

PA3188		sugar ABC transporter permease	-0.26	0.65	-	ABC transporters
PA3299	fadD1	long-chain-fatty-acid--CoA ligase	-0.65	0.91	octane oxidation	Fatty acid biosynthesis
PA3648	opr86	outer membrane protein Opr86	-0.42	0.83	-	-
PA3708	wspA	chemotaxis transducer	-0.54	0.72	-	Biofilm formation - Pseudomonas aeruginosa
PA3800	BamB	outer membrane protein assembly factor BamB	-0.54	0.59	-	-
PA3887	nhaP	Na+/H+ antiporter NhaP	-0.35	0.64	-	-
PA3987	leuS	leucine--tRNA ligase	-0.41	0.77	tRNA charging	Aminoacyl-tRNA biosynthesis
PA4234	uvrA	excinuclease ABC subunit A	-0.52	0.58	-	Nucleotide excision repair
PA4236	katA	catalase	-0.57	0.7	superoxide radicals degradation	Biosynthesis of antibiotics
PA4266	fusA1	elongation factor G	-0.59	0.86	-	-
PA4269	rpoC	DNA-directed RNA polymerase subunit beta'	-0.43	0.77	-	Metabolic pathways
PA4270	rpoB	DNA-directed RNA polymerase subunit beta	-0.47	0.83	-	Metabolic pathways
PA4292		phosphate transporter	-0.52	0.63	-	-
PA4310	pctB	chemotactic transducer PctB	-0.28	0.53	-	Bacterial chemotaxis
PA4317		hypothetical protein	-0.37	0.69	-	-

PA4366	sodB	superoxide dismutase	-0.49	0.66	superoxide radicals degradation	superoxide radicals degradation
PA4426		hypothetical protein	-0.42	0.68	-	-
PA4446	algW	AlgW protein	-0.68	0.69	-	-
PA4552	pilW	type 4 fimbrial biogenesis protein PilW	-0.48	0.63	-	-
PA4560	ileS	isoleucine--tRNA ligase	-0.23	0.69	tRNA charging	Aminoacyl-tRNA biosynthesis
PA4640	mqoB	malate:quinone oxidoreductase	-0.8	0.64	superpathway of glycolysis, pyruvate dehydrogenase, TCA, and glyoxylate bypass	Biosynthesis of antibiotics
PA4696	ilvI	acetolactate synthase 3 catalytic subunit	-0.59	0.84	L-isoleucine biosynthesis I (from threonine)	2-Oxocarboxylic acid metabolism
PA4733	acsB	acetyl-CoA synthetase	-0.86	0.81	cis-genanyl-CoA degradation	Biosynthesis of antibiotics
PA4735		hypothetical protein	-0.55	0.7	-	-
PA4744	infB	translation initiation factor IF-2	-0.33	0.69	-	-
PA4839	speA	arginine decarboxylase	-0.46	0.71	arginine degradation II	Arginine and proline metabolism
PA4851		hypothetical protein	-0.55	0.62	-	-
PA4942	hflK	protease subunit HflK	-0.43	0.7	-	-
PA4964	parC	DNA topoisomerase IV subunit A	-0.53	0.76	-	-
PA4967	parE	DNA topoisomerase IV subunit B	-0.73	0.8	-	-

PA5015	aceE	pyruvate dehydrogenase subunit E1	-0.61	0.91	lactate oxidation	Biosynthesis of antibiotics
PA5041	pilP	type 4 fimbrial biogenesis protein PilP	-0.38	0.48	-	-
PA5078		glucan biosynthesis protein G	-0.55	0.62	-	-
PA5136		hypothetical protein	-0.52	0.78	-	-
PA5192	pckA	phosphoenolpyruvate carboxykinase	-0.26	0.71	gluconeogenesis I	Biosynthesis of antibiotics
PA5217		iron ABC transporter substrate-binding protein	-0.41	0.66	-	ABC transporters
PA5556	atpA	ATP synthase subunit alpha	-0.63	0.36	adenosine ribonucleotides de novo biosynthesis	Metabolic pathways

Table 12: Proteins found in the MEblue module with corresponding network/pathway data from PseudoCYC and KEGG

Locus ID	Gene name	Protein	Gene sig.	Mod Mem	PseudoCYC	KEGG
PA0024	hemF	coproporphyrinogen III oxidase	-0.48	0.57	-	Biosynthesis of secondary metabolites
PA0081	fha1	Fha domain-containing protein	-0.44	0.8	-	Bacterial secretion system
PA0115		hypothetical protein	-0.5	0.74	-	-
PA0157	triB	resistance-nodulation-cell division (RND) efflux membrane fusion protein	-0.37	0.34	-	-
PA0319		hypothetical protein	-0.15	0.59	-	-
PA0355	pfpI	protease PfpI	-0.23	0.67	-	-
PA0382	micA	tRNA (guanine-N(7)-)-methyltransferase	-0.44	0.7	-	-
PA0413	chpA	chemotactic signal transduction system protein	-0.3	0.53	-	Biofilm formation - Pseudomonas aeruginosa
PA0435		hypothetical protein	-0.12	0.62	-	-
PA0602		ABC transporter	-0.71	0.8	-	Quorum sensing
PA0768	lepB	signal peptidase I	-0.46	0.55	-	Protein export
PA0778	icp	inhibitor of cysteine peptidase	-0.56	0.87	-	-
PA0794		aconitate hydratase	0.06	0.52	acetyl-CoA assimilation	acetyl-CoA assimilation

PA0795	prpC	methylcitrate synthase	-0.34	0.58	acetyl-CoA assimilation	acetyl-CoA assimilation
PA0837	slyD	peptidyl-prolyl cis-trans isomerase SlyD	-0.21	0.86	-	-
PA0888	aotJ	arginine/ornithine ABC transporter substrate-binding protein AotJ	-0.13	0.65	-	ABC transporters
PA0898	aruD	N-succinylglutamate 5-semialdehyde dehydrogenase	-0.32	0.65	L-arginine degradation II (AST pathway)	L-arginine degradation II (AST pathway)
PA1039		hypothetical protein	-0.18	0.59	-	-
PA1112		hypothetical protein	-0.47	0.55	-	-
PA1127		oxidoreductase	-0.11	0.66	-	-
PA1159		cold-shock protein	0.15	0.53	-	-
PA1206		hypothetical protein	0.12	0.37	-	-
PA1249	aprA	alkaline metalloproteinase	-0.32	0.78	-	Cationic antimicrobial peptide (CAMP) resistance
PA1288		hypothetical protein	-0.09	0.44	-	-
PA1304		oligopeptidase	-0.32	0.78	-	-
PA1361	PmpM	multidrug resistance protein PmpM	-0.38	0.83	-	-
PA1375	pdxB	erythronate-4-phosphate dehydrogenase	-0.46	0.77	pyridoxal 5'-phosphate biosynthesis I	pyridoxal 5'-phosphate biosynthesis I
PA1429		cation-transporting P-type ATPase	-0.13	0.65	-	-
PA1462		plasmid partitioning protein	-0.04	0.43	-	-
PA1483	cycH	cytochrome c-type biogenesis protein CycH	-0.4	0.53	-	-
PA1546	hemN	oxygen-independent coproporphyrinogen-III oxidase	-0.37	0.59	haem biosynthesis II (anaerobic)	haem biosynthesis II (anaerobic)

PA1596	htpG	chaperone protein HtpG	-0.27	0.63	-	-
PA1737		3-hydroxyacyl-CoA dehydrogenase	0.05	0.69	-	Benzoate degradation
PA1777	oprF	outer membrane porin F	-0.46	0.89	-	-
PA1800	tig	trigger factor	-0.23	0.44	-	-
PA1818	ldcA	lysine-specific pyridoxal 5'-phosphate-dependent carboxylase LdcA	-0.29	0.79	-	Arginine and proline metabolism
PA1829		hypothetical protein	-0.27	0.89	-	-
PA1830		hypothetical protein	0	0.45	-	-
PA1847	nfuA	Fe/S biogenesis protein NfuA	-0.15	0.69	-	-
PA1944		hypothetical protein	-0.29	0.4	-	-
PA2044		hypothetical protein	-0.3	0.66	-	-
PA2236	pslF	biofilm formation protein PslF	-0.51	0.78	-	Biofilm formation - Pseudomonas aeruginosa
PA2265		gluconate dehydrogenase	-0.3	0.65	-	Metabolic pathways
PA2331		hypothetical protein	-0.15	0.52	-	-
PA2462		hypothetical protein	-0.45	0.72	-	-
PA2493	mexE	resistance-nodulation-cell division (RND) multidrug efflux membrane fusion protein MexE	-0.23	0.41	-	-
PA2504		hypothetical protein	-0.42	0.67	-	-
PA2570	lecA	PA-I galactophilic lectin	-0.38	0.87	-	Biofilm formation - Pseudomonas aeruginosa
PA2619	infA	translation initiation factor IF-1	-0.12	0.57	-	-

PA2620	clpA	ATP-binding protease component ClpA	-0.42	0.65	-	-
PA2624	idh	isocitrate dehydrogenase	-0.08	0.49	ethylene biosynthesis V (engineered)	2-Oxocarboxylic acid metabolism
PA2626	trmU	tRNA-specific 2-thiouridylase MnmA	-0.24	0.81	-	Sulfur relay system
PA2633		hypothetical protein	-0.5	0.89	-	-
PA2688	pfeA	ferric enterobactin receptor	-0.34	0.79	-	Two-component system
PA2725		chaperone	-0.34	0.73	-	-
PA2730		hypothetical protein	-0.21	0.74	-	-
PA2755	eco	ecotin	-0.39	0.75	-	-
PA2776		hypothetical protein	-0.53	0.82	-	Arginine and proline metabolism
PA2826		glutathione peroxidase	-0.38	0.87	-	Arachidonic acid metabolism
PA2832	tpm	thiopurine S-methyltransferase	-0.4	0.45	-	-
PA2970	rpmF	50S ribosomal protein L32	-0.17	0.72	-	Ribosome
PA3013	foaB	3-ketoacyl-CoA thiolase	-0.35	0.6	-	alpha-Linolenic acid metabolism
PA3026		hypothetical protein	-0.46	0.57	-	Ether lipid metabolism
PA3031		hypothetical protein	-0.42	0.6	-	-
PA3038		porin	-0.17	0.54	-	-
PA3050	pyrD	dihydroorotate dehydrogenase	-0.4	0.49	-	Metabolic pathways
PA3082	gbt	glycine betaine transmethylase	-0.75	0.68	-	-
PA3112	accD	acetyl-CoA carboxylase carboxyltransferase subunit beta	-0.38	0.52	-	Biosynthesis of antibiotics

PA3115	fimV	motility protein FimV	-0.32	0.57	-	-
PA3162	rpsA	30S ribosomal protein S1	-0.4	0.68	-	Ribosome
PA3213		hypothetical protein	-0.34	0.46	-	ABC transporters
PA3214		hypothetical protein	-0.37	0.5	-	-
PA3297		ATP-dependent helicase	-0.15	0.53	-	-
PA3361	lecB	fucose-binding lectin PA-IIL	-0.36	0.68	-	Quorum sensing
PA3402		hypothetical protein	-0.59	0.72	-	-
PA3466	ATP-dependent RNA helicase		-0.11	0.4	-	-
PA3620	mutS	DNA mismatch repair protein MutS	-0.56	0.59	-	Mismatch repair
PA3627	ygbB	2-C-methyl-D-erythritol 2,4-cyclodiphosphate synthase	-0.39	0.55	-	Biosynthesis of antibiotics
PA3639	accA	acetyl-CoA carboxylase carboxyltransferase subunit alpha	-0.62	0.68	-	Biosynthesis of antibiotics
PA3667		cysteine desulfurase	-0.41	0.61	-	-
PA3692	lptF	outer membrane porin F	-0.47	0.78	-	-
PA3694		hypothetical protein	-0.39	0.57	-	-
PA3728		hypothetical protein	-0.42	0.62	-	-
PA3737	dsbC	thiol	-0.31	0.76	-	-
PA3764	mltF	membrane-bound lytic murein transglycosylase F	-0.4	0.79	-	-
PA3790	oprC	copper transport outer membrane porin OprC	-0.27	0.74	-	-
PA3799	Der	GTPase Der	-0.13	0.5	-	-
PA3801		hypothetical protein	-0.1	0.39	-	-
PA3878	narX	two-component sensor NarX	-0.45	0.91	-	Two-component system
PA3902		hypothetical protein	-0.09	0.64	-	-
PA3950		ATP-dependent RNA helicase	-0.28	0.73	-	-
PA3983		hypothetical protein	-0.5	0.87	-	-

PA4056	ribD	riboflavin-specific deaminase/reductase	-0.14	0.71	toxoflavin biosynthesis	Biosynthesis of secondary metabolites
PA4131		iron-sulfur protein	-0.47	0.77	-	-
PA4156	FvbA	TonB-dependent receptor	-0.56	0.78	-	-
PA4206	mexH	resistance-nodulation-cell division (RND) efflux membrane fusion protein	-0.71	0.76	-	Quorum sensing
PA4246	rpsE	30S ribosomal protein S5	-0.58	0.46	-	Ribosome
PA4252	rplX	50S ribosomal protein L24	-0.29	0.75	-	Ribosome
PA4275	nusG	transcription antitermination protein NusG	-0.32	0.5	-	-
PA4314	purU1	formyltetrahydrofolate deformylase	0.19	0.49	-	Glyoxylate and dicarboxylate metabolism
PA4373		hypothetical protein	-0.57	0.83	-	-
PA4390		hypothetical protein	-0.69	0.7	-	-
PA4415	mraY	phospho-N-acetylmuramoyl-pentapeptide-transferase	0	0.51	-	Metabolic pathways
PA4432	rpsI	30S ribosomal protein S9	-0.45	0.77	-	Ribosome
PA4500		ABC transporter	-0.32	0.42	-	ABC transporters
PA4526	pilB	type 4 fimbrial biogenesis protein PilB	-0.36	0.58	-	-
PA4553	pilX	type 4 fimbrial biogenesis protein PilX	-0.41	0.69	-	-
PA4557	lytB	4-hydroxy-3-methylbut-2-enyl diphosphate reductase	-0.25	0.47	-	Biosynthesis of antibiotics
PA4564		hypothetical protein	-0.4	0.64	-	-
PA4568	rplU	50S ribosomal protein L21	-0.59	0.79	-	Ribosome
PA4587	ccpR	cytochrome C551 peroxidase	-0.68	0.56	-	-
PA4595		ABC transporter ATP-binding protein	-0.47	0.61	-	-
PA4608		hypothetical protein	-0.26	0.63	-	-

PA4636		hypothetical protein	-0.08	0.51	-	-
PA4661	pagL	lipid A 3-O-deacylase	-0.56	0.6	-	-
PA4668	LolB	molecular chaperone LolB	-0.53	0.46	-	-
PA4738		hypothetical protein	-0.32	0.81	-	-
PA4739		hypothetical protein	-0.3	0.83	-	-
PA4758	carA	carbamoyl phosphate synthase small subunit	-0.6	0.55	L-arginine biosynthesis II (acetyl cycle)	Alanine, aspartate and glutamate metabolism
PA4760	dnaJ	molecular chaperone DnaJ	-0.1	0.66	-	-
PA4765	omlA	outer membrane lipoprotein OmlA	0.1	0.42	-	-
PA4808	selA	selenocysteine synthase	-0.29	0.57	-	Aminoacyl-tRNA biosynthesis
PA4867	ureB	urease subunit beta	-0.18	0.78	urea degradation II	Arginine biosynthesis
PA4876	osmE	OsmE family transcriptional regulator	-0.28	0.5	-	-
PA4879		hypothetical protein	-0.02	0.34	-	-
PA4931	dnaB	replicative DNA helicase	-0.34	0.69	-	DNA replication
PA4944	hfq	RNA-binding protein Hfq	-0.24	0.78	-	Quorum sensing
PA4972		hypothetical protein	-0.58	0.75	-	-
PA4991		hypothetical protein	-0.28	0.68	-	-
PA5022	KefA	potassium efflux protein KefA	-0.35	0.55	-	-
PA5117	typA	regulatory protein TypA	-0.36	0.62	-	-
PA5122		hypothetical protein	-0.46	0.75	-	-
PA5125	ntrC	two-component response regulator NtrC	-0.53	0.66	-	Two-component system
PA5130		hypothetical protein	-0.17	0.67	-	-
PA5153		amino acid ABC transporter substrate-binding protein	-0.49	0.42	-	-

PA5274	rnk	nucleoside diphosphate kinase regulator	-0.22	0.58	guanosine ribonucleotides de novo biosynthesis	guanosine ribonucleotides de novo biosynthesis
PA5278	dapF	diaminopimelate epimerase	-0.55	0.85	L-lysine biosynthesis I	Biosynthesis of amino acids
PA5300	cycB	cytochrome C5	-0.16	0.79	-	-
PA5304	dadA	D-amino acid dehydrogenase small subunit	-0.51	0.56	D-arginine degradation	Phenylalanine metabolism
PA5305		hypothetical protein	-0.11	0.71	-	-
PA5320	coaC	bifunctional phosphopantothenoylcysteine decarboxylase/phosphopantothenate synthase	-0.41	0.49	-	Metabolic pathways
PA5338	spoT	guanosine-3',5'-bis(diphosphate) 3'-pyrophosphohydrolase	-0.56	0.69	ppGpp biosynthesis	Purine metabolism
PA5414		hypothetical protein	-0.55	0.66	-	-
PA5443	uvrD	DNA-dependent helicase II	-0.31	0.5	-	Mismatch repair
PA5484		two-component sensor	-0.19	0.79	-	Two-component system

Table 13: Proteins found in the MEgreen module with corresponding network/pathway data from PseudoCYC and KEGG

Locus ID	Gene	Protein	Gene sig.	Mod Mem	PseudoCYC	KEGG
PA0102		Carbonic anhydrase	0.62	0.73	-	Nitrogen metabolism
PA0130	bauC	Putative 3-oxopropanoate dehydrogenase	0.56	0.6	-	beta-Alanine metabolism
PA0140	ahpF	Alkyl hydroperoxide reductase subunit F	0.66	0.78	-	-
PA0342	thyA	Thymidylate synthase	0.32	0.53	N-formyl-tetrahydrofolate biosynthesis	N-formyl-tetrahydrofolate biosynthesis
PA0381	thiG	Thiazole synthase	0.76	0.75	-	Metabolic pathways
PA0395	pilT	Twitching mobility protein	0.31	0.46	-	-
PA0399		Cystathionine beta-synthase	0.69	0.56	L-cysteine biosynthesis III (from L-homocysteine)	L-cysteine biosynthesis III (from L-homocysteine)
PA0407	gshB	Glutathione synthetase	0.75	0.79	glutathione biosynthesis	glutathione biosynthesis
PA0537		Uncharacterized protein	0.47	0.51	-	-
PA0546	metK	S-adenosylmethionine synthase	0.77	0.55	methionine and S-adenosylmethionine synthesis	methionine and S-adenosylmethionine synthesis
PA0609	trpE	Anthranilate synthase component 1	0.41	0.61	4-hydroxy-2-quinolone biosynthesis	4-hydroxy-2-quinolone biosynthesis
PA0649	trpG	Anthranilate synthase component 2	0.56	0.65	2-heptyl-3-hydroxy-4(1H)-quinolone biosynthesis	2-heptyl-3-hydroxy-4(1H)-quinolone biosynthesis
PA0650	trpD	Anthranilate phosphoribosyltransferase	0.41	0.41	L-tryptophan biosynthesis	L-tryptophan biosynthesis

PA0870	phhC	Aromatic-amino-acid aminotransferase	0.18	0.43	-	Biosynthesis of amino acids
PA0932	cysM	Cysteine synthase B	0.42	0.61	L-cysteine biosynthesis I	L-cysteine biosynthesis I
PA1023		Probable short-chain dehydrogenase	0.4	0.69	-	-
PA1091	fgtA	Flagellar glycosyl transferase, FgtA	0.34	0.33	-	-
PA1122		Peptide deformylase	0.53	0.78	-	-
PA1135	hchA	Protein/nucleic acid deglycase HchA	0.31	0.53	-	Microbial metabolism in diverse environments
PA1156	nrdA	Ribonucleoside-diphosphate reductase	0.48	0.59	-	Metabolic pathways
PA1162	dapE	Succinyl-diaminopimelate desuccinylase	0.58	0.78	L-lysine biosynthesis I	Biosynthesis of amino acids
PA1317	cyoA	Cytochrome bo(3) ubiquinol oxidase subunit 2	0.28	0.35	-	Metabolic pathways
PA1344		Probable short-chain dehydrogenase	0.43	0.42	-	-
PA1532	dnaX	DNA polymerase III subunit gamma/tau	0.32	0.54	-	DNA replication
PA1544	anr	Transcriptional activator protein anr	0.59	0.7	-	-
PA1618		Putative esterase PA1618	0.67	0.54	-	-
PA1641		Uncharacterized protein	0.29	0.32	-	-
PA1746		Macro domain-containing protein	0.59	0.52	-	-
PA1769		Putative phosphoenolpyruvate synthase regulatory protein	0.34	0.62	-	-

PA2302	ambE	AmbE	0.58	0.73	-	-
PA2363	HsiJ3	Uncharacterized protein	0.37	0.58	-	Biofilm formation - Pseudomonas aeruginosa
PA2386	pvdA	L-ornithine N(5)-monooxygenase	0.69	0.91	-	-
PA2393		Probable dipeptidase	0.31	0.44	-	-
PA2396	pvdF	Pyoverdine synthetase F	0.78	0.88	-	-
PA2399	pvdD	Pyoverdine synthetase D	0.68	0.81	-	-
PA2400	pvdJ	PvdJ	0.63	0.74	-	-
PA2402		Probable non-ribosomal peptide synthetase	0.47	0.7	-	-
PA2413	pvdH	L-2,4-diaminobutyrate:2-ketoglutarate 4-aminotransferase, PvdH	0.83	0.96	-	2-Oxocarboxylic acid metabolism
PA2483		Bac_luciferase domain-containing protein	0.18	0.53	-	-
PA2532	tpx	Thiol peroxidase	0.69	0.68	-	-
PA2764		AB hydrolase-1 domain-containing protein	0.38	0.54	-	-
PA2871		Uncharacterized protein	0.55	0.57	-	-
PA2979	kdsB	3-deoxy-manno-octulosonate cytidylyltransferase	0.2	0.33	CMP-3-deoxy-D-manno-octulosonate biosynthesis I	CMP-3-deoxy-D-manno-octulosonate biosynthesis I
PA3043	dgt2	Deoxyguanosinetriphosphate triphosphohydrolase-like protein	0.6	0.6	-	Purine metabolism
PA3107		O-succinylhomoserine sulfhydrylase	0.36	0.33	-	Cysteine and methionine metabolism

PA3138	uvrB	UvrABC system protein B	0.62	0.77	-	Nucleotide excision repair
PA3170		Amidohydro-rel domain-containing protein	0.67	0.9	-	Cysteine and methionine metabolism
PA3181	eda	2-dehydro-3-deoxy-phosphogluconate aldolase	0.28	0.48	Entner-Doudoroff pathway I	Carbon metabolism
PA3195	gapA	Glyceraldehyde-3-phosphate dehydrogenase	0.84	0.72	aerobic glycerol degradation I	Biosynthesis of amino acids
PA3266	cspA	Major cold shock protein CspA	0.67	0.46	-	-
PA3337	hldD	ADP-L-glycero-D-manno-heptose-6-epimerase	0.66	0.78	-	Lipopolysaccharide biosynthesis
PA3356		Gln-synt_C domain-containing protein	0.72	0.8	-	Alanine, aspartate and glutamate metabolism
PA3427		Probable short-chain dehydrogenase	0.68	0.83	-	-
PA3444	ssuD	Alkanesulfonate monooxygenase	0.59	0.85	-	Sulfur metabolism
PA3481		Iron-sulfur cluster carrier protein	0.33	0.55	-	-
PA3702	wspR	Probable two-component response regulator	0.62	0.74	-	Biofilm formation - Pseudomonas aeruginosa
PA3846		Isochorismatase domain-containing protein	0.75	0.8	-	-
PA3919		PINc domain-containing protein	0.75	0.68	-	-
PA3925		Probable acyl-CoA thiolase	0.78	0.79	fatty acid salvage	Benzoate degradation
PA3970	amn	AMP nucleosidase	0.39	0.63	-	Purine metabolism

PA4015		MaoC-like domain-containing protein	0.62	0.6	-	-
PA4112		Histidine kinase	0.32	0.56	-	-
PA4180		Probable acetolactate synthase large subunit	0.64	0.68	L-isoleucine biosynthesis I (from threonine)	2-Oxocarboxylic acid metabolism
PA4225	pchF	Pyochelin synthetase	0.76	0.85	L-ornithine degradation II (Stickland reaction)	Biosynthesis of siderophore group nonribosomal peptides
PA4226	pchE	Dihydroaeruginoic acid synthetase	0.68	0.75	pyochelin biosynthesis	Biosynthesis of siderophore group nonribosomal peptides
PA4228	pchD	Pyochelin biosynthesis protein PchD	0.48	0.66	pyochelin biosynthesis	Biosynthesis of siderophore group nonribosomal peptides
PA4356	xenB	Xenobiotic reductase	0.77	0.88	-	-
PA4401		Probable glutathione S-transferase	0.19	0.47	-	Glutathione metabolism
PA4406	lpxC	UDP-3-O-acyl-N-acetylglucosamine deacetylase	0.49	0.47	KDO-2-lipid A and peptidoglycan biosynthesis	Lipopolysaccharide biosynthesis
PA4465		Nucleotide-binding protein PA4465	0.61	0.41	-	-
PA4468	sodM	Superoxide dismutase [Mn]	0.36	0.5	superoxide radicals degradation	superoxide radicals degradation
PA4515	piuC	PKHD-type hydroxylase PiuC	0.81	0.77	-	-
PA4547	pilR	Response regulator protein PilR	0.37	0.52	-	Two-component system
PA4588	gdhA	Glutamate dehydrogenase	0.85	0.81	glutamate degradation III	Alanine, aspartate and glutamate metabolism

PA4625		Haemagg_act domain-containing protein	0.13	0.33	-	-
PA4645		Probable purine/pyrimidine phosphoribosyl transferase	0.42	0.48	-	Biosynthesis of secondary metabolites
PA4657		Renalase	0.86	0.85	-	-
PA4676		Carbonic anhydrase	0.41	0.47	-	Nitrogen metabolism
PA4749	glmM	Phosphoglucosamine mutase	0.56	0.56	-	Amino sugar and nucleotide sugar metabolism
PA4899		Probable aldehyde dehydrogenase	0.57	0.79	-	Arginine and proline metabolism
PA4939	hisZ	ATP phosphoribosyltransferase regulatory subunit	0.53	0.58	-	Biosynthesis of amino acids
PA5061		Uncharacterized protein	0.42	0.63	-	-
PA5110	fbp	Fructose-1,6-bisphosphatase class 1	0.48	0.48	gluconeogenesis I	Biosynthesis of antibiotics
PA5150		Probable short-chain dehydrogenase	0.81	0.93	-	-
PA5174	fabY	Beta-ketoacyl-[acyl-carrier-protein] synthase FabY	0.66	0.5	-	Fatty acid biosynthesis
PA5176		Nudix hydrolase domain-containing protein	0.61	0.72	-	Purine metabolism
PA5193	yrfI	heat shock protein HSP33	0.7	0.73	-	-
PA5204	argA	Amino-acid acetyltransferase	0.35	0.6	L-arginine biosynthesis II (acetyl cycle)	2-Oxocarboxylic acid metabolism
PA5215	gcvT	Aminomethyltransferase	0.48	0.41	-	Biosynthesis of antibiotics

PA5337	rpoZ	DNA-directed RNA polymerase subunit omega	0.32	0.49	-		Metabolic pathways
PA5483	algB	Alginate biosynthesis transcriptional regulatory protein AlgB	0.45	0.74	-		Two-component system
PA5496	nrdJb	NrdJb	0.32	0.43	-		-
PA5521		Probable short-chain dehydrogenase	0.81	0.86	-		-

	Locus ID	Gene	Protein		Amino acid	Position	PseudoCYC	KEGG

Biofilm	PA0041		Probable hemagglutinin	T	2028	-	-
	PA0041		Probable hemagglutinin	T	2030	-	-
	PA0095	vgrG1b	Type VI secretion system spike protein VgrG1b	S	707	-	Bacterial secretion system
	PA0095	vgrG1b	Type VI secretion system spike protein VgrG1b	S	711	-	Bacterial secretion system
	PA0155	pcaR	Transcriptional regulator PcaR	S	151	-	-
	PA0155	pcaR	Transcriptional regulator PcaR	S	158	-	-
	PA0181		Probable transcriptional regulator	S	18	-	-
	PA0305		Uncharacterized protein	T	645	-	Biosynthesis of antibiotics
	PA0323		Probable binding protein component of ABC transporter	S	59	-	ABC transporters
	PA0323		Probable binding protein component of ABC transporter	T	53	-	ABC transporters
	PA0337	ptsP	Phosphoenolpyruvate-protein phosphotransferase PtsP	S	303	-	Phosphotransferase system (PTS)
	PA0551	epd	D-erythrose-4-phosphate dehydrogenase	S	209	-	Metabolic pathways
	PA0551	epd	D-erythrose-4-phosphate dehydrogenase	S	213	-	Metabolic pathways

PA0689		PBP_domain domain-containing protein	T	144	-	-
PA0689		PBP_domain domain-containing protein	T	156	-	-
PA0690		Haemagg_act domain-containing protein	S	1196	-	-
PA0690		Haemagg_act domain-containing protein	S	1199	-	-
PA0752		Uncharacterized protein	T	500	-	Two-component system
PA1032	quiP	Acyl-homoserine lactone acylase QuiP	S	39	-	-
PA1032	quiP	Acyl-homoserine lactone acylase QuiP	T	43	-	-
PA1419		Probable transporter	S	245	-	-
PA1419		Probable transporter	T	244	-	-
PA1441		Flg_hook domain-containing protein	S	417	-	Flagellar assembly
PA1446	fliP	Flagellar biosynthetic protein FliP	S	163	-	Flagellar assembly
PA1770	ppsA	Phosphoenolpyruvate synthase	T	416	acetyl-CoA assimilation	Carbon metabolism
PA1865	fan1	Fanconi-associated nuclease 1 homolog	T	72	-	-
PA1938		Integrase catalytic domain-containing protein	S	11;13	-	-
PA2013	liuC	Putative 3-methylglutaconyl-CoA hydratase	S	243	L-leucine degradation I	L-leucine degradation I

PA2056		Probable transcriptional regulator	T	96	-	-
PA2056		Probable transcriptional regulator	T	97	-	-
PA2252		Probable AGCS sodium/alanine/glycine symporter	S	10	-	-
PA2402		Probable non-ribosomal peptide synthetase	T	2094	-	-
PA2623	icd	Isocitrate dehydrogenase [NADP]	S	115	anaerobic respiration	2-Oxocarboxylic acid metabolism
PA2812		Probable ATP-binding component of ABC transporter	S	299	-	-
PA2812		Probable ATP-binding component of ABC transporter	T	306	-	-
PA2827	msrB	Peptide methionine sulfoxide reductase MsrB	S	122	-	-
PA2827	msrB	Peptide methionine sulfoxide reductase MsrB	S	124	-	-
PA2827	msrB	Peptide methionine sulfoxide reductase MsrB	T	114	-	-
PA2878		Uncharacterized protein	T	109	-	-
PA2920		Probable chemotaxis transducer	T	244	-	Bacterial chemotaxis

PA3323		Peptidase_M24 domain-containing protein	T	214	-	-
PA3347		STAS domain-containing protein	T	40	-	Biofilm formation - *Pseudomonas aeruginosa*
PA3471		NAD-dependent malic enzyme	T	2	-	Carbon metabolism
PA3529		Probable peroxidase	S	2	-	-
PA3593		Probable acyl-CoA dehydrogenase	S	109	-	-
PA3593		Probable acyl-CoA dehydrogenase	S	111	-	-
PA3640	dnaE	DNA polymerase III subunit alpha	S	614	-	DNA replication
PA3640	dnaE	DNA polymerase III subunit alpha	T	606	-	DNA replication
PA3640	dnaE	DNA polymerase III subunit alpha	T	607	-	DNA replication
PA3795		Probable oxidoreductase	S	86	-	-
PA3961		Probable ATP-dependent helicase	S	179	-	-
PA3991		Uncharacterized protein	S	14	-	-
PA4001	sltB1	Soluble lytic transglycosylase B	T	291	-	-
PA4222		Probable ATP-binding component of ABC transporter	S	568	-	-
PA4269	rpoC	DNA-directed RNA polymerase subunit beta'	S	702	-	Metabolic pathways

	PA4373		Uncharacterized protein	T	59	-	-
	PA4408	ftsA	Cell division protein FtsA	T	249	-	-
	PA4408	ftsA	Cell division protein FtsA	T	251	-	-
	PA4581	rtcR	Transcriptional regulator RtcR	S	319	-	-
	PA4727	pcnB	Poly(A) polymerase I	S	434	-	RNA degradation
	PA5036	gltB	Glutamate synthase large chain	S	1468	ammonia assimilation cycle III	Alanine, aspartate and glutamate metabolism
	PA5036	gltB	Glutamate synthase large chain	T	1476	ammonia assimilation cycle III	Alanine, aspartate and glutamate metabolism
	PA5088		Uncharacterized protein	S	70	-	-
	PA5158		Probable outer membrane protein	S	209	-	-
	PA5158		Probable outer membrane protein	S	216	-	-
	PA5344	oxyR	OxyR	T	2	-	-
	PA5344	oxyR	OxyR	T	4	-	-
	PA5393		Uncharacterized protein	T	16	-	-
Planktonic							
	PA0041		Probable hemagglutinin	T	2028	-	-
	PA0041		Probable hemagglutinin	T	2030	-	-
	PA0153	pcaH	Protocatechuate 3,4-dioxygenase, beta subunit	S	165	protocatechuate degradation II (ortho-cleavage pathway)	protocatechuate degradation II (ortho-cleavage pathway)

	PA0153	pcaH	Protocatechuate 3,4-dioxygenase, beta subunit	S	167	protocatechuate degradation II (ortho-cleavage pathway)	protocatechuate degradation II (ortho-cleavage pathway)
	PA0305		Uncharacterized protein	T	645	-	Biosynthesis of antibiotics
	PA0411	pilJ	Protein PilJ	T	558	-	Biofilm formation - *Pseudomonas aeruginosa*
	PA0497		Fimbrial domain-containing protein	S	146	-	-
	PA0588		AAA_PrkA domain-containing protein	S	170	-	-
	PA0588		AAA_PrkA domain-containing protein	S	173	-	-
	PA0588		AAA_PrkA domain-containing protein	T	177	-	-
	PA0640		Probable bacteriophage protein	T	10	-	-
	PA0640		Probable bacteriophage protein	T	11	-	-
	PA0752		Uncharacterized protein	T	500	-	Two-component system
	PA1379		Probable short-chain dehydrogenase	T	185	-	-
	PA1391		Probable glycosyl transferase	S	6	-	-
	PA1441		Flg_hook domain-containing protein	S	417	-	Flagellar assembly
	PA1446	fliP	Flagellar biosynthetic protein FliP	S	163	-	Flagellar assembly

	PA1713	exsA	Exoenzyme S synthesis regulatory protein ExsA	S	63	-	Biofilm formation - *Pseudomonas aeruginosa*
	PA1713	exsA	Exoenzyme S synthesis regulatory protein ExsA	S	67	-	Biofilm formation - *Pseudomonas aeruginosa*
	PA1713	exsA	Exoenzyme S synthesis regulatory protein ExsA	T	68	-	Biofilm formation - *Pseudomonas aeruginosa*
	PA1714	exsD	ExsD	S	160	-	-
	PA1770	ppsA	Phosphoenolpyruvate synthase	T	416	acetyl-CoA assimilation	Carbon metabolism
	PA1859		Probable transcriptional regulator	T	47	-	-
	PA1859		Probable transcriptional regulator	T	48	-	-
	PA1967		Uncharacterized protein	S	3	-	-
	PA1967		Uncharacterized protein	S	8	-	-
	PA1967		Uncharacterized protein	S	10	-	-
	PA2016	liuR	Regulator of liu genes	S	2	-	-
	PA2016	liuR	Regulator of liu genes	S	8	-	-
	PA2016	liuR	Regulator of liu genes	T	4	-	-
	PA2072		Uncharacterized protein	S	392	-	-
	PA2072		Uncharacterized protein	S	394	-	-
	PA2616	trxB1	Thioredoxin reductase	S	2	thioredoxin pathway	thioredoxin pathway
	PA2623	icd	Isocitrate dehydrogenase [NADP]	S	115	anaerobic respiration	2-Oxocarboxylic acid metabolism

PA2920		Probable chemotaxis transducer	T	244	-	Bacterial chemotaxis
PA3312		Probable 3-hydroxyisobutyrate dehydrogenase	T	175	L-valine degradation I	L-valine degradation I
PA3593		Probable acyl-CoA dehydrogenase	S	109	-	-
PA3593		Probable acyl-CoA dehydrogenase	S	111	-	-
PA3640	dnaE	DNA polymerase III subunit alpha	S	614	-	DNA replication
PA3640	dnaE	DNA polymerase III subunit alpha	T	606	-	DNA replication
PA3640	dnaE	DNA polymerase III subunit alpha	T	607	-	DNA replication
PA3680	rsmJ	Ribosomal RNA small subunit methyltransferase J	S	247	-	-
PA3987	leuS	Leucine--tRNA ligase	S	179	tRNA charging	Aminoacyl-tRNA biosynthesis
PA3991		Uncharacterized protein	S	14	-	-
PA4235	ftnA	Bacterioferritin	T	80	-	Porphyrin and chlorophyll metabolism
PA4235	ftnA	Bacterioferritin	T	81	-	Porphyrin and chlorophyll metabolism
PA4269	rpoC	DNA-directed RNA polymerase subunit beta'	S	702	-	Metabolic pathways
PA4408	ftsA	Cell division protein FtsA	T	249	-	-
PA4408	ftsA	Cell division protein FtsA	T	251	-	-

	PA4869		Uncharacterized protein	S	97	-	-
	PA4902		Probable transcriptional regulator	S	181	-	-
	PA4929		GGDEF domain-containing protein	S	125	-	-
	PA5090	vgrG5	Type VI secretion system spike protein VgrG5	T	92	-	-

List of References

Akiyama, T., Williamson, K. S., Schaefer, R., Pratt, S., Chang, C. B. and Franklin, M. J. (2017) 'Resuscitation of Pseudomonas aeruginosa from dormancy requires hibernation promoting factor (PA4463) for ribosome preservation', *Proc Natl Acad Sci U S A,* 114(12), pp. 3204-3209.

Ali-Ahmad, A., Fadel, F., Sebban-Kreuzer, C., Ba, M., Pelissier, G. D., Bornet, O., Guerlesquin, F., Bourne, Y., Bordi, C. and Vincent, F. (2017) 'Structural and functional insights into the periplasmic detector domain of the GacS histidine kinase controlling biofilm formation in Pseudomonas aeruginosa', *Sci Rep,* 7(1), pp. 11262.

Allesen-Holm, M., Barken, K. B., Yang, L., Klausen, M., Webb, J. S., Kjelleberg, S., Molin, S., Givskov, M. and Tolker-Nielsen, T. (2006) 'A characterization of DNA release in Pseudomonas aeruginosa cultures and biofilms', *Mol Microbiol,* 59(4), pp. 1114-28.

Altelaar, A. F., Frese, C. K., Preisinger, C., Hennrich, M. L., Schram, A. W., Timmers, H. T., Heck, A. J. and Mohammed, S. (2013) 'Benchmarking stable isotope labeling based quantitative proteomics', *J Proteomics,* 88, pp. 14-26.

Arora, S. K., Ritchings, B. W., Almira, E. C., Lory, S. and Ramphal, R. (1998) 'The Pseudomonas aeruginosa flagellar cap protein, FliD, is responsible for mucin adhesion', *Infect Immun,* 66(3), pp. 1000-7.

Balaban, N. Q., Merrin, J., Chait, R., Kowalik, L. and Leibler, S. (2004) 'Bacterial persistence as a phenotypic switch', *Science,* 305(5690), pp. 1622-5.

Balasubramanian, D., Schneper, L., Kumari, H. and Mathee, K. (2013) 'A dynamic and intricate regulatory network determines Pseudomonas aeruginosa virulence', *Nucleic Acids Res,* 41(1), pp. 1-20.

Barekzi, N., Beinlich, K., Hoang, T. T., Pham, X. Q., Karkhoff-Schweizer, R. and Schweizer, H. P. (2000) 'High-frequency flp recombinase-mediated inversions of the oriC-containing region of the Pseudomonas aeruginosa genome', *J Bacteriol,* 182(24), pp. 7070-4.

Barraud, N., Storey, M. V., Moore, Z. P., Webb, J. S., Rice, S. A. and Kjelleberg, S. (2009) 'Nitric oxide-mediated dispersal in single- and multi-species biofilms of clinically and industrially relevant microorganisms', *Microb Biotechnol,* 2(3), pp. 370-8.

Belenky, P., Ye, J. D., Porter, C. B., Cohen, N. R., Lobritz, M. A., Ferrante, T., Jain, S., Korry, B. J., Schwarz, E. G., Walker, G. C. and Collins, J. J. (2015) 'Bactericidal Antibiotics Induce Toxic Metabolic Perturbations that Lead to Cellular Damage', *Cell Rep,* 13(5), pp. 968-80.

Benelli, D., La Teana, A. and Londei, P. (2017) 'Translation Regulation: The Archaea-Eukaryal Connection', *RNA Metabolism and Gene Expression in Archaea Nucleic Acids and Molecular Biology*, pp. 71-88.

Bernier, S. P., Lebeaux, D., DeFrancesco, A. S., Valomon, A., Soubigou, G., Coppee, J. Y., Ghigo, J. M. and Beloin, C. (2013) 'Starvation, together with the SOS response, mediates high biofilm-specific tolerance to the fluoroquinolone ofloxacin', *PLoS Genet,* 9(1), pp. e1003144.

Bhagirath, A. Y., Li, Y., Patidar, R., Yerex, K., Ma, X., Kumar, A. and Duan, K. (2019) 'Two Component Regulatory Systems and Antibiotic Resistance in Gram-Negative Pathogens', *Int J Mol Sci,* 20(7), pp. 1781.

Bigger, J. W. (1944) 'Treatment of staphyloccal infections with penicillin by intermittent sterilisation'.

Bonneau, A., Roche, B. and Schalk, I. J. (2020) 'Iron acquisition in Pseudomonas aeruginosa by the siderophore pyoverdine: an intricate interacting network including periplasmic and membrane proteins', *Sci Rep,* 10(1), pp. 120.

Borg, A., Holm, M., Shiroyama, I., Hauryliuk, V., Pavlov, M., Sanyal, S. and Ehrenberg, M. (2015) 'Fusidic acid targets elongation factor G in several stages of translocation on the bacterial ribosome', *J Biol Chem,* 290(6), pp. 3440-54.

Borriello, G., Richards, L., Ehrlich, G. D. and Stewart, P. S. (2006) 'Arginine or nitrate enhances antibiotic susceptibility of Pseudomonas aeruginosa in biofilms', *Antimicrob Agents Chemother,* 50(1), pp. 382-4.

Boynton, T. O., Daugherty, L. E., Dailey, T. A. and Dailey, H. A. (2009) 'Identification of Escherichia coli HemG as a novel, menadione-dependent flavodoxin with protoporphyrinogen oxidase activity', *Biochemistry,* 48(29), pp. 6705-11.

Brantl, S. (2004) 'Bacterial gene regulation: from transcription attenuation to riboswitches and ribozymes', *Trends Microbiol,* 12(11), pp. 473-5.

Brauner, A., Fridman, O., Gefen, O. and Balaban, N. Q. (2016) 'Distinguishing between resistance, tolerance and persistence to antibiotic treatment', *Nat Rev Microbiol,* 14(5), pp. 320-30.

Brencic, A., McFarland, K. A., McManus, H. R., Castang, S., Mogno, I., Dove, S. L. and Lory, S. (2009) 'The GacS/GacA signal transduction system of Pseudomonas aeruginosa acts exclusively through its control over the transcription of the RsmY and RsmZ regulatory small RNAs', *Mol Microbiol,* 73(3), pp. 434-45.

Brown, D. R., Barton, G., Pan, Z., Buck, M. and Wigneshweraraj, S. (2014a) 'Combinatorial stress responses: direct coupling of two major stress responses in Escherichia coli', *Microb Cell,* 1(9), pp. 315-317.

Brown, D. R., Barton, G., Pan, Z., Buck, M. and Wigneshweraraj, S. (2014b) 'Nitrogen stress response and stringent response are coupled in Escherichia coli', *Nat Commun,* 5, pp. 4115.

Burrows, L. L. (2012) 'Pseudomonas aeruginosa twitching motility: type IV pili in action', *Annu Rev Microbiol,* 66, pp. 493-520.

Buzzai, M., Bauer, D. E., Jones, R. G., Deberardinis, R. J., Hatzivassiliou, G., Elstrom, R. L. and Thompson, C. B. (2005) 'The glucose dependence of Akt-transformed cells can be reversed by pharmacologic activation of fatty acid beta-oxidation', *Oncogene,* 24(26), pp. 4165-73.

Cai, Y. (2018) 'Molecular mechanism of nitric oxide-mediated regulation of intracellular cyclic-di-GMP in Pseudomonas aeruginosa biofilms'.

Canova, M. J. and Molle, V. (2014) 'Bacterial serine/threonine protein kinases in host-pathogen interactions', *J Biol Chem,* 289(14), pp. 9473-9.

Castilho, B. A., Shanmugam, R., Silva, R. C., Ramesh, R., Himme, B. M. and Sattlegger, E. (2014) 'Keeping the eIF2 alpha kinase Gcn2 in check', *Biochim Biophys Acta,* 1843(9), pp. 1948-68.

Castro-Roa, D., Garcia-Pino, A., De Gieter, S., van Nuland, N. A., Loris, R. and Zenkin, N. (2013) 'The Fic protein Doc uses an inverted substrate to phosphorylate and inactivate EF-Tu', *Nat Chem Biol,* 9(12), pp. 811-7.

Cezairliyan, B. O. and Sauer, R. T. (2009) 'Control of Pseudomonas aeruginosa AlgW protease cleavage of MucA by peptide signals and MucB', *Mol Microbiol,* 72(2), pp. 368-79.

Chahrour, O., Cobice, D. and Malone, J. (2015) 'Stable isotope labelling methods in mass spectrometry-based quantitative proteomics', *J Pharm Biomed Anal,* 113, pp. 2-20.

Chakrabarti, A., Chen, A. W. and Varner, J. D. (2011) 'A review of the mammalian unfolded protein response', *Biotechnol Bioeng,* 108(12), pp. 2777-93.

Chawla, Y., Upadhyay, S., Khan, S., Nagarajan, S. N., Forti, F. and Nandicoori, V. K. (2014) 'Protein kinase B (PknB) of Mycobacterium tuberculosis is essential for growth of the pathogen in vitro as well as for survival within the host', *J Biol Chem,* 289(20), pp. 13858-75.

Chevalier, S., Bouffartigues, E., Bodilis, J., Maillot, O., Lesouhaitier, O., Feuilloley, M. G. J., Orange, N., Dufour, A. and Cornelis, P. (2017) 'Structure, function and regulation of Pseudomonas aeruginosa porins', *FEMS Microbiol Rev,* 41(5), pp. 698-722.

Choi, K. H., Gaynor, J. B., White, K. G., Lopez, C., Bosio, C. M., Karkhoff-Schweizer, R. R. and Schweizer, H. P. (2005) 'A Tn7-based broad-range bacterial cloning and expression system', *Nat Methods,* 2(6), pp. 443-8.

Choi, K. H. and Schweizer, H. P. (2005) 'An improved method for rapid generation of unmarked Pseudomonas aeruginosa deletion mutants', *BMC Microbiol,* 5, pp. 30.

Christensen, S. K., Mikkelsen, M., Pedersen, K. and Gerdes, K. (2001) 'RelE, a global inhibitor of translation, is activated during nutritional stress', *Proc Natl Acad Sci U S A,* 98(25), pp. 14328-33.

Chua, S. L., Yam, J. K., Hao, P., Adav, S. S., Salido, M. M., Liu, Y., Givskov, M., Sze, S. K., Tolker-Nielsen, T. and Yang, L. (2016) 'Selective labelling and eradication of antibiotic-tolerant bacterial populations in Pseudomonas aeruginosa biofilms', *Nat Commun,* 7, pp. 10750.

Connolly, E., Braunstein, S., Formenti, S. and Schneider, R. J. (2006) 'Hypoxia inhibits protein synthesis through a 4E-BP1 and elongation factor 2 kinase pathway controlled by mTOR and uncoupled in breast cancer cells', *Mol Cell Biol,* 26(10), pp. 3955-65.

Cooper (2000) 'Translation of mRNA', *The Cell: A Molecular Approach. 2nd edition*

Cornelis, P. and Dingemans, J. (2013) 'Pseudomonas aeruginosa adapts its iron uptake strategies in function of the type of infections', *Front Cell Infect Microbiol,* 3, pp. 75.

Costerton, J. W., Geesey, G. G. and Cheng, K. J. (1978) 'How Bacteria Stick', *Scientific American,* 238(1), pp. 86-&.

Costerton, J. W., Stewart, P. S. and Greenberg, E. P. (1999) 'Bacterial biofilms: a common cause of persistent infections', *Science,* 284(5418), pp. 1318-22.

Crabbe, A., Ostyn, L., Staelens, S., Rigauts, C., Risseeuw, M., Dhaenens, M., Daled, S., Van Acker, H., Deforce, D., Van Calenbergh, S. and Coenye, T. (2019) 'Host metabolites stimulate the bacterial proton motive force to enhance the activity of aminoglycoside antibiotics', *PLoS Pathog,* 15(4), pp. e1007697.

Cronan, J. E. and Thomas, J. (2009) 'Bacterial fatty acid synthesis and its relationships with polyketide synthetic pathways', *Methods Enzymol,* 459, pp. 395-433.

Cruz, J. W., Rothenbacher, F. P., Maehigashi, T., Lane, W. S., Dunham, C. M. and Woychik, N. A. (2014) 'Doc toxin is a kinase that inactivates elongation factor Tu', *J Biol Chem,* 289(11), pp. 7788-98.

da Cruz Nizer, W. S., Inkovskiy, V., Versey, Z., Strempel, N., Cassol, E. and Overhage, J. (2021) 'Oxidative Stress Response in Pseudomonas aeruginosa', *Pathogens,* 10(9).

Davey, H. M. and Hexley, P. (2011) 'Red but not dead? Membranes of stressed Saccharomyces cerevisiae are permeable to propidium iodide', *Environ Microbiol,* 13(1), pp. 163-171.

Depluverez, S., Devos, S. and Devreese, B. (2016) 'The Role of Bacterial Secretion Systems in the Virulence of Gram-Negative Airway Pathogens Associated with Cystic Fibrosis', *Front Microbiol,* 7, pp. 1336.

Derman, Y., Soderholm, H., Lindstrom, M. and Korkeala, H. (2015) 'Role of csp genes in NaCl, pH, and ethanol stress response and motility in Clostridium botulinum ATCC 3502', *Food Microbiol,* 46, pp. 463-470.

Diggle, S. P., Stacey, R. E., Dodd, C., Camara, M., Williams, P. and Winzer, K. (2006) 'The galactophilic lectin, LecA, contributes to biofilm development in Pseudomonas aeruginosa', *Environ Microbiol,* 8(6), pp. 1095-104.

Dolan, S. K., Kohlstedt, M., Trigg, S., Vallejo Ramirez, P., Kaminski, C. F., Wittmann, C. and Welch, M. (2020) 'Contextual Flexibility in Pseudomonas aeruginosa Central Carbon Metabolism during Growth in Single Carbon Sources', *mBio,* 11(2).

Durfee, T., Hansen, A. M., Zhi, H., Blattner, F. R. and Jin, D. J. (2008) 'Transcription profiling of the stringent response in Escherichia coli', *J Bacteriol,* 190(3), pp. 1084-96.

Dworkin, J. (2015) 'Ser/Thr phosphorylation as a regulatory mechanism in bacteria', *Curr Opin Microbiol,* 24, pp. 47-52.

Erill, I., Campoy, S. and Barbe, J. (2007) 'Aeons of distress: an evolutionary perspective on the bacterial SOS response', *FEMS Microbiol Rev,* 31(6), pp. 637-56.

Erill, I., Campoy, S., Kilic, S. and Barbe, J. (2016) 'The Verrucomicrobia LexA-Binding Motif: Insights into the Evolutionary Dynamics of the SOS Response', *Front Mol Biosci,* 3, pp. 33.

Field, T. R., White, A., Elborn, J. S. and Tunney, M. M. (2005) 'Effect of oxygen limitation on the in vitro antimicrobial susceptibility of clinical isolates of Pseudomonas aeruginosa grown planktonically and as biofilms', *Eur J Clin Microbiol Infect Dis,* 24(10), pp. 677-87.

Figueira, R., Brown, D. R., Ferreira, D., Eldridge, M. J., Burchell, L., Pan, Z., Helaine, S. and Wigneshweraraj, S. (2015) 'Adaptation to sustained nitrogen starvation by Escherichia coli requires the eukaryote-like serine/threonine kinase YeaG', *Sci Rep,* 5(October), pp. 17524.

Flemming, H. C. and Wingender, J. (2010) 'The biofilm matrix', *Nat Rev Microbiol,* 8(9), pp. 623-33.

Fowler, R. C. and Hanson, N. D. (2015) 'The OpdQ porin of Pseudomonas aeruginosa is regulated by environmental signals associated with cystic fibrosis including nitrate-induced regulation involving the NarXL two-component system', *Microbiologyopen,* 4(6), pp. 967-82.

Franklin, M. J., Nivens, D. E., Weadge, J. T. and Howell, P. L. (2011) 'Biosynthesis of the Pseudomonas aeruginosa Extracellular Polysaccharides, Alginate, Pel, and Psl', *Front Microbiol,* 2, pp. 167.

Gaidenko, T. A., Kim, T. J. and Price, C. W. (2002) 'The PrpC serine-threonine phosphatase and PrkC kinase have opposing physiological roles in stationary-phase Bacillus subtilis cells', *J Bacteriol,* 184(22), pp. 6109-14.

Gallique, M., Bouteiller, M. and Merieau, A. (2017) 'The Type VI Secretion System: A Dynamic System for Bacterial Communication?', *Front Microbiol,* 8, pp. 1454.

Germain, E., Castro-Roa, D., Zenkin, N. and Gerdes, K. (2013) 'Molecular mechanism of bacterial persistence by HipA', *Mol Cell,* 52(2), pp. 248-54.

Gibson, D. G., Young, L., Chuang, R. Y., Venter, J. C., Hutchison, C. A., 3rd and Smith, H. O. (2009) 'Enzymatic assembly of DNA molecules up to several hundred kilobases', *Nat Methods,* 6(5), pp. 343-5.

Goldova, J., Ulrych, A., Hercik, K. and Branny, P. (2011) 'A eukaryotic-type signalling system of Pseudomonas aeruginosa contributes to oxidative stress resistance, intracellular survival and virulence', *BMC Genomics,* 12, pp. 437.

Gronostajski, R. M. and Sadowski, P. D. (1985) 'The FLP recombinase of the Saccharomyces cerevisiae 2 microns plasmid attaches covalently to DNA via a phosphotyrosyl linkage', *Mol Cell Biol,* 5(11), pp. 3274-9.

Hachani, A., Lossi, N. S., Hamilton, A., Jones, C., Bleves, S., Albesa-Jove, D. and Filloux, A. (2011) 'Type VI secretion system in Pseudomonas aeruginosa: secretion and multimerization of VgrG proteins', *J Biol Chem,* 286(14), pp. 12317-27.

Hancock, R. E. and Brinkman, F. S. (2002) 'Function of pseudomonas porins in uptake and efflux', *Annu Rev Microbiol,* 56, pp. 17-38.

Hanks, S. K., Quinn, A. M. and Hunter, T. (1988) 'The protein kinase family: conserved features and deduced phylogeny of the catalytic domains', *Science,* 241(4861), pp. 42-52.

Harms, A., Fino, C., Sorensen, M. A., Semsey, S. and Gerdes, K. (2017) 'Prophages and Growth Dynamics Confound Experimental Results with Antibiotic-Tolerant Persister Cells', *MBio,* 8(6), pp. 1--18.

He, G. X., Kuroda, T., Mima, T., Morita, Y., Mizushima, T. and Tsuchiya, T. (2004) 'An H(+)-coupled multidrug efflux pump, PmpM, a member of the MATE family of transporters, from Pseudomonas aeruginosa', *J Bacteriol,* 186(1), pp. 262-5.

Hermansson, M. (1999) 'The DLVO theory in microbial adhesion', *Colloids and Surfaces B-Biointerfaces,* 14(1-4), pp. 105-119.

Heuston, S., Begley, M., Gahan, C. G. M. and Hill, C. (2012) 'Isoprenoid biosynthesis in bacterial pathogens', *Microbiology (Reading),* 158(Pt 6), pp. 1389-1401.

Hews, C. L., Cho, T., Rowley, G. and Raivio, T. L. (2019) 'Maintaining Integrity Under Stress: Envelope Stress Response Regulation of Pathogenesis in Gram-Negative Bacteria', *Front Cell Infect Microbiol,* 9, pp. 313.

Hill, D., Rose, B., Pajkos, A., Robinson, M., Bye, P., Bell, S., Elkins, M., Thompson, B., Macleod, C., Aaron, S. D. and Harbour, C. (2005) 'Antibiotic susceptabilities of Pseudomonas aeruginosa isolates derived from patients with cystic fibrosis under aerobic, anaerobic, and biofilm conditions', *J Clin Microbiol,* 43(10), pp. 5085-90.

Hmelo, L. R., Borlee, B. R., Almblad, H., Love, M. E., Randall, T. E., Tseng, B. S., Lin, C., Irie, Y., Storek, K. M., Yang, J. J., Siehnel, R. J., Howell, P. L., Singh, P. K., Tolker-Nielsen, T., Parsek, M. R., Schweizer, H. P. and Harrison, J. J. (2015) 'Precision-engineering the Pseudomonas aeruginosa genome with two-step allelic exchange', *Nat Protoc,* 10(11), pp. 1820-41.

Hobbs, M., Collie, E. S., Free, P. D., Livingston, S. P. and Mattick, J. S. (1993) 'PilS and PilR, a two-component transcriptional regulatory system controlling expression of type 4 fimbriae in Pseudomonas aeruginosa', *Mol Microbiol,* 7(5), pp. 669-82.

Hochachka, P. W., Buck, L. T., Doll, C. J. and Land, S. C. (1996) 'Unifying theory of hypoxia tolerance: molecular/metabolic defense and rescue mechanisms for surviving oxygen lack', *Proc Natl Acad Sci U S A,* 93(18), pp. 9493-8.

Hogrebe, A., von Stechow, L., Bekker-Jensen, D. B., Weinert, B. T., Kelstrup, C. D. and Olsen, J. V. (2018) 'Benchmarking common quantification strategies for large-scale phosphoproteomics', *Nat Commun,* 9(1), pp. 1045.

Hsu, F., Schwarz, S. and Mougous, J. D. (2009) 'TagR promotes PpkA-catalysed type VI secretion activation in Pseudomonas aeruginosa', *Mol Microbiol,* 72(5), pp. 1111-25.

Huang, B., Ru, K., Yuan, Z., Whitchurch, C. B. and Mattick, J. S. (2004) 'tonB3 is required for normal twitching motility and extracellular assembly of type IV pili', *J Bacteriol,* 186(13), pp. 4387-9.

Huse, M. and Kuriyan, J. (2002) 'The conformational plasticity of protein kinases', *Cell,* 109(3), pp. 275-82.

Irie, Y., Roberts, A. E. L., Kragh, K. N., Gordon, V. D., Hutchison, J., Allen, R. J., Melaugh, G., Bjarnsholt, T., West, S. A. and Diggle, S. P. (2017) 'The Pseudomonas aeruginosa PSL Polysaccharide Is a Social but Noncheatable Trait in Biofilms', *mBio,* 8(3).

Jakob, U., Muse, W., Eser, M. and Bardwell, J. C. (1999) 'Chaperone activity with a redox switch', *Cell,* 96(3), pp. 341-52.

Janczarek, M., Vinardell, J. M., Lipa, P. and Karas, M. (2018) 'Hanks-Type Serine/Threonine Protein Kinases and Phosphatases in Bacteria: Roles in Signaling and Adaptation to Various Environments', *Int J Mol Sci,* 19(10).

Justice, S. S., Hunstad, D. A., Cegelski, L. and Hultgren, S. J. (2008) 'Morphological plasticity as a bacterial survival strategy', *Nat Rev Microbiol,* 6(2), pp. 162-8.

Justice, S. S., Hunstad, D. A., Seed, P. C. and Hultgren, S. J. (2006) 'Filamentation by Escherichia coli subverts innate defenses during urinary tract infection', *Proc Natl Acad Sci U S A,* 103(52), pp. 19884-9.

Kanjee, U., Ogata, K. and Houry, W. A. (2012) 'Direct binding targets of the stringent response alarmone (p)ppGpp', *Mol Microbiol,* 85(6), pp. 1029-43.

Kant, S., Asthana, S., Missiakas, D. and Pancholi, V. (2017) 'A novel STK1-targeted small-molecule as an "antibiotic resistance breaker" against multidrug-resistant Staphylococcus aureus', *Sci Rep,* 7(1), pp. 5067.

Keto-Timonen, R., Hietala, N., Palonen, E., Hakakorpi, A., Lindstrom, M. and Korkeala, H. (2016) 'Cold Shock Proteins: A Minireview with Special Emphasis on Csp-family of Enteropathogenic Yersinia', *Front Microbiol,* 7, pp. 1151.

Kim, J. S., Chowdhury, N., Yamasaki, R. and Wood, T. K. (2018) 'Viable but non-culturable and persistence describe the same bacterial stress state', *Environ Microbiol,* 20(6), pp. 2038-2048.

Kim, J. S. and Wood, T. K. (2017) 'Tolerant, Growing Cells from Nutrient Shifts Are Not Persister Cells', *MBio,* 8(2).

Kindrachuk, K. N., Fernandez, L., Bains, M. and Hancock, R. E. (2011) 'Involvement of an ATP-dependent protease, PA0779/AsrA, in inducing heat shock in response to tobramycin in Pseudomonas aeruginosa', *Antimicrob Agents Chemother,* 55(5), pp. 1874-82.

King, P., Citron, D. M., Griffith, D. C., Lomovskaya, O. and Dudley, M. N. (2010) 'Effect of oxygen limitation on the in vitro activity of levofloxacin and other antibiotics administered by the aerosol route against Pseudomonas aeruginosa from cystic fibrosis patients', *Diagn Microbiol Infect Dis,* 66(2), pp. 181-6.

Kirchhoff, C. and Cypionka, H. (2017) 'Propidium ion enters viable cells with high membrane potential during live-dead staining', *J Microbiol Methods,* 142, pp. 79-82.

Klein, M., Schermuly, R. T., Ellinghaus, P., Milting, H., Riedl, B., Nikolova, S., Pullamsetti, S. S., Weissmann, N., Dony, E., Savai, R., Ghofrani, H. A., Grimminger, F., Busch, A. E. and Schafer, S. (2008) 'Combined tyrosine and serine/threonine kinase inhibition by sorafenib prevents progression of experimental pulmonary hypertension and myocardial remodeling', *Circulation,* 118(20), pp. 2081-90.

Klevens, R. M., Edwards, J. R., Richards, C. L., Jr., Horan, T. C., Gaynes, R. P., Pollock, D. A. and Cardo, D. M. (2007) 'Estimating health care-associated infections and deaths in U.S. hospitals, 2002', *Public Health Rep,* 122(2), pp. 160-6.

Korch, S. B., Henderson, T. A. and Hill, T. M. (2003) 'Characterization of the hipA7 allele of Escherichia coli and evidence that high persistence is governed by (p)ppGpp synthesis', *Molecular Microbiology,* 50(4), pp. 1199-1213.

Koritzinsky, M., Magagnin, M. G., van den Beucken, T., Seigneuric, R., Savelkouls, K., Dostie, J., Pyronnet, S., Kaufman, R. J., Weppler, S. A., Voncken, J. W., Lambin, P., Koumenis, C., Sonenberg, N. and Wouters, B. G. (2006) 'Gene expression during acute and prolonged hypoxia is regulated by distinct mechanisms of translational control', *EMBO J,* 25(5), pp. 1114-25.

Koromilas, A. E. (2015) 'Roles of the translation initiation factor eIF2alpha serine 51 phosphorylation in cancer formation and treatment', *Biochim Biophys Acta,* 1849(7), pp. 871-80.

Kostakioti, M., Hadjifrangiskou, M. and Hultgren, S. J. (2013) 'Bacterial biofilms: development, dispersal, and therapeutic strategies in the dawn of the postantibiotic era', *Cold Spring Harb Perspect Med,* 3(4), pp. a010306.

Krupa, A. and Srinivasan, N. (2005) 'Diversity in domain architectures of Ser/Thr kinases and their homologues in prokaryotes', *BMC Genomics,* 6, pp. 129.

Kumar, C. M. S., Chugh, K., Dutta, A., Mahamkali, V., Bose, T., Mande, S. S., Mande, S. C. and Lund, P. A. (2021) 'Chaperonin Abundance Enhances Bacterial Fitness', *Front Mol Biosci,* 8, pp. 669996.

Kussmaul, L. and Hirst, J. (2006) 'The mechanism of superoxide production by NADH:ubiquinone oxidoreductase (complex I) from bovine heart mitochondria', *Proc Natl Acad Sci U S A,* 103(20), pp. 7607-12.

Kwan, B. W., Valenta, J. A., Benedik, M. J. and Wood, T. K. (2013) 'Arrested protein synthesis increases persister-like cell formation', *Antimicrob Agents Chemother,* 57(3), pp. 1468-73.

Lai, S., Safaei, J. and Pelech, S. (2016) 'Evolutionary Ancestry of Eukaryotic Protein Kinases and Choline Kinases', *J Biol Chem,* 291(10), pp. 5199-205.

Lee, J. H., Pestova, T. V., Shin, B. S., Cao, C., Choi, S. K. and Dever, T. E. (2002) 'Initiation factor eIF5B catalyzes second GTP-dependent step in eukaryotic translation initiation', *Proc Natl Acad Sci U S A,* 99(26), pp. 16689-94.

Lemke, J. J., Sanchez-Vazquez, P., Burgos, H. L., Hedberg, G., Ross, W. and Gourse, R. L. (2011) 'Direct regulation of Escherichia coli ribosomal protein promoters by the transcription factors ppGpp and DksA', *Proc Natl Acad Sci U S A,* 108(14), pp. 5712-7.

Leprivier, G., Remke, M., Rotblat, B., Dubuc, A., Mateo, A. R., Kool, M., Agnihotri, S., El-Naggar, A., Yu, B., Somasekharan, S. P., Faubert, B., Bridon, G., Tognon, C. E., Mathers, J., Thomas, R., Li, A., Barokas, A., Kwok, B., Bowden, M., Smith, S., Wu, X., Korshunov, A., Hielscher, T., Northcott, P. A., Galpin, J. D., Ahern, C. A., Wang, Y., McCabe, M. G., Collins, V. P., Jones, R. G., Pollak, M., Delattre, O., Gleave, M. E., Jan, E., Pfister, S. M., Proud, C. G., Derry, W. B., Taylor, M. D. and Sorensen, P. H. (2013) 'The eEF2 kinase confers resistance to nutrient deprivation by blocking translation elongation', *Cell,* 153(5), pp. 1064-79.

Leprivier, G., Rotblat, B., Khan, D., Jan, E. and Sorensen, P. H. (2015) 'Stress-mediated translational control in cancer cells', *Biochim Biophys Acta,* 1849(7), pp. 845-60.

Levine, A. J. (1997) 'p53, the cellular gatekeeper for growth and division', *Cell,* 88(3), pp. 323-31.

Li, P., Xu, D., Ma, T., Wang, D., Li, W., He, J., Ran, T. and Wang, W. (2018) 'Crystal structures of the kinase domain of PpkA, a key regulatory component of T6SS, reveal a general inhibitory mechanism', *Biochem J,* 475(13), pp. 2209-2224.

Li, Y., Chen, L., Zhang, P., Bhagirath, A. Y. and Duan, K. (2020) 'ClpV3 of the H3-Type VI Secretion System (H3-T6SS) Affects Multiple Virulence Factors in Pseudomonas aeruginosa', *Front Microbiol,* 11, pp. 1096.

Lin, J., Zhang, W., Cheng, J., Yang, X., Zhu, K., Wang, Y., Wei, G., Qian, P. Y., Luo, Z. Q. and Shen, X. (2017) 'A Pseudomonas T6SS effector recruits PQS-containing outer membrane vesicles for iron acquisition', *Nat Commun,* 8, pp. 14888.

Liu, L., Wise, D. R., Diehl, J. A. and Simon, M. C. (2008a) 'Hypoxic reactive oxygen species regulate the integrated stress response and cell survival', *J Biol Chem,* 283(45), pp. 31153-62.

Liu, M., Zhang, Y., Inouye, M. and Woychik, N. A. (2008b) 'Bacterial addiction module toxin Doc inhibits translation elongation through its association with the 30S ribosomal subunit', *Proc Natl Acad Sci U S A,* 105(15), pp. 5885-90.

Luscher, A., Moynie, L., Auguste, P. S., Bumann, D., Mazza, L., Pletzer, D., Naismith, J. H. and Kohler, T. (2018) 'TonB-Dependent Receptor Repertoire of Pseudomonas aeruginosa for Uptake of Siderophore-Drug Conjugates', *Antimicrob Agents Chemother,* 62(6).

Macek, B. and Mijakovic, I. (2011) 'Site-specific analysis of bacterial phosphoproteomes', *Proteomics,* 11(15), pp. 3002-11.

Macia, M. D., Rojo-Molinero, E. and Oliver, A. (2014) 'Antimicrobial susceptibility testing in biofilm-growing bacteria', *Clin Microbiol Infect,* 20(10), pp. 981-90.

Maisonneuve, E., Castro-Camargo, M. and Gerdes, K. (2013) '(p)ppGpp controls bacterial persistence by stochastic induction of toxin-antitoxin activity', *Cell,* 154(5), pp. 1140-1150.

Maisonneuve, E. and Gerdes, K. (2014) 'Molecular mechanisms underlying bacterial persisters', *Cell,* 157(3), pp. 539-48.

Maisonneuve, E., Shakespeare, L. J., Jorgensen, M. G. and Gerdes, K. (2011) 'Bacterial persistence by RNA endonucleases', *Proc Natl Acad Sci U S A,* 108(32), pp. 13206-11.

Malinverni, J. C. and Silhavy, T. J. (2011) 'Assembly of Outer Membrane beta-Barrel Proteins: the Bam Complex', *EcoSal Plus,* 4(2).

Mann, E. E. a. W. D. J. (2015) 'Pseudomonas biofilm matrix composition and niche biology', 36(4), pp. 893--916.

Manning, G. and Hunter, T. (2010) 'Chapter 56 - Eukaryotic Kinomes: Genomics and Evolution of Protein Kinases A2 - Bradshaw, Ralph A', in Dennis, E.A. (ed.) *Handbook of Cell Signaling (Second Edition)*. San Diego: Academic Press, pp. 393-397.

Manning, G., Whyte, D. B., Martinez, R., Hunter, T. and Sudarsanam, S. (2002) 'The protein kinase complement of the human genome', *Science,* 298(5600), pp. 1912-34.

Marshall, K. C., Stout, R. and Mitchell, R. (1971) 'Mechanism of the Initial Events in the Sorption of Marine Bacteria to Surfaces', *Journal of General Microbiology,* 68(3), pp. 337-348.

McEwen, E., Kedersha, N., Song, B., Scheuner, D., Gilks, N., Han, A., Chen, J. J., Anderson, P. and Kaufman, R. J. (2005) 'Heme-regulated inhibitor kinase-mediated phosphorylation of eukaryotic translation initiation factor 2 inhibits translation, induces stress granule formation, and mediates survival upon arsenite exposure', *J Biol Chem,* 280(17), pp. 16925-33.

Michalska, M. and Wolf, P. (2015) 'Pseudomonas Exotoxin A: optimized by evolution for effective killing', *Front Microbiol,* 6, pp. 963.

Minandri, F., Imperi, F., Frangipani, E., Bonchi, C., Visaggio, D., Facchini, M., Pasquali, P., Bragonzi, A. and Visca, P. (2016) 'Role of Iron Uptake Systems in Pseudomonas aeruginosa Virulence and Airway Infection', *Infect Immun,* 84(8), pp. 2324-2335.

Mitchell, C., Morris, P. W. and Vary, J. C. (1992) 'Identification of proteins phosphorylated by ATP during sporulation of Bacillus subtilis', *J Bacteriol,* 174(8), pp. 2474-7.

Mougous, J. D., Gifford, C. A., Ramsdell, T. L. and Mekalanos, J. J. (2007) 'Threonine phosphorylation post-translationally regulates protein secretion in Pseudomonas aeruginosa', *Nat Cell Biol,* 9(7), pp. 797-803.

Mukhopadhyay, S., Kapatral, V., Xu, W. B. and Chakrabarty, A. M. (1999) 'Characterization of a hank's type serine/threonine kinase and serine/threonine phosphoprotein phosphatase in Pseudomonas aeruginosa', *Journal of Bacteriology,* 181(21), pp. 6615-6622.

Murphy, J. R. (2011) 'Mechanism of diphtheria toxin catalytic domain delivery to the eukaryotic cell cytosol and the cellular factors that directly participate in the process', *Toxins (Basel),* 3(3), pp. 294-308.

Navarre, W. W., Zou, S. B., Roy, H., Xie, J. L., Savchenko, A., Singer, A., Edvokimova, E., Prost, L. R., Kumar, R., Ibba, M. and Fang, F. C. (2010) 'PoxA, yjeK, and elongation factor P coordinately modulate virulence and drug resistance in Salmonella enterica', *Mol Cell,* 39(2), pp. 209-21.

Neidig, A., Yeung, A. T., Rosay, T., Tettmann, B., Strempel, N., Rueger, M., Lesouhaitier, O. and Overhage, J. (2013) 'TypA is involved in virulence, antimicrobial resistance and biofilm formation in Pseudomonas aeruginosa', *BMC Microbiol,* 13, pp. 77.

Nguyen, A. T., O'Neill, M. J., Watts, A. M., Robson, C. L., Lamont, I. L., Wilks, A. and Oglesby-Sherrouse, A. G. (2014) 'Adaptation of iron homeostasis pathways by a Pseudomonas aeruginosa pyoverdine mutant in the cystic fibrosis lung', *J Bacteriol,* 196(12), pp. 2265-76.

Nguyen, D., Joshi-Datar, A., Lepine, F., Bauerle, E., Olakanmi, O., Beer, K., McKay, G., Siehnel, R., Schafhauser, J., Wang, Y., Britigan, B. E. and Singh, P. K. (2011) 'Active starvation responses mediate antibiotic tolerance in biofilms and nutrient-limited bacteria', *Science,* 334(6058), pp. 982-6.

Nguyen, H. A., El Khoury, T., Guiral, S., Laaberki, M. H., Candusso, M. P., Galisson, F., Foucher, A. E., Kesraoui, S., Ballut, L., Vallet, S., Orelle, C., Zucchini, L., Martin, J., Page, A., Attieh, J., Aghajari, N., Grangeasse, C. and Jault, J. M. (2017) 'Expanding the Kinome World: A New Protein Kinase Family Widely Conserved in Bacteria', *J Mol Biol,* 429(20), pp. 3056-3074.

Nolen, B., Taylor, S. and Ghosh, G. (2004) 'Regulation of protein kinases; controlling activity through activation segment conformation', *Mol Cell,* 15(5), pp. 661-75.

O'Toole, G., Kaplan, H. B. and Kolter, R. (2000) 'Biofilm formation as microbial development', *Annu Rev Microbiol,* 54, pp. 49-79.

O'Toole, G. A. and Kolter, R. (1998) 'Initiation of biofilm formation inPseudomonas fluorescensWCS365 proceeds via multiple, convergent signalling pathways: a genetic analysis', *Molecular Microbiology,* 28(3), pp. 449-461.

Ochsner, U. A., Vasil, M. L., Alsabbagh, E., Parvatiyar, K. and Hassett, D. J. (2000) 'Role of the Pseudomonas aeruginosa oxyR-recG operon in oxidative stress defense and DNA repair: OxyR-dependent regulation of katB-ankB, ahpB, and ahpC-ahpF', *J Bacteriol,* 182(16), pp. 4533-44.

Oliver, A., Baquero, F. and Blazquez, J. (2002) 'The mismatch repair system (mutS, mutL and uvrD genes) in Pseudomonas aeruginosa: molecular characterization of naturally occurring mutants', *Mol Microbiol,* 43(6), pp. 1641-50.

Pan, J., Zha, Z., Zhang, P., Chen, R., Ye, C. and Ye, T. (2017a) 'Serine/threonine protein kinase PpkA contributes to the adaptation and virulence in Pseudomonas aeruginosa', *Microb Pathog,* 113(October), pp. 5-10.

Pan, X., Dong, Y., Fan, Z., Liu, C., Xia, B., Shi, J., Bai, F., Jin, Y., Cheng, Z., Jin, S. and Wu, W. (2017b) 'In vivo Host Environment Alters Pseudomonas aeruginosa Susceptibility to Aminoglycoside Antibiotics', *Front Cell Infect Microbiol,* 7, pp. 83.

Pereira, S. F., Gonzalez, R. L., Jr. and Dworkin, J. (2015) 'Protein synthesis during cellular quiescence is inhibited by phosphorylation of a translational elongation factor', *Proc Natl Acad Sci U S A,* 112(25), pp. E3274-81.

Pereira, S. F., Goss, L. and Dworkin, J. (2011) 'Eukaryote-like serine/threonine kinases and phosphatases in bacteria', *Microbiol Mol Biol Rev,* 75(1), pp. 192-212.

Perez-Martinez, I. and Haas, D. (2011) 'Azithromycin inhibits expression of the GacA-dependent small RNAs RsmY and RsmZ in Pseudomonas aeruginosa', *Antimicrob Agents Chemother,* 55(7), pp. 3399-405.

Petrova, O. E. and Sauer, K. (2009) 'A novel signaling network essential for regulating Pseudomonas aeruginosa biofilm development', *PLoS Pathog,* 5(11), pp. e1000668.

Pissaridou, P., Allsopp, L. P., Wettstadt, S., Howard, S. A., Mavridou, D. A. I. and Filloux, A. (2018) 'The Pseudomonas aeruginosa T6SS-VgrG1b spike is topped by a PAAR protein eliciting DNA damage to bacterial competitors', *Proc Natl Acad Sci U S A,* 115(49), pp. 12519-12524.

Polikanov, Y. S., Blaha, G. M. and Steitz, T. A. (2012) 'How hibernation factors RMF, HPF, and YfiA turn off protein synthesis', *Science,* 336(6083), pp. 915-8.

Potrykus, K., Murphy, H., Philippe, N. and Cashel, M. (2011) 'ppGpp is the major source of growth rate control in E. coli', *Environ Microbiol,* 13(3), pp. 563-575.

Prigent-Combaret, C., Vidal, O., Dorel, C. and Lejeune, P. (1999) 'Abiotic surface sensing and biofilm-dependent regulation of gene expression in Escherichia coli', *J Bacteriol,* 181(19), pp. 5993-6002.

Prisic, S. and Husson, R. N. (2014) 'Mycobacterium tuberculosis Serine/Threonine Protein Kinases', *Microbiol Spectr,* 2(5).

Ravichandran, A., Sugiyama, N., Tomita, M., Swarup, S. and Ishihama, Y. (2009) 'Ser/Thr/Tyr phosphoproteome analysis of pathogenic and non-pathogenic Pseudomonas species', *Proteomics,* 9(10), pp. 2764-75.

Rosenberg, M., Azevedo, N. F. and Ivask, A. (2019) 'Propidium iodide staining underestimates viability of adherent bacterial cells', *Sci Rep,* 9(1), pp. 6483.

Rotblat, B., Grunewald, T. G., Leprivier, G., Melino, G. and Knight, R. A. (2013) 'Anti-oxidative stress response genes: bioinformatic analysis of their expression and relevance in multiple cancers', *Oncotarget,* 4(12), pp. 2577-90.

S.E.H. West, H. P. S., C. Dall, AK. Sample and L.J. Runyen-Janecky (1994) 'Construction of improved Escherichia-Pseudomonas shuttle vectors derived from pUC 18/l 9 and sequence of the region required for their replication in Pseudomonas aeruginosa'.

Sajid, A., Arora, G., Gupta, M., Singhal, A., Chakraborty, K., Nandicoori, V. K. and Singh, Y. (2011) 'Interaction of Mycobacterium tuberculosis elongation factor Tu with GTP is regulated by phosphorylation', *J Bacteriol,* 193(19), pp. 5347-58.

Sampedro, I., Parales, R. E., Krell, T. and Hill, J. E. (2015) 'Pseudomonas chemotaxis', *FEMS Microbiol Rev,* 39(1), pp. 17-46.

Sandro F. F. Pereiraa, R. L. G. J. b., and Jonathan Dworkina,1 (2015) 'Protein synthesis during cellular quiescence is inhibited by phosphorylation of a translational elongation factor'.

Sarg, B., Helliger, W., Talasz, H., Forg, B. and Lindner, H. H. (2006) 'Histone H1 phosphorylation occurs site-specifically during interphase and mitosis: identification of a novel phosphorylation site on histone H1', *J Biol Chem,* 281(10), pp. 6573-80.

Sauer, K., Camper, A. K., Ehrlich, G. D., Costerton, J. W. and Davies, D. G. (2002) 'Pseudomonas aeruginosa displays multiple phenotypes during development as a biofilm', *Journal of Bacteriology,* 184(4), pp. 1140-1154.

Schumacher, M. A., Piro, K. M., Xu, W., Hansen, S., Lewis, K. and Brennan, R. G. (2009) 'Molecular mechanisms of HipA-mediated multidrug tolerance and its neutralization by HipB', *Science,* 323(5912), pp. 396-401.

Schweizer, H. P. (1992) 'Alielic exchange in Pseudomonas aeruginosa using novel ColE1-type vectors and a family of cassettes containing a portable oriT and the counter-selectable Baciiius subtiiis sacB marker'.

Schweizer, H. P. (2003) 'Applications of the Saccharomyces cerevisiae Flp-FRT system in bacterial genetics', *J Mol Microbiol Biotechnol,* 5(2), pp. 67-77.

Schweizer, H. P. (2004) 'Molecular Tools for Genetic Analysis of Pseudomonads'.

Schweizer, H. P. (2012) 'Understanding efflux in Gram-negative bacteria: opportunities for drug discovery', *Expert Opin Drug Discov,* 7(7), pp. 633-42.

Sissi, C. and Palumbo, M. (2010) 'In front of and behind the replication fork: bacterial type IIA topoisomerases', *Cell Mol Life Sci,* 67(12), pp. 2001-24.

Sivaneson, M., Mikkelsen, H., Ventre, I., Bordi, C. and Filloux, A. (2011) 'Two-component regulatory systems in Pseudomonas aeruginosa: an intricate network mediating fimbrial and efflux pump gene expression', *Mol Microbiol,* 79(5), pp. 1353-66.

Snyder, E., Gordon, D. M. and Stoebel, D. M. (2012) 'Escherichia coli lacking RpoS are rare in natural populations of non-pathogens', *G3 (Bethesda),* 2(11), pp. 1341-4.

Sonnleitner, E., Schuster, M., Sorger-Domenigg, T., Greenberg, E. P. and Blasi, U. (2006) 'Hfq-dependent alterations of the transcriptome profile and effects on quorum sensing in Pseudomonas aeruginosa', *Mol Microbiol,* 59(5), pp. 1542-58.

Southey-Pillig, C. J., Davies, D. G. and Sauer, K. (2005) 'Characterization of temporal protein production in Pseudomonas aeruginosa biofilms', *J Bacteriol,* 187(23), pp. 8114-26.

Stancik, I. A., Sestak, M. S., Ji, B., Axelson-Fisk, M., Franjevic, D., Jers, C., Domazet-Loso, T. and Mijakovic, I. (2018) 'Serine/Threonine Protein Kinases from Bacteria, Archaea and Eukarya Share a Common Evolutionary Origin Deeply Rooted in the Tree of Life', *J Mol Biol,* 430(1), pp. 27-32.

Starosta, A. L., Lassak, J., Jung, K. and Wilson, D. N. (2014) 'The bacterial translation stress response', *FEMS Microbiol Rev,* 38(6), pp. 1172-201.

Steinmetz, M., Le Coq, D., Aymerich, S., Gonzy-Treboul, G. and Gay, P. (1985) 'The DNA sequence of the gene for the secreted Bacillus subtilis enzyme levansucrase and its genetic control sites', *Mol Gen Genet,* 200(2), pp. 220-8.

Stewart, P. S., Franklin, M. J., Williamson, K. S., Folsom, J. P., Boegli, L. and James, G. A. (2015) 'Contribution of stress responses to antibiotic tolerance in Pseudomonas aeruginosa biofilms', *Antimicrob Agents Chemother,* 59(7), pp. 3838-47.

Stolle, A. S., Meader, B. T., Toska, J. and Mekalanos, J. J. (2021) 'Endogenous membrane stress induces T6SS activity in Pseudomonas aeruginosa', *Proc Natl Acad Sci U S A,* 118(1).

Su, S., Panmanee, W., Wilson, J. J., Mahtani, H. K., Li, Q., Vanderwielen, B. D., Makris, T. M., Rogers, M., McDaniel, C., Lipscomb, J. D., Irvin, R. T., Schurr, M. J., Lancaster, J. R., Jr., Kovall, R. A. and Hassett, D. J. (2014) 'Catalase (KatA) plays a role in protection against anaerobic nitric oxide in Pseudomonas aeruginosa', *PLoS One,* 9(3), pp. e91813.

Talavera, A., Hendrix, J., Versees, W., Jurenas, D., Van Nerom, K., Vandenberk, N., Singh, R. K., Konijnenberg, A., De Gieter, S., Castro-Roa, D., Barth, A., De Greve, H., Sobott, F., Hofkens, J., Zenkin, N., Loris, R. and Garcia-Pino, A. (2018) 'Phosphorylation decelerates conformational dynamics in bacterial translation elongation factors', *Sci Adv,* 4(3), pp. eaap9714.

Tanaka, S. Y., Narita, S. and Tokuda, H. (2007) 'Characterization of the Pseudomonas aeruginosa Lol system as a lipoprotein sorting mechanism', *J Biol Chem,* 282(18), pp. 13379-84.

Tashiro, Y., Nomura, N., Nakao, R., Senpuku, H., Kariyama, R., Kumon, H., Kosono, S., Watanabe, H., Nakajima, T. and Uchiyama, H. (2008) 'Opr86 is essential for viability and is a potential candidate for a protective antigen against biofilm formation by Pseudomonas aeruginosa', *J Bacteriol,* 190(11), pp. 3969-78.

Thomas, G. G. (1996) 'Hypoxia-mediated selection of cells with diminished apoptotic potential in solid tumours'.

Tolker-Nielsen, T. (2015) 'Biofilm Development', *Microbiol Spectr,* 3(2), pp. MB-0001-2014.

Tribelli, P. M., Lujan, A. M., Pardo, A., Ibarra, J. G., Fernandez Do Porto, D., Smania, A. and Lopez, N. I. (2019) 'Core regulon of the global anaerobic regulator Anr targets central metabolism functions in Pseudomonas species', *Sci Rep,* 9(1), pp. 9065.

Troxell, B. and Hassan, H. M. (2013) 'Transcriptional regulation by Ferric Uptake Regulator (Fur) in pathogenic bacteria', *Front Cell Infect Microbiol,* 3, pp. 59.

Trunk, K., Benkert, B., Quack, N., Munch, R., Scheer, M., Garbe, J., Jansch, L., Trost, M., Wehland, J., Buer, J., Jahn, M., Schobert, M. and Jahn, D. (2010) 'Anaerobic adaptation in Pseudomonas aeruginosa: definition of the Anr and Dnr regulons', *Environ Microbiol,* 12(6), pp. 1719-33.

Tyson, J. R., O'Neil, N. J., Jain, M., Olsen, H. E., Hieter, P. and Snutch, T. P. (2018) 'MinION-based long-read sequencing and assembly extends the Caenorhabditis elegans reference genome', *Genome Res,* 28(2), pp. 266-274.

Ude, S., Lassak, J., Starosta, A. L., Kraxenberger, T., Wilson, D. N. and Jung, K. (2013) 'Translation elongation factor EF-P alleviates ribosome stalling at polyproline stretches', *Science,* 339(6115), pp. 82-5.

Unterholzner, S. J., Poppenberger, B. and Rozhon, W. (2013) 'Toxin-antitoxin systems: Biology, identification, and application', *Mob Genet Elements,* 3(5), pp. e26219.

Van Gennip, M., Christensen, L. D., Alhede, M., Phipps, R., Jensen, P. O., Christophersen, L., Pamp, S. J., Moser, C., Mikkelsen, P. J., Koh, A. Y., Tolker-Nielsen, T., Pier, G. B., Hoiby, N., Givskov, M. and Bjarnsholt, T. (2009) 'Inactivation of the rhlA gene in Pseudomonas aeruginosa prevents rhamnolipid production, disabling the protection against polymorphonuclear leukocytes', *APMIS,* 117(7), pp. 537-46.

Varadarajan, A. R., Allan, R. N., Valentin, J. D. P., Castaneda Ocampo, O. E., Somerville, V., Pietsch, F., Buhmann, M. T., West, J., Skipp, P. J., van der Mei, H. C., Ren, Q., Schreiber, F., Webb, J. S. and Ahrens, C. H. (2020) 'An integrated model system to gain mechanistic insights into biofilm-

associated antimicrobial resistance in Pseudomonas aeruginosa MPAO1', *NPJ Biofilms Microbiomes,* 6(1), pp. 46.

Walters, M. C., 3rd, Roe, F., Bugnicourt, A., Franklin, M. J. and Stewart, P. S. (2003) 'Contributions of antibiotic penetration, oxygen limitation, and low metabolic activity to tolerance of Pseudomonas aeruginosa biofilms to ciprofloxacin and tobramycin', *Antimicrob Agents Chemother,* 47(1), pp. 317-23.

Wang, Y. G., Ning, Y., Alam, G. N., Jankowski, B. M., Dong, Z. H., Nor, J. E. and Polverini, P. J. (2013) 'Amino Acid Deprivation Promotes Tumor Angiogenesis through the GCN2/ATF4 Pathway', *Neoplasia,* 15(8), pp. 989-997.

Wei, Q. and Ma, L. Z. (2013) 'Biofilm matrix and its regulation in Pseudomonas aeruginosa', *Int J Mol Sci,* 14(10), pp. 20983-1005.

Whitney, J. C., Quentin, D., Sawai, S., LeRoux, M., Harding, B. N., Ledvina, H. E., Tran, B. Q., Robinson, H., Goo, Y. A., Goodlett, D. R., Raunser, S. and Mougous, J. D. (2015) 'An interbacterial NAD(P)(+) glycohydrolase toxin requires elongation factor Tu for delivery to target cells', *Cell,* 163(3), pp. 607-19.

Williamson, K. S., Richards, L. A., Perez-Osorio, A. C., Pitts, B., McInnerney, K., Stewart, P. S. and Franklin, M. J. (2012) 'Heterogeneity in Pseudomonas aeruginosa biofilms includes expression of ribosome hibernation factors in the antibiotic-tolerant subpopulation and hypoxia-induced stress response in the metabolically active population', *J Bacteriol,* 194(8), pp. 2062-73.

Wolf, H., Chinali, G. and Parmeggiani, A. (1974) 'Kirromycin, an inhibitor of protein biosynthesis that acts on elongation factor Tu', *Proc Natl Acad Sci U S A,* 71(12), pp. 4910-4.

Wongsaroj, L., Saninjuk, K., Romsang, A., Duang-Nkern, J., Trinachartvanit, W., Vattanaviboon, P. and Mongkolsuk, S. (2018) 'Pseudomonas aeruginosa glutathione biosynthesis genes play multiple roles in stress protection, bacterial virulence and biofilm formation', *PLoS One,* 13(10), pp. e0205815.

Wood, L. F., Leech, A. J. and Ohman, D. E. (2006) 'Cell wall-inhibitory antibiotics activate the alginate biosynthesis operon in Pseudomonas aeruginosa: Roles of sigma (AlgT) and the AlgW and Prc proteases', *Mol Microbiol,* 62(2), pp. 412-26.

Wood, T. K., Knabel, S. J. and Kwan, B. W. (2013) 'Bacterial persister cell formation and dormancy', *Appl Environ Microbiol,* 79(23), pp. 7116-21.

Wood, T. K., Song, S. and Yamasaki, R. (2019) 'Ribosome dependence of persister cell formation and resuscitation', *J Microbiol,* 57(3), pp. 213-219.

Xie, K., Peng, H., Hu, H., Wang, W. and Zhang, X. (2013) 'OxyR, an important oxidative stress regulator to phenazines production and hydrogen peroxide resistance in Pseudomonas chlororaphis GP72', *Microbiol Res,* 168(10), pp. 646-53.

Yamaguchi, Y. and Inouye, M. (2011) 'Regulation of growth and death in Escherichia coli by toxin-antitoxin systems', *Nat Rev Microbiol,* 9(11), pp. 779-90.

Yao, H., Jepkorir, G., Lovell, S., Nama, P. V., Weeratunga, S., Battaile, K. P. and Rivera, M. (2011) 'Two distinct ferritin-like molecules in Pseudomonas aeruginosa: the product of the bfrA gene is a bacterial ferritin (FtnA) and not a bacterioferritin (Bfr)', *Biochemistry,* 50(23), pp. 5236-48.

Ye, J., Kumanova, M., Hart, L. S., Sloane, K., Zhang, H., De Panis, D. N., Bobrovnikova-Marjon, E., Diehl, J. A., Ron, D. and Koumenis, C. (2010) 'The GCN2-ATF4 pathway is critical for tumour cell survival and proliferation in response to nutrient deprivation', *EMBO J,* 29(12), pp. 2082-96.

Zhang, Y. L., Zhang, J. J., Hoeflich, K. P., Ikura, M., Qing, G. L. and Inouye, M. (2003) 'MazF cleaves cellular mRNAs specifically at ACA to block protein synthesis in Escherichia coli', *Molecular Cell,* 12(4), pp. 913-923.

Zhu, W., Soonpaa, M. H., Chen, H., Shen, W., Payne, R. M., Liechty, E. A., Caldwell, R. L., Shou, W. and Field, L. J. (2009) 'Acute doxorubicin cardiotoxicity is associated with p53-induced inhibition of the mammalian target of rapamycin pathway', *Circulation,* 119(1), pp. 99-106.

Zhu, X., Feng, C., Zhou, L., Li, Z., Zhang, Y. and Pan, J. (2021a) 'Impacts of Ser/Thr Protein Kinase Stk1 on the Proteome, Twitching Motility, and Competitive Advantage in Pseudomonas aeruginosa', *Frontiers in Microbiology,* 12.

Zhu, X., Feng, C., Zhou, L., Li, Z., Zhang, Y. and Pan, J. (2021b) 'Impacts of Ser/Thr Protein Kinase Stk1 on the Proteome, Twitching Motility, and Competitive Advantage in Pseudomonas aeruginosa', *Front Microbiol,* 12, pp. 738690.

Zoncu, R., Efeyan, A. and Sabatini, D. M. (2011) 'mTOR: from growth signal integration to cancer, diabetes and ageing', *Nat Rev Mol Cell Biol,* 12(1), pp. 21-35.